NASA SP-249

COSMIC GAMMA RAYS

NATIONAL AERONAUTICS AND SPACE ADMINISTRATION

NASA SP-249

COSMIC GAMMA RAYS

FLOYD WILLIAM STECKER

Goddard Space Flight Center

Scientific and Technical Information Office 1971
NATIONAL AERONAUTICS AND SPACE ADMINISTRATION
Washington, D.C.

For sale by the Superintendent of Documents,
U.S. Government Printing Office, Washington, D.C. 20402
Price $1.25
Library of Congress Catalog Card Number 70–609224

PREFACE

The scientific potential of γ-ray astronomy has long been recognized from a theoretical standpoint by investigators in the fields of cosmic-ray research and high-energy astrophysics. Gamma-ray studies can help answer questions concerning the nature and origin of cosmic rays, both galactic and extragalactic; the nature of supernovae, pulsars, and powerful radio sources; the extent and importance of antimatter in the universe; and the nature of the universe in the distant past.

The advent of satellite-borne γ-ray telescopes has recently made γ-ray astronomy a reality. The first observations, as discussed in this book, have already provided important information on galactic and extragalactic cosmic rays and interstellar gas. These observations may also have great cosmological significance. The second generation of γ-ray telescopes is already in the development stage.

It therefore seems most appropriate at this time for a comprehensive theoretical monograph to appear on the scene to aid in the planning of future γ-ray astronomy experiments and in the interpretation of future experimental results. It should be of value both as a reference and as a text.

JOHN F. CLARK
Director, Goddard Space Flight Center
Greenbelt, Md.

Foreword

It is a far cry from the early years of cosmic-ray exploration when it was widely supposed that the primary cosmic radiation consists mainly of γ-rays. Today we know that cosmic γ-rays are relatively scarce, and that the high-energy particles bombarding the Earth from outer space are mostly atomic nuclei and electrons. These fast ions have "forgotten" their original directions of motion, owing to their tortuous paths in the magnetic fields of interstellar space. Unlike the photons of optical or radio astronomy, which travel in essentially straight lines, they provide no directional clues to their sources. This explains in part the avid search for point sources of cosmic γ-rays, which must be generated as secondaries of the high-energy charged particles at the sites of origin.

There is every reason to believe that high-energy γ-rays are produced not only at cosmic-ray sources but also in the interstellar and intergalactic media. Study of this diffuse radiation can also provide significant astrophysical information.

The very low flux of photons with energies exceeding tens or hundreds of megaelectron volts, and the high background of charged particles, makes their detection extremely difficult. However, the importance of the quest guarantees that the search will go on.

The author of this timely monograph has made noteworthy contributions to the theory of production and interactions of cosmic γ-rays. In the present work he has resisted the temptation to treat specific models of possible point sources of γ-rays; such models are as yet highly speculative. His central purpose has been to summarize fundamental processes that are likely to play an important role in future research in this discipline.

The specialist in astrophysics and cosmology, the interested physicist, and the graduate student will all find this monograph very useful.

Maurice M. Shapiro
Laboratory for Cosmic Ray Physics
Naval Research Laboratory
Washington, D.C.

Introduction

Gamma-ray astrophysics is one of the newest branches of physical science. Although some theoretical work has been produced, particularly in the past decade, it was not until September 1968 that the actual discovery of cosmic γ-rays (above 100 MeV) was announced in the literature. This momentous discovery, the work of an MIT research team headed by Kraushaar, Clark, and Garmire, not only proved the existence of cosmic γ-rays but also showed that most of those detected originated in the plane of our galaxy.

Although observations have been attempted by many other experimental groups, their results, for the most part, have been either negative or inconclusive, allowing only the determination of upper limits on the diffuse cosmic γ-ray flux and the flux from possible point sources. However, present detectors should be sensitive enough, according to theoretical estimates, to measure diffuse γ-ray fluxes and possibly fluxes from a few point sources. Most recently, Vette, Gruber, Matteson, and Peterson have obtained measurements of the cosmic γ-ray background spectrum between 1 and 6 MeV and have found this spectrum to be of an unexpected nature which may have great cosmological significance.

No attempt is made here to list and discuss these observational attempts in detail; such listings may be found in recent reviews. Neither is it the author's intention to construct crude models for possible point sources of cosmic γ-rays. The emphasis here is on a discussion of the basic γ-ray production processes themselves. In addition, the discussion is confined to the simple cases of the production of diffuse γ-radiation in the galaxy and metagalaxy, where the fluxes are directly proportional to the products of quantities like gas densities and cosmic-ray intensities.

Finally, no attempt is made here to repeat in detail derivations of the classical electromagnetic production processes of bremsstrahlung, magnetobremsstrahlung (synchrotron radiation), and Compton collisions, which are given in many references such as Heitler, Shklovskii, and Ginzburg and Syrovatskii. However, the results of these production processes are discussed.

Most of this book is devoted to a detailed discussion of the high-energy processes, primarily in the realm of modern particle physics, which

lead to the production of cosmic γ-rays. The physics of these processes is then applied to the problems of astronomy and cosmic-ray physics which γ-ray astronomy is best suited to solve. The final section is devoted to what may turn out to be the most significant area of γ-ray astronomy; i.e., an examination of the cosmological significance of the energy spectra of extragalactic γ-radiation.

An appendix by Donald Kniffen contains a discussion of γ-ray telescopes and the latest techniques being developed for the detection of cosmic γ-rays.

Acknowledgments

This book, in large part, is based on research performed during the past 4 years at Harvard College Observatory, Smithsonian Astrophysical Observatory, and NASA Goddard Space Flight Center.

Particular thanks are due Giovanni Fazio for his many and invaluable contributions.

Thanks go to Henri Mitler, Frank C. Jones, Martin Rees, Richard McCray, Reuven Ramaty, Gerald Share, and David Morgan for their discussion and critical comments. Thanks, also, go to Joseph Bredekamp for programing most of the numerical calculations found throughout the book.

I am grateful to John F. Clark for writing the preface, to Maurice Shapiro for writing the foreword, and to Donald Kniffen for his help in balancing out the book by contributing an appendix on γ-ray telescopes from the viewpoint of an active experimentalist in the field. I also thank George Clark, Giovanni Fazio, Glenn Frye, Kenneth Greisen, William Kraushaar, Lawrence Peterson, Maurice Shapiro, Gerald Share, and James Vette for contributing information on their γ-ray telescopes, some of it prior to final independent publication.

I also wish to thank the *Astrophysical Journal*, *Astrophysics and Space Science*, the *Journal of Geophysical Research*, and *Nature* for permission to include here much material that appeared in essentially the same form in previously published articles of mine in those journals.

F. W. S.

CONTENTS

1

Basic Interactions

GAMMA-RAY PRODUCTION FROM THE DECAY OF SECONDARY PARTICLES PRODUCED IN COSMIC-RAY INTERACTIONS

1-1 INTRODUCTION

The importance of studying cosmic γ-radiation has been recognized for some time, and for fundamental reasons. These energetic photons are the direct product of interactions which are basic to high-energy astrophysics and cosmic-ray physics. Gamma-ray-producing interactions involve the basic constituents of the universe: cosmic rays, interstellar and intergalactic gas, cosmic radio waves, the universal blackbody radiation, starlight, and cosmic magnetic fields. In addition, γ-ray observations allow us to test for the presence of significant amounts of antimatter in the universe.

Gamma rays suffer negligible absorption in most cases of astrophysical interest and they travel in straight lines from their sources. In this they differ from cosmic rays which, being charged particles, have their motions continually altered by interactions with cosmic magnetic fields. Therefore, much can be learned about cosmic-ray sources and interactions by studying the spatial and energy distribution of the γ-rays they produce.

Recent laboratory studies of high-energy interactions utilizing proton accelerators have provided us with much information on the nature of these interactions up to $\sim$30-GeV energies. This information can be supplemented by studies of cosmic-ray interactions at higher energies occurring in the atmosphere. The knowledge gained from earthbound studies of high-energy interactions may then be applied to astronomical problems involving cosmic-ray and annihilation phenomena.

1-2 THE DETERMINATION OF GAMMA-RAY PRODUCTION SPECTRA DUE TO COSMIC-RAY INTERACTIONS WITH INTERSTELLAR AND INTERGALACTIC GAS

For our discussion of the production of cosmic γ-rays in high-energy interactions, it will be useful to define a source function $q(E_\gamma)$ such that

411-892 O - 71 - 2

$q(E_\gamma)dE_\gamma$ represents the number of γ-rays having energies in the range between E_γ and $E_\gamma + dE_\gamma$ produced per unit volume per unit time; $q(E_\gamma)$ can be written as the product

$$q(E_\gamma) = n\nu_c\langle\zeta\rangle \tag{1-1}$$

where n is the density of target nuclei in the medium considered, ν_c is the collision frequency per target nucleus, and $\langle\zeta\rangle$ is the average number (multiplicity) of γ-rays with energy E_γ produced per collision. If we define an average collision cross section $\langle S\rangle$, then ν_c is given by

$$\nu_c = \langle S\rangle 4\pi I_{\rm cr} \tag{1-2}$$

where $I_{\rm cr}$ is the average directional intensity of cosmic rays (in units of $\rm cm^{-2}\ s^{-1}\ sr^{-1}$), and the factor of 4π comes from integration over solid angle. Equations (1–1) and (1–2) then combine to give

$$q(E_\gamma) = 4\pi n\langle S\rangle\langle\zeta\rangle I_{\rm cr} \tag{1-3}$$

In general, for the production of γ-rays, ζ and S are functions of the primary cosmic-ray energy $E_{\rm pr}$. Therefore, we define

$$\sigma(E_\gamma|E_{\rm pr}) \equiv \zeta(E_{\rm pr})S(E_\gamma|E_{\rm pr}) \tag{1-4}$$

and write

$$q(E_\gamma) = 4\pi n \int dE_{\rm pr}\,\sigma(E_\gamma|E_{\rm pr})I(E_{\rm pr}) \tag{1-5}$$

Note that, in general, n and $I_{\rm cr}$ and therefore $q(E_\gamma)$ are functions of spatial location $\mathbf{r}$.

We can now derive an expression for the directional intensity of γ-rays of energy E_γ observed at the Earth. The flux reaching the Earth after being produced in a differential source volume dV located at a point $\mathbf{r}$ is given by

$$\begin{aligned} dF_\gamma(E_\gamma, \mathbf{r}) &= \frac{1}{4\pi r^2}\, q(E_\gamma, \mathbf{r})\ dV \\ &= \frac{1}{4\pi r^2}\, q(E_\gamma, \mathbf{r}) r^2\ d\Omega\ dr \end{aligned} \tag{1-6}$$

Thus, the directional intensity $dI_\gamma(E_\gamma, \mathbf{r})$ reduces to

$$dI_\gamma(E_\gamma, \mathbf{r}) = \frac{dF_\gamma(E_\gamma, \mathbf{r})}{d\Omega} = \frac{q(E_\gamma, \mathbf{r})\ dr}{4\pi} \tag{1-7}$$

and the total specific intensity is, therefore,

$$I_\gamma(E_\gamma) = \frac{1}{4\pi} \int dr\, q(E_\gamma, \mathbf{r}) \tag{1-8}$$

If, in addition, we take into account the effects of absorption of γ-rays by the medium, we must include an exponential absorption factor of the form $\exp\,[-\int dr\ \kappa(E_\gamma, \mathbf{r})]$, where $\kappa(E_\gamma, \mathbf{r})$ is the absorption of the medium per unit pathlength. Thus, the more general form of equation (1–8), which takes absorption into account, is

$$I_\gamma(E_\gamma) = \frac{1}{4\pi} \int dr\, q(E_\gamma, \mathbf{r})\ \exp\left[-\int_0^r dr'\, \kappa(E_\gamma, \mathbf{r}')\right] \tag{1-9}$$

We will now derive the source function $q(E_\gamma, \mathbf{r})$ for γ-ray production. By generalizing equation (1–5) to include collisions between various nuclides of cosmic rays and interstellar gas, we can express this function as

$$q(E_\gamma, \mathbf{r}) = 4\pi \sum_{j,k} n_j(\mathbf{r}) \int dE_k \sigma_{jk}(E_\gamma | E_k) I(E_k, \mathbf{r}) \tag{1-10}$$

so that the total γ-ray source function is obtained by summing over all the possible contributions from collisions between gas nuclei of type j and cosmic-ray nuclei of type k. We must also allow for various distinct γ-ray production interactions that can take place between two specified nuclei, j and k. To do this, we express the cross section $\sigma_{jk}(E_\gamma | E_k)$ as a sum over the contributions from various secondary particles which can be produced in the interaction and can subsequently decay to produce γ-rays. Denoting these particles as secondary particles of type s, we therefore write

$$\sigma_{jk}(E_\gamma | E_k) = \sum_s \int dE_s \langle \zeta_{\gamma,s} \rangle f_s(E_\gamma | E_s) \sigma_{jk,s}(E_s | E_k) \tag{1-11}$$

where $\langle \zeta_{\gamma,s} \rangle$ is the average number of γ-rays produced by the decay of a secondary of type s and $f_s(E_\gamma | E_s)$ is an energy distribution function, normalized so that

$$\int_0^{E_s} dE_\gamma f_s(E_\gamma | E_s) = 1$$

which gives the probability that a γ-ray of energy E_γ will result from the decay of a secondary s having an energy E_s.

But this breakdown is still insufficient for the specification of γ-ray production interactions. We indicate this by citing the following example:

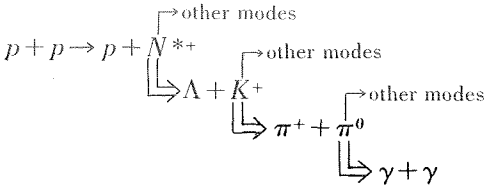

In this example we consider an interaction between two protons. We have chosen to follow a particular decay chain which results in the production of two γ-rays and is given by the double arrows. In this decay chain, we first produce an intermediate nonstrange isobar, N^{*+}, which decays in $\sim 10^{-23}$ s into a lambda hyperon and a positive K-meson (kaon). The kaon, in turn, decays in $\sim 10^{-8}$ s into a positive and a neutral π-meson (pion). The neutral pion then decays in $\sim 10^{-16}$ s, yielding two γ-rays. At each stage in the chain, there are branches into other possible decay modes which occur with specified probabilities (branching ratios). For example, the isobar could have decayed into a proton and a neutral pion and this alternate decay mode would have produced γ-rays having a different energy spectrum in the rest frame of the observer (hereafter referred to as the laboratory system (ls)).

Therefore, we must determine the sum over all possible γ-ray-producing decay modes d involving secondary particles of type s to evaluate the right-hand side of equation (1–11); i.e.,

$$\langle \zeta_{\gamma,\, s} \rangle f_s(E_\gamma \mid E_s) = \prod_d \langle \zeta_{\gamma,\, ds} \rangle f_{ds}(E_\gamma \mid E_s) \tag{1–12}$$

where, for decay modes involving l intermediate secondaries,

$$\langle \zeta_{\gamma,\, ds} \rangle = \zeta_{s'} R_{s'} \zeta_{s''} R_{s''} \cdots \zeta_{s(l)} R_{s(l)} \zeta_\gamma R_\gamma \tag{1–13}$$

Here, the quantities denoted by R indicate branching ratios for the production of various intermediate secondaries. The distribution function $f_{ds}(E_\gamma \mid E_s)$ is given by

$$f_{ds}(E_\gamma \mid E_s) = \int\int \cdots \int dE_{s'}\, dE_{s''} \cdots dE_{s(l)} f(E_\gamma \mid E_{s(l)}) f(E_{s(l)} \mid E_{s(l-1)}) \cdots f(E_{s'} \mid E_s) \tag{1–14}$$

Fortunately, long chain decay modes for γ-ray production turn out to have such small probabilities that they may be neglected.

1–3 GAMMA-RAY-PRODUCING DECAY MODES

We will consider the γ-rays produced from the following secondary particle decay channels: the electromagnetic decays

$$\pi^0 \rightarrow 2\gamma \tag{1–15}$$

$$\Sigma^0 \rightarrow \Lambda + \gamma \tag{1–16}$$

and also the weak decays

$$K^{\pm} \rightarrow \pi^{\pm} + \pi^0 \tag{1–17}$$

$$K_1^0 \rightarrow 2\pi^0 \tag{1–18}$$

$$K_2^0 \rightarrow 3\pi^0 \tag{1–19}$$

$$K_2^0 \rightarrow \pi^+ + \pi^- + \pi^0 \tag{1–20}$$

$$\Lambda \rightarrow n + \pi^0 \tag{1–21}$$

and

$$\Sigma^+ \rightarrow p + \pi^0 \tag{1–22}$$

followed by $\pi^0 \rightarrow 2\gamma$. Table 1–1 shows some of the features of γ-ray production from the decays of p-p secondaries.

The hyperons can be created by associated production or in hyperon-antihyperon pairs; i.e., by the reactions

$$N + N \rightarrow N + Y + K + \cdots \tag{1–23}$$

and

$$N + N \rightarrow N + N + Y + \bar{Y} + \cdots \tag{1–24}$$

TABLE 1–1.—*Gamma-Ray Multiplicity and Branching Ratios From Hyperon and Meson Decays* [a]

Decay mode	Branching ratio R	Multiplicity ζ_γ	$R\zeta_\gamma$
$\pi^0 \rightarrow 2\gamma$	1.00	2	2.00
$\Sigma^0 \rightarrow \Lambda + \gamma$	1.00	1	1.00
$K^{\pm} \rightarrow \pi^{\pm} + \pi^0$	0.215	2	.430
$K_1^0 \rightarrow 2\pi^0$	$\frac{1}{2}$(0.311)	4	.622
$K_2^0 \rightarrow 3\pi^0$	$\frac{1}{2}$(0.265)	6	.795
$K_2^0 \rightarrow \pi^+ + \pi^- + \pi^0$	$\frac{1}{2}$(0.114)	2	.114
$\Lambda \rightarrow n + \pi^0$	0.331	2	.662
$\Sigma^+ \rightarrow p + \pi^0$	0.510	2	1.02

[a] The reactions $\Xi^0 \rightarrow \Lambda + \pi^0$ and $\Omega^- \rightarrow \Xi^- + \pi^0$ may also occur, but production of the Ξ^0 and Ω^- hyperons is so rare that these decays will not be considered.

where the N denotes nucleon and the Y denotes hyperon. They may also arise from such reactions as

$$N+N\rightarrow N^*+N+\cdots \tag{1-25}$$

(where the asterisk denotes an isobar) followed by

$$N^*\rightarrow Y+K$$

and

$$N+N\rightarrow Y^*+N+K+\cdots \tag{1-26}$$

followed by

$$Y^*\rightarrow Y+\pi\text{'s}$$
$$\rightarrow N+\pi\text{'s}$$

which have end products similar to those of reactions (1–23) and (1–24), but whose resultant momentum and angular distributions are affected by the formation of the intermediate isobar. (Unless otherwise specified, the symbol N stands for nucleon, Y for any hyperon, K for any kaon, N^* for any nonstrange isobar, and Y^* for any strange isobar.) We may note also that at very high energies, as first pointed out by Fermi (1951), pions and kaon-antikaon pairs can be produced as what might be pictured as a quasithermal boson gas.

The experimental results of p–p interactions indicate the following features.

(1) For p–p machine data where the primary beam momentum is less than 10 GeV/c (what will be hereafter referred to as the low-energy region) secondaries are produced primarily through an intermediate stage involving isobar production; for example,[1]

$$p+p\rightarrow\Delta(1.238)+N$$

followed by (1–27)

$$\Delta(1.238)\rightarrow N+\pi$$

and

$$p+p\rightarrow\Sigma(1.385)+N+K$$

followed by (1–28)

$$\Sigma(1.385)\rightarrow\Lambda+\pi$$

---

[1] We adopt here the contemporary notation for isobar designations. The quantity in the parentheses is the rest mass of the isobar in GeV/c^2. N^* and Δ represent nonstrange isobars having isospins 1/2 and 3/2, respectively. $\Lambda(\ )$ and $\Sigma(\ )$ represent isobars of strangeness -1 having isospins 0 and 1, respectively. $\Xi(\ )$ represents isobars of strangeness -2.

(2) The character of the interaction changes so that for "high" energies (primary proton energy greater than 10 GeV), the p–p interactions continue to yield only one or two isobars, with perhaps as many as four secondary mesons (K or π), but the bulk of the secondary mesons produced at high energies results from the formation of a quasithermal meson gas (Fermi, 1951; Heisenberg, 1952; and Landau, 1953), containing up to one-half the energy of the system and localized to one or two centers of excitation (sometimes referred to as fireballs), which move much more slowly in the center-of-mass system than do the baryon isobars. (See Daniel et al., 1963.)

1-4 KINEMATICS

The reactions that we consider involve energies at least of the order of magnitude of the rest masses of the particles involved. Therefore, we must use the results of the special theory of relativity to describe their kinematics. The following is a discussion of the kinematics that will be needed to describe the reactions listed in the previous section.

Special relativity makes use of a four-vector algebra with the corresponding four-momenta and four-velocities defined as the vectors

$$p^{(4)} = (\mathbf{p}, iE) \tag{1-29}$$

and

$$\beta^{(4)} = (\boldsymbol{\beta}, i) \tag{1-30}$$

In equations (1–29) and (1–30), the superscript denotes a four-vector, $\boldsymbol{\beta} \equiv \mathbf{v}/c$, and the speed of light c is taken equal to unity (as it will be hereafter).

The Lorentz transformation can be expressed as an orthogonal transformation that corresponds to a rotation through an angle ϕ in a complex four-vector space. Figure 1–1(a) shows that the β of the Lorentz trans-

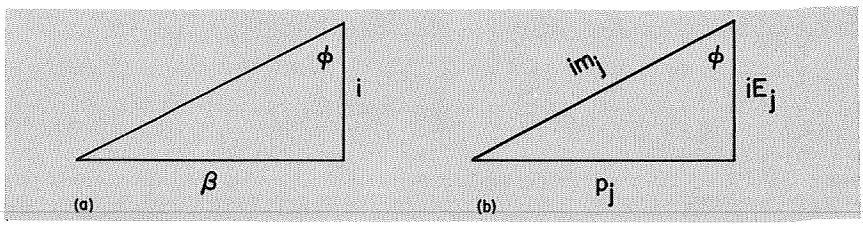

FIGURE 1–1.—Relativistic energy momentum and velocity triangles. (a) β triangle. (b) p–E triangle.

formation is then equal to tanh ϕ. It follows that, under this rotation, the "length" of the four-vector momentum

$$|p^{(4)}|^2 = |\mathbf{p}^2 - E^2| = m^2 \tag{1-31}$$

is an invariant and serves to define the proper mass m.

In figure 1–1(b) the subscript j serves as the index of each of the various particles involved in the reaction.

If we want to transform our kinetic equations from one system to another by performing a Lorentz transformation specified by the velocity β_2 (for example, we will later be concerned with transformations from center-of-momentum systems (cms) to laboratory systems (ls) and vice versa), the corresponding transformation, being simply a rotation in our complex four-space, can be performed merely by adding the angles $\phi = \tanh^{-1} \beta$. Thus, if we label quantities in the original system with the subscript 1, the transformation quantities with the subscript 2, and the transformed quantities with the subscript 3, we can write

$$\phi_3 = \phi_1 + \phi_2 \tag{1-32}$$

and

$$\beta_1 = \tanh \phi_1 \qquad \beta_2 = \tanh \phi_2 \tag{1-33}$$

therefore,

$$\beta_3 = \tanh (\phi_1 + \phi_2) = \frac{\tanh \phi_1 + \tanh \phi_2}{1 + \tanh \phi_1 \tanh \phi_2} = \frac{\beta_1 + \beta_2}{1 + \beta_1 \beta_2} \tag{1-34}$$

To find ϕ for the cms, we just add the four-momenta of all the particles involved in the reaction. Then, it follows from figure 1–1(b) that

$$\tanh \phi_{\text{cms}} = \beta_{\text{cms}} = \frac{\sum_j p_j}{\sum_j E_j} \tag{1-35}$$

From figure 1–1(a), we see that we can write

$$p = m \sinh \phi = \frac{m\beta}{(1-\beta^2)^{1/2}} \tag{1-36}$$

and

$$E = m \cosh \phi = \frac{m}{(1-\beta^2)^{1/2}} \tag{1-37}$$

We also introduce here a very useful quantity called the Lorentz factor γ, which is defined as

$$\gamma \equiv \frac{E}{m} = (1-\beta^2)^{-1/2} = \cosh \phi \tag{1-38}$$

As a particular case of equation (1–35), a case that we will be primarily concerned with later on, we consider a proton of energy E in the ls colliding with a proton at rest in the ls. We then find

$$\beta_{\text{cms}} = \frac{\sum p_j}{\sum E_j} = \frac{(E^2-m^2)^{1/2}}{E+m} = \left(\frac{\gamma-1}{\gamma+1}\right)^{1/2} \tag{1-39}$$

and

$$\gamma_{\text{cms}} = (1-\beta_{\text{cms}}^2)^{-1/2} = [\tfrac{1}{2}(\gamma+1)]^{1/2} \tag{1-40}$$

which, for $\gamma \gg 1$, reduces to

$$\gamma_{\text{cms}} \simeq (\tfrac{1}{2}\gamma)^{1/2} \tag{1-41}$$

We can use the definition (1–38) with equation (1–32) to obtain directly the Lorentz transformation for γ. We find

$$\begin{aligned} \gamma_3 = \cosh \phi_3 &= \cosh (\phi_1 + \phi_2) \\ &= \cosh \phi_1 \cosh \phi_2 + \sinh \phi_1 \sinh \phi_2 \\ &= \gamma_1\gamma_2 + \gamma_1\beta_1 \gamma_2\beta_2 \\ &= \gamma_2[\gamma_1 + \beta_2(\gamma_1\beta_1)] \end{aligned} \tag{1-42}$$

which, together with the definition (1–38), yields the energy transformation relation

$$E_3 = \gamma_2[E_1 + \beta_2 p_1] \tag{1-43}$$

Similarly, we also obtain the momentum transformation relation

$$\begin{aligned} p_3 &= m \sinh \phi_3 \\ &= m \sinh \phi_1 \cosh \phi_2 + m \cosh \phi_1 \sinh \phi_2 \\ &= \gamma_2[p_1 + \beta_2(m\gamma_1)] \\ &= \gamma_2[p_1 + \beta_2 E_1] \end{aligned} \tag{1-44}$$

From the similarity of the β and p–E triangles of figure 1–1, we can recover the Lorentz contraction formulas by analogy with equations

(1–43) and (1–44). Therefore, we obtain

$$x_3 = \gamma_2(x_1 + \beta_2 t_1) \tag{1–45}$$

and

$$t_3 = \gamma_2(t_1 + \beta_2 x_1) \tag{1–46}$$

where x is understood to be the displacement in the direction of motion, just as p has been understood to be under a similar restraint. We will find it useful to generalize our transformations by looking at reactions in a two-dimensional x–y plane, x being taken to be at angle θ with the axis of the Lorentz transformation. Therefore, under the Lorentz transformation, $z_3 = z_1$. We can then define a direction of motion by the angular parameter θ, such that

$$\tan \theta_{1,3} = \frac{\dfrac{dy_{1,3}}{dt_{1,3}}}{\dfrac{dx_{1,3}}{dt_{1,3}}} \tag{1–47}$$

From the definition (1–47) and equations (1–45) and (1–46), we immediately obtain the transformation relation for θ:

$$\tan \theta_3 = \frac{\sin \theta_1}{\gamma_2[\cos \theta_1 + (\beta_2/\beta_1)]} \tag{1–48}$$

Equations (1–43) through (1–45) can now be further generalized by the replacements

$$p \rightarrow p \cos \theta \tag{1–49}$$

and

$$x \rightarrow x \cos \theta \tag{1–50}$$

which define the axis of the Lorentz transformation, where p and x now represent the total magnitudes of these vectors in three-space.

We now consider the kinematics of two-body collisions and the kinematics of particle decay. For our purposes, we may limit ourselves to two- and three-body decays, since we need discuss only the decay reactions (1–15) through (1–22) and isobar decays where not more than three particles are produced (Morrison, 1963). It should be noted that of the decay modes (1–15) through (1–22), only the $K^{\pm}$ and K_2^0 channels involve three decay products. In those cases, the three particles produced have essentially identical masses, which simplifies the treatment.

First, we consider the reaction

$$a + b \rightarrow c + d + \cdots \tag{1–51}$$

where particle b is the target particle, at rest in the ls. Since the length of the total four-momentum is invariant, we have

$$[\Sigma p_{\text{ls}}^{(4)}]^2 = [\Sigma p_{\text{cms}}^{(4)}]^2 \tag{1-52}$$

or

$$p_a^2 - (E_a + m_b)^2 = -(E_a' + E_b')^2 \tag{1-53}$$

where quantities in the cms will be denoted by primes. We now let E' represent the total energy in the cms. Then, from equation (1–53)

$$\begin{aligned} E' = E_a' + E_b' &= [(E_a + m_b)^2 - p_a^2]^{1/2} \\ &= [m_a^2 + m_b^2 + 2m_b E_a]^{1/2} \end{aligned} \tag{1-54}$$

Using the four-momentum invariant inner product

$$[p_a^{(4)} \cdot (p_a^{(4)} + p_b^{(4)})]_{\text{ls}} = [p_a^{(4)} \cdot (p_a^{(4)} + p_b^{(4)})]_{\text{cms}} \tag{1-55}$$

we obtain expressions for the individual cms energies of particles a and b. Thus, we obtain

$$E_a' = \frac{E'^2 + m_a^2 - m_b^2}{2E'} \tag{1-56}$$

and

$$E_b' = \frac{E'^2 + m_b^2 - m_a^2}{2E'} \tag{1-57}$$

To obtain the threshold energies for the creation of particles c, d, . . ., we write

$$E_{\text{th}}' = m_a + m_b + \Delta m = m_c + m_d + \cdots \tag{1-58}$$

where Δm is the mass difference between the incoming and outgoing particles as defined by equation (1–58). In the case that we have been considering, where one particle is at rest in the ls, we note that the threshold energy is the energy of the incoming particle which is equivalent to just enough available energy in the cms (given by eq. (1–54)) to produce the rest mass of all the outgoing particles (given by eq. (1–58)). Thus, we equate equations (1–54) and (1–58) to obtain

$$m_a + m_b + \Delta m = [m_a^2 + m_b^2 + 2m_b (E_a)_{\text{th}}]^{1/2} \tag{1-59}$$

which reduces to

$$(E_a)_{\text{th}} = \left(1 + \frac{m_a}{m_b} + \frac{\Delta m}{2m_b}\right)\Delta m + m_a \tag{1-60}$$

In terms of kinetic energy $T = (E - m) = (\gamma - 1)m$, we have

$$T_{\text{th}} = \left(1 + \frac{m_a}{m_b} + \frac{\Delta m}{2m_b}\right)\Delta m \tag{1-61}$$

Table 1–2 lists cms energies for a p–p system as a function of laboratory energy, derived from equation (1–40).

Let us now consider the decay of a particle of mass M into two particles of mass m_a and m_b, respectively. From equations (1–56) and (1–57), we find that in the rest system of mass M

$$E'_a = \frac{M^2 + m_a^2 - m_b^2}{2M} \tag{1-62}$$

TABLE 1–2.—*Transformation From Laboratory Energy to cms Energy in* p–p *Collisions*

$T_{\text{ls}} = E_p - m_p$, GeV	$\gamma_p = E_p/m_p$	γ_{cms}	$Q = 2m_p(\gamma_c - 1)$, GeV
0.0	1.00	1.00	0.0
0.5	1.53	1.13	.235
1.0	2.07	1.24	.447
1.5	2.60	1.34	.641
2.0	3.13	1.44	.821
2.5	3.67	1.53	.989
3.0	4.20	1.61	1.149
3.5	4.73	1.69	1.300
4.0	5.26	1.77	1.444
4.5	5.80	1.84	1.583
5.0	6.33	1.91	1.716
5.5	6.86	1.98	1.844
6.0	7.40	2.05	1.968
6.5	7.93	2.11	2.088
7.0	8.46	2.18	2.205
7.5	9.00	2.23	2.318
8.0	9.53	2.29	2.428
8.5	10.06	2.35	2.536
9.0	10.59	2.41	2.641
9.5	11.13	2.46	2.744
10.0	11.66	2.52	2.844

and

$$E'_b = \frac{M^2 + m_b^2 - m_a^2}{2M} \tag{1-63}$$

The rest system of mass M must also be the cms of the two decay particles. Therefore, they are given equal and opposite momenta of magnitude p' in this system. Using equations (1–43) and (1–49), we obtain the Lorentz transformation to an ls where the original mass M had an energy $E_M = \gamma M$. This transformation is given by

$$E_{a,b} = \gamma(E'_{a,b} + \beta p' \cos\theta') \tag{1-64}$$

Equations (1–62) through (1–64) then yield the energies of the decay particles in the ls. These energies are given by

$$E_{a,b} = \frac{E_M}{M}\left[\left(\frac{M^2 + m_{a,b}^2 - m_{b,a}^2}{2M}\right) + \left(1 - \frac{M^2}{E_M^2}\right)^{1/2} \times p'(M, m_a, m_b)\cos\theta'\right] \tag{1-65}$$

where $p'(M, m_a, m_b)$ is given implicitly by the conservation of energy relation

$$(p'^2 + m_a^2)^{1/2} + (p'^2 + m_b^2)^{1/2} = M \tag{1-66}$$

Equation (1–65) immediately yields the following results:

(1) If $\langle\cos\theta'\rangle = 0$, i.e., if we have equal emission in the forward and backward directions in the cms,

$$\langle E_{a,b}\rangle = E_M\left(\frac{M^2 + m_{a,b}^2 - m_{b,a}^2}{2M^2}\right) \tag{1-67}$$

(2) If particle M decays isotropically, i.e., if there is equal probability of emission in all directions in the cms, the normalized angular distribution function for the emitted particles is given by

$$f(\theta')\, d\theta' = \frac{d\Omega(\theta')}{4\pi} = \frac{1}{2}\sin\theta'\, d\theta' \tag{1-68}$$

We will now make some useful substitutions in equation (1–65) to write it in the form

$$E(\theta') = E_M(\eta + \beta\kappa\cos\theta') \tag{1-69}$$

so that

$$dE(\theta') = \beta E_M \kappa \sin \theta' \, d\theta' \tag{1-70}$$

where

$$\eta \equiv \mu/M$$

is the dimensionless ratio of the cms energy of the daughter particle to the mass of the parent particle, and $\kappa \equiv p'/M$ is the dimensionless ratio of the cms momentum of the daughter particle to the mass of the parent particle. Consequently,

$$f(E)\, dE = \frac{f(\theta')}{dE/d\theta'}\, dE = \frac{1}{2\beta\kappa E_M}\, dE \tag{1-71}$$

As a check on the normalization of $f(E)$, we note that

$$\int_{E_{\min}}^{E_{\max}} f(E)\, dE = \frac{1}{2\beta\kappa E_M} \int_{E_M(\eta-\beta\kappa)}^{E_M(\eta+\beta\kappa)} dE = \frac{2\beta\kappa E_M}{2\beta\kappa E_M} = 1 \tag{1-72}$$

This function is graphed in figure 1–2.

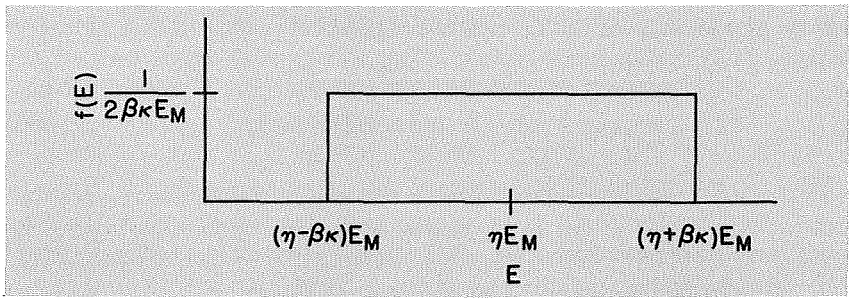

FIGURE 1–2.—The form of the energy distribution function for a particle formed isotropically from two-body decay.

(3) If we have a case where a particle of mass M decays into two particles of equal mass m, e.g., $K_1^0 \rightarrow 2\pi^0$, equation (1–65) reduces to

$$E_m = \frac{1}{2} E_M + \left(\frac{E_M^2}{M^2} - 1\right)^{1/2} \left(\frac{1}{4} M^2 - m^2\right)^{1/2} \cos \theta' \tag{1-73}$$

If, in addition, the decay is isotropic in θ', the average energy $\langle E_m \rangle$ and the half-width of the energy distribution Δ_m of decay particles having mass m are given by

$$\langle E_m \rangle = \frac{1}{2} E_M \tag{1-74}$$

and

$$\Delta_m = \left[\left(\frac{E_M^2}{M^2} - 1 \right) \left(\frac{1}{4} M^2 - m^2 \right) \right]^{1/2} \tag{1-75}$$

We find a discrete energy for the decay particles in the ls; i.e., $\Delta_m = 0$, only for two cases: (*a*) $E_M^2/M^2 = 1$, i.e., the particle of mass M is at rest in the ls; and (*b*) $m = \frac{1}{2}M$, i.e., the decay particles have no kinetic energy in the cms.

(4) If particle M decays into two particles, one of which has mass zero, e.g., $\Sigma^0 \rightarrow \Lambda + \gamma$, equation (1–65) reduces to

$$E_m = \frac{E_M}{M} \left[\frac{M^2 + m^2}{2M} + \left(1 - \frac{M^2}{E_M^2} \right)^{1/2} p'(M, m) \cos \theta' \right] \tag{1-76}$$

and

$$E_0 = \frac{E_M}{M} \left[\frac{M^2 - m^2}{2M} + \left(1 - \frac{M^2}{E_M^2} \right)^{1/2} p'(M, m) \cos \theta' \right] \tag{1-77}$$

Since, for a particle of mass zero $p = E$, we find

$$p'(M, m) = \frac{M^2 - m^2}{2M} \tag{1-78}$$

and thus

$$E_0 = \frac{E_M}{M} \left(\frac{M^2 - m^2}{2M} \right) \left[1 + \left(1 - \frac{M^2}{E_M^2} \right)^{1/2} \cos \theta' \right]$$

$$= E_M \eta(M, m) (1 + \beta_M \cos \theta') \tag{1-79}$$

(5) If both decay particles have mass zero, e.g., $\pi^0 \rightarrow 2\gamma$, equation (1–65) reduces to

$$E_0 = \tfrac{1}{2} E_M \left[1 + \left(1 - \frac{M^2}{E_M^2} \right)^{1/2} \cos \theta' \right]$$

$$= \tfrac{1}{2} M \gamma_M (1 + \beta_M \cos \theta') \tag{1-80}$$

In particular, for $M^2/E^2 \ll 1$, i.e., for ultrarelativistic particles, equation (1–80) reduces to

$$E_0 = E_M \cos^2 (\tfrac{1}{2}\theta') \tag{1-81}$$

and the energy distribution then has the corresponding parameters

$$\langle E_0 \rangle = \tfrac{1}{2} E_M \qquad \Delta_0 = \tfrac{1}{2} E_M \tag{1-82}$$

This function is shown in figure 1–3.

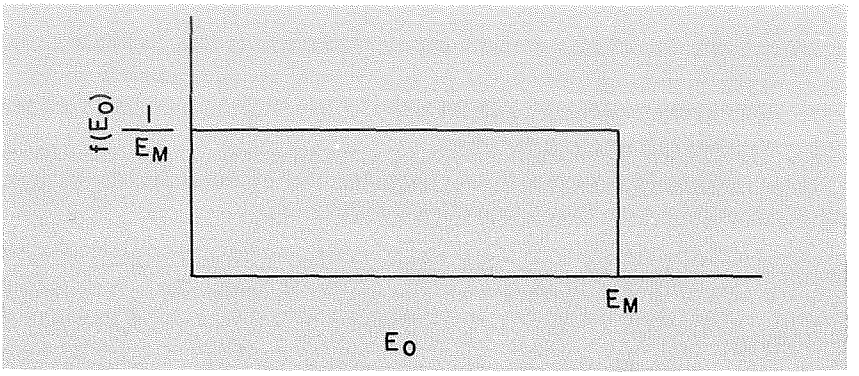

FIGURE 1–3.—The form of the energy distribution function for γ-rays resulting from the decay of relativistic neutral pions.

The ultrarelativistic form for equation (1–79) yields a distribution function that is similar in form to that of figure 1–3, with the resultant E_0 given by the simplified expression

$$E_0 = 2E_M\eta(M, m)\ \cos^2(\tfrac{1}{2}\theta') \tag{1–83}$$

with $\eta(M, m)$ defined by equation (1–79).

It should be noted that the kinematics of equation (1–65) can be applied to isobar decay as well as to the weak and electromagnetic decays of the various particles. Thus, we can make a distinction between the three-body final state in a reaction such as

$$p + p \rightarrow p + \Lambda + K^+ \tag{1–84}$$

and the double two-body kinematics problem posed by a reaction such as

$$p + p \rightarrow p + N^{*+} \tag{1–85}$$

followed by

$$N^{*+} \rightarrow \Lambda + K^+ \tag{1–86}$$

Clearly, the kinematics of reaction (1–86) is more restrained than is that of reaction (1–85), even though the mass of N^* has an associated uncertainty $\hbar/\tau_d$, where τ_d is the decay time of the isobar and $\hbar$ is Planck's constant divided by 2π.

1-5 THE EVALUATION OF THE SOURCE FUNCTIONS DUE TO VARIOUS DECAY MODES

1-5a The Decay Mode $\pi^0 \rightarrow 2\gamma$

Equation (1–80) can be used to write an expression for the energy of a γ-ray produced by the decay $\pi^0 \rightarrow 2\gamma$. This energy is then given by

$$E_\gamma = \tfrac{1}{2} m_\pi \gamma_\pi (1 + \beta_\pi \cos \theta') \tag{1–87}$$

Equation (1–71) reduces to give the γ-ray energy-distribution function. This result, together with the limits implied by equation (1–87), yields the Green's function for the decay $f_{ds}(E_\gamma | E_s)$ of equation (1–14). The result is

$$f(E_\gamma | E_\pi) = \begin{cases} (E_\pi^2 - m_\pi^2)^{-1/2} & \text{for } \tfrac{1}{2} E_\pi (1 - \beta_\pi) \leq E_\gamma \leq \tfrac{1}{2} E_\pi (1 + \beta_\pi) \\ 0 & \text{otherwise} \end{cases} \tag{1–88}$$

We note also that, for the neutral-pion decay,

$$R_{\gamma,\, \pi^0 \rightarrow 2\gamma} \simeq 1 \tag{1–89}$$

and

$$\zeta_{\gamma,\, \pi^0 \rightarrow 2\gamma} = 2 \tag{1–90}$$

Thus, the contribution of neutral-pion decay to the source function of equation (1–10) reduces to

$$q(E_\gamma, \mathbf{r}) = 4\pi n(\mathbf{r}) \int dE_p \, I(E_p, \mathbf{r}) \int_{E_{\pi,\,\min}}^{E_{\pi,\,\max}} dE_\pi \, \sigma(E_\pi | E_p) \cdot 2 \cdot 1 \cdot (E_\pi^2 - m_\pi^2)^{-1/2} \tag{1–91}$$

where the limits $E_{\pi,\max}$ and $E_{\pi,\min}$ can be found from the following considerations.

The quantity $E_{\pi,\max}$ is the maximum energy that a pion can have and still produce a γ-ray of energy E_γ. We note that as $E \rightarrow \infty$ the ultra-relativistic form of the pion/γ-ray energy relation given by equation (1–81) becomes valid, so that

$$E_{\pi,\,\max} = \frac{E_\gamma}{[\cos^2 (\tfrac{1}{2}\theta')]_{\min}} \rightarrow \infty \tag{1–92}$$

since

$$[\cos^2 (\tfrac{1}{2}\theta')]_{\min} = 0$$

From conservation of energy, we note that, for the two γ-rays produced in the decay,

$$E_\pi = E_{\gamma,a} + E_{\gamma,b} \tag{1-93}$$

In the extreme case where the γ-rays are emitted in the direction of motion, $\cos\theta' = 1, -1$,

$$E_{\gamma,\min} = \tfrac{1}{2}E_\pi(1-\beta_\pi) \tag{1-94}$$

and

$$E_{\gamma,\max} = \tfrac{1}{2}E_\pi(1+\beta_\pi) \tag{1-95}$$

Thus, corresponding to the highest energy $E_{\gamma,\max}$ that can be emitted by a pion of energy E_π, a γ-ray of energy $E_{\gamma,\min}$ is also emitted such that

$$E_{\gamma,\max} + E_{\gamma,\min} = \tfrac{1}{2}E_\pi(1+\beta_\pi) + \tfrac{1}{2}E_\pi(1-\beta_\pi) = E_\pi \tag{1-96}$$

We can use equations (1–94) and (1–95) to express $E_{\gamma,\min}$ in terms of $E_{\gamma,\max}$ by noting that

$$(E_{\gamma,\min})(E_{\gamma,\max}) = \tfrac{1}{4}E_\pi^2(1-\beta_\pi^2) = \tfrac{1}{4}m_\pi^2 \tag{1-97}$$

so that

$$E_\pi = E_{\gamma,\max} + E_{\gamma,\min} = E_{\gamma,\max} + \frac{m_\pi^2}{4E_{\gamma,\max}} \tag{1-98}$$

This criterion can then be reversed to put a lower limit on the pion energy integration by writing equation (1–98) as

$$E_{\pi,\min} = E_\gamma + \frac{m_\pi^2}{4E_\gamma} \tag{1-99}$$

where $E_{\pi,\min}$ is now the minimum energy that a pion needs to produce a γ-ray of energy E_γ. Thus, equation (1–91) reduces to

$$q_{\pi^0}(E_\gamma, \mathbf{r}) = 8\pi n(\mathbf{r}) \int dE_p I(E_p, \mathbf{r}) \int_{E_\gamma + m_\pi^2/4E_\gamma}^{\infty} dE_\pi \frac{\sigma(E_\pi|E_p)}{(E_\pi^2 - m_\pi^2)^{1/2}} \tag{1-100}$$

1–5b The Decay Mode $\Sigma^0 \rightarrow \Lambda + \gamma$

The energy distribution function and energy transformation equation for the Σ^0 decay are given by equations (1–71) and (1–79) as follows:

$$E_\gamma = E_{\Sigma^0}\,\eta(\Sigma^0, \Lambda)(1+\beta_\Sigma \cos\theta') \tag{1-101}$$

and

$$f(E_\gamma|E_{\Sigma^0})\,dE_\gamma = \frac{dE_\gamma}{2E_{\Sigma^0}\beta_{\Sigma^0}\eta(\Sigma^0,\,\Lambda)} \tag{1–102}$$

where

$$\eta(\Sigma^0,\,\Lambda) = \frac{m_{\Sigma^0}^2 - m_\Lambda^2}{2m_{\Sigma^0}^2} \tag{1–103}$$

The evaluation of the source function for the Σ^0 decay can then be made in a manner similar to that used for the π^0 decay. For the Σ^0 decay, we have

$$R_{\gamma,\,\Sigma^0\to\Lambda+\gamma} \simeq 1 \tag{1–104}$$

and

$$\zeta_{\gamma,\,\Sigma^0\to\Lambda+\gamma} = 1 \tag{1–105}$$

The distribution function $f(E_\gamma|E_{\Sigma^0})$ is then written explicitly in terms of E_Σ as

$$f(E_\gamma|E_{\Sigma^0}) = \begin{cases} \dfrac{1}{2\eta(\Sigma^0,\,\Lambda)\,(E_\Sigma^2 - m_\Sigma^2)^{1/2}} & \\ & \text{for } E_{\Sigma^0}\eta(1-\beta_{\Sigma^0}) \leqslant E_\gamma \leqslant E_{\Sigma_0}\eta(1-\beta_{\Sigma^0}) \\ 0 & \text{otherwise} \end{cases} \tag{1–106}$$

Thus, equation (1–10) reduces to

$$q_{\Sigma^0}(E_\gamma,\,\mathbf{r}) = \frac{2\pi}{\eta(\Sigma^0,\,\Lambda)}\,n(\mathbf{r}) \int dE_p\, I(E_p,\,\mathbf{r}) \int_{E_{\Sigma,\,\min}}^{E_{\Sigma,\,\max}} dE_\Sigma\, \frac{\sigma(E_\Sigma|E_p)}{(E_\Sigma^2 - m_\Sigma^2)^{1/2}} \tag{1–107}$$

where the limits $E_{\Sigma,\,\max}$ and $E_{\Sigma,\,\min}$ are deduced from equation (1–101). By analogy with equations (1–97) and (1–98), we find for the case of Σ^0 decay

$$(E_{\gamma,\,\min})\,(E_{\gamma,\,\max}) = E_\Sigma^2\eta^2(1-\beta_{\Sigma^0}^2) = \eta^2 m_\Sigma^2 = \mu^2 \tag{1–108}$$

where μ, as before, is the cms energy of the γ-ray. From equation (1–101), we find

$$E_{\Sigma,\,\max} = \frac{E_\gamma}{\eta(1-\beta_\Sigma)} \to \infty \qquad \text{as } \beta_\Sigma \to 1 \tag{1–109}$$

and

$$E_{\Sigma,\,\min} = \frac{E_\gamma}{\eta(1+\beta_\Sigma)} \to \frac{E_\gamma}{2\eta} \qquad \text{as } \beta_\Sigma \to 1 \tag{1–110}$$

We will later show that the case $\beta_\Sigma \to 1$ is the only one of importance to cosmic γ-ray production from Σ^0 decay. Thus, the source function for the production of cosmic γ-rays through the decay of secondary Σ^0 particles produced in high-energy cosmic p–p collisions is given by

$$q_{\Sigma^0}(E_\gamma, \mathbf{r}) = \frac{2\pi}{\eta(\Sigma^0, \Lambda)} n(\mathbf{r}) \int dE_p \, I(E_p, \mathbf{r}) \int_{\frac{E_\gamma}{2\overline{\eta}}}^{\infty} dE_\Sigma \frac{\sigma(E_\Sigma|E_p)}{(E_\Sigma^2 - m_\Sigma^2)^{1/2}} \tag{1-111}$$

where $M_\Sigma = 1.192$ GeV and $\mu = 7.466 \times 10^{-2}$ GeV, so $\eta^{-1} = 15.96$.

1–5c The Decay Mode $K_1^0 \to 2\pi^0 \to 4\gamma$

For this two-step process, we must express the Green's function, $f_{K_1^0 \to 4\gamma}(E_\gamma|E_K)$ in the form

$$f_{K_1^0 \to 4\gamma}(E_\gamma|E_K) = \int dE_{\pi^0} f_{\pi^0 \to 2\gamma}(E_\gamma|E_{\pi^0}) \, f_{K_1^0 \to 2\pi^0}(E_{\pi^0}|E_K) \tag{1-112}$$

where, as we have already shown (eq. (1–88)),

$$f_{\pi^0 \to 2\gamma}(E_\gamma|E_{\pi^0}) = \frac{1}{(E_\pi^2 - m_\pi^2)^{1/2}} \qquad \text{for } \tfrac{1}{2}E_\pi(1-\beta_\pi) \leq E_\gamma \leq \tfrac{1}{2}E_\pi(1+\beta_\pi)$$

$$= 0 \qquad \text{otherwise} \tag{1-113}$$

The function $f_{K_1^0 \to 2\pi^0}(E_\pi|E_K)$ can be derived from equations (1–71) and (1–73). Since the decay is isotropic in the cms, we have

$$f_{K_1^0 \to 2\pi^0}(E_\pi|E_K) = \tfrac{1}{2}\Delta_K^{-1} \qquad \text{for } \tfrac{1}{2}E_K - \Delta_K \leq E_\pi \leq \tfrac{1}{2}E_K + \Delta_K$$

$$= 0 \qquad \text{otherwise} \tag{1-114}$$

where Δ_K is the half-width of the square distribution function. From equation (1–75), we have

$$\Delta_K = \left[\left(\frac{E_K^2}{m_K^2} - 1\right)\left(\frac{m_K^2}{4} - m_\pi^2\right)\right]^{1/2} \tag{1-115}$$

Figure 1–4 schematically illustrates the relationships between E_{K^0}, E_{π^0}, and E_γ for the decay mode $K_1^0 \to 2\pi^0 \to 4\gamma$.

Referring to figure 1–4, we see that a neutral kaon of energy E_K (point A on the E_{K^0} scale) will decay to produce two neutral pions having

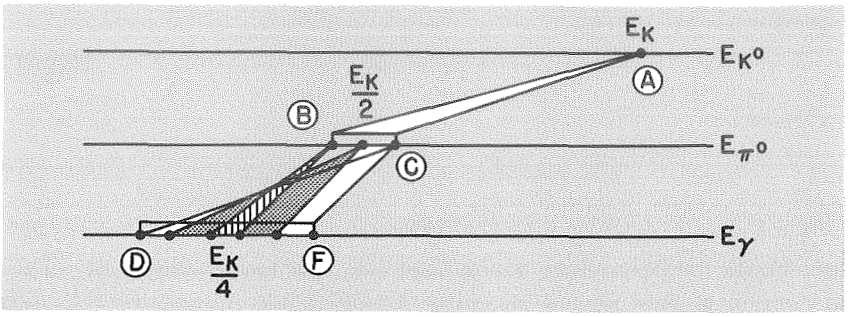

FIGURE 1–4. — The relationships between E_{K^0}, E_{π^0}, and E_γ for the decay mode $K_1^0 \rightarrow 2\pi^0 \rightarrow 4\gamma$.

energies in the range between B and C (when it decays via the K_1^0 mode), where

$$E_\pi(B) = \tfrac{1}{2}E_K - \Delta_K \tag{1–116}$$

and

$$E_\pi(C) = \tfrac{1}{2}E_K + \Delta_K \tag{1–117}$$

The resultant γ-rays have energies on the E_γ scale that lie between points D and F, such that

$$E_\gamma(D) = \frac{1}{2}\left(\frac{E_K}{2} + \Delta_K\right) - \Delta_\pi(C) \tag{1–118}$$

and

$$E_\gamma(F) = \frac{1}{2}\left(\frac{E_K}{2} + \Delta_K\right) + \Delta_\pi(C) \tag{1–119}$$

We have already found from equation (1–99) that

$$E_{\pi,\,\min} = E_\gamma + \frac{m_\pi^2}{4E_\gamma}$$

Now we must determine the minimum energy that the K_1^0 meson state needs to produce a neutral pion of energy E_π. If we define[2]

$$\kappa \equiv \left(1 - \frac{4m_\pi^2}{m_K^2}\right)^{1/2} \simeq 0.840 \tag{1–120}$$

[2] Note important difference with equation (1–69). From equation (1–120) on, $\kappa \equiv 2p'/M$.

equation (1–115) yields

$$\Delta_K = \tfrac{1}{2} E_K \beta \kappa \tag{1–121}$$

followed by

$$(E_{\pi,\,\max})(E_{\pi,\,\min}) = \tfrac{1}{4} E_K^2 (1 - \kappa^2 \beta_K^2) \tag{1–122}$$

We can see that equation (1–122) is analogous to equation (1–97) and would further reduce to the limit $\frac{1}{4} m_K^2$ if κ approached unity. This, of course, is as it should be, since a value for κ of unity would imply a decay into massless particles. Thus, equation (1–122) is a generalization of equation (1–97) for the case of decay into two particles having finite and equal masses. We also note from equation (1–121) that a value of zero for κ implies a monoenergetic spectrum of neutral pions, in agreement with our previous discussion of equation (1–75).

Using equations (1–42) and (1–49), we find

$$E_K = \left(\frac{m_K^2}{2m_\pi^2}\right)(1 + \beta_\pi \kappa \cos \theta') E_\pi \tag{1–123}$$

and therefore kaons capable of producing pions of energy E_π are restricted to the energy range

$$\left(\frac{m_K^2}{2m_\pi^2}\right)(1 - \beta_\pi \kappa) E_\pi \leq E_K \leq \left(\frac{m_K^2}{2m_\pi^2}\right)(1 + \beta_\pi \kappa) E_\pi \tag{1–124}$$

In the nonrelativistic and extreme relativistic cases, where $\beta_K \ll 1$ and $\beta_K \simeq 1$, we can use equations (1–115) and (1–116) to determine the limits on the range of kaons of energy E_K which contribute pions of energy E_π as

$$E_K \simeq 2E_\pi \qquad \text{for } \beta_K \ll 1 \tag{1–125}$$

and

$$E_{K,\,\max} \simeq 12.8\, E_\pi \tag{1–126}$$

$$E_{K,\,\min} \simeq 1.09\, E_\pi \tag{1–127}$$

for $\beta_K \simeq \beta_\pi \simeq 1$.

Finally, for the decay mode $K_1^0 \rightarrow 4\gamma$ we have

$$R_{K_1^0 \rightarrow 4\gamma} \simeq 0.156 \tag{1–128}$$

and

$$\zeta_{K_1^0 \rightarrow 4\gamma} = 4 \tag{1–129}$$

We can thus reduce equation (1–10) in this case to obtain the source function

$$q_{K_1^0}(E_\gamma, \mathbf{r}) = 3.11\pi n(\mathbf{r}) \int dE_p\, I(E_p, \mathbf{r}) \int_{E_\gamma + (m_\pi^2/4E_\gamma)}^{\infty} \frac{dE_\pi}{(E_\pi^2 - m_\pi^2)^{1/2}}$$

$$\times \int_{(6.89-5.78\beta_\pi)E_\pi}^{(6.89+5.78\beta_\pi)E_\pi} \frac{dE_K \sigma(E_{K^0}|E_p)}{(E_{K^0}^2 - m_{K^0}^2)^{1/2}} \quad (1\text{–}130)$$

since

$$\sigma(E_{K_1^0}|E_p) = \tfrac{1}{2}\sigma(E_{K^0}|E_p) \quad (1\text{–}131)$$

1–5d The Decay Mode $K^\pm \to \pi^\pm + \pi^0 \to \pi^\pm + 2\gamma$

The kinematics for this decay are exactly the same as for the decay $K_1^0 \to 2\pi^0 \to 4\gamma$. If we neglect the small difference between the kinetic energies released in the above decays ($Q_{K^0} = 228.0$ MeV, $Q_{K^\pm} = 219.2$ MeV), the only significant difference for our purposes is that the $K^\pm$ two-body decay produces only half as many γ-rays as the $K_1^0 \to 4\gamma$ decay. The relevant numerical quantities are

$$\kappa \simeq 0.84 \quad (1\text{–}132)$$

$$R \simeq 0.215 \quad (1\text{–}133)$$

$$\zeta = 2 \quad (1\text{–}134)$$

for

$$K^\pm \to \pi^\pm + \pi^0$$

(See eqs. (1–120), (1–128), and (1–129).) The expression for the source functions from $K^\pm$ decay is then similar in form to equation (1–130) and is given by

$$q_{K^\pm}(E_\gamma, \mathbf{r}) = 2.15\pi n(\mathbf{r}) \int dE_p\, I(E_p, \mathbf{r})$$

$$\times \int_{E_\gamma + (m_\pi^2/4E_\gamma)}^{\infty} \frac{dE_p}{(E_\pi^2 - m_\pi^2)^{1/2}} \int_{(6.78-5.69\beta_\pi)E_\pi}^{(6.78+5.69\beta_\pi)E_\pi} \frac{dE_K \sigma(E_{K^\pm}|E_p)}{(E_{K^\pm}^2 - m_{K^\pm}^2)^{1/2}} \quad (1\text{–}135)$$

1–5e The Decay Mode $\Lambda \to n + \pi^0$ for Unpolarized Λ Particles

The energy-distribution function and energy-transformation equation for unpolarized $\Lambda \to n + \pi^0$ decay are given by equations (1–65) and (1–71) as follows:

$$f_{\Lambda \to n+\pi^0}(E_\pi|E_\Lambda) = \frac{1}{2\Delta_K} \qquad \text{for } E_\Lambda \eta(\Lambda, \pi^0) - \Delta_{\Lambda\pi^0} \leq E_\pi \leq E_\Lambda \eta(\Lambda, \pi^0) + \Delta_{\Lambda\pi^0}$$

$$0 \qquad \text{otherwise} \quad (1\text{–}136)$$

and

$$E_\pi = E_\Lambda \eta(\Lambda, \pi^0) + \Delta_{\Lambda\pi^0} \cos\theta' \tag{1-137}$$

where

$$\eta(\Lambda, \pi^0) = \frac{m_\Lambda^2 + m_\pi^2 - m_n^2}{2m_\Lambda^2} \simeq 0.152 \tag{1-138}$$

$$\Delta_{\Lambda\pi^0} = \tfrac{1}{2} E_\Lambda \beta \kappa_{\Lambda,\pi^0} \tag{1-139}$$

and

$$\kappa_{\Lambda\pi^0} = \frac{2p'}{m_\Lambda} \tag{1-140}$$

and p' being given implicitly by

$$(m_\pi^2 + p'^2)^{1/2} + (m_n^2 + p'^2)^{1/2} = m_\Lambda \tag{1-141}$$

Noting that

$$\left.\begin{aligned} m_\Lambda &\simeq 1115.44 \text{ MeV} \\ m_n &\simeq 939.55 \text{ MeV} \end{aligned}\right\} \tag{1-142}$$

and

$$m_{\pi^0} \simeq 134.97 \text{ MeV}$$

we find from equation (1–141) that

$$p' \simeq 103.6 \qquad \text{MeV}/c \tag{1-143}$$

and

$$\kappa_{\Lambda\pi} \simeq 0.186$$

Thus, we obtain

$$f_{\Lambda\to n+\pi^0}(E_\pi | E_\Lambda) = \frac{5.38}{(E_\Lambda^2 - m_\Lambda^2)^{1/2}} \tag{1-144}$$

Using the same techniques used to derive equation (1–124), we can now find the limits on the E_Λ distribution.

From equations (1–42) and (1–49), we obtain

$$\gamma_\Lambda = \gamma_\pi \gamma'_\pi (1 + \beta_\pi \beta'_\pi \cos\theta') \tag{1-145}$$

or

$$E_\Lambda = E_\pi E'_\pi \left(\frac{m_\Lambda}{m_\pi^2}\right)^2 (1 + \beta_\pi \beta'_\pi \cos\theta') = \left(\frac{m_\Lambda}{m_\pi^2}\right)(E'_\pi + \beta_\pi p'_\pi \cos\theta') E_\pi \tag{1-146}$$

By using equations (1–138) and (1–140), we may further reduce equation (1–146) to the form

$$E_\Lambda = \left(\frac{m_\Lambda}{m_\pi}\right)^2 \left[\eta(\Lambda, \pi^0) + \beta_\pi \frac{\kappa(\Lambda, \pi^0)}{2} \cos\theta'\right] E_\pi \qquad (1\text{–}147)$$

so that

$$\left(\frac{m_\Lambda}{m_\pi}\right)^2 \left(\eta - \beta_\pi \frac{\kappa}{2}\right) E_\pi \leq E_\Lambda \leq \left(\frac{m_\Lambda}{m_\pi}\right)^2 \left(\eta + \beta_\pi \frac{\kappa}{2}\right) E_\pi \qquad (1\text{–}148)$$

Using the numerical values given in equations (1–138) and (1–143), we then find

$$(10.52 - 6.44\beta_\pi) E_\pi \leq E_\Lambda \leq (10.52 + 6.44\beta_\pi) E_\pi \qquad (1\text{–}149)$$

Equation (1–147) is analogous to equation (1–123) and reduces to equation (1–123) for the case of decay into two particles of equal mass, where $\eta = 1/2$. The nonrelativistic and extreme relativistic limits of equation (1–137) for the parent Λ yield

$$E_\Lambda = 6.58 E_\pi \qquad \text{for } \beta_\Lambda \ll 1 \qquad (1\text{–}150)$$

and

$$\left.\begin{aligned} E_{\Lambda,\,\max} &= 16.96 E_\pi \\ E_{\Lambda,\,\min} &= 4.08 E_\pi \end{aligned}\right\} \qquad \text{for } \beta_\pi \simeq \beta_\Lambda \simeq 1 \qquad (1\text{–}151)$$

Noting that

$$R_{\Lambda \to n + \pi^0} \simeq 0.331$$

and

$$\zeta_{\gamma,\,\Lambda \to n + \pi^0} = 2 \qquad (1\text{–}152)$$

we can reduce equation (1–10) to yield the source function

$$q_\Lambda(E_\gamma, \mathbf{r}) = 44.9 n(\mathbf{r}) \int dE_p\, I(E_p, \mathbf{r}) \int_{E_\gamma + m_\pi^2/4E_\gamma}^{\infty} \frac{dE_\pi}{(E_\pi^2 - m_\pi^2)^{1/2}} \times \int_{(10.52 - 6.44\beta_\pi)E_\pi}^{(10.52 + 6.44\beta_\pi)E_\pi} \frac{dE_\Lambda \sigma(E_\Lambda | E_p)}{(E_\Lambda^2 - m_\Lambda^2)^{1/2}} \qquad (1\text{–}153)$$

In equation (1–153) we have used the double Green's function reduction

$$f_{\Lambda \to n + 2\gamma}(E_\gamma | E_\Lambda) = \int dE_\pi f_{\pi^0 \to 2\gamma}(E_\gamma | E_\pi) f_{\Lambda \to n + \pi^0}(E_\pi | E_\Lambda) \qquad (1\text{–}154)$$

1-5f The Decay Mode $\Sigma^+ \to p + \pi^0$ for Unpolarized Σ^+ Particles

The kinematics of this decay are exactly the same as those for the $\Lambda \to n + \pi^0$ decay; only the numerical values for the masses involved

are different. For this decay we have

$$m_{\Sigma^+} \simeq 1189.4 \text{ MeV}$$

and

$$m_p \simeq 938.26 \text{ MeV} \tag{1-155}$$

so that

$$\eta \simeq 0.195$$

$$p' \simeq 189.03 \text{ MeV}/c$$

and

$$\kappa \simeq 0.318$$

We also have, for this decay,

$$R_{\Sigma^+ \to p+\pi^0} \simeq 0.510$$

and

$$\zeta_{\gamma,\, \Sigma^+ \to p+\pi^0} \approx 2 \tag{1-156}$$

so that

$$q_{\Sigma^+}(E_\gamma, \mathbf{r}) = 40.3n(\mathbf{r}) \int dE_p\, I(E_p, \mathbf{r}) \int_{E_\gamma + (m_\pi/4E_\gamma)}^{\infty} \frac{dE_\pi}{(E_\pi^2 - m_\pi^2)^{1/2}}$$

$$\times \int_{(15.32-12.50\beta_\pi)E_\pi}^{(15.32+12.50\beta_\pi)E_\pi} \frac{dE_{\Sigma^+}\sigma(E_{\Sigma^+}|E_p)}{(E_{\Sigma^+}^2 - m_{\Sigma^+}^2)^{1/2}} \tag{1-157}$$

where

$$E_{\Sigma^+,\,\min} = 5.13E_\pi \qquad \text{for } \beta_{\Sigma^+} \ll 1 \tag{1-158}$$

and

$$E_{\Sigma^+,\,\min} = 2.82E_\pi \qquad \text{for } \beta_{\Sigma^+} \simeq 1 \tag{1-159}$$

1-5g The Three-Body Decay Modes $K_2^0 \to 3\pi^0$ and $K_2^0 \to \pi^+ + \pi^- + \pi^0$

We will treat these three-body decay modes by using the approximation $m_{\pi^\pm} \simeq m_{\pi^0} \equiv m_\pi$. We will also make use of the empirical fact that the K_2^0 mode is that of a spinless particle that decays isotropically into an S state.

The energy distribution function for the decay is given implicitly by

$$w = \frac{2\pi}{\hbar} M^2\, d^3 \left(\frac{dN}{dQ}\right) \tag{1-160}$$

where w is the decay rate into the three-differential energy region specified by the energies of the three particles formed in the decay, and dN/dQ is the density, in energy space, of the final states of the decay, with each degenerate state counted separately.

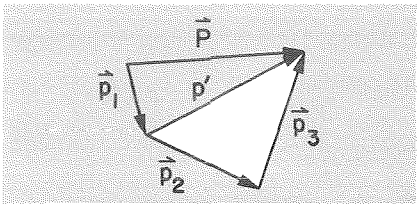

FIGURE 1–5.—The momentum vectors used in the derivation of equation (1–176).

The quantity M is the matrix element for the transition from the K_2^0 state to the 3π state and is of the form

$$M = \langle 3\pi | K_2^0 \rangle = (\text{spin and parity part}) \int d\tau_1 \, d\tau_2 \, d\tau_3 e^{i\epsilon_1 t} \, e^{i\epsilon_2 t} \, e^{i\epsilon_3 t} \cdots \propto (\epsilon_1 \epsilon_2 \epsilon_3)^{-1/2} \qquad (1\text{–}161)$$

where $d\tau$ represents an element of space-time volume, the subscripts denote the three decay pions, and the ϵ's denote the energies of each of the three pions. Thus,

$$M^2 \propto \frac{1}{\epsilon_1 \epsilon_2 \epsilon_3} \qquad (1\text{–}162)$$

We define

$$E = \epsilon_1 + \epsilon_2 + \epsilon_3 \qquad (1\text{–}163)$$

and

$$\mathbf{P} = \mathbf{p}_1 + \mathbf{p}_2 + \mathbf{p}_3 \qquad (1\text{–}164)$$

in order to derive the phase-space part of equation (1–160). The derivation given here is essentially that given by Williams (1961). First, $\mathbf{p}_1$ is specified, leaving $\mathbf{p}'$ and ϵ' to be distributed among particles 2 and 3 as shown in figure 1–5. Then the phase-space volume for particles 2 and 3 is given by

$$U' = \int d\Omega_2 \int_0^{p_2(\theta_2)} p_2^2 \, dp_2 \qquad (1\text{–}165)$$

where $p_2(\theta_2)$ is the maximum momentum of particle 2 in direction θ_2. The remaining integration over particle 1 is given by

$$U = \int d\Omega_1 \int_0^{p_1(\theta_1)} p_1^2 \, dp_1 U' \qquad (1\text{–}166)$$

so that

$$N = \frac{V^2}{h^6} U = \frac{V^2}{h^6} \int d\Omega_1 \int_0^{p_1(\theta_1)} p_1^2 \, dp_1 \int d\Omega_2 \int_0^{p_2(\theta_2)} p_2^2 \, dp_2 \qquad (1\text{–}167)$$

and

$$d^3\left(\frac{dN}{dQ}\right) = d^3\left(\frac{dN}{dE}\right)_Q = \frac{d}{dE}\left\{\frac{V^2}{\hbar^6}\, d\Omega_1\, d\Omega_2\, p_1^2\, dp_1 \int_0^{p_2(\theta_2)} p_2^2\, dp_2\right\} \tag{1-168}$$

Letting p_2 be the independent momentum variable, we can write

$$\frac{dN}{dE} = \frac{dN}{dp_2}\frac{dp_2}{dE} \tag{1-169}$$

where

$$\frac{dE}{dp_2} = \frac{d\epsilon_1}{dp_2} + \frac{d\epsilon_2}{dp_2} + \frac{d\epsilon_3}{dp_2} \tag{1-170}$$

Now, ϵ_1 is fixed, so $d\epsilon_1/dp_2 = 0$. We also note that

$$\epsilon_{2,3}^2 = p_{2,3}^2 + m_\pi^2 \tag{1-171}$$

so that

$$\epsilon_{2,3}\, d\epsilon_{2,3} = p_{2,3}\, dp_{2,3} \tag{1-172}$$

or

$$\frac{d\epsilon_{2,3}}{dp_{2,3}} = \frac{p_{2,3}}{\epsilon_{2,3}} \tag{1-173}$$

Thus, from equations (1-170) and (1-173) we find

$$\frac{dE}{dp_2} = \frac{p_2}{\epsilon_2} + \frac{p_3}{\epsilon_3}\frac{dp_3}{dp_2} \tag{1-174}$$

Since $\mathbf{p}_1$ is fixed, and since fixing θ_2 merely specifies a coordinate axis, we have

$$\left(\frac{dp_3}{dp_2}\right)_{p_1} = -\cos\,\theta_{2,3} = -\frac{\mathbf{p}_2 \cdot \mathbf{p}_3}{p_2 p_3} \tag{1-175}$$

whereupon, by combining equations (1-168), (1-169), (1-174), and (1-175), we obtain the result

$$d^3\left(\frac{dN}{dE}\right) = \frac{V^2}{\hbar^6}\frac{\epsilon_2\epsilon_3 p_1^2 p_2^3\, d\Omega_1\, d\Omega_2\, dp_1}{p_2^2(E-\epsilon_1) - \epsilon_2 \mathbf{p}_2 \cdot (\mathbf{P}-\mathbf{p}_1)} \tag{1-176}$$

Referring to figure 1-6, we can write

$$p_3^2 = p_1^2 + p_2^2 + 2p_1p_2\cos\,\theta \tag{1-177}$$

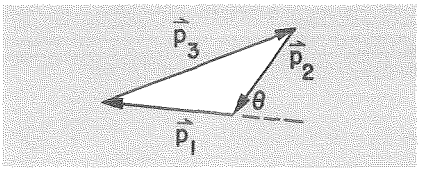

FIGURE 1–6.—The momentum vectors used in the derivation of equation (1–184).

so that

$$\mathbf{p}_2 \cdot (\mathbf{P} - \mathbf{p}_1) = \mathbf{p}_2 \cdot (\mathbf{p}_2 + \mathbf{p}_3) = p_2^2 + \mathbf{p}_2 \cdot \mathbf{p}_3 = \tfrac{1}{2}(p_1^2 - p_2^2 - p_3^2) + p_2^2 = p_1 p_2 \cos\theta \qquad (1\text{–}178)$$

Substituting equation (1–178) into equation (1–176), we obtain

$$d^3\left(\frac{dN}{dE}\right) = \frac{V^2}{\hbar^6} \frac{\epsilon_1 \epsilon_2 \epsilon_3 p_1 p_2^3 \, d\Omega_1 \, d\Omega_2 \, d\epsilon_1}{p_2^2(\epsilon_2 + \epsilon_3) + \epsilon_2 p_1 p_2 \cos\theta} \qquad (1\text{–}179)$$

The integration over the arbitrary $d\Omega_1$ yields 4π. We can write $d\Omega_2$ in the form

$$d\Omega_2 = 2\pi \, d(\cos\theta) \qquad (1\text{–}180)$$

For a specified ϵ_1, we have

$$d\epsilon_2 + d\epsilon_3 = 0 \qquad (1\text{–}181)$$

Using equation (1–181) in combination with equation (1–177), we obtain

$$-\epsilon_3 \, d\epsilon_2 = \epsilon_2 \, d\epsilon_2 + \frac{p_1 \epsilon_2}{p_2} \cos\theta \, d\epsilon_2 + p_1 p_2 \, d(\cos\theta) \qquad (1\text{–}182)$$

Thus,

$$-p_1 p_2^2 \, d(\cos\theta) = [p_2(\epsilon_1 + \epsilon_3) + \epsilon_2 p_1 \cos\theta] \, d\epsilon_2 \qquad (1\text{–}183)$$

whereupon equation (1–179) reduces to

$$d^2\left(\frac{dN}{dE}\right) = \frac{8\pi^2 V^2}{h^6} \epsilon_1 \epsilon_2 \epsilon_3 \, d\epsilon_1 \, d\epsilon_2 \qquad (1\text{–}184)$$

with the use of equation (1–183).

Substituting equations (1–184) and (1–163) into equation (1–160), we find

$$w \propto d\epsilon_1 \, d\epsilon_2 \propto dt_1 \, dt_2 \qquad (1\text{–}185)$$

where t_1 and t_2 are the kinetic energies of particles 1 and 2, respectively.

Because of the three-way symmetry of the kinetic relations in the problem of the decay into three particles of equal (or approximately equal) mass, equation (1–185) can be better expressed in the form

$$w \propto dt_i\, dt_k \qquad (i \neq k,\ i, k = 1, 2, 3) \tag{1–186}$$

This fact prompted Dalitz (1953) to introduce a plot of particle decays into a triangular energy space as shown in figure 1–7.

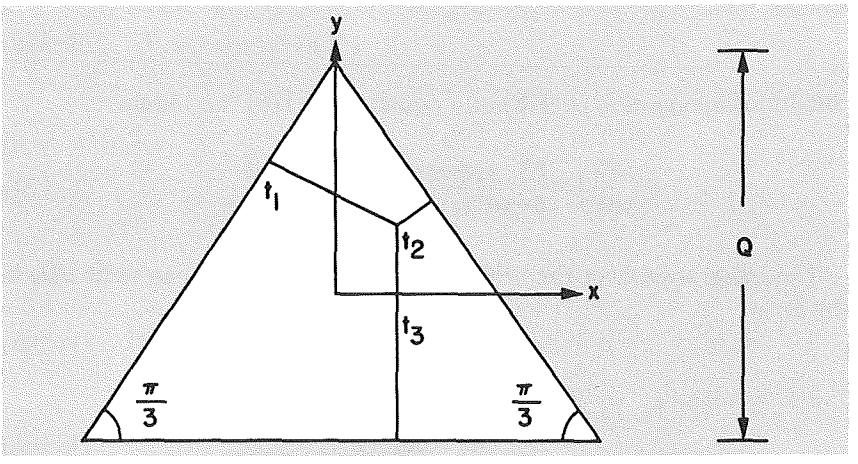

FIGURE 1–7.—The Dalitz triangle.

In this plot, the perpendicular distances from each side are proportional to the kinetic energies t_i of each of the decaying particles. The geometry of the triangle insures that $\Sigma t_i = Q$, Q being the total kinetic energy, $m_K - 3m_\pi$, released in the decay. From figure 1–7, we can see that

$$x = \frac{t_2 - t_1}{3^{1/2} Q}$$

and

$$y = \frac{Q - t_3}{3Q} \tag{1–187}$$

in units normalized to Q, so that a uniformity in $dt_i\, dt_k$ corresponds to a uniformity in $dx\, dy$. Thus, the uniform distribution of the decay points on the Dalitz plot, which is obtained experimentally, indicates a constancy in the matrix element M of equation (1–160) for the case of K_2^0 decay.

A more symmetric coordinate system for the Dalitz plot is obtained

by transformation to polar coordinates. In the polar coordinate system (ρ, ϕ)

$$\epsilon_1 = \tfrac{1}{3} m_K [1 + A\rho \cos(\phi - \tfrac{2}{3}\pi)]$$

$$\epsilon_2 = \tfrac{1}{3} m_K [1 + A\rho \cos(\phi + \tfrac{2}{3}\pi)] \qquad (1\text{–}188)$$

and

$$\epsilon_3 = \tfrac{1}{3} m_K (1 + A\rho \cos\phi)$$

where $A = Q/m_K$ (Fabri, 1954).

The condition of conservation of momentum further restricts the allowed area in the Dalitz plot, since we have the triangular relations

$$p_1 \leqslant p_2 + p_3$$

$$p_2 \leqslant p_1 + p_3 \qquad (1\text{–}189)$$

and

$$p_3 \leqslant p_1 + p_2$$

where

$$p_{1,2,3}^2 = \epsilon_{1,2,3}^2 - m_\pi^2 \qquad (1\text{–}190)$$

The limiting case is specified by the collinear distribution of momenta, where the equalities hold. From equations (1–188), (1–189), and (1–190), it is found that the limiting curve is given by

$$\rho_{\max}^2 = \frac{\frac{Q^2}{9}}{1 + B(1 + \rho \cos 3\phi)} \qquad (1\text{–}191)$$

so that all points on the Dalitz plot with $\rho \leqslant \rho_{\max}$ are allowed. In equation (1–191)

$$B = \frac{\frac{1}{2}A}{(1 - \frac{1}{2}A)^2} \qquad (1\text{–}192)$$

The nonrelativistic limit of the limiting curve is obtained in the event that $A \to 0$, which implies $B \to 0$ and $\rho_{\max} \to Q/3$. Thus, the nonrelativistic limiting curve is a circle, as shown in figure 1–8.

Equation (1–191) indicates only a slight distortion of the circle when relativistic effects are taken into account, since

$$A \simeq 0.19 \qquad B \simeq 0.11 \qquad \text{for } K_2^0 \to 3\pi^0 \text{ decay}$$

and (1–193)

$$A \simeq 0.17 \qquad B \simeq 0.10 \qquad \text{for } K_2^0 \to \pi^+ + \pi^- + \pi^0 \text{ decay}$$

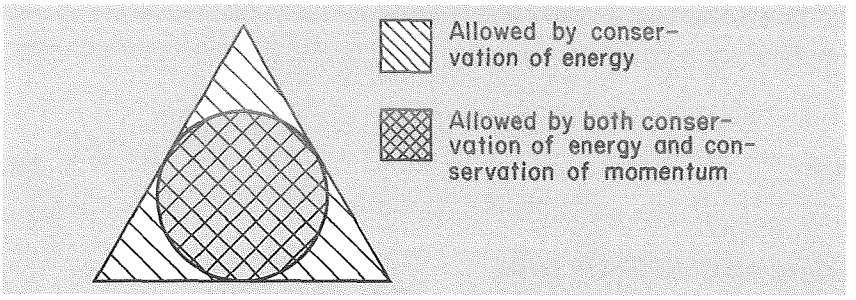

FIGURE 1–8.—Kinematic boundaries on the Dalitz triangle.

This small distortion will be further obliterated when the energy spectrum is spread out by transformation from the cms of the decay to the ls. Thus, we will find the nonrelativistic approximation quite adequate.

Referring to figure 1–9, we wish to find the energy distribution function $\Phi(\epsilon)$ for one of the particles; the results for the other two particles will be identical from symmetry considerations. Denoting this energy (in the cms of the kaon) as ϵ, we see from figure 1–9 that the probability for decay into the energy region between ϵ and $\epsilon + d\epsilon$ is proportional to the area in the rectangle. (There is uniformity within the circular area.) Thus,

$$\Phi(\epsilon)\ d\epsilon = K\lambda(\epsilon)\ d\epsilon \tag{1–194}$$

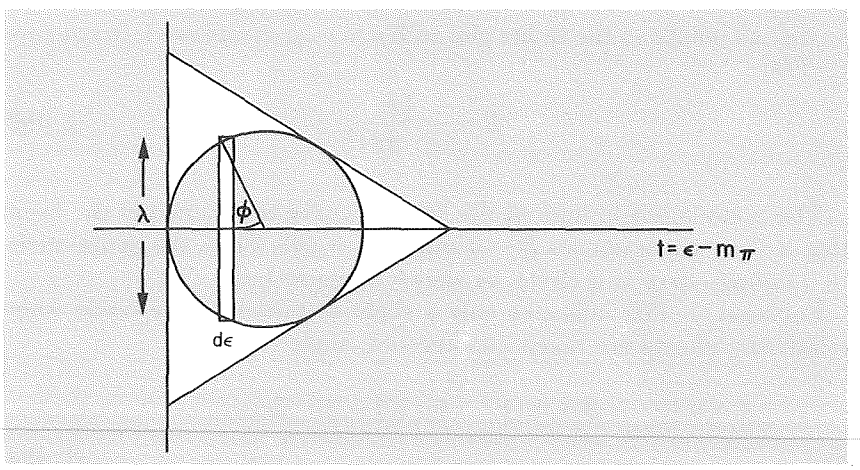

FIGURE 1–9.—The Dalitz diagram used in the derivation of equation (1–201).

where K is a normalization constant, such that

$$\int_{m_\pi}^{\epsilon_{max}} \Phi(\epsilon)\, d\epsilon = 1 = K \int_{m_\pi}^{\epsilon_{max}} \lambda(\epsilon)\, d\epsilon \qquad (1\text{–}195)$$

Referring to figure 1–9, we express λ and ϵ in terms of ϕ as

$$\lambda = \tfrac{2}{3} Q \sin \phi \qquad (1\text{–}196)$$

and

$$\epsilon - m_\pi = \tfrac{1}{3} Q (1 - \cos \phi) \qquad d\epsilon = \tfrac{1}{3} Q \sin \phi\, d\phi \qquad (1\text{–}197)$$

so that

$$K = \int_{m_\pi}^{\epsilon_{max}} \lambda\, d\epsilon = \int_0^\pi \frac{2Q^2}{9} \sin^2 \phi\, d\phi = \frac{Q^2}{9} \int_0^{2\pi} (1 - \cos^2 \phi)\, d\phi$$

$$= \pi \left(\frac{Q}{3}\right)^2 \qquad (1\text{–}198)$$

From equations (1–194) and (1–198), we find

$$\Phi(\epsilon)\, d\epsilon = \frac{1}{\pi (\frac{1}{3} Q)^2} \lambda(\epsilon)\, d\epsilon \qquad (1\text{–}199)$$

and, eliminating ϕ from equation (1–196) by using equation (1–197), we obtain

$$\lambda(\epsilon) = \frac{2}{3} Q \sin \left\{ 2 \left[\sin^{-1} \left(\frac{3}{2} \frac{\epsilon - m_\pi}{Q} \right)^{1/2} \right] \right\} \qquad (1\text{–}200)$$

so that

$$\Phi(\epsilon)\, d\epsilon = \frac{6}{\pi Q} \sin \left\{ 2 \left[\sin^{-1} \left(\frac{3}{2} \frac{\epsilon - m_\pi}{Q} \right)^{1/2} \right] \right\} d\epsilon \qquad (1\text{–}201)$$

Figure 1–10 shows $\Phi(\epsilon)$.

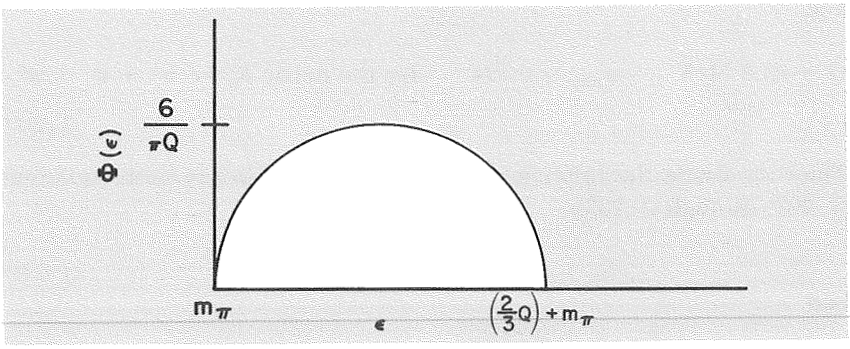

FIGURE 1–10.—The cms energy distribution function for pions formed in K_2^0 decay.

In the transformation to the ls,

$$E_\pi = \gamma_K(\epsilon + \beta_K p \cos\theta) \tag{1-202}$$

Thus

$$E_{\pi,\max} = \gamma_K\left(\frac{2}{3}Q + m_\pi + \Delta_{K,\max}\right) \tag{1-203}$$

where

$$\Delta_{K,\max} = \kappa(\epsilon_{\max})\,\beta_K(\tfrac{1}{2}E_K) \tag{1-204}$$

and

$$\kappa(\epsilon_{\max}) = \kappa_{\max} = 2\left[\frac{\left(\frac{2}{3}Q + m_\pi\right)^2 - m_\pi^2}{m_K^2}\right]^{1/2} \tag{1-205}$$

Thus

$$E_{\pi,\max} = E_K\left(\frac{m_\pi + \frac{2}{3}Q}{m_K} + \frac{1}{2}\beta_K\kappa_{\max}\right) \tag{1-206}$$

Again, we wish to determine the energy range of K_2^0-mesons that produce pions of energy E_π. In this case, however, we must take account of the finite range of decay energies E instead of the unique two-body decay energies we have previously considered. Setting $\eta \equiv \epsilon/m_K$, we again find

$$E_K = \left(\frac{m_K}{m_\pi}\right)^2 [\eta + \tfrac{1}{2}\beta_\pi\kappa\cos\theta']E_\pi \tag{1-207}$$

but in this case, η and κ are not constants but are functions of ϵ. The quantities Q and $\kappa_{\max}$ are given by

$$Q \simeq 93.0 \text{ MeV} \qquad \kappa_{\max} \simeq 0.560 \qquad \text{for the decay } K_2^0 \to 3\pi^0 \tag{1-208}$$

and

$$Q \simeq 83.8 \text{ MeV} \qquad \kappa_{\max} \simeq 0.534 \qquad \text{for the decay } K_2^0 \to \pi^+ + \pi^- + \pi^0 \tag{1-209}$$

Thus we obtain the limiting values for $K_2^0 \to 3\pi^0$ decay from equations (1–203) through (1–205):

$$E_K \simeq 2.53E_\pi \qquad \text{for } \beta_K \ll 1 \tag{1-210}$$

and

$$\left.\begin{aligned} E_{K,\max} &\simeq 9.27E_\pi \\ E_{K,\min} &\simeq 1.59E_\pi \end{aligned}\right\} \qquad \text{for } \beta_K \simeq \beta \simeq 1 \tag{1-211}$$

For $K_2^0 \rightarrow \pi^+ + \pi^- + \pi^0$ decay

$$E_K \simeq 2.56 E_\pi \qquad \text{for } \beta_K \ll 1 \tag{1-212}$$

and

$$\left.\begin{aligned} E_{K,\max} &\simeq 8.96 E_\pi \\ E_{K,\min} &\simeq 1.64 E_\pi \end{aligned}\right\} \qquad \text{for } \beta_K \simeq \beta_\pi \simeq 1 \tag{1-213}$$

The appropriate constants for the two decay modes of K_2^0 considered are

$$\zeta = 6 \qquad R \simeq 0.265 \qquad \text{for } K_2^0 \rightarrow 3\pi^0 \tag{1-214}$$

and

$$\zeta = 2 \qquad R \simeq 0.114 \qquad \text{for } K_2^0 \rightarrow \pi^+ + \pi^- + \pi^0 \tag{1-215}$$

We will thus neglect the small kinematic differences between the $K_2^0 \rightarrow 3\pi^0$ and $K_2^0 \rightarrow \pi^+ + \pi^- + \pi^0$ decay modes and use the quantities derived for the $K_2^0 \rightarrow 3\pi^0$ mode, which contributes more than six times as many γ-rays as does the $K_2^0 \rightarrow \pi^+ + \pi^- + \pi^0$ mode.

We also note that

$$\frac{\sigma(E_{K_2^0}|E_p)}{\sigma(E_{K^0}|E_p)} = \frac{1}{2} \tag{1-216}$$

This, together with equations (1–10) through (1–14), (1–99), (1–207), (1–214), and (1–215), yields the source spectrum

$$q_{K_2^0}(E_\gamma, \mathbf{r}) = 11.43 n(\mathbf{r}) \int dE_p I(E_p, \mathbf{r}) \int_{E_\gamma + (m_\pi^2/4E_\gamma)}^{\infty} \frac{dE_\pi}{(E_\pi^2 - m_\pi^2)^{1/2}}$$
$$\times \int_{m_\pi}^{m_\pi + 2/3Q} \frac{d\epsilon \Phi(\epsilon)}{\kappa(\epsilon)} \int_{\left(\frac{m_K}{m_\pi}\right)^2 [\eta(\epsilon) - \beta_\pi \kappa(\epsilon)/2] E_\pi}^{\left(\frac{m_K}{m_\pi}\right)^2 [\eta(\epsilon) + \beta_\pi \kappa(\epsilon)/2] E_\pi} \frac{dE_K \sigma(E_K|E_p)}{(E_K^2 - m_K^2)^{1/2}} \tag{1-217}$$

1-6 SUMMARY OF VARIOUS KINEMATIC PROPERTIES OF THE IMPORTANT GAMMA-RAY-PRODUCING DECAY MODES

In our discussion in the previous section, we established the Lorentz transformation equation for the two-body decay process given by equation (1–69). When we evaluate the cosmic γ-ray production spectrum later on, we will find it useful to give our results in the form of a log-log plot covering the many decades in energy which are of astrophysical significance. At this point, before we summarize the kinematic properties described in the previous section, we digress a bit to point out an addi-

tional symmetry property which holds for logarithmic energy spectra that is implicit in equation (1–69) for two-body decays.

From equation (1–69), it follows that a particle which is the product of a two-body decay will have an ls energy which lies between the minimum and maximum values obtained when $\cos\theta' = \pm 1$. These values are

$$E_{s,\,\min} = E_{\rm pr}(\eta - \beta\rho) \tag{1–218}$$

and

$$E_{s,\,\max} = E_{\rm pr}(\eta + \beta\rho) \tag{1–219}$$

where $E_{\rm pr}$ and E_s are the energies of the primary and secondary particles, respectively. We have replaced the quantity κ in equation (1–69) by ρ to avoid confusion with the definition of κ in the previous section. The product

$$(E_{s,\,\min})(E_{s,\,\max}) = (\eta^2 - \beta^2\rho^2)E_{\rm pr}^2 \tag{1–220}$$

We now define a geometric mean for the energy range of the secondary particle

$$E_s = E_{s,\,\min}E_{s,\,\max} = (\eta^2 - \beta^2\rho^2)^{1/2}E_{\rm pr} \tag{1–221}$$

Thus, in the nonrelativistic limit,

$$E_s \simeq \eta E_{\rm pr} \simeq \mu \qquad (\gamma \simeq 1,\ \beta \ll 1) \tag{1–222}$$

where μ, as before, is the energy of the secondary in the rest system of the decaying primary.

In the relativistic limit,

$$\tilde{E}_s \simeq (\eta^2 - \rho^2)^{1/2}E_{\rm pr} = (M_s/M_{\rm pr})E_{\rm pr} = \gamma M_s \qquad (\beta \simeq 1) \tag{1–223}$$

In particular, for photon secondaries

$$\tilde{E}_\gamma = \eta(1 - \beta^2)^{1/2}E_{\rm pr} = \mu \tag{1–224}$$

We have thus proved an important kinematic property regarding the energy range of secondary γ-rays that are the product of two-body decays; viz,

> The geometric mean of the energy range of secondary γ-rays which are produced in all two-body decays is equal to the energy of the γ-rays in the rest system of the decaying primary μ and is independent of the energy of the primary particle.

Also, since

$$\log E_\gamma = \tfrac{1}{2}(\log E_{\gamma,\,\min} + \log E_{\gamma,\,\max}) = \log \mu \qquad (1\text{–}225)$$

it follows that, on logarithmic plots of the energy spectra of these γ-rays, the rest-system energy μ will lie halfway between the extremum energies.

We are particularly concerned with decays that are isotropic in the rest system of the decaying particle, such as the π^0 and Σ^0 decays, which we have previously considered. For these decays, we have already shown that the resultant γ-ray energy distribution function is only a function of the momentum of the primary; indeed this function is a constant which is inversely proportional to this momentum for a given primary, within a range proportional to the momentum of the primary, and vanishes outside this range. Thus, for decays of parent particles with a wide range of primary energies, γ-ray spectra are generated which are made up of a superposition of rectangular spectra, as shown in figure 1–11. Higher energy primaries produce the γ-rays at the extremes of the spectrum. We therefore deduce a second important kinematic property, which holds for two-body decays that produce γ-rays isotropically in the rest system of the decaying primary; viz,

> The energy spectra of γ-rays produced isotropically in the rest system of the decaying primary will be symmetric on a logarithmic plot with respect to $E_\gamma = \mu$ and will peak at $E_\gamma = \mu$.

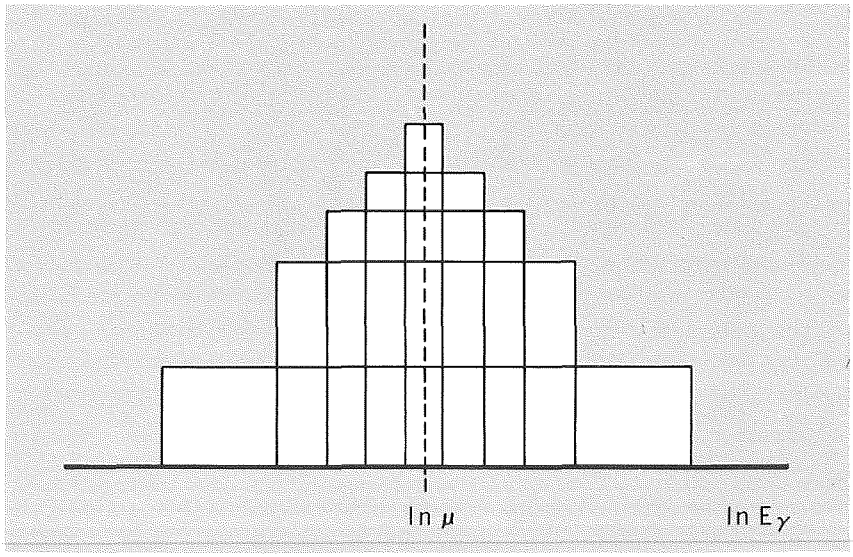

FIGURE 1–11.—Ideal superposition of γ-ray energy spectra from π^0 of Σ^0 particles having discrete values of energy.

The properties of the various decay modes discussed in the previous section are given in table 1–3.

TABLE 1–3.—*Kinematic Properties of γ-Ray-Producing Decay Modes*

Decay mode ($1 \rightarrow 2$)	$E_1(\beta_1 \ll 1)$	$E_{1,\min}(\beta_1 \simeq 1)$	$E_{1,\max}(\beta_1 \simeq 1)$	$\tilde{E}_2(\beta_1 \ll 1)$	$\tilde{E}_2(\beta_1 \simeq 1)$
$\pi^0 \rightarrow 2\gamma$	$2E_\gamma$	E_γ	∞	$M_\pi/2$	$M_\pi/2$
$\Sigma^0 \rightarrow \Lambda + \gamma$	E_γ/η	$E_\gamma/2\eta$	∞	$\frac{M_\Sigma^2 - M_\Lambda^2}{2M_\Sigma}$	$\frac{M_\Sigma^2 - M_\Lambda^2}{2M_\Sigma}$
$K_1^0 \rightarrow 2\pi^0$	$2E_\pi$	$1.11E_\pi$	$12.7E_\pi$	$M_K/2$	$0.272E_K$
$K^\pm \rightarrow \pi^\pm + \pi^0$	$2.01E_\pi$	$1.09E_\pi$	$12.5E_\pi$	$0.498M_K$	$0.274E_K$
$\Lambda \rightarrow n + \pi^0$	$6.58E_\pi$	$4.08E_\pi$	$16.96E_\pi$	$0.152E_\Lambda$	$0.121E_\Lambda$
$\Sigma^+ \rightarrow p + \pi^0$	$5.13E_\pi$	$2.82E_\pi$	$27.82E_\pi$	$0.195E_\Sigma$	$0.113E_\Sigma$
$K_2^0 \rightarrow 3\pi^0$	$2.53E_\pi$	$1.59E_\pi$	$9.27E_\pi$		
$K^0 \rightarrow \pi^+ + \pi^- + \pi^0$	$2.56E_\pi$	$1.64E_\pi$	$8.96E_\pi$		

Gamma-Ray Production From Cosmic Electron-Positron Annihilation

2-1 CROSS SECTIONS AND ANNIHILATION RATES

As is well known, electrons and positrons may interact electromagnetically and thereby annihilate to produce γ-rays. This annihilation may occur in the following ways.[1]

(1) A free positron may annihilate with a free electron to produce, most frequently, two γ-rays; i.e.,

$$e^+ + e^- \rightarrow \gamma + \gamma \tag{2-1}$$

(2) A positron and electron of low (typically thermal) energy may first combine to form a hydrogenlike system known as positronium. The positronium may then annihilate, usually into two or three γ-rays.

We can discuss these annihilations with much more confidence and exactness than we can discuss the γ-ray production from high-energy inelastic collisions (as we will in a later chapter) because here we can use the results of quantum electrodynamics, which we know to be a very successful theory, whereas there is presently no really good theoretical understanding of particle production in high-energy interactions. Consequently, we will be forced to use a phenomenological description in the discussion of the high-energy processes.

2-2 THE FREE-ANNIHILATION GAMMA-RAY SPECTRUM

The cross section for free positron annihilation as a function of energy was first deduced by Dirac (1930). An excellent presentation of the theory

[1] Positrons may annihilate with bound electrons to produce a single photon, with momentum being conserved by the binding nucleus. However, the cross section for this process is always less than $\pi r_0^2 Z^5/(137)^4$, where the atomic number Z is almost always 1 or 2 under astrophysical conditions. Therefore, the single-photon annihilation can be neglected in the following discussion (Heitler, 1960).

is given by Heitler (1960). The most important annihilation mode of the free electron-positron system is the annihilation

$$e^+ + e^- \rightarrow \gamma + \gamma \tag{2-1}$$

The frequency of this annihilation is 372 times greater than that of the free three-photon annihilation and we may neglect all but the two-photon mode in our consideration of the γ-ray spectrum from free $e^+ - e^-$ annihilations. (However, as we shall see later, the three-photon mode becomes important when we consider the effect of positronium formation by positrons of energies less than 5 keV.)

The differential cross section for γ-ray production in the collision cms of a free two-photon annihilation may be written as

$$d\sigma = \frac{\sigma_0}{2\gamma_c^2 \beta_c} \phi(\chi|\gamma) d\chi \tag{2-2}$$

where $\sigma_0 = \pi r_0^2 = 2.5 \times 10^{-25}$ cm^2, using the definition of the classical radius of the electron, $r_0 = \frac{e^2}{m_e c^2} = 2.8 \times 10^{-13}$ cm; γ is the Lorentz factor of the positron; $\beta = \left[1 - \left(\frac{1}{\gamma^2}\right)\right]^{1/2}$; the cms Lorentz factor and the velocity are given by

$$\gamma_c = \left(\frac{\gamma + 1}{2}\right) \qquad \text{and} \qquad \beta_c = \left(\frac{\gamma - 1}{\gamma + 1}\right)^{1/2} \tag{2-3}$$

χ is the cosine of the angle between the incoming positron and the outgoing γ-ray in the cms; and $\phi(\chi|\gamma)$, the angular distribution function, is defined as

$$\phi(\chi|\gamma) = \frac{1 + \beta_c^2(2 - \chi^2)}{1 - \beta_c^2 \chi^2} - \frac{2\beta_c^4 (1 - \chi^2)^2}{(1 - \beta_c^2 \chi^2)^2} \tag{2-4}$$

The energy of an annihilation γ-ray in the ls is given by the Doppler relation as

$$E_\gamma = (m_e c^2)\ \gamma_c^2 (1 + \beta_c \chi) \tag{2-5}$$

If we now define the dimensionless energy $\eta = E_\gamma / m_e c^2$, we may use equations (2–3) and (2–5) to determine the normalized distribution func-

tion that uniquely relates χ to the laboratory Lorentz factor of the positron and the laboratory energy of the γ-ray as follows:

$$f(\chi|\gamma, \eta) = 2(\gamma^2 - 1)^{-1/2}\delta[\chi - \chi_0(\eta, \gamma)]$$

where

$$\chi_0(\eta, \gamma) \equiv \frac{(2\eta - 1) - \gamma}{(\gamma^2 - 1)^{1/2}} \tag{2-6}$$

The total number of γ-rays produced per second by a positron of energy $\gamma m_e c^2$ is

$$Q_{\text{total}}(\gamma) = \frac{2\sigma_0 n_e \beta c}{2\gamma_c^2 \beta_c} \int_{-1}^{1} d\chi\, \phi(\chi|\gamma)$$

$$= \frac{2\sigma_0 n_e c}{\gamma} \int_{-1}^{1} d\chi\, \phi(\chi|\gamma)$$

where n_e is the number density of electrons in the medium.

Therefore, the γ-ray source spectrum from the annihilation of cosmic-ray positrons with a density $n(\gamma)$ cm^{-3} is given by

$$Q(\eta) = 4n_e\sigma_0 c \int_1^{\infty} d\gamma \frac{n(\gamma)}{\gamma(\gamma^2 - 1)^{1/2}} \int_{-1}^{1} d\chi\, \phi(\chi|\gamma)\delta[\chi - \chi_0(\eta, \gamma)] \tag{2-7}$$

We now wish to integrate over the delta function in equation (2–7). The result of this integration is to replace the last integral in equation (2–7) by a function $\Phi(\eta, \gamma)$ such that

$$\Phi(\eta, \gamma) = \begin{cases} \phi[\chi_0(\eta, \gamma), \gamma] & \text{for} \quad |\chi_0| \leq 1 \\ 0 & \text{for} \quad |\chi_0| > 1 \end{cases} \tag{2-8}$$

We may, therefore, replace the integral over $d\chi$ by the algebraic function $\phi[\chi_0(\eta, \gamma), \gamma]$, provided the limiting condition on χ_0 is transformed into a limiting condition on the integration over $d\gamma$. The limiting conditions $\chi_0 = \pm 1$ correspond to the relations

$$\eta_{\pm} = \gamma_c^2(1 \pm \beta_c) \tag{2-9}$$

It follows from equation (2–9) that the product

$$\eta_+\eta_- = \gamma_c^4(1 - \beta_c^2) = \gamma_c^2 = \tfrac{1}{2}(\gamma + 1) \tag{2-10}$$

and the sum

$$\eta_+ + \eta_- = 2\gamma_c^2 = \gamma + 1 \tag{2-11}$$

Therefore, η_+ and η_- are the roots of the quadratic equation

$$\eta^2 - 2\gamma_c^2\eta + \gamma_c^2 = 0 \tag{2-12}$$

which can be solved for γ_c in terms of η to give

$$\gamma_c^2 = \frac{\eta^2}{2\eta - 1} = \tfrac{1}{2}(\gamma + 1) \tag{2-13}$$

or

$$\gamma = \frac{\eta^2 + (\eta - 1)^2}{2\eta - 1} \tag{2-14}$$

which is finite and positive for $\eta > 1/2$ and has a minimum of $\gamma = 1$ at $\eta = 1$.

Figure 2–1 shows the curve defined by equation (2–14) split into the branches defined by the physical extremes $\chi = \pm 1$. Also shown are the asymptotes $\eta = 1/2$ and $\eta = \gamma + 1/2$, the line defining $\chi = 0$, and the shaded region corresponding to the physical values of $|\chi| \leq 1$. It can be

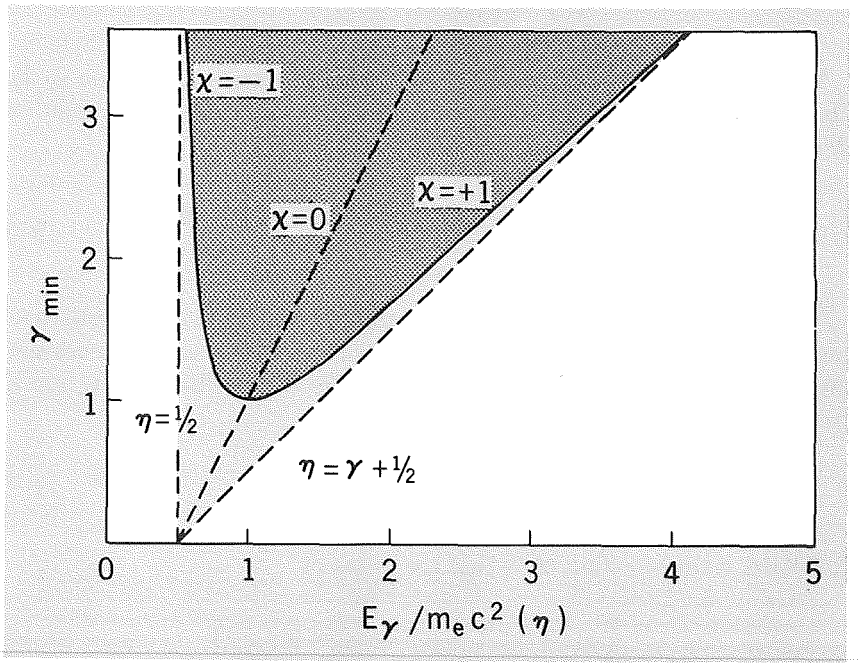

FIGURE 2–1.—The kinematic limits on the positron Lorentz factor involved in the determination of the laboratory energies of the annihilation γ-rays produced (Stecker, 1969a).

seen from figure 2–1 that the physical range of γ defined by the shaded region ($|\chi| \leq 1$) is bounded on the bottom by the curve of equation (2–14) and is unbounded on the top.

Figure 2–1 indicates that no γ-ray can be produced from an annihilation process that has an energy less than or equal to $\frac{1}{2}m_e c^2$. This physical restriction may be seen more clearly as a direct consequence of equation (2–9), since

$$\eta_- \leq \eta \leq \eta_+ \tag{2–15}$$

where

$$\eta_- = \gamma_c^2(1-\beta_c) = \frac{1-\beta_c}{1-\beta_c^2} = \frac{1}{1+\beta_c} > \frac{1}{2} \tag{2–16}$$

Thus η_- may approach, but never reach 1/2 as $\gamma_c \to \infty$. On the other hand

$$\eta_+ = \gamma_c^2(1+\beta_c) = \frac{1}{1-\beta_c} \tag{2–17}$$

which increases without bound as $\gamma_c \to \infty$.

The general restriction on the range of η may be designated by the introduction of the Heaviside step function $H_+(\eta_0)$, which is defined by the relation

$$H_+(\eta_0) = \begin{cases} 1 & \text{for } \eta > \eta_0 \\ 0 & \text{for } \eta \leq \eta_0 \end{cases} \tag{2–18}$$

We may therefore rewrite equation (2–7) in the form

$$Q(\eta) = 4H_+\left(\frac{1}{2}\right) n_{e^-}\sigma_0 c \int_{G(\eta)}^{\infty} d\gamma \, \frac{n(\gamma)}{\gamma(\gamma^2-1)^{1/2}} \, \phi[\chi_0(\eta, \gamma), \gamma] \tag{2–19}$$

where

$$G(\eta) = \frac{\eta^2 + (\eta-1)^2}{2\eta - 1} \tag{2–20}$$

From the general results which we have obtained, we can immediately arrive at formulas for asymptotic spectra that can be used as guides in the examination of the results of numerical calculations. These are obtained as follows:

(1) For two-photon annihilations at rest, it follows from equation (2–5) that the annihilation γ-ray spectrum (AGS) is simply a line at energy $\eta = 1$ (0.51 MeV). This is, of course, a familiar and expected result.

(2) The AGS from the two-photon annihilation of an ultrarelativistic positron may be obtained from a consideration of the angular

distribution function $\phi(\chi|\gamma)$, given by equation (2–4). At ultrarelativistic energies, the angular distribution function peaks sharply at $\chi = \pm 1$ so that the γ-rays resulting from the annihilation lie close to the asymptotes of figure 2–1; viz, $\eta = 1/2$ and $\eta = \gamma + 1/2$. This result, as pointed out by Heitler (1960), may be discussed physically as follows: In an ultrarelativistic annihilation, the resultant photons are emitted in a sharply backward and sharply forward direction in the collision cms. In the ls, the forward photon carries off almost all the energy of the collision and the backward photon carries off an energy between about 0.25 and 0.5 MeV. Therefore, the AGS for $\eta \gg 1$ may be obtained by using the approximate production cross section

$$\sigma_A(\eta|\gamma) \simeq \sigma_A(\gamma)\delta(\eta - \gamma) \qquad \text{for} \qquad \eta \gg 1 \tag{2–21}$$

The total cross section for free annihilation of positrons into γ-ray pairs was first calculated by Dirac (1930) and is given by

$$\sigma_A = \frac{\sigma_0}{\gamma+1}\left[\frac{\gamma^2+4\gamma+1}{(\gamma^2-1)^{1/2}} \ln\left[\gamma+(\gamma^2-1)^{1/2}\right] - \frac{\gamma+3}{(\gamma^2-1)^{1/2}}\right] \tag{2–22}$$

At nonrelativistic energies ($\gamma \simeq 1$), equation (2–22) reduces to the asymptotic form

$$\sigma_A \rightarrow \frac{\sigma_0\gamma}{(\gamma^2-1)^{1/2}} \rightarrow \frac{\sigma_0}{\beta} \qquad (\beta \ll 1) \tag{2–23}$$

At extreme relativistic energies ($\gamma \gg 1$), equations (2–21) and (2–22) reduce to the asymptotic form

$$\sigma_A \rightarrow \sigma_0\left[\frac{\ln(2\gamma)-1}{\gamma}\right] \qquad (\gamma \gg 1) \tag{2–24}$$

and $Q(\eta) \rightarrow n_e\sigma_0 cn(\eta)[\ln(2\eta) - 1]/\eta$ as has been noted by Ginzburg and Syrovatskii (1964). A free positron and free electron may also annihilate to produce three or more γ-rays. The cross section for the process

$$e^+ + e^- \rightarrow \zeta\gamma \tag{2–25}$$

is of the order

$$\sigma_{A,\,\zeta\gamma} \simeq \alpha^{(\zeta-2)}\sigma_{A,\,2\gamma} \tag{2–26}$$

where

$$\alpha = \frac{e^2}{\hbar c} \simeq \frac{1}{137} \tag{2–27}$$

The cross section for three-photon annihilation in the nonrelativistic limit ($\beta \ll 1$) is also inversely proportional to β and is given by Ore and Powell (1949).

$$\sigma_{A,3\gamma} \rightarrow \frac{4}{3}(\pi^2 - 9)\alpha \frac{r_0^2}{\beta} \qquad \beta \ll 1$$
$$\simeq \frac{\sigma_{A,2\gamma}}{372} \tag{2-28}$$

In our discussion we can neglect processes involving $\zeta > 3$, where cross sections contain increasingly large factors of α.

2–3 THE ANNIHILATION GAMMA-RAY SPECTRUM FROM POSITRONIUM FORMATION

A positron and electron of low (typically thermal) energy may first combine to form a hydrogenlike system known as positronium (which we will here designate by the symbol Π). The positronium may then annihilate into γ-rays. We must therefore consider processes of the type

$$e^+ + e^- \rightarrow \Pi \qquad \Pi \rightarrow \zeta\gamma \tag{2-29}$$

Here again, we can neglect processes involving $\zeta > 3$.

The positronium system, which is similar in structure to the hydrogen atom, can exist in the ground state ($L = 0$) either as a triplet ($^3S_1$), called orthopositronium by analogy with the spectral designation for hydrogen, or as a singlet ($^1S_0$) called parapositronium (also by analogy with hydrogen). In the triplet state, the spins of the electron and positron are parallel, whereas in the singlet state they are antiparallel. Since the positronium system has well-defined values of the quantum numbers L and S and has no net charge, the system is in an eigenstate of charge conjugation.

The positronium annihilations, unlike the free annihilations, obey selection rules since positronium is in an eigenstate of charge conjugation C, and C is conserved in electromagnetic interactions.

If ζ photons are produced in the final state, then

$$C = (-1)^\zeta \tag{2-30}$$

It can be shown that under particle exchange, positronium obeys a kind of generalized Pauli principle and changes sign. The exchange of

particles involves the exchange of the product of the space, spin, and charge-conjugation parts of the wave function. Therefore,

$$(-1)^{l}(-1)^{S+1}C=-1 \tag{2-31}$$

where l is the orbital angular-momentum quantum number and S is the spin quantum number. By combining equations (2–30) and (2–31), we obtain the selection rule

$$l+S=\zeta \tag{2-32}$$

We may therefore specify the processes given by equation (2–29) as

$$e^{+}+e^{-}\rightarrow \Pi(^{1}S_{0}) \hookrightarrow 2\gamma \tag{2-33}$$

and

$$e^{+}+e^{-}\rightarrow \Pi(^{3}S_{1}) \hookrightarrow 3\gamma \tag{2-34}$$

Processes involving $l\neq 0$ can be neglected (Deutsch, 1953).

The positronium annihilation rate, or inverse lifetime, is equal to the product of four times the free-annihilation cross section, the relative velocity of the electron and positron, and the overlap probability of the electron and positron wave functions. The factor of 4 is required because the free-annihilation cross section is an average over all four possible relative spin orientations of the positron and electron; viz, up-up, up-down, down-up, and down-down; whereas the positronium system annihilates from a definite orientation state.

If we designate the probability density of the wave function as the square of its absolute value $|\psi|^2$ in the usual notation, we then find

$$\begin{aligned}\tau_{2\gamma}^{-1}&=4\sigma_{A,2\gamma}v|\psi(0)|^{2}\\&=4\pi r_{0}^{2}\frac{c}{v}v\frac{1}{\pi}\left(\frac{1}{2a_{0}}\right)^{3}\\&=\frac{r_{0}^{2}c}{2a_{0}^{3}}=\alpha^{4}\frac{c}{2a_{0}}\end{aligned} \tag{2-35}$$

or

$$\tau_{2\gamma}=\alpha^{-4}\frac{2a_{0}}{c}=1.25\times 10^{-10}\ \text{s} \tag{2.36}$$

where a_0 is the Bohr radius given by

$$a_{0}=\alpha^{-2}r_{0}=5.29\times 10^{-13}\ \text{cm} \tag{2-37}$$

v is the electron velocity and $|\psi(0)|$ is the absolute magnitude of the wave function at the origin of the system. The effective Bohr radius for positronium is twice that of hydrogen, and this is taken into account. The factor $|\psi(0)|^2$ is just the effective electron density seen by the positron.

The lifetime for positronium annihilation into three γ-rays is derived from the free-annihilation cross section given by equation (2–28) through the use of the same method as that used in the derivation of equation (2–36). We thus obtain (Ore and Powell, 1949)

$$\tau^{-1}_{^3S_1 \to 3\gamma} = \frac{2}{9\pi}(\pi^2 - 9)\frac{\alpha^5 c}{a_0} \tag{2–38}$$

or

$$\tau_{^3S_1 \to 3\gamma} = 1.4 \times 10^{-7}\ \text{s} \tag{2–39}$$

This result can also be expressed as

$$\frac{\sigma_{f,3\gamma}}{\sigma_{f,2\gamma}} = 3\,\frac{\tau^{-1}_{^3S_1 \to 3\gamma}}{\tau^{-1}_{^1S_0 \to 2\gamma}} \tag{2–40}$$

Here again, the factor of 3 in equation (2–40) expresses the difference in probability between a singlet and triplet interaction (3/4 versus 1/4).

The lifetimes for both the two- and three-photon annihilations of positronium are so short that for galactic γ-ray production, we may consider the annihilation to take place effectively at the time that positronium is formed. Since the probability for positronium formation in the triplet state is three times the probability for positronium formation in the singlet state, it follows from equations (2–33) and (2–34) that 3/4 of the positronium formed in the galaxy undergoes three-photon annihilation.

2–4 THE GAMMA-RAY SPECTRA FROM ELECTRON-POSITRON ANNIHILATION

The energy spectrum of the two-photon annihilation in the cms of the electron-positron pair is a single line at $E_\gamma = m_e \simeq 0.511$ MeV, as can easily be seen from considerations of conservation of energy and momentum. The natural width of this line due to the uncertainty principle is small, being on the order of

$$\Delta E = \frac{\hbar}{\tau} \simeq 5.3 \times 10^{-12}\ \text{MeV} \tag{2–41}$$

Dominant broadening can be expected to be due to the Doppler effect, and is of the order

$$\frac{\Delta E}{E} = \frac{\Delta E}{m_e c^2} = \beta \tag{2-42}$$

The effect of astrophysical conditions on the broadening of the 0.51-MeV line from two-photon annihilation can be determined as follows:

In free e^+–e^- annihilations, we may consider a gas or plasma at temperature T. Then the distribution of the component of particle velocity along the line of sight of the observed γ-ray is of the form

$$f(\beta_{||})\,d\beta_{||} = \left(\frac{b}{\pi}\right)^{1/2} e^{-b\beta_{||}^2} d\beta_{||} \tag{2-43}$$

where

$$b \equiv \frac{m_e c^2}{2kT} \tag{2-44}$$

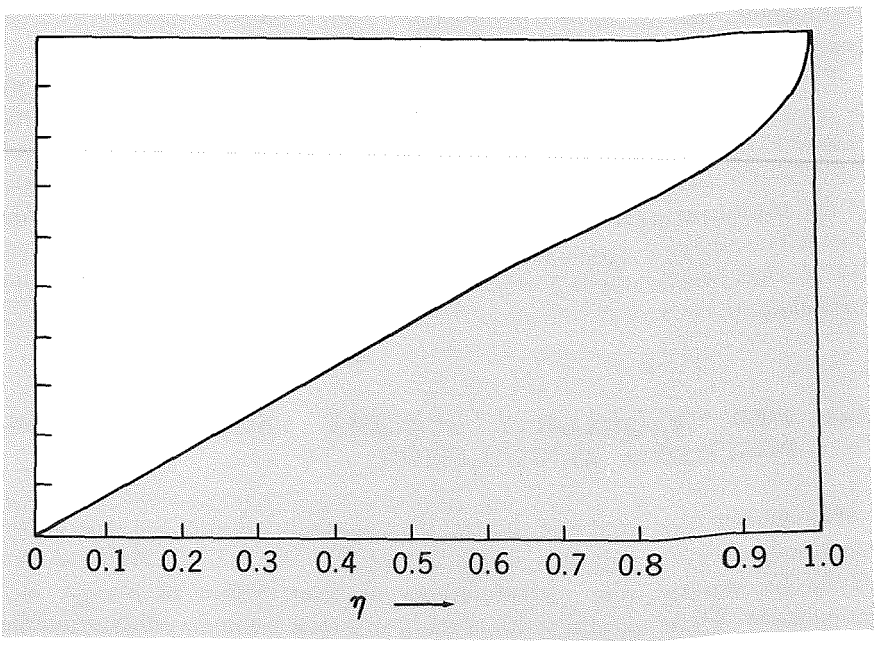

FIGURE 2–2.—Energy spectrum of γ-rays resulting from the three-photon annihilation of an electron and a positron. The abscissa is the photon energy in units of $m_e c^2$, and the ordinate is proportional to the number of photons per unit energy interval (from Ore and Powell, 1949).

It follows from equations (2–42) and (2–43) that the spectral-line shape has the gaussian form

$$f(\eta)\ d\eta = \left(\frac{b}{\pi}\right)^{1/2} \exp\left[-b\left(\frac{\eta-1}{\eta}\right)^2\right] d\eta \qquad (2\text{–}45)$$

Equation (2–45) has the same form as equation (2–43), since the number of collisions involving velocity v is proportional to $\sigma v \simeq \sigma_0 c$, independent of v.

The magnitude of the broadening is of the order

$$\Delta\eta = \left(\frac{\Delta E_\gamma}{m_e c^2}\right) \simeq b^{-1/2} \simeq 1.8 \times 10^{-5} T^{1/2} \qquad (2\text{–}46)$$

so that for $T = 100$ K, $\Delta E \simeq 10^{-1}$ keV. However, we have shown in the last section that most of the annihilations near rest occur following the formation of positronium by positrons having an average energy of about 35 eV. It therefore follows from the results of the previous section and equation (2–42) that 75 percent of the resultant annihilations occur via the three-photon channel and 25 percent produce a two-photon line with a Doppler width of about 5 keV.

The energy spectrum from the three-photon annihilation is continuous, as allowed by conservation of momentum. It has been calculated by Ore and Powell (1949) to be of the form

$$F(\eta) = \frac{2}{\pi^2 - 9}\left[\frac{\eta(1-\eta)}{(2-\eta)^2} - \frac{2(1-\eta)^2}{(2-\eta)^3}\ln(1-\eta) + \frac{2-\eta}{\eta} + \frac{2(1-\eta)}{\eta^2}\ln(1-\eta)\right] \qquad (2\text{–}47)$$

The function $F(\eta)$ is shown in figure (2–2). $F(\eta)$ is normalized so that

$$\int_0^1 F(\eta)\ d\eta = 1 \qquad (2\text{–}48)$$

GAMMA-RAY PRODUCTION FROM COSMIC PROTON-ANTIPROTON INTERACTIONS

3-1 INTRODUCTION

A topic of importance to both cosmology and particle physics is the existence or nonexistence of antimatter in the universe (Alfvén, 1965). It is therefore of interest to determine the extent to which γ-ray astronomy may be useful in determining the existence of cosmologically distributed antimatter and antimatter sources in which matter-antimatter interactions take place.

For the purpose of discussion, we define the terms "RG" and "CR" as follows. An RG (rest-gas) proton (or antiproton) is one possessing negligible kinetic energy with respect to the surrounding gas in an astronomical system. For example, nuclei of the galactic interstellar gas clouds from which stars are formed may be considered RG nuclei. A CR (cosmic-ray) proton (or antiproton) would be one possessing relativistic energy. We may thus envision four situations for discussion in which matter and antimatter might interact:

(1) RG matter + RG antimatter (RG–$\overline{\text{RG}}$)
(2) RG matter + CR antimatter (RG–$\overline{\text{CR}}$)
(3) CR matter + RG antimatter (CR–$\overline{\text{RG}}$)
(4) CR matter + CR antimatter (CR–$\overline{\text{CR}}$)

Although astrophysics has revealed many surprising phenomena, we would be hard put to imagine a system in which the number of RG nuclei did not greatly outnumber the number of CR nuclei. Indeed, the evolution of such a system from a more balanced one would violate the second law of thermodynamics. Therefore, if we let the number of RG nuclei in a typical system be N and the number of CR nuclei in the system be of the order ϵN, with $\epsilon \ll 1$, then typical interaction rates would have the properties

$$\frac{R(\text{RG}-\overline{\text{CR}})}{R(\text{RG}-\overline{\text{RG}})} \sim \frac{R(\text{CR}-\overline{\text{RG}})}{R(\text{RG}-\overline{\text{RG}})} \sim \epsilon \qquad (3\text{-}1)$$

$$\frac{R(\mathrm{CR}-\overline{\mathrm{CR}})}{R(\mathrm{CR}-\overline{\mathrm{RG}})} \sim \frac{R(\mathrm{CR}-\overline{\mathrm{CR}})}{R(\mathrm{RG}-\overline{\mathrm{CR}})} \sim \epsilon \tag{3-2}$$

and

$$\frac{R(\mathrm{CR}-\overline{\mathrm{CR}})}{R(\mathrm{RG}-\overline{\mathrm{RG}})} \sim \epsilon^2 \tag{3-3}$$

We will thus assume that the likelihood of CR–$\overline{\mathrm{CR}}$ interactions is negligible compared to the likelihood of RG–$\overline{\mathrm{CR}}$ or CR–$\overline{\mathrm{RG}}$ interactions that will produce γ-rays of similar characteristics, and we may limit ourselves to the discussion of RG–$\overline{\mathrm{RG}}$ and RG–$\overline{\mathrm{CR}}$ (or CR–$\overline{\mathrm{RG}}$) interactions.

3-2 THE GAMMA-RAY SOURCE SPECTRUM

The γ-ray source spectrum from p–$\bar{p}$ interactions of the RG–$\overline{\mathrm{CR}}$ type is given by (cf. eqs. (1–10) through (1–14))

$$q_{\mathrm{RG}-\overline{\mathrm{CR}}}(E_\gamma) = 4\pi n_p(\mathbf{r}) \int dE_{\bar{p}} I(E_{\bar{p}}, \mathbf{r}) \sum_s \int dE_s \sigma_s(E_s|E_{\bar{p}}) \times \sum_d \zeta_{\gamma d} R_{\gamma d} f_{ds}(E_\gamma|E_s) \tag{3-4}$$

For interactions of the CR–$\overline{\mathrm{RG}}$ type, we use the corresponding expression

$$q_{\mathrm{CR}-\overline{\mathrm{RG}}}(E_\gamma) = 4\pi n_{\bar{p}}(\mathbf{r}) \int dE_p I(E_p, \mathbf{r}) \sum_s \int dE_s \sigma_s(E_s|E_p) \times \sum_d \zeta_{\gamma d} R_{\gamma d} f_{ds}(E_\gamma|E_s) \tag{3-5}$$

The notation for equations (3–4) and (3–5) is the same as that used in chapter 1. The quantity $n(\mathbf{r})$ is the number of target nucleons in the medium per cubic centimeter as a function of position; $I(E, \mathbf{r})$ is the differential cosmic-ray particle flux in $\mathrm{cm^{-2}\text{-}s^{-1}\text{-}sr^{-1}\text{-}GeV^{-1}}$. The subscript p stands for proton, $\bar{p}$ for antiproton, s for secondary particle produced in the collision, and d for decay mode. The production function $\sigma_s(E_s|E_p)$ represents the cross section for production of secondary particles of type s and energy E_s in a collision of primary energy E_p, $\zeta_{\gamma d}$ represents the number of γ-rays produced in the decay mode d, $R_{\gamma d}$ is the branching ratio for the decay mode d (the probability that a secondary particle s will decay via mode d) and $f_{ds}(E_\gamma|E_s)$ is the normalized distribution function representing the probability that a secondary

particle with energy E_s will decay to produce a γ-ray of energy E_γ. For the purposes of discussion, we will restrict ourselves to $p-\bar{p}$ interactions.

The situation for matter-antimatter annihilations occurring near rest is somewhat different. In this case, we will find it more convenient to speak of particle densities instead of fluxes or intensities. We thus make the transformation

$$\int dE_k I_k(E_k, \mathbf{r}) \rightarrow \frac{n_k(\mathbf{r})}{4\pi} \int dv\, v f(v) = \frac{n_k(\mathbf{r})\langle v \rangle}{4\pi} \tag{3-6}$$

where v is the relative velocity between the annihilating nucleon and antinucleon, which we can consider to be a thermal velocity, and $f(v)$ is a normalized distribution function representing the distribution of relative velocities between the interacting nucleons.

The γ-ray source spectrum from $p-\bar{p}$ interactions at or near rest is given by

$$q_{\mathrm{RG}-\overline{\mathrm{RG}}}(E_\gamma) = n_p(\mathbf{r}) n_{\bar{p}}(\mathbf{r}) \int dv f(v) v \sum_s \int dE_s \sigma_s(E_s|v) \times \sum_d \zeta_{\gamma d} R_{\gamma d} f_{ds}(E_\gamma|E_s) \tag{3-7}$$

The form of equation (3–7) suggests that the introduction of the term "emission measure" be defined in analogy with its use in astrophysics (Shklovskii, 1960).

We therefore define the "emission measure" B as

$$B = \int dr n_p(\mathbf{r}) n_{\bar{p}}(\mathbf{r}) \tag{3-8}$$

It follows from equation (3–7) that

$$I_{\mathrm{RG}-\overline{\mathrm{RG}}}(E_\gamma) = \frac{1}{4\pi} \int dr q(\mathbf{r}) \alpha B \tag{3-9}$$

3–3 CROSS SECTIONS FOR PROTON-ANTIPROTON ANNIHILATIONS NEAR REST

We now state more precisely what we mean by a "rest gas." We define a rest gas to be a gas of particles such that no particle in the gas has an energy greater than 286 MeV. This rather liberal definition of rest is sufficient to insure that the only secondary particles produced in RG–$\overline{\mathrm{RG}}$ interactions that yield γ-rays are secondary mesons produced by nucleon-

antinucleon annihilation. Our restriction leaves out interactions of the type

$$p + \bar{p} \rightarrow p + \bar{p} + \pi^0 \tag{3-10}$$

since the threshold for reactions of this type is 286 MeV. (See ch. 1.)

Since the threshold for nonannihilation, inelastic, p–$\bar{p}$ interactions that produce particles other than π^0-mesons is even greater, it follows that in the RG–$\overline{\text{RG}}$ case, only annihilations; i.e., reactions of the form

$$p + \bar{p} \rightarrow \text{bosons} \hookrightarrow \text{neutral pions} \hookrightarrow \gamma\text{-rays} \tag{3-11}$$

need be considered.

Table 3–1 lists the experimental cross sections for free p–$\bar{p}$ annihilation as a function of incident antiproton kinetic energy at accelerator energies. Also listed are β_{cms} and the product of the annihilation cross section (σ_A) and cms velocity (β_{cms}). It can be seen from table 3–1 that the product of cms velocity and annihilation cross section is constant over a very large energy range. For nonrelativistic energies,

$$\beta_{\text{cms}} \simeq \tfrac{1}{2}\beta \qquad (\beta \ll 1) \tag{3-12}$$

β being the relative velocity of the particles. We find experimentally that

$$\sigma_A \simeq \frac{4.8 \times 10^{-26}\ \text{cm}^2}{\beta} \simeq \frac{1.4 \times 10^{-15}\ \text{cm}^3\text{-s}^{-1}}{v} \tag{3-13}$$

TABLE 3–1.—*Experimental Cross Sections for* p–$\bar{\text{p}}$ *Annihilation as a Function of Incident Antiproton Kinetic Energy*

$T_{\bar{p}}$, MeV	σ_A, mb	$\beta_{\bar{p}}$, cms	$\beta_{\bar{p}}\sigma_A$, mb	Reference
25 to 40	192 ±34	0.13	25	Loken and Derrick (1963).
45	175 ±45	.15	26	Cork et al. (1962).
40 to 55	155 ±27	.16	25	Loken and Derrick (1963).
55 to 80	118 ±26	.20	24	Loken and Derrick (1963).
90	101 ± 9	.22	22	Cork et al. (1962).
145	99 ± 8	.28	28	Cork et al. (1962).
245	66 ± 6	.36	24	Cork et al. (1962).
7000	23.6 ± 3.4	~1	24	Ferbel et al. (1965).

At all energies above 25 MeV, we find that table 3–1 agrees with the theoretical cross section

$$\sigma_A = \frac{\pi r_p^2}{\beta_{\text{cms}}} \tag{3–14}$$

taking

$$r_p = 0.87 \times 10^{-13} \text{ cm} \tag{3–15}$$

as the proton (or antiproton) radius and using the model of Koba and Takeda (1958) in which the nucleon acts as a black absorbing sphere of radius r_p.

At lower energies ($\lesssim 10$ MeV, which correspond to annihilations of matter and antimatter gases at a temperature $\lesssim 10^{11}$ K), coulomb forces play a dominant role in the matter-antimatter interaction process. At energies $\lesssim$ 100 eV, bound systems of protons and antiprotons can be formed as an intermediate stage before annihilation. The situation is similar to the case of positronium formation discussed in the last chapter. As was the case there, we find that under astrophysical conditions, the lifetime of the p–$\bar{p}$ system against annihilation is much shorter than its lifetime against breakup, so that the cross section for bound-state formation becomes the effective annihilation cross section. Until recently the effect of coulomb interactions on matter-antimatter annihilation was largely neglected and theoretical cross sections for bound-state formation processes had not been calculated. However, recently Morgan and Hughes (1970) have calculated the cross sections for the radiative capture processes

$$e^- + e^+ \rightarrow \Pi_e + \gamma \tag{3–16}$$

and

$$p + \bar{p} \rightarrow \Pi_p + \gamma \tag{3–17}$$

and the atomic processes

$$\bar{\text{H}} + \text{H} \rightarrow \Pi_p + (\Pi_e \text{ or } e^- + e^+) \tag{3–18}$$

$$\text{H}_2 + \text{H} \rightarrow \Pi_p + (\Pi_e \text{ or } e^- + e^+) + (\text{H or } p + e^-) \tag{3–19}$$

$$\text{H}_2 + \bar{\text{H}}_2 \rightarrow 2\Pi_p + (\text{various combinations of } 2e^-, 2e^+) \tag{3–20}$$

$$\text{H}_2 + \bar{\text{H}}_2 \rightarrow \Pi_p + (\Pi_e \text{ or } e^+ + e^-) + (\text{various combinations of } p, \bar{p}, e^+, \text{ and } 1e^-) \tag{3–21}$$

$$p + \bar{\text{H}} \rightarrow \Pi_p + e^+ \tag{3–22}$$

$$p + \bar{\text{H}}_2 \rightarrow \Pi_p + (\Pi_e \text{ or } e^+ + e^-) + (\bar{\text{H}} \text{ or } \bar{p} + e^+) \tag{3–23}$$

$$e^- + \bar{H} \rightarrow \Pi_e + \bar{p} \tag{3-24}$$

and

$$e^+ + H \rightarrow \Pi_e + p \tag{3-25}$$

where we have used the symbols Π_p and Π_e to denote the bound states of the $p-\bar{p}$ and $e^- - e^+$ systems, respectively. Reactions (3–24) and (3–25) have already been discussed in the previous chapter with regard to the annihilation of secondary cosmic-ray positrons in a tenuous neutral hydrogen gas. The cross sections for these reactions, as calculated by Cheshire (1964), will be given in a later chapter. With regard to $p-\bar{p}$ annihilation in intergalactic space, three processes in particular can be expected to be of the greatest importance:

(1) Direct annihilations, such as (3–11), at energies greater than 10 MeV, where the cross section can be well represented by equations (3–14) and (3–15).

(2) Direct annihilations at energies below 10 MeV, where the mutual coulomb attraction of the proton and antiproton distort the wave functions of the two particles with a resultant increase in the direct-annihilation cross section. When the cross section given by equation (3–14) is corrected for this effect, the cross-section formula becomes modified to

$$\sigma_A = \frac{2\pi\alpha/\beta}{1-\exp(-2\pi\alpha/\beta)} \frac{\pi r_p^2}{\beta_{\text{cms}}} \tag{3-26}$$

where α is the fine structure constant. For $p-\bar{p}$ interactions at energies much less than 4 MeV, where $\beta \ll 2\pi\alpha$, equation (3–26) reduces to

$$\sigma_A \simeq \frac{4\pi^2\alpha r_p^2}{\beta^2} \qquad \beta \ll 2\pi\alpha \tag{3-27}$$

Thus, at an energy of about 4 MeV, there is a transition in the velocity dependence of the annihilation cross section from $\sigma_A \sim \beta^{-1}$ to $\sigma_A \sim \beta^{-2}$. The same is true for electron-positron interactions at energies of the order of 2 keV where $\beta \approx 2\pi\alpha$.

(3) In interactions between neutral atomic gases of hydrogen and antihydrogen at thermal energies, the $H-\bar{H}$ rearrangement collision, reaction (3–18), becomes the dominant mode of $p-\bar{p}$ annihilation.

Morgan and Hughes (1970) have calculated the annihilation cross section for this reaction and found that, to within 20 percent for energies between 10^{-3} and 1 eV (corresponding to thermal velocities at temperatures between 10 K and 10^4 K)

$$\sigma_{\mathrm{H-H},A} \simeq (0.31 a_0^2)\beta^{-0.64} \tag{3-28}$$

where a_0 is the Bohr radius of the hydrogen atom.

Radiative capture reactions of the form of equation (3–17) can be shown to be insignificant. The cross section for annihilations of this type (Morgan and Hughes, 1970) is

$$\sigma_{A,r} = \frac{128}{3\sqrt{3}}\alpha\left(\frac{m_e}{m_p}\right)^2\left[\ln\left(\frac{\alpha}{\beta}\right) + 0.20 + 0.25\left(\frac{\alpha}{\beta}\right)^{-2/3}\right]\frac{\sigma_0}{\beta^2} \tag{3-29}$$

Equation (3–29) is accurate to within at least 1 percent when $\beta \leqslant \alpha/7$ and is exact in the limit as $\beta \to 0$. The radiative capture cross section for the electron-positron system, viz, $e^+ + e^- \to \Pi_e + \gamma$, is given by the same formula without the quantity $(m_e/m_p)^2$. For p–$\bar{p}$ annihilations at all energies of interest $\sigma_{A,r} \ll \sigma_A$; however, in the case of electron-positron annihilation (in an ionized medium) $\sigma_{A,r} > \sigma_A$ for interactions at energies less than 20 eV.

In figure 3–1 we give the cross section versus temperature, energy, and thermal velocity for the reactions expected to be of importance for cosmological problems (intergalactic p–$\bar{p}$ annihilations). Figure 3–2 shows the values for total-annihilation cross section times velocity (proportional to the annihilation rate) calculated by Morgan and Hughes, which should be valid for astrophysical and cosmological problems at the temperatures and kinetic energies indicated.

We may now make use of equations (3–17), (3–18), (3–27), and (3–28) in order to reduce equation (3–7) to a simpler form. To do this, let us assume that matter-antimatter annihilations are taking place at thermal energies in three temperature regions defined as

Region I:	$10^{11}\ \mathrm{K} \lesssim T \lesssim 10^{13}\ \mathrm{K}$	
Region II:	$10^4\ \mathrm{K} \lesssim T \lesssim 10^{11}\ \mathrm{K}$	(3–30)
Region III:	$10\ \mathrm{K} \lesssim T \lesssim 10^4\ \mathrm{K}$	

It follows from the equations cited above that in each of these regions the annihilation cross section varies as some inverse power of the veloc-

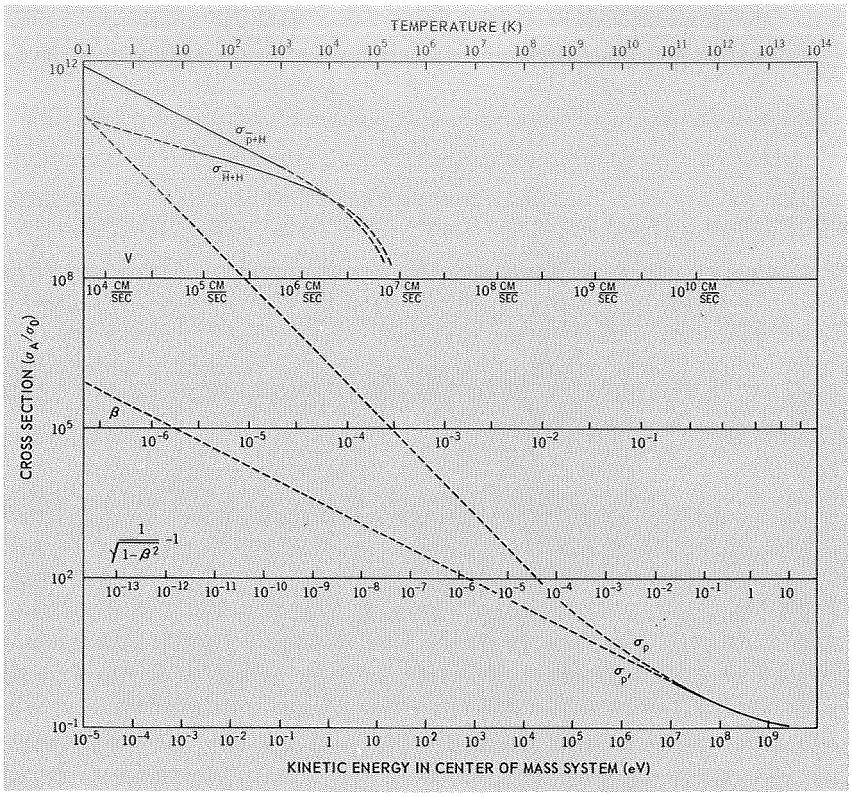

FIGURE 3–1.—Proton-antiproton annihilation cross sections as a function of temperature and kinetic energy for free nucleons and atoms (Morgan and Hughes, 1970). The curve marked σ_ρ takes into account the mutual coulomb attraction between the proton and antiproton; the curve marked $\sigma_{\rho'}$ is an extrapolation from the accelerator data that fails to take this effect into account.

ity. We can write an expression for this cross section for each of the temperature regions defined above thus

$$\begin{aligned}
&\text{Region I:} && \sigma(E_s|v) \simeq \sigma_{\mathrm{I}} \left(\frac{v}{c}\right)^{-1} \\
&\text{Region II:} && \sigma(E_s|v) \simeq \sigma_{\mathrm{II}} \left(\frac{v}{c}\right)^{-2} \qquad (3\text{–}31) \\
&\text{Region III:} && \sigma(E_s|v) \simeq \sigma_{\mathrm{III}} \left(\frac{v}{c}\right)^{-0.64}
\end{aligned}$$

where

$$\sigma_{\mathrm{I}} = 4.8 \times 10^{-26} \text{ cm}^2$$

and

$$\begin{aligned}
\sigma_{\mathrm{II}} &= 2.2 \times 10^{-27} \text{ cm}^2 \qquad (3\text{–}32) \\
\sigma_{\mathrm{III}} &= 2.6 \times 10^{-18} \text{ cm}^2
\end{aligned}$$

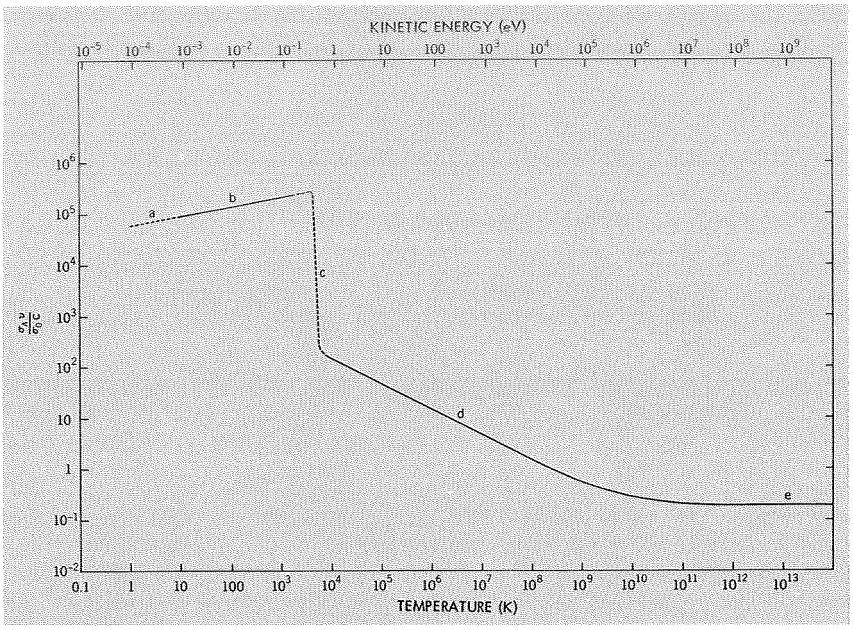

FIGURE 3–2.—Cross section times velocity for hydrogen-antihydrogen annihilation of nucleons given as a sum for the interactions shown in figure 3–1 integrated over a Maxwell-Boltzmann distribution at temperature T and taking ionization into account (Morgan and Hughes, 1970). (*a*) $\sigma_{H+\bar{H}}$ (extrapolated. (*b*) $\sigma_{H+\bar{H}}$ (calculated). (*c*) $\sigma_{H+\bar{H}}$, $\sigma_{p+\bar{H}}$, $\sigma_{p+\bar{H}}$, and $\sigma_{p+\bar{p}}$. multiplied by appropriate factors to take account of fractional ionization. (*d*) $\sigma_{p+\bar{p}}$, taking coulomb attraction into account. (*e*) $\sigma_{p+\bar{p}}$, from high-energy accelerator data.

We will write for all three regions

$$\sigma(E_s|v) = \sigma_i \left(\frac{v}{c}\right)^{-\delta_i} f(E_s) \tag{3–33}$$

where δ_i is the exponent of the power-law velocity dependence of $\sigma(E_s|v)$ as given in equation (3–31) and where, as in previous discussions

$$\int_0^\infty dE_s f(E_s) \equiv 1 \tag{3–34}$$

If we assume that the velocity distribution of the interacting nucleons and antinucleons is thermal and can be represented by the normalized maxwellian distribution

$$f_M(v) = \sqrt{\frac{2}{\pi}} \left(\frac{m}{kT}\right)^{3/2} v^2 \exp\left(-\frac{mv^2}{2kT}\right) \tag{3–35}$$

at some given temperature T; and in addition, if we define a normalized energy spectrum of the γ-radiation in the rest frame of the gas,

$$\zeta_\gamma f(E_{\gamma 0}) \equiv \sum_s \int dE_s f(E_s) \sum_d \zeta_{\gamma d} R_{\gamma d} f_{ds}(E_{\gamma 0}|E_s) \tag{3-36}$$

and smear it out by the distribution function,

$$D(E_\gamma|E_{\gamma 0}) \equiv \left(\frac{mc^2}{2\pi kT}\right)^{1/2} \exp\left[-\frac{mc^2}{2kT}\left(\frac{E_\gamma - E_{\gamma 0}}{E_{\gamma 0}}\right)^2\right] \tag{3-37}$$

to take account of the thermal Doppler broadening of the γ-ray spectrum, we may write equation (3–7) in the form

$$q_{\mathrm{RG}-\overline{\mathrm{RG}}}(E_\gamma, \mathbf{r}) = n_p(\mathbf{r})\, n_{\bar{p}}(\mathbf{r}) \sigma_i c^{\delta_i} \zeta_\gamma \left(\frac{2}{\pi}\right)^{1/2} \left(\frac{m}{kT}\right)^{3/2}$$

$$\times \int dv\, v^{(3-\delta_i)} \exp\left(-\frac{mv^2}{2kT}\right) \int dE_{\gamma 0} D(E_\gamma|E_{\gamma 0}) f(E_{\gamma 0}) \tag{3-38}$$

From the relation

$$\int_0^\infty dv\, v^{(3-\delta_i)} \exp -\frac{mv^2}{2kT} = \frac{1}{2} \Gamma\left(2 - \frac{\delta_i}{2}\right) \left(\frac{2kT}{m}\right)^{\left(2-\frac{\delta_i}{2}\right)} \tag{3-39}$$

where $\Gamma(x)$ is the well-known gamma function

$$\Gamma(x) \equiv \int_0^\infty dy\, y^{x-1} e^{-y} \tag{3-40}$$

which has the property, for integral arguments,

$$\Gamma(N+1) = N! \tag{3-41}$$

equation (3–38) may be further specified to read

$$q_{\mathrm{RG}-\overline{\mathrm{RG}}}(E_\gamma, \mathbf{r}) = n_p(\mathbf{r})\, n_{\bar{p}}(\mathbf{r}) \sigma_i c^{\delta_i} \zeta_\gamma \frac{2}{\pi^{1/2}} \Gamma\left(2 - \frac{\delta_i}{2}\right)$$

$$\times \left(\frac{2kT}{m}\right)^{1/2(1-\delta_i)} \int dE_{\gamma 0}\, D(E_\gamma|E_{\gamma 0}) f(E_{\gamma 0}) \tag{3-42}$$

Let us now utilize equation (3–42) to specifically discuss the tempera-

ture regions I, II, and III defined earlier. In region I, $\delta_{\mathrm{I}} = 1$, and therefore, from equation (3–7),

$$\int dv f(v) v \sigma_{\mathrm{I}} c v^{-1} = \sigma_{\mathrm{I}} c \int dv f(v) v \cdot v^{-1} = \sigma_{\mathrm{I}} c \int dv f(v)$$

$$= \sigma_{\mathrm{I}} c \tag{3–43}$$

since $\int dv f(v) \equiv 1$ by definition.

We therefore find that in region I,

$$q_{\mathrm{RG}-\overline{\mathrm{RG}}}(E_\gamma, \mathbf{r}) = n_p(\mathbf{r}) n_{\bar{p}}(\mathbf{r}) \sigma_{\mathrm{I}} c \zeta_\gamma \int dE_{\gamma 0} D(E_\gamma | E_{\gamma 0}) f(E_{\gamma 0})$$

$$\text{for } 10^{11}\ \mathrm{K} \lesssim T \lesssim 10^{13}\ \mathrm{K} \tag{3–44}$$

In temperature regions II and III, we cannot make the simplification given by equation (3–43); however, we can make a different simplification. In these temperature regions, $\beta \ll 1$, and Doppler broadening due to thermal effects provides only a negligible distortion on the γ-ray spectrum. Thus, in these temperature regions, we may write

$$D(E_\gamma | E_{\gamma 0}) \simeq \delta(E_\gamma - E_{\gamma 0}) \qquad (\beta \ll 1) \tag{3–45}$$

and therefore

$$\int dE_{\gamma 0} D(E_\gamma | E_{\gamma 0}) f(E_{\gamma 0}) \simeq f(E_\gamma) \tag{3–46}$$

In region II, $\delta_{\mathrm{II}} = 2$, and by reducing equation (3–42) and making use of the approximation (3–46), we obtain

$$q_{\mathrm{RG}-\overline{\mathrm{RG}}}(E_\gamma, \mathbf{r}) = n_p(\mathbf{r}) n_{\bar{p}}(\mathbf{r}) \sigma_{\mathrm{II}} c \zeta_\gamma \left(\frac{2mc^2}{\pi kT}\right)^{1/2} f(E_\gamma)$$

$$\text{for } 10^{4}\ \mathrm{K} \lesssim T \lesssim 10^{11}\ \mathrm{K} \tag{3–47}$$

In region III, $\delta_{\mathrm{III}} = 0.64$, and again reducing equation (3–42) and using the approximation (3–46), we find

$$q_{\mathrm{RG}-\overline{\mathrm{RG}}}(E_\gamma, \mathbf{r}) = n_p(\mathbf{r}) n_{\bar{p}}(\mathbf{r}) \sigma_{\mathrm{III}} c \zeta_\gamma \left[\frac{2}{\pi^{1/2}} \Gamma(1.68) \left(\frac{2kT}{mc^2}\right)^{0.18}\right] f(E_\gamma)$$

$$\text{for } 10\ \mathrm{K} \lesssim T \lesssim 10^{4}\ \mathrm{K} \tag{3–48}$$

We will consider more detailed applications of equations (3–44), (3–47), and (3–48) in a later chapter when we consider cosmological

formulations of these equations. However, it might be useful at this point to consider a simplified numerical example of these equations.

Present theoretical conceptions, based on recent empirical studies, indicate that the intergalactic medium is probably a very tenuous ionized gas with an average density of 10^{-7} to 10^{-5} atom per cubic centimeter at a temperature between 10^4 and 10^6 K, which places it in our temperature region II. It is found experimentally that approximately three γ-rays of energy greater than 100 MeV are produced for each p–$\bar{p}$ annihilation (i.e., $\zeta_\gamma = 3$). From equations (3–8), (3–9) and (3–47), and by taking $T = 10^6$ K, we find

$$I_{\mathrm{RG}-\overline{\mathrm{RG}}}(E_\gamma > 100\ \mathrm{MeV}) \simeq \frac{3B}{4\pi}\,\sigma_{\mathrm{II}}\,c\left(\frac{2mc^2}{\pi kT}\right)^{1/2}$$
$$\simeq 4.1 \times 10^{-14} B\ (\mathrm{cm^{-2}\text{-}s^{-1}\text{-}sr^{-1}}) \qquad (3\text{–}49)$$

Recent measurements (Clark, Garmire, and Kraushaar, 1968) have indicated that the isotropic flux of cosmic γ-rays in this energy region is $\lesssim 10^{-4}$ $\mathrm{cm^{-2}\text{-}s^{-1}\text{-}sr^{-1}}$. This places an upper limit on the emission measure B:

$$B \leqslant 2.4 \times 10^9 \qquad \mathrm{cm^{-5}} \qquad (3\text{–}50)$$

and, from equation (3–8), indicates that by dividing by the visible radius of the universe R_u,

$$\langle n_p n_{\bar{p}} \rangle = \frac{B}{R_u} \lesssim 2.4 \times 10^{-19} \qquad \mathrm{cm^{-6}} \qquad (3\text{–}51)$$

Thus, if $n_p \gtrsim 10^{-7}$ $\mathrm{cm^{-3}}$, the mean density of antimatter in intergalactic space is $\lesssim 2 \times 10^{-12}$ particles per cubic centimeter.

We will now go on to calculate the energy spectrum $f(E_\gamma)$.

3–4 MESON PRODUCTION AND THE STATISTICAL MODEL OF MATSUDA

In considering the production of mesons from p–$\bar{p}$ annihilation, we refer to the simple statistical model of Matsuda (1966) and the data of the Columbia University group presented in the Matsuda reference.

The Matsuda model assumes that shortly after annihilation the total energy of the p–$\bar{p}$ system (equal to $2m_p$) is distributed in an interaction volume Ω and that the system reaches thermal equilibrium. Since in the

annihilation the wave packets of the two particles completely overlap in an S state, then for

$$\Omega \simeq \left(\frac{\hbar}{m_\pi c}\right)^3$$

$$n_s \simeq \frac{\langle \zeta \rangle_{\text{expt}}}{\Omega} \tag{3-52}$$

$$\sigma \simeq \left(\frac{\hbar}{m_\pi c}\right)^2$$

(where n_s is the density of secondary particles produced) we find that the mean free path of the meson produced, l_{mfp}, is

$$l_{\text{mfp}} = \frac{1}{n_s \sigma} \simeq 10^{-1} \lambda_{\text{st}} \tag{3-53}$$

for an experimentally observed average number of mesons produced, ζ_{expt}, where λ_{st} is the distance traveled by the meson during the strong interaction in time $t_{\text{st}} = \lambda_{\text{st}} c^{-1} \simeq 10^{-23}$ s. Thus, we find that there is enough time available for the created mesons to collide with each other and reach thermal equilibrium before they leave the interaction volume Ω. Matsuda then assumes that there exists a quantized energy level $\epsilon_\tau > 0$ for each type of meson ($\tau = \pi, \rho, \omega, \eta, K, K^*$, etc.) produced in the annihilation. The whole system reaches a thermal equilibrium given by the parameter $\Phi = 1/kT$ at temperature T, which is therefore the same for each nonstrange boson (type $\sigma = \pi$, ρ, ω, η, etc.) or strange meson pair (type $\nu = K\bar{K}$, $K^*\bar{K}^*$, etc.). We designate the statistical weights by

$$g_\tau = (2S_\tau + 1)(2T_\tau + 1) \tag{3-54}$$

T_τ being the isospin of particle τ. Because the created mesons are bosons, we obtain

$$\langle \zeta_\tau \rangle = \frac{g_\tau}{e^{\Phi \epsilon_\tau} - 1} \tag{3-55}$$

Matsuda then introduces the chemical potential parameter ϵ_0 associated with the production of each particle and related to the observed average energy $\langle E_\tau \rangle$ of each particle through the relation

$$\epsilon_\tau = \langle E_\tau \rangle - \epsilon_0 \tag{3-56}$$

which must satisfy the condition

$$\epsilon_0 < \langle E_\tau \rangle \tag{3-57}$$

so that for nonstrange mesons equation (3–55) becomes

$$\langle \zeta_\sigma \rangle = \frac{g_\sigma}{\exp\left[\Phi(\langle E_\sigma \rangle - \epsilon_0)\right] - 1} \tag{3–58}$$

For pairs of strange mesons, equation (3–55) becomes

$$\langle \zeta_\nu \rangle = \frac{g_\nu}{\exp\left[\Phi(\langle E_\nu \rangle - 2\epsilon_0)\right] - 1} \tag{3–59}$$

since the formation of each meson involves energy ϵ_0.

The observed average energies of the various mesons produced in p–$\bar{p}$ annihilations at rest are listed by Matsuda and given here in table 3–2. We find that by specifying

$$\frac{1}{\Phi} = 150 \text{ MeV}$$

and (3–60)

$$\epsilon_0 = 295 \text{ MeV}$$

we obtain excellent agreement with the experimental production rate, as shown in table 3–2. The total average number of produced particles calculated from equations (3–58) and (3–59) is

$$\langle \zeta_{\text{Total}} \rangle = \sum_\sigma \langle \zeta_\sigma \rangle + \sum_\nu 2\langle \zeta_\nu \rangle = 4.37 \tag{3–61}$$

TABLE 3–2.—*Average Energies and Production Rates for Various Particles Produced in* p–$\bar{\text{p}}$ *Annihilations at Rest*

[Matsuda, 1966]

τ, particle or pair	Average energy, MeV	Calculated production rate	Experimental production rate
π	380	3.96	3.94 ± 0.33
ρ	850	2.3×10^{-1}	$(2.5 \pm 0.6) \times 10^{-1}$
ω	940	4.2×10^{-2}	$(4.5 \pm 0.7) \times 10^{-2}$
η	860	2.4×10^{-2}	$(1.4 \pm 0.5) \times 10^{-2}$
$K\bar{K}$	$(K)660$	3.1×10^{-2}	$(3.3 \pm 1.6) \times 10^{-2}$
$K\bar{K}^*, \bar{K}K^*$		20.6×10^{-3}	$(8.8 \pm 1.8) \times 10^{-3}$
$K^*\bar{K}^*$	$(K^*)980$	3.8×10^{-3}	$(3.9 \pm 0.7) \times 10^{-3}$

The value given by the experimental results is

$$\langle \zeta_{\text{Total}} \rangle_{\text{expt}} = 4.34 \tag{3-62}$$

which also agrees well with the calculation.

Both the experimental data and the simple statistical model of Matsuda indicate that in $p-\bar{p}$ annihilations at rest, ρ-meson production is an order of magnitude less important than pion production and that production of other mesons is at least two orders of magnitude less frequent than pion production. Table 3–3 shows the decay schemes of these mesons that lead to final-state γ-rays and other relevant data. Table 3–4 shows some recent data on meson production indicating that about 20 percent of the γ-rays produced arise through nonpionic meson production. The largest nonpion contribution to the γ-ray spectrum is due to the ρ-meson decay schemes

$$\begin{array}{l} \rho^{\pm} \rightarrow \pi^{\pm} + \pi^0 \\ \qquad\quad \hookrightarrow \gamma + \gamma \end{array} \tag{3-63}$$

The ρ meson is an isospin triplet ($T=1$) constructed from two pions,

TABLE 3–3.—*Decay Modes, Branching Ratios, and γ-Ray Multiplicities for Various Particles Produced in* p–$\bar{\text{p}}$ *Annihilations*

Decay mode	Branching ratio, R	$\zeta_\gamma R$
$\rho^{\pm} \rightarrow \pi^{\pm} + \pi^0$	~ 1.00	2.0
$\omega \rightarrow \pi^+ + \pi^- + \pi^0$	.89	1.78
$\rightarrow \pi^0 + \gamma$	.10	.30
$\eta \rightarrow \gamma + \gamma$	.386	.78
$\rightarrow 3\pi^0$ or $\pi^0 + 2\gamma$	.308	1.5
$\rightarrow \pi^+ + \pi^- + \pi^0$	.250	.5
$\rightarrow \pi^+ + \pi^- + \gamma$	.055	.05
$K^{\pm} \rightarrow \pi^{\pm} + \pi^0$ [a]	.215	.43
K_0 $K_1^0 \rightarrow \pi^0 + \pi^0$	.155	.62
K_0 $K_2^0 \rightarrow \pi^0 + \pi^0 + \pi^0$	.133	.80
K_0 $K_2^0 \rightarrow \pi^+ + \pi^- + \pi^0$	.067	.1
$K^* \rightarrow K + \pi$	—	—

[a] Other γ-ray-producing decay modes have negligible branching ratios.

TABLE 3–4.—*Production Rates for Various Meson-Producing Channels in* $p-\bar{p}$ *Annihilations at Rest*

[From Baltay et al., 1964]

Channel	Rate, %	ζ_γ	$\zeta_\gamma R$
$\rho^0\pi^0$	1.4 ± 0.2	2	2.8
$\rho^\pm\pi^\mp$	2.9 ± 0.4	2	5.8
$\rho^0\pi^+\pi^-$ [a]	$5.8\ ^{+0.3}_{-1.3}$	0	0
$\rho^0\rho^0$	0.4 ± 0.3	0	0
$\rho^0\pi^+\pi^-\pi^0$	7.3 ± 1.7	2	14.6
$\rho^\pm\pi^\mp\pi^+\pi^-$	6.4 ± 1.8	2	12.8
$\omega^0\pi^+\pi^-$ [a]	3.8 ± 0.4	2	7.6
$\eta^0\pi^+\pi^-$ [a]	1.2 ± 0.3	~ 2.6	3.1
$\omega^0\rho^0$	0.7 ± 0.3	2	—
$\eta^0\rho^0$	0.22 ± 0.17	~ 2.6	—

[a] Includes cases where $\pi^+\pi^-$ were from ρ^0 decay.

each having $T=1$. Evaluation of the Clebsch-Gordon coefficients for this construction yields

$$|\rho^+\rangle = \frac{1}{\sqrt{2}}\left(|\pi^+\rangle|\pi^0\rangle - |\pi^0\rangle|\pi^+\rangle\right)$$

$$|\rho^0\rangle = \frac{1}{\sqrt{2}}\left(|\pi^+\rangle|\pi^-\rangle - |\pi^-\rangle|\pi^+\rangle\right) \tag{3–64}$$

$$|\rho^-\rangle = \frac{1}{\sqrt{2}}\left(|\pi^0\rangle|\pi^-\rangle - |\pi^-\rangle|\pi^0\rangle\right)$$

Since the ρ^0 construction does not contain any $|\pi^0\rangle|\pi^0\rangle$ terms,

$$|\langle\pi^0\pi^0|\rho^0\rangle|^2 = 0 \tag{3–65}$$

and, therefore,

$$\rho^0 \not\to \pi^0 + \pi^0 \tag{3–66}$$

Gamma rays from $\rho^\pm$ decay (reaction (3–63)) possess an average energy of 210 MeV, not much different from the 190-MeV average energy given to γ-rays from the directly produced pions that are an order of magnitude more frequent. Because other mesons are produced even less frequently than the ρ mesons, we can conclude that mesons other than pions have a negligible effect on the total γ-ray spectrum from $p-\bar{p}$ annihilation.

3–5 SELECTION RULES

If we assume that the large majority of γ-rays from RG–$\overline{\text{RG}}$ interactions arise through π^0 decay (as was shown in the previous section), equation (3–36) reduces to

$$f(E_\gamma) = \int_{E\gamma+(m_\pi^2/4E\gamma)}^{\infty} dE_\pi \frac{f_A(E_\pi)}{(E_\pi^2 - m_\pi^2)^{1/2}} \tag{3–67}$$

as we showed in our derivation of equation (1–100).

The process

$$p + \bar{p} \rightarrow \pi^0 \tag{3–68}$$

is, of course, forbidden by conservation of momentum. The process

$$p + \bar{p} \rightarrow \pi^0 + \pi^0 \tag{3–69}$$

is also forbidden since p–$\bar{p}$ annihilations at rest occur predominantly from the S states of the p–$\bar{p}$ system.

The selection rule that forbids reaction (3–69) follows from conservation of G conjugation parity.

The process of G conjugation is an extension of charge (C) conjugation, which holds for neutral as well as charged particles. It is defined as

$$G = Ce^{i\pi T_2} \tag{3–70}$$

where C is the charge-conjugation operator and T_2 is the second component of the isospin vector. From (3–70) we can show the commutation relation

$$[\mathbf{T}, G] = 0 \tag{3–71}$$

Thus, we may describe particle states as simultaneous eigenstates of both G and T.

It can be shown (Sakurai, 1964) that systems having baryon number 0 are in an eigenstate of G. The p–$\bar{p}$ system is just such a system. For this system

$$G = (-1)^{L+S+T} \tag{3–72}$$

where L, S, and T are the orbital, spin, and isospin quantum numbers of the state, respectively.

In a state consisting of a single pion, $L = 0, S = 0, T = 1$, and, therefore, $G = -1$. In a final state consisting of ζ_π pions, G is given by

$$G = (-1)^{\zeta_\pi} \tag{3–73}$$

The selection rules (3–72) and (3–73) indicate that for an S-state annihilation ($L=0$), the final state consisting of two neutral pions is strictly forbidden (Lee and Yang, 1956).

Therefore, the extremum γ-ray energies that we would expect from this decay would result from interactions of the type

$$p+\bar{p}\rightarrow \pi^+ + \pi^- + \pi^0 \tag{3–74}$$

resulting in pions with the given maximum energy

$$\begin{aligned} E_{\pi^0,\,\max} &= \frac{1}{2(2m_p)}\left[(2m_p)^2 + m_{\pi^0}^2 - (2m_{\pi^\pm})^2\right] \\ &= m_p - \frac{3}{4}\frac{m_\pi^2}{m_p} \simeq 923 \text{ MeV} \end{aligned} \tag{3–75}$$

Thus, the annihilation γ-rays are limited to the energy region

$$\tfrac{1}{2}\left[E_{\pi^0,\,\min} - (E_{\pi^0,\,\max}^2 - m_\pi^2)^{1/2}\right] \leq E_\gamma \leq \tfrac{1}{2}\left[E_{\pi^0,\,\max} + (E_{\pi^0,\,\max}^2 - m_\pi^2)^{1/2}\right] \tag{3–76}$$

or 5 MeV $\leq E_\gamma \leq$ 919 MeV.

The process

$$p+\bar{p}\rightarrow \gamma+\gamma \tag{3–77}$$

may also occur; but this process, involving the electromagnetic emission (em) of two photons, is of the order

$$\sigma_{\text{em}} = \alpha^2 \sigma_{A,\,\text{strong}} \simeq \frac{2.6\times 10^{-30}\ \text{cm}^2}{\beta} \tag{3–78}$$

and therefore this process may be neglected as a significant contribution to γ-ray production.

3–6 THE GAMMA-RAY SPECTRUM FROM PROTON-ANTIPROTON ANNIHILATIONS AT REST

As we showed in the previous section, we can neglect the contribution from the decay of mesons other than neutral pions in calculations of the γ-ray spectrum from p–$\bar{p}$ annihilations at rest. The normalized γ-ray spectrum was calculated numerically from the relation (3–68) by the author, with the normalized distribution function $f_A(E_\pi)$ taken from the calculations of Maksimenko (1958), based on the statistical theory of multiple particle production.

The resultant spectrum, up to 750 MeV, is shown in figure 3–3. Frye and Smith (1966) have recently calculated the γ-ray spectrum from p–$\bar{p}$

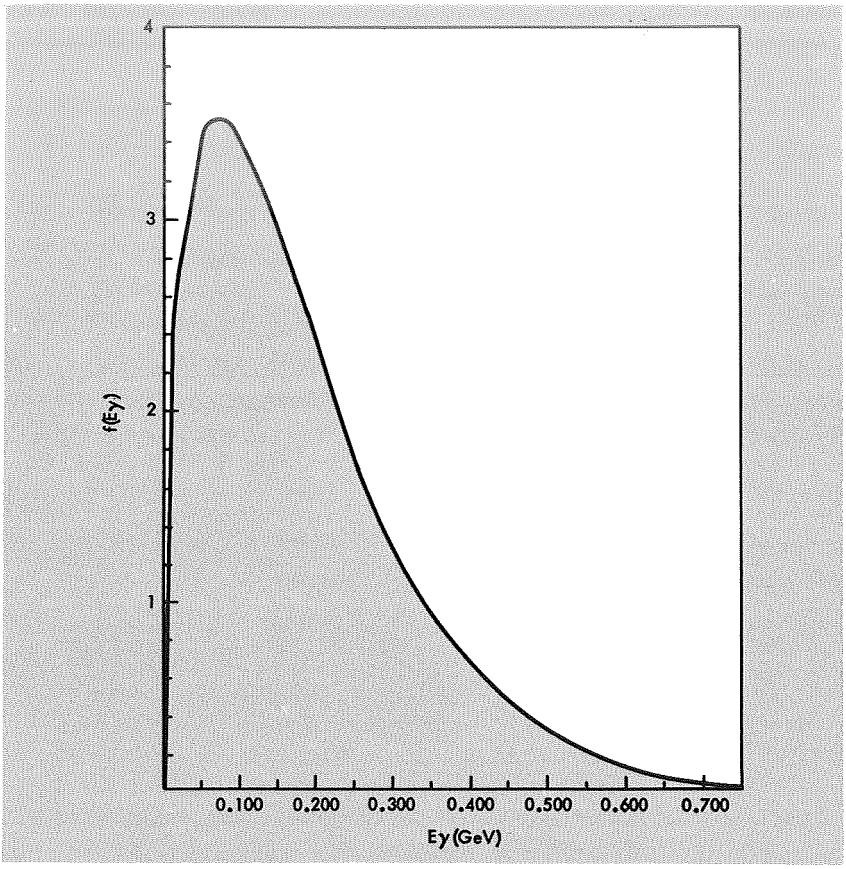

FIGURE 3–3.—Normalized γ-ray spectrum from p–$\bar{p}$ annihilation.

annihilation up to 500 MeV, based on recent measurements of charged pions from p–$\bar{p}$ annihilation by the Columbia University group. The excellent agreement between the results of figure 3–3 and the calculations of Frye and Smith not only serves as a mutual check on the calculations but also supports our previous conclusion that mesons other than pions have a negligible effect on the total γ-ray spectrum from p–$\bar{p}$ annihilation at rest.

The absolute magnitude of the γ-ray spectrum from p–$\bar{p}$ annihilation at rest is obtained from equation (3–44), (3–47), or (3–48), depending upon the temperature region involved.

3–7 PROTON-ANTIPROTON ANNIHILATIONS IN FLIGHT

We now turn our attention to RG–$\overline{\text{CR}}$ interactions. Here, because of limitations in the data, as well as kinematic and dynamic similarities that

would make the γ-ray spectra from such interactions difficult to distinguish from the γ-ray spectra of the much more prevalent RG–CR interactions, we will present only a qualitative treatment.

An excellent review article on high-energy interactions of antiprotons in hydrogen has been presented by Baltay et al. (1964). For high-energy p–$\bar{p}$ interactions, annihilations of the types

$$p + \bar{p} \rightarrow p + \bar{p} + \text{bosons} \tag{3–79}$$

$$p + \bar{p} \rightarrow \begin{cases} N + \bar{N}^* + \text{bosons} \\ N^* + \bar{N} + \text{bosons} \\ N^* + \bar{N}^* + \text{bosons} \end{cases} \tag{3–80}$$

and

$$p + \bar{p} \rightarrow \begin{cases} Y + \bar{Y} \\ Y + \bar{Y}^* + \text{bosons} \\ Y^* + \bar{Y} + \text{bosons} \\ Y^* + \bar{Y}^* + \text{bosons} \end{cases} \tag{3–81}$$

may occur, as well as annihilations of the type previously considered.

Reactions of the type given by equation (3–80) seem to occur frequently and to be of a similar nature as p–p interactions. For example (Ferbel et al., 1962, and Ferbel et al., 1965), p–$\bar{p}$ interactions in the 3- to 4-GeV/c range lead to strong production of the $\Delta(1.238)$ isobar, while at 7 GeV/c no single resonance seems to dominate. The angular distribution of the outgoing baryons is strongly peaked in the forward and backward directions in the collision cms. All these facts hold true for the p–p interactions as we will discuss in detail in chapter 6. In the energy range where production of the $\Delta(1.238)$ isobar predominates, production of neutral pions occurs at roughly the same rate in both p–p and p–$\bar{p}$ interactions, as indicated in table 3–5 (Baltay et al., 1964).

This fact, too, strongly highlights the similarity between p–p and nonannihilation p–$\bar{p}$ interactions at similar energies. Thus, in the 3- to

TABLE 3–5.—*Cross Sections for Inelastic Single Neutral-Pion Production in* p–$\bar{\text{p}}$ *Interactions as a Function of Incident Momentum*

Reaction	Collision momentum, GeV/c	Cross section, mb
$\bar{p} + p \rightarrow \bar{p} + p + \pi^0$	3.25	2.3 ± 0.5
$p + p \rightarrow p + p + \pi^0$	3.67	2.9 ± 0.3

4-GeV/c range, neutral (and charged) pion production is dominated by the channel

$$\begin{array}{ccc} & \Delta+\bar{N} & \\ \nearrow & & \searrow \\ p+\bar{p} & & N+\bar{N}+\pi^0 \\ \searrow & & \nearrow \\ & \bar{\Delta}+N & \end{array} \qquad (3\text{–}82)$$

It may therefore be assumed that the nonannihilation RG–$\overline{\text{CR}}$ (or CR–$\overline{\text{RG}}$) interactions will lead to γ-ray spectra with the same characteristics as those from high-energy p–p interactions. (See chs. 5 and 6.) Experiments also show that in p–$\bar{p}$ interactions between 1.6 and 7.0 GeV/c (Böckmann et al., 1966), nonannihilation production of pions increases with respect to annihilation production. At 5.7 GeV/c, the cross sections for the two processes are comparable (and also are comparable to the cross section for inelastic p–p interactions).

Böckmann et al. (1966) find these values for the cross sections at 5.7 GeV/c:

$$\begin{array}{ll} p+\bar{p}\rightarrow p+\bar{p}+\text{bosons (inelastic)} & 24.8\pm 2.0 \text{ mb} \\ p+\bar{p}\rightarrow \text{bosons (annihilation)} & 22.5\pm 2.0 \text{ mb} \end{array} \qquad (3\text{–}83)$$

The pion multiplicity in annihilation interactions rises slowly with energy, as shown in table 3–6.

The cross sections in tables 3–7 and 3–8 are comparable in magnitude to those given in chapter 5 for hyperon production in p–p interactions. As in p–p interactions, these cross sections are small relative to pion-production cross sections, but increase with energy. The outgoing hyperons are observed to be emitted strongly in the forward and backward directions, as in the case of p–p interactions. Also, in interactions involving final-state Y- and π-production, resonances (strange isobars) of the type

$$Y^*\rightarrow Y+\pi \qquad (3\text{–}84)$$

are commonly produced.

TABLE 3–6.—*Average Pion Multiplicity in Annihilation Interactions as a Function of Incident Momentum*

Momentum, GeV/c	Multiplicity	Reference
0	~ 4.3	Matsuda (1966)
3.25	~ 6.0	Baltay et al. (1964)
5.7	~ 7.3	Böckmann et al. (1966)

TABLE 3–7.—*Cross Sections for Hyperon-Antihyperon Production in* $p-\bar{p}$ *Interactions*

Final state	Cross section, μb	
	3.25 GeV/c	3.69 GeV/c
$\Lambda\bar{\Lambda}$	87 ± 13	94 ± 14
$\Lambda\bar{\Sigma}^0$, $\bar{\Lambda}\Sigma^0$	56 ± 11	76 ± 14
$\Sigma^+\bar{\Sigma}^-$, $\Sigma^-\Sigma^+$	38 ± 11	56 ± 14
$\Xi^-\Xi^+$	4 [a]	5 [a]
$\Lambda\bar{\Lambda} + n\pi^0$, $\Lambda\bar{\Sigma}^0 + n\pi^0$, $\bar{\Lambda}\Sigma^0 + n\pi^0$	102 ± 39	122 ± 43
$\Lambda\bar{\Lambda}\pi^+\pi^-$	15 ± 6	30 ± 9
$\Sigma^\pm\bar{\Lambda}\pi^\mp$, $\bar{\Sigma}^\pm\Lambda\pi^\mp$	51 ± 18	143 ± 45
$\Sigma^\pm\bar{\Sigma}^\mp\pi^0$	7 ± 5	28 ± 19
$KN(\bar{\Lambda}$ or $\bar{\Sigma})$, $K\bar{N}(\Lambda$ or $\Sigma)$	24 ± 10	41 ± 14
Total antihyperon production	438 ± 52	710 ± 78

[a] Based on one event at each energy.

TABLE 3–8.—*Cross Sections for the Reaction* $p + \bar{p} \rightarrow \Lambda + \bar{\Lambda}$ *as a Function of Incident Momentum*

Momentum, GeV/c	Cross section, μb	Reference
1.61	57 ± 18	Button et al. (1961)
3.25	87 ± 13	Baltay et al. (1964)
3.69	94 ± 14	Baltay et al. (1964)

We can summarize the findings for high-energy $p-\bar{p}$ interactions as follows:

(1) There are two distinct types of pion-production processes that may be considered: (*a*) annihilations and (*b*) inelastic pion production without annihilation.
(2) The ratio of occurrence of process (*b*) relative to process (*a*) increases with increasing energy between 1.6 and 7.0 GeV/c and is approximately 1 at 5.7 GeV/c.
(3) Inelastic interactions (without annihilation) are very similar to $p-p$ interactions and exhibit similar resonance production and forward-backward peaking.

(4) Strange particles are produced in similar quantities in both inelastic $p-p$ and $p-\bar{p}$ interactions.

For these reasons, we may assume that

(1) An "isobar-plus-fireball" model, similar to that discussed in chapter 5 may be applicable to high-energy $p-\bar{p}$ interactions. In this case, annihilation interactions may be included as an added contribution to the fireball component.

(2) At high energies ($E_\gamma > 5$ GeV) there is at present no reason to assume that the characteristics of the γ-ray spectrum from $p-\bar{p}$ interactions will differ from those of the γ-ray spectrum from $p-p$ interactions.

GAMMA-RAY ABSORPTION MECHANISMS

4–1 INTRODUCTION

In this chapter, we wish to discuss the various processes that are of astrophysical importance in depleting γ-rays in the galaxy and the universe. By "absorption" we will mean not only those processes in which the γ-ray completely disappears, such as pair-production, but also those processes in which the γ-ray is scattered out of the energy range of interest, as can occur in the case of Compton scattering.

We will consider two basic categories of absorption processes: Absorption of γ-rays in matter and absorption of γ-rays through interactions with radiation. The latter process is of importance because of the recently discovered 2.7 K blackbody radiation field which is now believed to fill the universe and to be a remnant of the initial cosmological "big-bang."

4–2 ABSORPTION OF GAMMA RAYS THROUGH INTERACTIONS WITH RADIATION

Let us first consider the effects of the universal radiation field on the intensity of cosmic γ-rays. The attenuation process of importance here is the pair-production process

$$\gamma + \gamma_{bb} \rightarrow e^+ + e^- \tag{4–1}$$

where γ represents the cosmic γ-ray and γ_{bb} the low-energy blackbody photon with which it interacts. This process can only take place if the total energy of the γ-rays in the cms of the interaction is greater than or equal to $2m_ec^2$. The cross section for reaction (4–1) can be calculated using quantum electrodynamics and a derivation may be found in Jauch and Rohrlich (1955). The importance of reaction (4–1) in astrophysics was first pointed out by Nikishov (1961) in considering interactions of γ-rays with ambient starlight photons and with the discovery of the universal thermal radiation. Gould and Schréder (1966, 1967a, b) and Jelly (1966) were quick to point out the opacity of the universe to γ-rays

of energy above 10^{14} eV. Stecker (1969c) and Fazio and Stecker (1970) generalized these calculations by including cosmological effects at high redshifts. (See ch. 13.)

In discussing reaction (4–1), we will generally follow the discussion of Gould and Schréder (1967a, b) with one important difference: At the time Gould and Schréder published their papers, it was generally thought that the universal blackbody radiation field was at a temperature of 3.0 K. More recent measurements (Stokes, Partridge, and Wilkinson, 1967) have yielded a temperature of 2.7 K for the blackbody radiation with a corresponding photon energy density of 0.25 eV/cm^3 instead of the value of 0.38 eV/cm^3 used by Gould and Schréder. Therefore, we have corrected the Gould and Schréder results to correspond to a 2.7 K radiation field.

In order to determine the threshold energy for reaction (4–1), we make use of the same procedure used in the derivation of equation (1–59) and start with the four-momentum invariance given by equation (1–52). Again, if we denote cms quantities by a prime and note that

$$E'_{e^+} = E'_{e^-} \equiv E'_e \tag{4–2}$$

equation (1–52) reduces to

$$\begin{aligned}(2E'_e)^2 &= (E_{\mathrm{bb}} + E_\gamma)^2 - |(\mathbf{p}_{\mathrm{bb}} + \mathbf{p}_\gamma)|^2 \\ &= (E^2_{\mathrm{bb}} + 2E_{\mathrm{bb}}E_\gamma + E^2_\gamma) - (E^2_{\mathrm{bb}} + E^2_\gamma - 2E_{\mathrm{bb}}E_\gamma \cos\theta) \\ &= 2E_{\mathrm{bb}}E_\gamma(1 - \cos\theta)\end{aligned} \tag{4–3}$$

To determine the threshold energy for reaction (4–1), we only need to specify that at this energy both the electron and the positron are produced at rest in the cms of the interaction. The minimum energy required is the one which corresponds to a head-on collision ($\cos\theta = -1$). Equation (4–3) then reduces to the relation specifying the threshold energy as

$$E_{\gamma,\,\mathrm{th}} = \frac{m_e^2}{E_{\mathrm{bb}}} \tag{4–4}$$

where, as in chapter 1, we have used the convention $c = 1$. It is interesting to note here the similarity between equation (4–4) and equation (1–97) for neutral pion decay. This is no accident and can be seen by picturing the pion decay run backward; however, instead of a pion, we picture the reverse decay of a particle made up of an electron and a positron stuck together, with a total rest mass of $2m_e$.

If we consider a typical blackbody photon to have an energy of approximately 10^{-9} MeV, then from equation (4–4) we find a threshold energy of approximately 2.5×10^{8} MeV for reaction (4–1). However, this threshold is somewhat blurred because the blackbody photons are not all at the same energy, but have a Bose-Einstein distribution in energy given by the well-known formula

$$n(E_{\mathrm{bb}}) = \frac{1}{\pi^2 \hbar^3 c^3} \frac{E_{\mathrm{bb}}^2}{1 - \exp\ (E_{\mathrm{bb}}/kT)} \tag{4–5}$$

We must also allow for the various possible values of cos θ given by the isotropic distribution (1–68) as

$$f(\theta) = \tfrac{1}{2} \sin\ \theta \tag{4–6}$$

The cross section for (4–1) is given by Jauch and Rohrlich (1955)

$$\sigma(E_{\mathrm{bb}}, E_\gamma) = \tfrac{1}{2}\sigma_0(1-\beta_e'^2)\ \left[(3-\beta_e'^4)\ \ln \frac{1+\beta_e'}{1-\beta_e'} - 2\beta_e'(2-\beta_e'^2)\right] \tag{4–7}$$

where the cms velocity of the electron (or positron) is given by

$$\beta_e' = \left(1 - \frac{m_e^2}{E_{\mathrm{bb}} E_\gamma}\right)^{1/2} \tag{4–8}$$

The absorption coefficient for γ-radiation against pair-production by interactions with the blackbody radiation is given by

$$\kappa_{\gamma\gamma}(E_\gamma) = \iint dE_{\mathrm{bb}}\ d\theta\ \frac{\sin\ \theta}{2}\ n(E_{\mathrm{bb}})\sigma(E_{\mathrm{bb}}, E_\gamma)(1 - \cos\ \theta) \tag{4–9}$$

Gould and Schréder (1967) have reduced equation (4–9) to the form

$$\kappa_{\gamma\gamma}(E_\gamma) = \alpha^3(\pi r_0)^{-1}\left(\frac{kT}{mc^2}\right)^3 f(\nu) \tag{4–10}$$

where

$$\nu \equiv \frac{(mc^2)^2}{E_\gamma kT} \tag{4–11}$$

They find that the function $f(\nu)$ has a maximum value ≈ 1 at $\nu \approx 1$ and that $f(\nu)$ has the asymptotic forms given by

$$f(\nu) \rightarrow \tfrac{1}{3}\pi^3 \nu\ \ln\ (0.117\nu) \qquad \text{for } \nu \ll 1$$

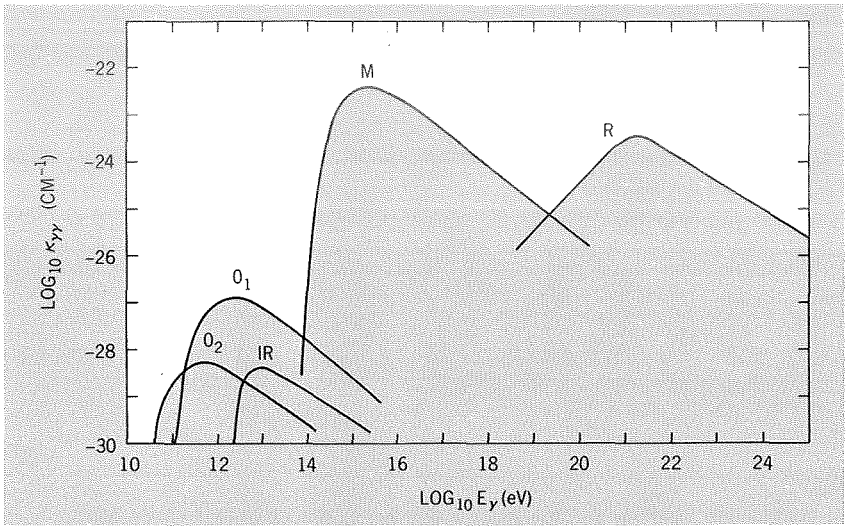

FIGURE 4–1.—Absorption probability per unit distance by $\gamma+\gamma' \rightarrow e^+ + e^-$ as a function of photon energy for γ-rays traversing the cosmic-photon gas. The contributions from the optical (O_1 and O_2), infrared (IR), microwave (M), and radio (R) cosmic-photon gas are shown. Absorption at lower energies by X-ray photons is negligible. O_1 represents the contribution from the light of population II stars; O_2 that from population I stars (from Gould and Schréder, 1967a, b); M is corrected to 2.7 K.

and

$$f(\nu) \rightarrow (\tfrac{1}{4}\pi\nu)^{1/2}e^{-\nu}\left(1+\frac{75}{8\nu}+\cdots\right) \qquad \text{for } \nu \gg 1 \qquad (4\text{–}12)$$

They have also calculated $\kappa_{\gamma\gamma}$ for γ-ray interactions with various photon fields in intergalactic space. The results of their numerical calculation are shown in figure 4–1.

4–3 ABSORPTION OF GAMMA RAYS THROUGH INTERACTIONS WITH MATTER

There are two types of interactions of importance to be considered here. The first is the Compton scattering interaction

$$\gamma + e^- \rightarrow \gamma + e^- \qquad (4\text{–}13)$$

whose cross section is given by the Klein-Nishima formula

$$\sigma_c(E_\gamma) = 2\sigma_0\left\{\frac{1+\epsilon}{\epsilon^2}\left[\frac{2(1+\epsilon)}{1+2\epsilon}-\frac{1}{\epsilon}\ln(1+2\epsilon)\right]+\frac{1}{2\epsilon}\ln(1+2\epsilon) - \frac{1+3\epsilon}{(1+2\epsilon)^2}\right\} \qquad (4\text{–}14)$$

where we have defined

$$\epsilon \equiv \frac{E_\gamma}{mc^2} \tag{4–15}$$

In the asymptotic limits,

$$\sigma_c \rightarrow \frac{8}{3}\sigma_0(1-2\epsilon+5.2\epsilon^2-13.3\epsilon^3+\cdots) \qquad \text{for } \epsilon \ll 1 \tag{4–16}$$

and

$$\sigma_c \rightarrow \frac{\sigma_0}{\epsilon}\left[\frac{1}{2}+\ln 2\epsilon\right] \qquad \text{for } \epsilon \gg 1 \tag{4–17}$$

Electrons play the dominant role in the Compton scattering of γ-rays. As we mentioned previously, Compton scattering does not eliminate the γ-ray per se, but will in all probability result in the transfer of some the energy of the γ-ray to the electron, thus absorbing the γ-ray's energy. For γ-rays of energy $E_\gamma \gg mc^2$, almost all of the energy of the γ-ray is absorbed, and then we can consider that the γ-ray has "disappeared."

In some cases it is useful to define an "absorption cross section" σ_a, such that

$$\sigma_a = \left(\frac{\Delta E_\gamma}{E_\gamma}\right)\sigma_c \tag{4–18}$$

where ΔE_γ is the average amount of energy transferred from the γ-ray to the electron. It is then found that (Heitler, 1954)

$$\sigma_a = \epsilon\sigma_c \qquad \text{for } \epsilon \ll 1 \tag{4–19}$$

and

$$\sigma_a = \sigma_c\left[\frac{\ln 2\epsilon - \frac{5}{6}}{\ln 2\epsilon + \frac{1}{2}}\right] \qquad \text{for } \epsilon \gg 1 \tag{4–20}$$

The second type of γ-ray absorption process in matter that we must consider involves the conversion of a γ-ray into an electron-positron pair in the electrostatic field of a charged particle or nucleus. If we designate such a charge field by the symbol CF, such an interaction may be symbolically written as

$$\gamma + \text{CF} \rightarrow e^+ + e^- + \text{CF} \tag{4–21}$$

The conversion interaction, or pair-production as it is usually called, has a cross section that involves an extra factor of the fine structure constant, $\alpha = e^2/hc$, since it involves an intermediate interaction with an electrostatic field. At nonrelativistic energies, this cross section is a complicated function of energy which must be determined numerically.

(See Heitler, 1954, for further details.) However, a closed analytic approximation for this cross section may be given for energies greater than 1 MeV, which corresponds to the energy region where the pair-production cross section becomes more important than the Compton scattering cross section in the determination of the γ-ray mass absorption coefficient for hydrogen gas.

For pair-production in the field of a nucleus of atomic number Z, the cross section for reaction (4–21) is given by

$$\sigma_p = \frac{\alpha}{\pi}\sigma_0\left(\frac{28}{9}\ln 2\epsilon - \frac{218}{27}\right)Z^2 \qquad \text{for } 1 \ll \epsilon \ll \alpha^{-1}Z^{-1/3} \tag{4–22}$$

which is the energy region where electron screening of the nuclear charge field may be neglected. The no-screening case, of course, also holds for an ionized gas (plasma).

In the energy region where the complete screening approximation is valid,

$$\sigma_p = \frac{\alpha}{\pi}\sigma_0\left[\frac{28}{9}\ln\left(183Z^{-1/3}\right) - \frac{2}{27}\right]Z^2 \qquad \text{for } \epsilon \gg \alpha^{-1}Z^{-1/3} \tag{4–23}$$

The threshold energy for pair-production in the field of an atomic nucleus is, of course, $2m_ec^2$. In the case of pair-production in the field

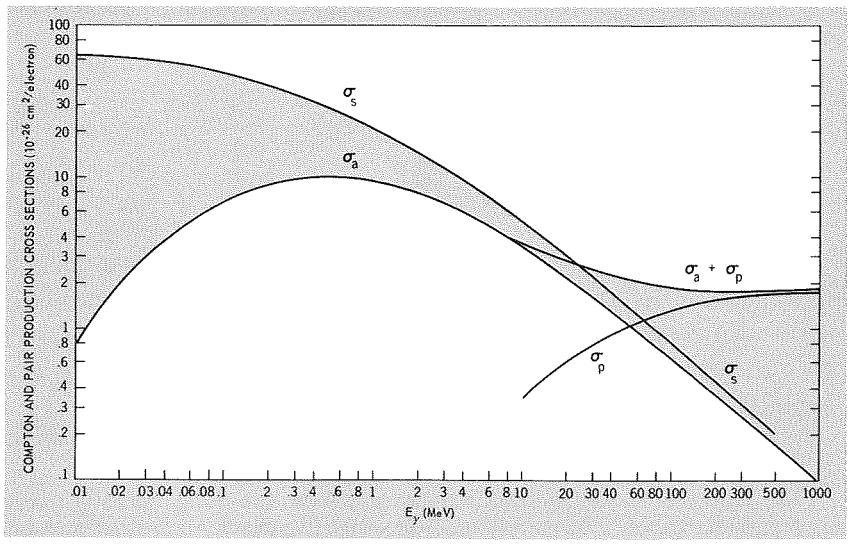

FIGURE 4–2.—Compton scattering (σ_s), Compton absorption (σ_a), pair-production and total ($\sigma_a + \sigma_p$) cross sections as a function of γ-ray energy for absorption of γ-rays in hydrogen gas (based in part on work of Nelmes, 1953).

of atomic electrons, the threshold energy for (4–21) is $4m_e c^2$. Above this energy, the pair-production cross section must be modified to include the additional contribution of the electrons and this may be done approximately by making the replacement

$$Z^2 \rightarrow Z^2(1 + \xi^{-1}Z^{-1}) \tag{4–24}$$

in equations (4–22) and (4–23), where the quantity ξ varies from ≈ 2.6 at $E_\gamma \approx 6.5$ MeV to ≈ 1.2 at $E_\gamma \approx 100$ MeV. For γ-ray energies above 200 MeV, $\xi \approx 1$; and the pair-production cross section has an approximately constant value of 1.8×10^{-26} cm^2, according to the results of Trower (1966). The values of the various cross sections for γ-ray absorption in matter, as discussed in this section, are shown in figure 4–2.

411-892 O - 71 - 7

2

Galactic Gamma Rays

The Form of the Cosmic Gamma-Ray Production Spectrum From Galactic Cosmic-Ray Interactions for Gamma-Ray Energies Less Than 1 GeV

5-1 INTRODUCTION

In chapter 1, general formulas were derived for the calculation of the γ-ray spectrum due to secondary particles produced in cosmic-ray collisions with atoms of the interstellar or intergalactic gas.

This chapter will deal with a calculation of the γ-ray spectrum for $E_\gamma < 1$ GeV. In this energy region the analysis is complicated by the lack of a complete understanding of the various modes of pion production. Therefore, the analysis will be carried out in two steps. The first step will be a discussion of the general properties of γ-ray spectra from neutral pion decay, with a determination of the various features of such spectra that must, in general, hold true. This discussion will include the results of analytic and numerical calculations of normalized γ-ray spectra from ideal neutral pion energy distributions. Such results serve two purposes:

(1) They add to an understanding of the salient features of γ-ray spectra from neutral pion decay.
(2) They serve as a test for the accuracy of similar numerical computations where an analytic comparison cannot be obtained.

The general features of γ-ray spectra resulting from neutral pion decay should be kept in mind whenever a discussion of a particular result is desired. The general results will prove invaluable as a guide in discussing the results of the particular model used in the numerical calculations.

Following the general analysis of γ-ray spectra from neutral pion decay, a specific model will be chosen that will be used for numerical calculation of the γ-ray spectrum below 1 GeV. This model is of necessity an oversimplification of the true physics of pion production, but it can be made to fit the present accelerator data to an extent that is adequate for our purposes. The model is of the "isobar-plus-fireball" type. The terms "isobar" and "fireball" are here loosely defined to characterize the main features of the model. The model assumes that at accelerator energies

there exist two dominant modes of pion production. Thus we may speak of two pion components: The isobar component, which dominates pion production in collisions where the cosmic-ray protons have energies in the low GeV range; and the fireball component, which supplies the main bulk of pions for $p-p$ collisions of initial energy greater than 5 GeV.

5-2 GENERAL PROPERTIES OF THE GAMMA-RAY SPECTRUM FROM THE DECAY $\pi^0 \rightarrow \gamma + \gamma$

More neutral pions are produced in high-energy collisions than any other γ-ray-producing secondary particle. We will therefore turn our attention to the properties of the γ-ray spectrum produced by the decay

$$\pi^0 \rightarrow \gamma + \gamma \tag{5-1}$$

We will consider a normalized distribution of neutral pions; i.e., $f(E_\pi)$ such that

$$\int dE_\pi f(E_\pi) = 1 \tag{5-2}$$

We have already shown in chapter 1 how the γ-ray spectrum is related to the neutral pion spectrum. In terms of normalized distribution functions, this relation may be expressed as

$$F(E_\gamma) = \int_\epsilon^\infty dE_\pi \frac{f(E_\pi)}{(E_\pi^2 - m_\pi^2)^{1/2}} \tag{5-3}$$

where $F(E_\gamma)$ is a normalized γ-ray distribution function resulting from the decay of neutral pions, and

$$\epsilon = E_\gamma + \frac{m_\pi^2}{4E_\gamma} \tag{5-4}$$

(See derivation of eq. (1-100).)

Equation (5-4) can be written in the quadratic form

$$E_\gamma^2 - \epsilon E_\gamma + \frac{m_\pi^2}{4} = 0 \tag{5-5}$$

This equation has two roots, $E_{\gamma 1}$ and $E_{\gamma 2}$, such that

$$\epsilon(E_{\gamma 1}) = \epsilon(E_{\gamma 2}) \tag{5-6}$$

Since these roots are solutions of a quadratic equation given by equation (5–5), they must satisfy the condition

$$E_{\gamma 1} \cdot E_{\gamma 2} = \frac{m_\pi^2}{4} \tag{5–7}$$

We will find it useful to express equation (5–7) in logarithmic form and to define

$$\nu \equiv \ln \frac{m_\pi}{2}$$

$$\delta_1 \equiv \nu - \ln E_{\gamma 1}$$

and

$$\delta_2 \equiv \nu - \ln E_{\gamma 2} \tag{5–8}$$

Equation (5–7) then reduces to

$$\delta_1 = -\delta_2 \tag{5–9}$$

or

$$|\delta_1| = |\delta_2| \equiv \delta \tag{5–10}$$

It follows from equation (5–6) that

$$\epsilon(\nu - \delta) = \epsilon(\nu + \delta) \tag{5–11}$$

and therefore

$$F(\nu - \delta) = F(\nu + \delta) \tag{5–12}$$

where the function F is now expressed in terms of $\ln E_\gamma$. Equation (5–12) expresses a useful symmetry on a graph of $F(\ln E_\gamma)$. On a graph of this type, the curve defined by $F(\ln E_\gamma)$ is symmetric about the line $\ln E_\gamma = \nu$ and thus reflects into itself about this line. This property is illustrated in figure 5–1.

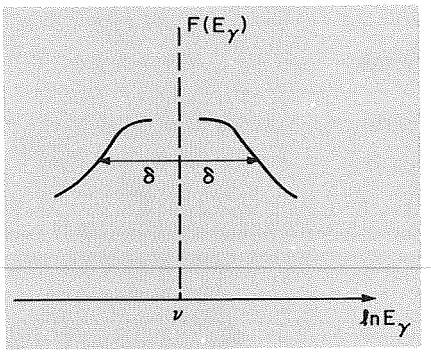

FIGURE 5–1.—A schematic representation of the form of $F(\ln E_\gamma)$ expressing the implications of equation (5–12).

Equation (5–11) can also be expressed as

$$F(E_\gamma) = F\left(\frac{m_\pi^2}{4E_\gamma}\right) \tag{5–13}$$

which is easily seen to be a direct consequence of equations (5–4) and (5–5). Thus, for the important asymptotic cases where the γ-ray spectral distribution function can be approximated by a power law with exponent Γ of the form

$$F(E_\gamma) \rightarrow KE_\gamma^\Gamma \qquad \text{for } E_\gamma > \tilde{E} \tag{5–14}$$

which we will later show to be of astrophysical significance, it follows that

$$F(E_\gamma) \rightarrow K'E^\Gamma \qquad \text{for } E_\gamma < \frac{m_\pi^2}{4\tilde{E}} \tag{5–15}$$

where

$$K' = K(\tfrac{1}{2}m_\pi)^{-2\Gamma} \tag{5–16}$$

Let us now define

$$G(E_\pi) = \frac{f(E_\pi)}{(E_\pi^2 - m_\pi^2)^{1/2}} \tag{5–17}$$

From physical restrictions, it follows that

$$f(E_\pi) \geq 0 \tag{5–18}$$

and

$$(E_\pi^2 - m_\pi^2)^{1/2} \geq 0 \tag{5–19}$$

so that

$$G(E_\pi) \geq 0 \tag{5–20}$$

We can now rewrite equation (5–3) as the functional relation

$$F[\epsilon] = \int_\epsilon^\infty dt\ G(t) \tag{5–21}$$

where t is a dummy variable of integration.

It follows that

$$F[\epsilon_\alpha] = F[\epsilon_\beta] + \int_{\epsilon_\alpha}^{\epsilon_\beta} dt\ G(t) \tag{5–22}$$

where

$$\epsilon_\alpha < \epsilon_\beta$$

and, from equation (5–20),

$$F[\epsilon_\alpha] \geq F[\epsilon_\beta] \qquad \text{for } \epsilon_\alpha < \epsilon_\beta \tag{5–23}$$

Equation (5–23) shows that $F[\epsilon]$ is a monotonically decreasing functional of ϵ.

In order to relate $F[\epsilon]$ to $F(E_\gamma)$, we must consider the quantity

$$\epsilon' \equiv \frac{\partial \epsilon}{\partial E_\gamma} \tag{5–24}$$

From equation (5–4), it follows that

$$\epsilon' = 1 - \frac{m_\pi^2}{4E_\gamma^2} \tag{5–25}$$

Using equations (5–8) and (5–25), we obtain

$$\epsilon' < 0 \qquad \text{for } \ln E_\gamma < \nu$$

$$\epsilon' = 0 \qquad \text{for } \ln E_\gamma = \nu$$

and

$$\epsilon' > 0 \qquad \text{for } \ln E_\gamma > \nu \tag{5–26}$$

We now write

$$\frac{\partial \epsilon}{\partial \delta} = \epsilon' \frac{\partial E_\gamma}{\partial \delta} \tag{5–27}$$

so that

$$\epsilon_\beta = \epsilon_\alpha + \Delta\epsilon = \epsilon_\alpha + \frac{\partial \epsilon}{\partial \delta} \Delta\delta \tag{5–28}$$

From equations (5–8) and (5–10), it follows that

$$\frac{\partial E_\gamma}{\partial \delta} > 0 \qquad \text{for } \ln E_\gamma = \nu + \delta$$

and (5–29)

$$\frac{\partial E_\gamma}{\partial \delta} < 0 \qquad \text{for } \ln E_\gamma = \nu - \delta$$

Thus, from equations (5–26), (5–28), and (5–29), we obtain

$$\frac{\partial \epsilon}{\partial \delta} = 0 \qquad \text{for } \ln E_\gamma = \nu \tag{5–30}$$

and

$$\frac{\partial \epsilon}{\partial \delta} > 0 \qquad \text{at all other points} \tag{5–31}$$

This result, combined with equations (5–26) and (5–27), yields the conclusion that ϵ increases monotonically with δ. Since $F[\epsilon]$ is a monotonically decreasing functional of ϵ, it follows that $F[\delta]$ is a monotonically decreasing functional of δ. Thus, $F[\delta]$ is a maximum at $\delta=0$ and decreases more and more with increasing δ. It follows that $F(E_\gamma)$ is a maximum at $\ln E_\gamma=\nu$; i.e., at $E_\gamma=\frac{1}{2}m_\pi$ and that this is, in fact, the only maximum. Note that these results were reached by less rigorous arguments in our general discussion in section 1–6.

Our results are illustrated in figure 5–2, which shows the general form of $F(E_\gamma)$.

We will further illustrate our results with two ideal distribution functions of pion energy.

Distribution A:

$$f(E_\pi)=\delta(E_\pi-E_0)$$

In this case,

$$F(E_\gamma)=\int_\epsilon^\infty dE_\pi \frac{\delta(E_\pi-E_0)}{(E_\pi^2-m_\pi^2)^{1/2}}$$

$$=\begin{cases}\dfrac{1}{(E_0^2-m_\pi^2)^{1/2}} & \text{for } E_0>\epsilon \\ 0 & \text{otherwise}\end{cases} \qquad (5\text{–}32)$$

To find the limits in terms of E_γ, we need only solve equation (5–5) to obtain

$$E_0>\epsilon \quad \text{implies } E_{\gamma 1}\leq E_\gamma \leq E_{\gamma 2}$$

where

$$E_{\gamma 1}=\tfrac{1}{2}[E_0-(E_0^2-m_\pi^2)^{1/2}]$$

and

$$E_{\gamma 2}=\tfrac{1}{2}[E_0+(E_0^2-m_\pi^2)^{1/2}] \qquad (5\text{–}33)$$

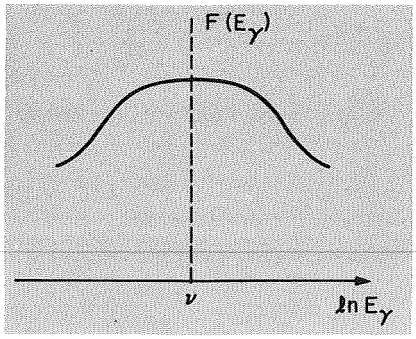

FIGURE 5–2.—A schematic representation of the form $F(\ln E_\gamma)$ expressing the implications of equations (5–12), (5–23), and (5–31).

Distribution B:

$$f(E_\pi) = \begin{cases} (E_B - E_A)^{-1} & \text{for } E_A \leq E_\pi \leq E_B \\ 0 & \text{otherwise} \end{cases}$$

In this case,

$$F(E_\gamma) = \begin{cases} (E_B - E_A)^{-1} \int_{E_A}^{E_B} \dfrac{dE_\pi}{(E_\pi^2 - m_\pi^2)^{1/2}} & \text{for } E_A \geq \epsilon \\ (E_B - E_A)^{-1} \int_{\epsilon}^{E_B} \dfrac{dE_\pi}{(E_\pi^2 - m_\pi^2)^{1/2}} & \text{for } E_A \leq \epsilon \leq E_B \\ 0 & \text{for } \epsilon \geq E_B \end{cases} \tag{5-34}$$

The integral

$$\int \frac{dt}{(t^2 - m^2)^{1/2}} = \ln\,[t + (t^2 - m^2)^{1/2}] + \text{constant} \tag{5-35}$$

Therefore, if we define

$$\begin{aligned} E_{A1} &= \tfrac{1}{2}[E_A - (E_A^2 - m_\pi^2)^{1/2}] & E_{A2} &= \tfrac{1}{2}[E_A + (E_A^2 - m_\pi^2)^{1/2}] \\ \text{and} & & & \qquad (5\text{-}36) \\ E_{B1} &= \tfrac{1}{2}[E_B - (E_B^2 - m_\pi^2)^{1/2}] & E_{B2} &= \tfrac{1}{2}[E_B + (E_B^2 - m_\pi^2)^{1/2}] \end{aligned}$$

we find

$$F(E_\gamma) = \begin{cases} (E_B - E_A)^{-1} \ln\left(\dfrac{E_{B2}}{E_{A2}}\right) & \text{for } E_{A1} \leq E_\gamma \leq E_{A2} \\ (E_B - E_A)^{-1} \ln\left(\dfrac{E_{B2}}{E_\gamma}\right) & \text{for } E_{B1} \leq E_\gamma \leq E_{A1} \text{ and } E_{A2} \leq E_\gamma \leq E_{B2} \\ 0 & \text{otherwise} \end{cases} \tag{5-37}$$

These results are shown schematically in figure 5–3.

5-3 THE ISOBAR-PLUS-FIREBALL MODEL

In this model, we will assume that in collisions at accelerator energies all pions are produced in either of two ways:

(1) Via intermediate production and decay of the Δ(1.238) nonstrange isobar (sometimes also referred to as an excited baryon or baryon resonance). The isobar is assumed to carry momentum directly forward or backward in the cms of the collision with an equal

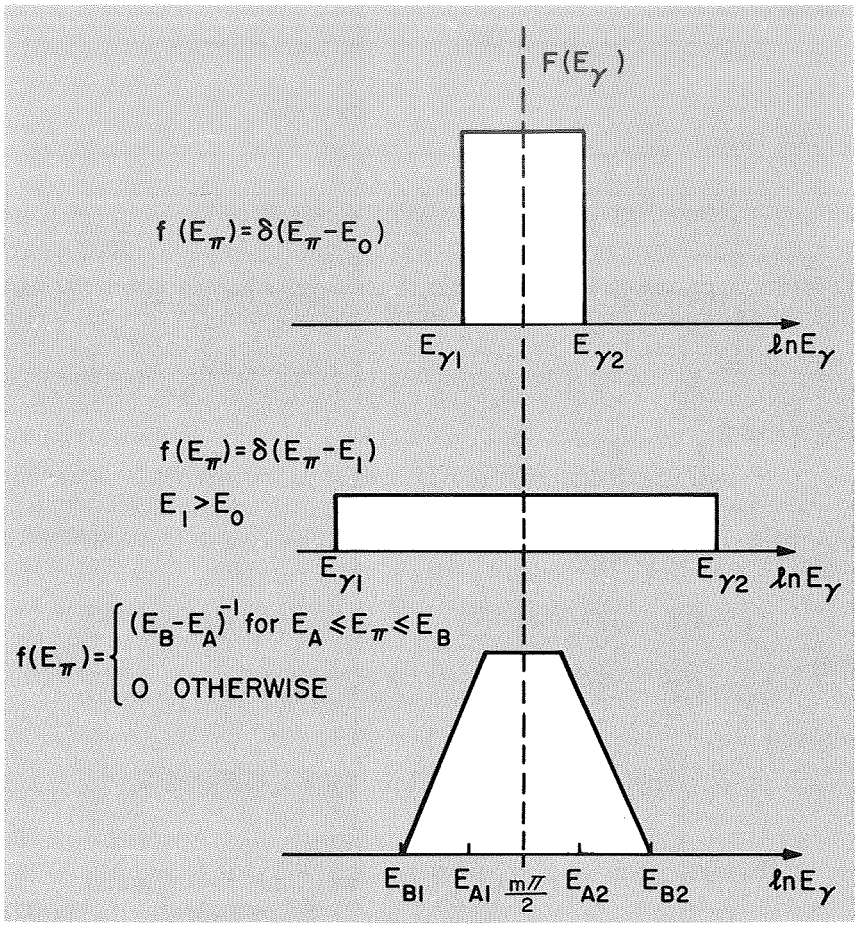

FIGURE 5–3.—Some ideal γ-ray spectra resulting from the decay of some ideal spectra of neutral pions.

probability. This property of isobar production in nucleon-nucleon interactions is well indicated from accelerator studies and has been discussed theoretically (see, e.g., the review by D. R. O. Morrison, 1963).

(2) From the energy remaining available in the cms of the collision, a thermal pion "gas" is created where the pions are given an energy distribution which is very similar to a Maxwell-Boltzmann distribution (Morrison, 1963). This phenomenon sometimes is referred to as a fireball in cosmic-ray nuclear emulsion studies and will be referred to as a fireball here. Its conception dates back to some of Fermi's early research into the problem of pion production in cosmic-ray collisions (Fermi, 1951). Our low-energy fireball is

assumed to be roughly at rest with respect to the cms of the collision with its pions directed isotropically in this system. As an illustration, figure 5–4 shows schematically the situation resulting from a TeV (10^3 GeV) collision of the type we will discuss in the next chapter. The large difference in the behavior of the mesons and baryons emanating from the collision leads to asymptotic forms for the high-energy γ-ray spectrum described in that chapter.

The situation for low-energy collisions is not that simple, as is shown in figure 5–5. As is indicated, it is much harder to distinguish between the two modes of pion production because of the similarity in the momenta involved. There is no large disparity in cms momenta as in the case of a TeV collision.

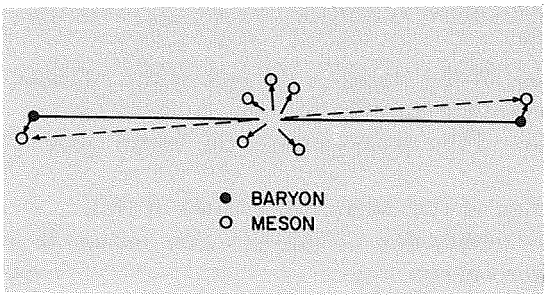

FIGURE 5–4.—A schematic representation of the distribution of secondary pions resulting from a p–p collision in the teraelectron volt energy range.

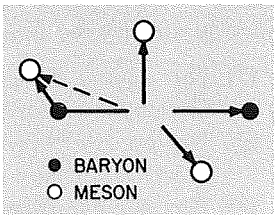

FIGURE 5–5.—A schematic representation of the distribution of secondary pions resulting from a p–p collision in the gigaelectron volt energy range.

Indeed, we may even conceptually fuse the two components and envision all the created pions together as having an elongated cms momentum distribution whose anisotropy is a function of collision energy. A simple model of this type has been used by Hayakawa et al. (1964) in their calculations of the cosmic γ-ray spectrum. However, the two-component model presented here utilizes the more detailed results of more recent accelerator experiments. Among the most striking of these results is the complete dominance of the $\Delta(1.238)$ production mode in collisions where $E_p < 3$ GeV (Muirhead, 1965 (p. 666)). Indeed, even for collisions below the threshold for production of the mass peak at 1.238 GeV, there is evidence that this resonance (whose mass distribution extends below 1.238 GeV) affects the pion energy distribution (Focardi et al., 1965). We will assume here that below 3.16 GeV, all pion production occurs through the intermediate 1.238 resonance. This hypothesis is in agreement with the observation that at about 0.6-GeV proton kinetic energy, the neutral pion distribution is

isotropic, since in this energy range the isobar enhancement would be formed at rest in the cms. The model is also in agreement with the observation of an increasing asymmetry in pion momentum toward the forward and backward directions as E_p increases, since at higher energies the isobars tend to carry more and more momentum in the forward and backward directions.

5–4 CALCULATION OF THE GAMMA-RAY SPECTRUM FROM THE ISOBAR PION COMPONENT

We are now ready to specify the parameters needed for the numerical calculation of the γ-ray spectrum from the isobar pion component, hereafter referred to as the i-process component. For our model we need to specify the following:

(1) The energy distribution of the isobar in the cms of the collision.
(2) The angular distribution of the isobar in the cms.
(3) The energy distribution of the decay pions in the BARS (baryon-isobar rest system).
(4) The angular distribution of the decay pions in the BARS.
(5) The cross section for production of the $\Delta(1.238)$ isobar as a function of initial proton energy.

In our model the isobars are assumed to decay isotropically in the BARS. The energy distribution of the decay pions is obtained from the Breit-Wigner form of the isobar mass distribution. The isobar mass distribution is assumed to peak at $M_0^*=1.238$ GeV and have a width of 0.1 GeV. The Breit-Wigner distribution is given by

$$\mathscr{F}(M^*)=\frac{1}{\pi}\frac{\Gamma}{(M^*-M_0^*)^2+\Gamma^2} \tag{5–38}$$

We denote the pion energy in the BARS by the symbol μ, which was used in chapter 1. In terms of isobar mass, μ is then given by

$$\mu=\frac{M^{*2}+M_\pi^2-M_p^2}{2M^*} \tag{5–39}$$

The normalized distribution function for μ is related to the normalized Breit-Wigner mass distribution by the transformation

$$\mathscr{F}(\mu)=\frac{\mathscr{F}(M^*)}{d\mu/dM^*} \tag{5–40}$$

which yields

$$\mathscr{F}(\mu)=\frac{\Gamma}{\pi}\left\{[\{\mu+[\mu^2+(M_p^2-M_\pi)^2]^{1/2}-M_0^*\}^2+\Gamma^2]\left[1-\frac{\mu}{\mu+(\mu^2+M_p^2-M_\pi^2)^{1/2}}\right]\right\}^{-1} \tag{5-41}$$

Equation (5–41) was solved numerically by the author (Stecker, 1970) as a check on an intermediate step in the complete numerical solution. The results are graphed in figure 5–6 along with the BARS γ-ray distribution, which results from this pion distribution and is given by

$$f(E'_\gamma)=\int_{E'_\gamma+(M_\pi^2/4E'_\gamma)}^{\infty}\frac{d\mu\,\mathscr{F}(\mu)}{(\mu^2-M_\pi^2)^{1/2}} \tag{5-42}$$

In the actual calculation of the γ-ray spectrum, we must take into account the kinematic limits on the allowed pion energy. There is only a limited amount of energy available for pion production. In order to specify a maximum BARS pion energy $\mu_{\max}$, we note that in the extreme case, where all the cms energy of the collision is transformed into the mass of the resonance,

$$M^*_{\max}=(2\gamma_c-1)\,M_p \tag{5-43}$$

Thus we can define

$$\mu_{\max}=\frac{M^{*2}_{\max}+M_\pi^2-M_p^2}{2M^*_{\max}} \tag{5-44}$$

We must then renormalize the distribution function over μ so that its integral over the allowed energy region is equal to unity. We thus define a renormalizing weighting factor

$$w_{\rm rn}\equiv\left[\int_{m_\pi}^{\mu_{\max}(E_p)}d\mu\;\mathscr{F}(\mu)\right]^{-1} \tag{5-45}$$

which multiplies the distribution $\mathscr{F}(\mu)$.

We specify in our model, as before, that the isobars carry momentum either directly forward or directly backward in the cms (Morrison, 1963). We further assume that the low-energy *i*-process produces pions through the two-stage decay

$$\begin{array}{l} p+p\rightarrow p+\Delta^+(1.238) \\ \qquad\qquad\quad \hookrightarrow p+\pi^0 \\ \qquad\qquad\qquad\quad \hookrightarrow 2\gamma \end{array} \tag{5-46}$$

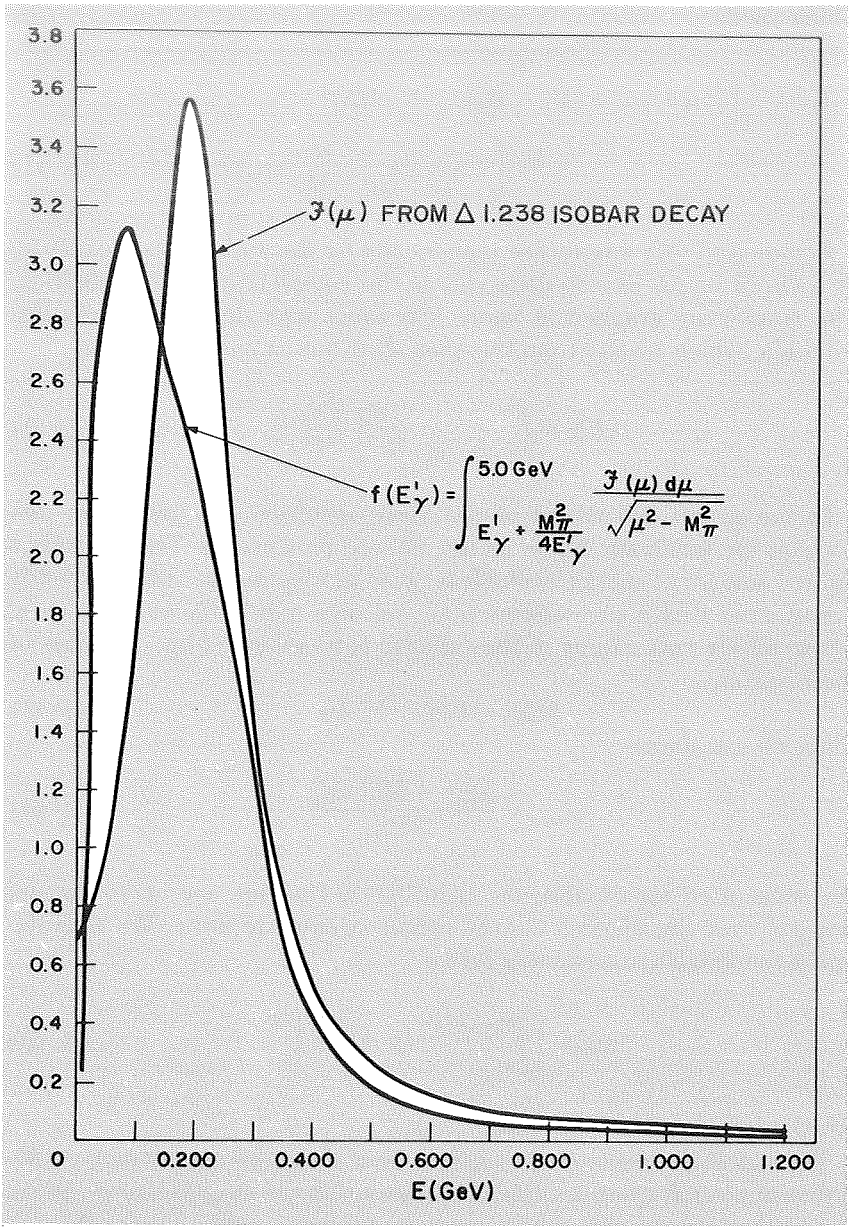

FIGURE 5–6.—The energy distribution function of pions in the BARS resulting from the decay of the Δ(1.238) isobar and the energy distribution function of γ-rays in the BARS resulting from the decay of these pions (Stecker, 1970).

Let E_c be the total energy of the collision in the cms; i.e.,

$$E_c = 2M_p\gamma_c \tag{5–47}$$

Furthermore, let us designate the energy of the isobar and proton in the cms system of the collision by E_{ci} and E_{cp}, respectively. It has been shown in chapter 1 (see eq. (1–62)) that

$$E_{ci}=\frac{E_c^2+M^{*2}-M_p^2}{2E_c} \tag{5–48}$$

The energy of the forwardly and backwardly produced isobars in the laboratory system are then

$$E_f=\gamma_c(E_{ci}+\beta_c p_{ci}) \tag{5–49}$$

and

$$E_b=\gamma_c(E_{ci}-\beta_c p_{ci}) \tag{5–50}$$

with

$$p_{ci}=(E_{ci}^2-M^{*2})^{1/2} \tag{5–51}$$

We may therefore write

$$\sigma(E_i|E_p)=\frac{\sigma_i(E_p)}{2}\left[\delta(E_i-E_f)+\delta(E_i-E_b)\right] \tag{5–52}$$

We now wish to determine the normalized γ-ray energy distribution function for the i-process decay of the $\Delta(1.238)$ isobar. As we showed in our discussion of equation (1–14), since the i-process is a two-stage process, the determination of the distribution function $f_{di}(E_\gamma|E_i)$ requires an integration over an additional energy parameter. We may, if we wish, specify this parameter as E_π as in chapter 1; however, since type i decays are symmetric in the BARS, it will be simpler to use E'_γ (the energy of the decay γ-ray in the BARS). We can then specify

$$f_{di}(E_\gamma|E_i)=\int dE'_\gamma f(E'_\gamma) f_i(E_\gamma|E_i, E'_\gamma) \tag{5–53}$$

In the first stage of the decay, the energy of the resultant neutral pion in the BARS is again uniquely determined and is given by

$$\mu_i=\frac{M_i^{*2}+M_\pi^2-M_N^2}{2M^*} \tag{5–54}$$

Therefore, the magnitude of the BARS momentum of the neutral pion is also unique. We can thus define the convenient parameter ρ_i by the relation

$$\rho_i\equiv\frac{p_{\pi,i}}{M^*}=\frac{(\mu_i^2-M_\pi^2)^{1/2}}{M^*} \tag{5–55}$$

In the pion rest system, each of the two decay γ-rays is given an energy $\frac{1}{2}M_\pi$. Thus, in transforming to the BARS, we find

$$E'_\gamma = \gamma'_\pi \tfrac{1}{2} M_\pi (1 + \beta'_\pi \cos\phi) = \tfrac{1}{2}(\mu_i + \rho_i M_i^* \cos\phi) \tag{5-56}$$

where ϕ is the angle between the γ-ray momentum vector in the pion rest system and the pion momentum vector in the BARS.

Once again, the decay is isotropic in the rest system of the decaying particle (i.e., in cos ϕ), so we obtain

$$f(E'_\gamma) = \begin{cases} \dfrac{1}{\rho_i M_i^*} & \text{for } L_i \leq E'_\gamma \leq U_i \\ 0 & \text{otherwise} \end{cases} \tag{5-57}$$

where, from equation (5–56), we find

$$L_i \equiv \tfrac{1}{2}(\mu_i - \rho_i M_i^*)$$

and (5–58)

$$U_i \equiv \tfrac{1}{2}(\mu_i + \rho_i M^*)$$

Once E'_γ is specified, we need only extend the reasoning used in the derivation of equation (1–106) to obtain

$$f(E_\gamma | E_i, E'_\gamma) = \begin{cases} \dfrac{M^*}{2E'_\gamma (E_i^2 - M^{*2})^{1/2}} & \text{for } E_{\gamma 1} \leq E_\gamma \leq E_{\gamma 2} \\ 0 & \text{otherwise} \end{cases} \tag{5-59}$$

so that as $\beta_i \to 1$,

$$E_{i,\,\max}(E_\gamma) \to \infty$$

and (5–60)

$$E_{i,\,\min}(E_\gamma) \to \left(\frac{M}{2E'_\gamma}\right) E_\gamma$$

Through the use of equation (1–8), equation (1–10) in this case reduces to

$$I_i(E_\gamma) = \tfrac{1}{2}\langle nL \rangle \int dE_p I(E_p) w_{\rm rn}(E_p) \int dE_i \left[\frac{M^*}{(E_i^2 - M^{*2})^{1/2}}\right] \sigma(E_i | E_p) R_i \times \int_{L(E_\gamma, E_i)}^{U(E_\gamma, E_i)} \frac{dE'_\gamma}{E'_\gamma} \int_{E'_\gamma + (M_\pi^2/4E'_\gamma)}^{\mu_{\max}(E_p)} d\mu \frac{\mathscr{F}(\mu)}{(\mu^2 - M_\pi^2)^{1/2}} \tag{5-61}$$

where $w_{\rm rn}$ is defined by equation (5–45), $\mu_{\max}$ is defined by equation (5–44), E'_γ is the γ-ray energy in the BARS, $R_i = 2/3$ is the branching

ratio for the neutral pion decay mode of the $\Delta(1.238)$ isobar,

$$U(E_\gamma, E_i) = \frac{E_\gamma}{\gamma_i(1-\beta_i)} \tag{5-62}$$

$$L(E_\gamma, E_i) = \frac{E_\gamma}{\gamma_i(1+\beta_i)} \tag{5-63}$$

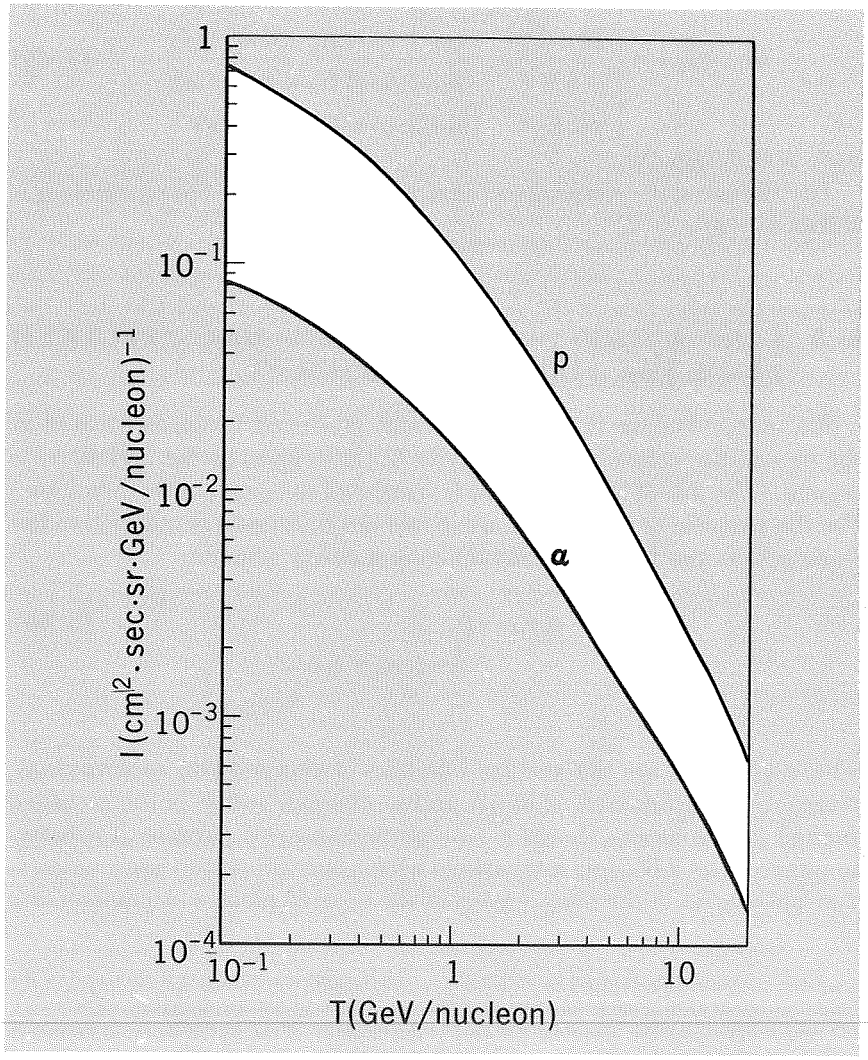

FIGURE 5–7.—The differential cosmic-ray proton and alpha particle kinetic-energy spectra.

and

$$\langle nL \rangle \equiv \int_0^{L_{\text{eff}}} dr\, n(\mathbf{r}) \tag{5-64}$$

with the cosmic-ray intensity in the galaxy $I(E_p)$ assumed to be constant.

The integrations in equation (5–61) were carried out numerically by the author (Stecker, 1970). The product $R_i\sigma_i(E_p)$ (in millibarns) was approximated by a function which was taken to be a three-part power law of the form

$$R_i\sigma_i(E_p) = \begin{cases} 0 & \text{for} \quad E_p < 1.48 \text{ GeV} \\ 10^{-1}\, E_p^{6.7} & \text{for } 1.48 < E_p < 1.88 \text{ GeV} \\ 6.9 & \text{for } 1.88 < E_p < 3.16 \text{ GeV} \\ 69\, E_p^{-2} & \text{for } 3.16 < E_p < 10 \text{ GeV} \end{cases} \tag{5-65}$$

with σ_i in millibarns.[1]

The differential cosmic-ray proton intensity used in the calculation is shown in figure 5–7.

5–5 CALCULATION OF THE GAMMA-RAY SPECTRUM FROM THE FIREBALL COMPONENT

We now calculate the γ-ray spectrum produced by pions created in the cms of the collision. We will refer to these pions as the fireball component. (The use of the term here is restricted to our previous definition.) For the purpose of discussion, we define the f-process (as opposed to the i-process) as the following production and decay scheme:

$$\begin{aligned} p + p &\rightarrow p + p + F \\ &\hookrightarrow \zeta_{\pm}\pi^{\pm} + \zeta_0\pi^0 \\ &\hookrightarrow 2\zeta_0\gamma \end{aligned} \tag{5-66}$$

where $\zeta_{\pm}$ and ζ_0 are the average numbers of charged and neutral pions, respectively (a function of initial proton energy), and F is the so-called fireball. By no means should F be regarded as a real particle; it is better to picture it as a bosonic nonparticle whose only properties are a momentary possession of the mass energy of the created pions and a momentary

[1] Such a cross section is an approximation which assumes complete dominance of the i-process for neutral pion production in collisions involving kinetic energies below 1 GeV but which maintains the observed E^{-2} energy dependence of the $\Delta(1.238)$ cross section in various channels for kinetic energies above 2 GeV (Muirhead, 1965; Ellis et al., 1968; and Connolley et al., 1967).

occupation of the interaction volume centered at the center of momentum of the collision and therefore moving at β_c with respect to the ls.

We assume that the fireball decays isotropically with a cms energy distribution which is roughly independent of energy. The justification for this assumption comes both from accelerator studies (Morrison, 1963, and Fidecaro et al., 1962) and from studies of interactions of cosmic rays in the atmosphere (Fowler and Perkins, 1964). Accelerator studies (Morrison, 1963) of p–p interactions for energies up to 30 GeV give a charged-pion transverse-momentum distribution that fits an empirical law of the form

$$f_\pi(p_\perp) \propto p_\perp e^{-2p_\perp/\langle p_\perp\rangle_\pi} \tag{5–67}$$

Studies at 300 GeV (Guseva et al., 1962) fit this law very well. (There is only a change in normalization involved, indicating an increased multiplicity.) It has also been observed that $\langle p_\perp\rangle_\pi$ is roughly constant in p–p collisions involving energies of up to 10^4 GeV (Fowler and Perkins, 1964). If neutral pions also obey this law, we would expect that the resultant γ-rays would have a transverse-momentum distribution of the form

$$f_\gamma(p_\perp) \propto e^{-p_\perp/\langle p_\perp\rangle_\gamma} \tag{5–68}$$

with

$$\langle p_\perp\rangle_\gamma = \tfrac{1}{2}\langle p_\perp\rangle_\pi \tag{5–69}$$

Data confirm this exponential distribution for $p_\perp > 0.1$ GeV in p–p collisions involving energies up to 10^4 GeV (Fowler and Perkins, 1964). Accelerator experiments (Fidecaro et al., 1962) measuring the γ-ray spectrum from p–p interactions at 23.1 GeV have substantiated indications of an exponential distribution of neutral pions in the cms. The data are well represented by an energy distribution function of the form

$$f(E_\gamma^{(c)}) \propto e^{-4E_\gamma^{(c)}} \tag{5–70}$$

Figure 5–8 shows the average cms energy distribution of γ-rays produced in 23.1 GeV p–p interactions as measured by Fidecaro et al. (1962).

Thus, over a wide range of energies

$$f_\pi(p_\perp) \propto p_\perp e^{-2p_\perp/\langle p_\perp\rangle_\pi} \tag{5–71}$$

The quantity $p_\perp$ is a relativistic invariant that is proportional to the cms momentum of the pion and, therefore (relativistically), to its cms

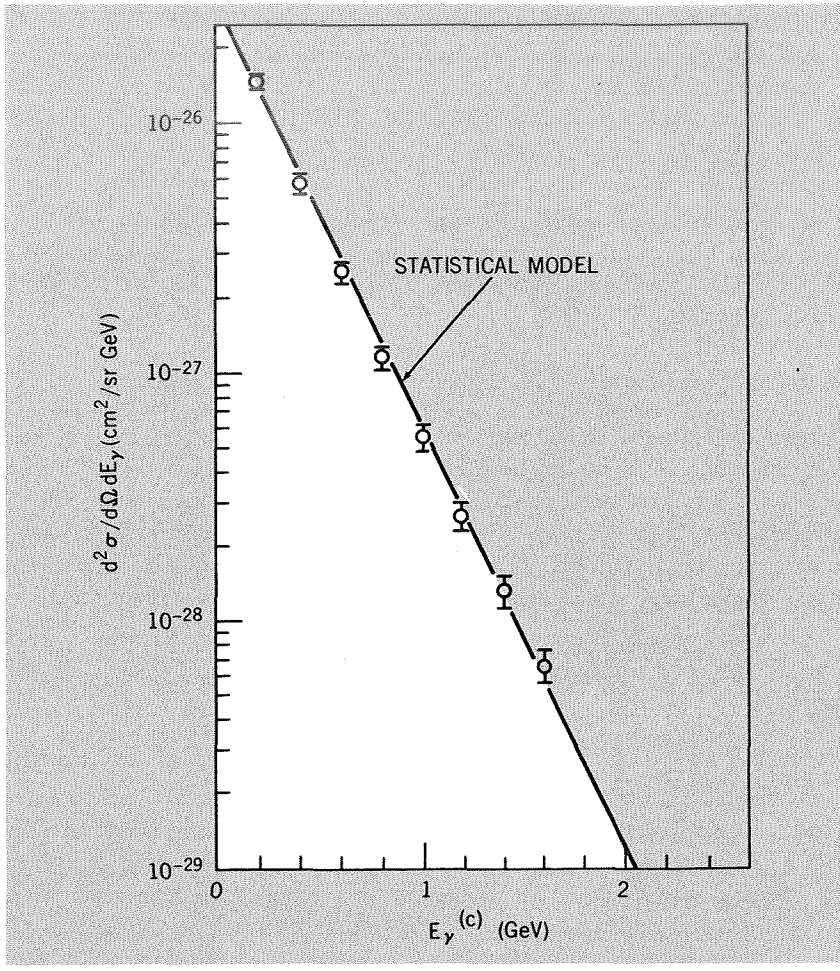

FIGURE 5–8.—Gamma-ray cms energy spectrum integrated over angles as given by Fidecaro et al. (1962). The solid line has a slope of −3.86.

energy. Letting ξ stand for cms pion energy, we may therefore use the approximation

$$\mathscr{F}(\xi) \propto \xi e^{-2\xi/\langle\xi\rangle} \tag{5–72}$$

Since $\langle\xi\rangle \simeq 0.5$, independent of energy for collisions involving energies up to 10^4 GeV, we find that

$$\mathscr{F}(\xi) = \frac{1}{Z}\,\xi e^{-4\xi} \tag{5–73}$$

with the normalization constant Z defined by

$$Z = \int_{m_\pi}^{\mu_{\max}(E_p)} d\xi \; \xi e^{-4\xi} \tag{5–74}$$

so that

$$\int_{m_\pi}^{\mu_{\max}(E_p)} d\xi \; \mathscr{F}(\xi) = 1 \tag{5–75}$$

Evidence for a two-component pion production model with the f-process component producing pions isotropically in the collision cms has been presented by Dekkers et al. (1965). Their work indicates that the i-component yields a very large positive-to-negative pion ratio. Thus, the negative pions arise principally through the f-process. It is also found that at accelerator energies, most negative pions are produced isotropically in the cms (the remaining ones are consistent with a small contribution from $N^* \rightarrow N\pi\pi$ decays).

We have thus assumed that the i-process plus the f-process provide all the pions produced; i.e.,

$$\zeta_f \sigma_f \equiv [\zeta(E_p)\sigma(E_p)]_{\text{Total}} - \sigma_i(E_p) \tag{5–76}$$

The function $[\zeta(E_p)\sigma(E_p)]_{\text{Total}}$ is shown in figure 5–9.

It has been shown that a γ-ray of energy $E_\gamma^{(c)}$ in the cms may have any laboratory energy E_γ within the range

$$\gamma_c E_\gamma^{(c)}(1 - \beta_c) \leq E_\gamma \leq \gamma_c E_\gamma^{(c)}(1 + \beta_c) \tag{5–77}$$

Under our assumption of uniform cms pion emission for the f-process, there is a constant production probability

$$f(E_\gamma | E_\gamma^{(c)}) = \frac{1}{2\gamma_c \beta_c E_\gamma^{(c)}} \tag{5–78}$$

within this energy range. It follows from equation (5–77) that the integral over the source function with respect to $E_\gamma^{(c)}$ is bounded by the upper and lower limits, U_F and L_F, respectively, where

$$U_F(E_\gamma, E_p) = \frac{E_\gamma}{\gamma_c(1 - \beta_c)} \tag{5–79}$$

and

$$L_F(E_\gamma, E_p) = \frac{E_\gamma}{\gamma_c(1 + \beta_c)} \tag{5–80}$$

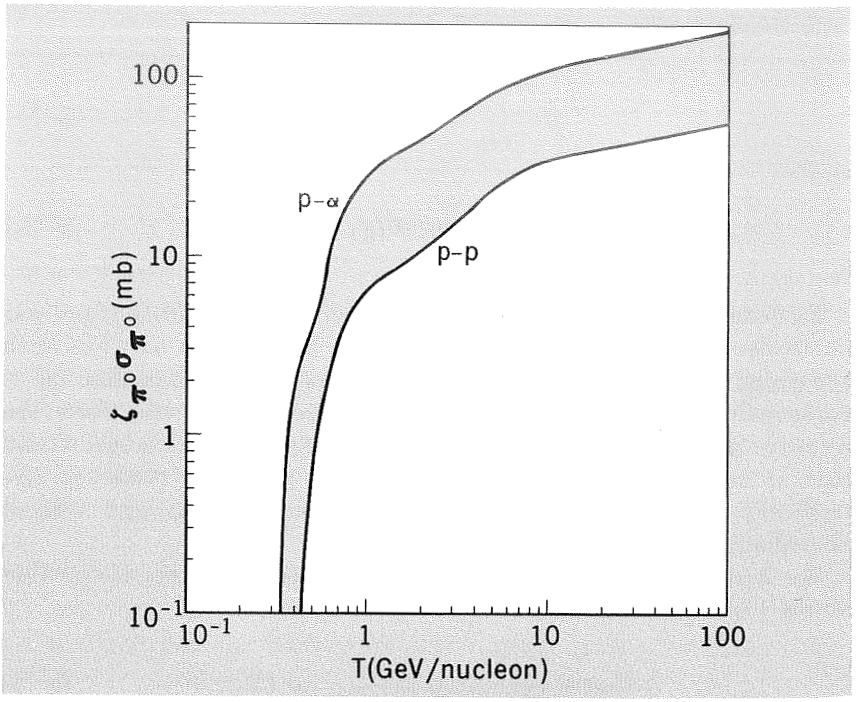

FIGURE 5–9.—Cross section times multiplicity for neutral pion production. Data for p–p interactions as summarized by Muirhead (1965). Data for p–α interactions from Prokoshkin and Tiapkin (1957a, b), Batson et al. (1959), and Kozodaev et al. (1960).

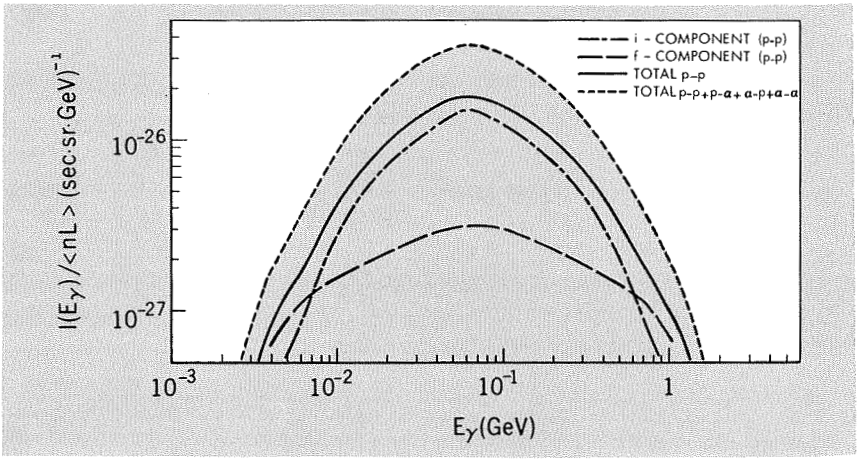

FIGURE 5–10.—The calculated differential production spectrum of γ-rays produced in cosmic-ray interactions based on the "isobar-plus-fireball" model described in the text (Stecker, 1970)

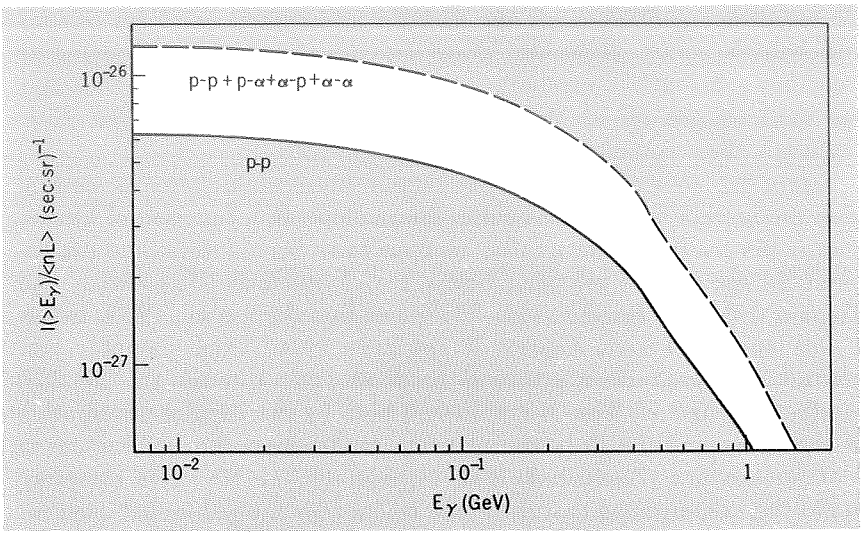

FIGURE 5–11.—Calculated integral production spectrum based on the results of figure 5–6 (Stecker, 1970).

since only γ-rays within this cms energy range will produce γ-rays of laboratory energy E_γ.

Therefore, the complete formula for the γ-ray spectrum arising from the f-process is

$$I_f(E_\gamma) = \frac{\langle nL\rangle}{2}\int dE_p \frac{\zeta_f(E_p)\sigma_f(E_p)I(E_p)}{\gamma_c(E_p)\beta_c(E_p)} \times \int_{L_r(E_\gamma,E_p)}^{U_F(E_\gamma,E_p)} \frac{dE_\gamma^{(c)}}{E_\gamma^{(c)}} \int_{E_\gamma^{(c)}+(m_\pi^2/4E_\gamma^{(c)})}^{\mu\max(E_p)} d\xi \frac{\mathscr{F}(\xi)}{(\xi^2-m_\pi^2)^{1/2}} \qquad (5\text{–}81)$$

The resultant f-process spectrum was obtained numerically by the same methods previously described for the evaluation of the i-process spectrum (Stecker, 1970). The results of the numerical integration are shown in figure 5–10. Figure 5–10 also shows the total spectrum produced by summation of the i- and f-components. The integral spectrum is given in figure 5–11.

5–6 COSMIC GAMMA RAYS PRODUCED IN COSMIC-RAY p–α AND α–p INTERACTIONS

Up to this point, we have restricted ourselves to a discussion of cosmic γ-ray production in cosmic-ray p–p interactions. The details of particle production in p–p interactions have been well studied in recent accelera-

tor experiments. Such is not the case for interactions involving protons and helium nuclei. However, these interactions may be expected to provide a substantial contribution to the total γ-ray production of roughly the same magnitude as the contribution from p–p interactions. Consequently these interactions cannot be neglected.

Figure 5–9 shows the total cross section times multiplicity for neutral pion production and proton-helium interactions as a function of kinetic energy per nucleon. These cross sections have been determined experimentally for kinetic energies below 1 GeV/nucleon (Prokoshkin and Tiapkin, 1957a, b; Batson et al., 1959; and Kozodaev et al., 1960). Below 1 GeV/nucleon kinetic energy, it has been found experimentally that neutral pion production proceeds predominantly through the $\Delta(1.238)$ production channel. This is manifested both by the angular distribution of the pions and the 2:1 ratio of neutral-to-positive pion production in p–n interactions (Prokoshkin and Tiapkin, 1957a). We have therefore made the assumptions that the same isobar-plus-fireball model used for p–p interactions is also valid for p–α and α–p interactions, that the i-process dominates below a total energy of 3.16 GeV/nucleon, and that the energy dependences of the cross sections for the i-process and the f-process are the same for nucleon-nucleon collisions in all of these interactions (charge independence). For interactions involving kinetic energies greater than 1 GeV/nucleon, the cross-section data were extrapolated by assuming that the energy dependence of the pion multiplicity has the same form for α–p and p–α interactions as for p–p interactions. We assume also that the cross section for $\Delta(1.238)$ production decreases with energy as E^{-2}, as is the case for p–p interactions. The assumption is also made that the pions are produced primarily in interactions which simulate free nucleon-nucleon interactions (Batson et al., 1959), but with shadowing corrections as given by Kozodaev et al. (1960).

The energy spectrum of cosmic-ray alpha particles at solar minimum is shown in figure 5–7. These particles produce γ-rays by interacting with the interstellar gas (primarily α–p interactions). To this contribution we must add the contribution of cosmic-ray protons interacting with helium nuclei in the interstellar gas (p–α interactions). Interstellar helium is estimated to make up approximately 36 percent of the nucleons in the interstellar medium so that the ratio of helium nucleons to hydrogen nucleons is 0.57 (Allen, 1963).

The differential energy spectrum of cosmic γ-rays from α–p and p–α interactions was calculated based on the intensities and cross sections given in figures 5–7 and 5–9, respectively, and on the assumptions given above (Stecker, 1970). The results of this calculation, when added to the results of the p–p calculations, yield the total spectrum given in figure 5–10. The total integral production spectrum is shown in figure 5–11.

The Form of the Cosmic Gamma-Ray Production Spectrum From Galactic Cosmic-Ray Interactions for Gamma-Ray Energies Greater Than 1 GeV: The Effect of the Decay of Nucleon Isobars and Hyperons on the Cosmic Gamma-Ray Spectrum

6–1 INTRODUCTION

Several workers (Pollack and Fazio, 1963; Ginzburg and Syrovatskii, 1964; Gould and Burbidge, 1965; Hayakawa et al., 1964; Garmire and Kraushaar, 1965; Lieber, Milford, and Spergel, 1965; Dilworth, Maraschi, and Perola, 1968; and Stecker, Tsuruta, and Fazio, 1968) have discussed the production of cosmic γ-rays by the collision of high-energy protons with interstellar and intergalactic gas. Many others have studied cosmic-ray pion production in high-energy interactions. Out of these studies have come various phenomenological models for pion production, sometimes referred to as "pionization." Among these models are the hydrodynamical and "fireball" models. (For a general review, see Fujimoto and Hayakawa, 1967; see also the discussion in ch. 5.) Gamma rays result through the reactions

$$p + p \rightarrow p + p + \text{pions} \tag{6–1}$$

followed by

$$\pi^0 \rightarrow \gamma + \gamma$$

Pal and Peters (Peters, 1962, and Pal and Peters, 1964) have pointed out the significance of the production and decay of hyperons and excited baryons (isobars) as a source of pions in high-energy interactions, which may be of particular importance in producing high-energy pions. In chapter 1 we discussed the details of the γ-ray spectra generated from the formation of various secondary particles produced in p–p interactions. These calculations and the results of recent proton accelerator experiments indicate that in high-energy p–p interactions, the production of the hyperons Σ^+, Σ^0, and Λ and unstable baryon resonances $N^*(1.410)$ and $N^*(1.688)$ and their subsequent decay may be important sources of

very-high-energy γ-ray photons. Although the production cross sections for these particles are relatively low, a substantial fraction of the initial interaction energy is transferred to these particles and hence to the resultant γ-radiation. In this chapter we will use the new accelerator data to calculate the cosmic γ-ray energy spectrum caused by the decay of these particles and to determine at what γ-ray energies the decay of these particles may provide a significant source of cosmic γ-rays. Our discussion will be based on that given by Stecker et al. (1968).

6-2 GAMMA-RAY PRODUCTION MECHANISMS

The basic types of production reactions that we will consider in addition to the usual process denoted by expressions (6–1) are hyperon production:

$$p + p \rightarrow N + Y + K + \text{bosons} \tag{6–2}$$

and nucleon isobar production:

$$p + p \rightarrow N^{*+} + p + \text{bosons} \tag{6–3}$$

The symbols N, Y, K, and N^{*+} denote a nucleon (proton, neutron), a hyperon, a kaon, and a positive nucleon isobar, respectively. Experimental data are available for these reactions for incident-proton energies up to 30 GeV. These reactions produce γ-rays primarily by the decay schemes

$$\begin{aligned} \Sigma^0 &\rightarrow \Lambda + \gamma \\ \Lambda &\rightarrow n + \pi^0 \\ &\qquad \hookrightarrow 2\gamma \\ \Sigma^+ &\rightarrow p + \pi^0 \\ &\qquad \hookrightarrow 2\gamma \end{aligned} \tag{6–4}$$

for the hyperons, and

$$\begin{aligned} N^{*+} &\rightarrow p + \pi^0 \\ &\qquad \hookrightarrow 2\gamma \end{aligned} \tag{6–5}$$

for the isobars. A particular nucleon isobar of isotopic spin $\frac{1}{2}$ will be denoted by the symbol $N^*(M^*)$, where the symbol M^* will be taken to denote its most probable rest mass in GeV.

These decay schemes are of two basic types: The neutral sigma decay, which directly produces one γ-ray, and decays that we will designate as being of type i which indirectly produce two γ-rays from

the decay of a heavy baryon, here denoted by $B_i (i = \Sigma^+, \Lambda, N^{*+})$, as follows:

$$\begin{array}{l} B_i \rightarrow N + \pi^0 \\ \qquad\quad \hookrightarrow 2\gamma \end{array} \tag{6-6}$$

This decay scheme will be referred to, as before, as an "i-process."

6-3 THE DIFFERENTIAL PRODUCTION CROSS SECTIONS OF HYPERONS AND NUCLEON ISOBARS

In order to calculate the cosmic γ-ray spectrum produced from the decay of hyperons and nucleon isobars, we must first determine the differential production cross sections $\sigma_s(E_s|E_p)$, which are defined as the cross sections for the production of a secondary particle of type s with energy E_s by a proton of energy E_p colliding with a proton at rest. These differential production cross sections are determined from proton accelerator experiments and cosmic-ray shower studies. Such studies have indicated that in high-energy collisions the forward baryon retains most of its energy, between 50 and 65 percent. (See, e.g., Baradzei et al., 1962, and Daniel et al., 1963.) This baryon is strongly directed forward, a tendency manifested even at accelerator energies (Morrison, 1963). We will therefore approximate the differential production cross sections for the forwardly produced baryons by the expression

$$\sigma_s(E_s|E_p) = \tfrac{1}{2}\,\sigma_s(E_p)\,\delta[E_s - \eta_s(E_p)] \tag{6-7}$$

where $\eta_s = \chi(E_p - M_p) + M_s$.

Thus, χ designates the fraction of initial energy carried off by the forward baryon, which has been excited to a nucleon isobar N^* or hyperon Y. After deexcitation it is thus equal to the fraction of incident energy carried off by the forward nucleon *plus* the most energetic pion. We will take χ to be a constant and equal to 0.6 in all cases.[1]

The factor of $\frac{1}{2}$ in equation (6–7) is included to take account of the fact that only one-half of the baryons are produced in the forward direction.

---

[1] There is even some indication that in collisions where baryon excitation occurs, the fraction of energy retained by the forward excited baryon may be higher than in collisions where excitation does not take place (Kazuno, 1964). Peak and Woolcott (1965) have studied cosmic-ray interactions with 5×10^2 GeV $\leq E_p \leq 5 \times 10^4$ GeV and find indications that the nucleon retains approximately 55 percent of its initial energy; about 25 percent of the energy goes into pionization (see sec. 4–3) and the other 20 percent may go to an isobar-decay pion. With the data presented in this paper, we find that the average fraction of energy relegated to the i-process pion is 23 percent, in agreement with the conjecture of Peak and Woolcott. Thus, the Peak and Woolcott data may indicate a value of χ as high as 0.75.

We will neglect the backwardly directed baryons, since they will produce low-energy γ-rays only, and will produce them at a negligible rate compared with those produced by the more usually considered π-decay process, which we will soon discuss.

Tables 6–1 and 6–2 give the empirical data for the total cross sections of hyperons and nucleon isobars, respectively, as obtained in proton

TABLE 6–1.—*Hyperon Cross-Section Data*

Proton momentum, GeV/c	Lambda cross section, mb	Neutral sigma cross section, mb	Positive sigma cross section, mb	Reference
4.7	0.051	0.049	0.083	[a]
6	.259	.077	.....	[b]
10	.472	.196	.239	[c]
23.1	Lambda + neutral sigma cross section = 0.77			[d]
24.5	Lambda + neutral sigma cross section = 1.13			[e]

[a] Louttit et al., 1961.
[b] Chinowsky, 1966.
[c] Holmgren et al., 1967.
[d] CERN HBC and IEP groups, 1961.
[e] Bartke et al., 1963.

TABLE 6–2.—*Isobar Cross-Section Data* [a]

Incident momentum, GeV/c	Cross section, mb					Reference
	$\Delta(1.238)$	$N^*(1.410)$	$N^*(1.518)$	$N^*(1.688)$	$N^*(2.190)$	
2.85	3.8	.....	.....	.....	.....	[b]
4.55	1.5	0.63	0.68	0.7	.....	[b]
6	.376	.....	.....	.....	.....	[c]
6.06	.6	.65	.45	.5	.....	[b]
7.88	.41	.45	.31	.46	.....	[b]
10	.184	.544	.196	.562	.....	[c]
15	.142	.602	.160	.638	.....	[c]
20	.....	.660	.170	.560	0.128	[c]
30	.....	.744	.166	.576	.108	[c]

[a] For reaction channels of the type $p + p \rightarrow N^{*+} + p$ only.
[b] Blair et al., 1966.
[c] Anderson et al., 1966.

TABLE 6–3.—*Production and Decay Parameters for* Λ, Σ^+, Σ^0, N*(1.410), and N*(1.688)

[Rosenfeld et al., 1965]

Particle	Decay scheme	Mass, GeV	Production threshold energy (GeV) in p–p collision	Branching ratio for γ-producing modes	Assumed production cross section at high energies, mb	Decay time, s
$N^*(1.688)$.....	$N^{*+}(1.688) \rightarrow N+\pi^0$	1.688	1.80	[a] 0.33	0.6	$\sim 10^{-23}$
$N^*(1.410)$.....	$N^{*+}(1.410) \rightarrow N+\pi^0$	1.410	1.24	[a].33	.6	$< 10^{-23}$
Σ^+.....	$\Sigma^+ \rightarrow p+\pi^0$	1.189	1.90	.510	.8	$\sim 10^{-10}$
Σ^0.....	$\Sigma^0 \rightarrow \Lambda+\gamma$	1.192	1.90	1.00	.4	$< 10^{-14}$
Λ.....	$\Lambda \rightarrow n+\pi^0$	1.115	1.70	.331	.4	$\sim 10^{-10}$

[a] For simplicity, it is assumed that all decays occur via the i-process. More precisely, ~ 10 to 15 percent of the decays occur via the production of 2 pions.

accelerator experiments. These cross sections are related to the differential cross sections by the condition

$$\zeta_s(E_p)\sigma_s(E_p) = \int dE_s\, \sigma_s(E_s|E_p) \qquad (6\text{–}8)$$

where ζ_s is the number of particles of type s produced per collision.

Table 6–3 gives a summary of the properties of the production and decay of the hyperons and nucleon isobars with which we will concern ourselves in this calculation. In this table we have also listed the value we have assigned to the quantity $\sigma_s(E_p)$ for $E_p > 25$ GeV. We have assumed in all cases that the total cross sections have attained an asymptotic constant value above this energy. There is good evidence that this is the case for the production of the isobars that we consider (see table 6–2), but the poor data on hyperon production above 10 GeV leave some uncertainty about the validity of the assumption of constant σ_{Σ^+}, σ_{Σ^0}, and σ_Λ at high energy. Cosmic-ray studies (Wolfendale, 1963; Peters, 1962; Yekutieli, 1961; Pal and Peters, 1964; and Kazuno, 1964) indicate that the production of isobars and hyperons is significant at energies from 10^3 to 10^6 GeV. We note that $\Delta(1.238)$ and $N^*(1.518)$ production cross sections seem to decrease rapidly with increasing energy (see table 6–2),[2] whereas the isobars we have considered seem to maintain fairly constant cross sections between 5 and 30 GeV. At higher energies

[2] The cross section for $N^*(1.518)$ may reach a constant value at high energies, but it is so small compared to the others that it may be considered to be negligible.

there may be significant contributions from the production of heavier resonances (both strange and nonstrange), as well as to those in other charge states (e.g., $N^{*0}(1.688)$). However, there are indications of strong inhibition of the production of resonances involving a change in isotopic spin and involving masses greater than 2 GeV (Morrison, 1963).

In this discussion we have neglected the contribution of kaons to the cosmic γ-ray spectrum. It should not affect our results significantly for the following reasons:

(1) Kaon pairs are produced directly in the cms of the collision in the same manner as the pions of equation (6–1). Therefore, when the kaons decay through channels that produce neutral pions, they will produce the same spectral characteristics as the neutral-pion fireball component. (See sec. 6–4c.)

(2) The ratio of kaon-to-pion production is only 0.10 to 0.20 (Osborne and Wolfendale, 1963), so that only a marked difference in their production and decay schemes would affect the overall γ-ray spectrum predicted.

We note also that we have an additional contribution of Λ particles from the decay $\Sigma^0 \rightarrow \Lambda + \gamma$ to consider, apart from the Λ particles created directly. This will increase somewhat the contribution of the Λ component; however, the spectral characteristics of this component will remain unaltered.

We have not discussed the effect of the production of boson resonances such as the η, ρ, and ω mesons, as well as possible unknown resonances of higher mass. Data on such production in cosmic-ray showers are practically nil, although there is some evidence for it (Nishimura, 1967). (It is possible to speculate that the so-called fireballs, presumably created in high-energy interactions, may be either heavy boson resonances or baryon-antibaryon pairs.) (See sec. 6–4c.)

While the cross-section data for hyperon and baryon-resonance production are still sparse, we hope to have more data in the future.

6–4 THE COSMIC GAMMA-RAY SPECTRUM

A detailed discussion of the γ-ray spectra produced by the formation of various secondaries in p–p interactions has already been given in chapter 1. In general, the differential γ-ray spectrum resulting from secondary particles formed in p–p collisions is given by

$$I(E_\gamma) = \int_0^{L_{\text{eff}}} dr\, n(\mathbf{r}) \sum_s \int_{E_{\text{th},s}}^{\infty} dE_p\, I(E_p, \mathbf{r}) \int_{E_{s,\min}}^{E_{s,\max}} dE_s\, \sigma_s(E_s|E_p) \times \sum_d \zeta_d R_d f_{ds}(E_\gamma|E_s) \qquad (6\text{–}9)$$

where $\mathbf{r}$ is the radial vector from the Earth to the source, $n(\mathbf{r})$ is the density of interstellar and intergalactic gas, L_{eff} is an effective integration length, E_p is the energy of the cosmic-ray proton involved in the collision, and $I(E_p, \mathbf{r})$ is the differential flux of cosmic-ray primaries. The index s denotes a type of secondary particle produced, the index d a decay mode that leads to the production of a γ-ray, ζ_d the number of γ-rays produced in this mode, and R_d the branching ratio for decay mode d. The limits on the integrals are determined by the kinematics of the processes involved; e.g., $E_{\text{th},s}$, the lower limit on the E_p integration, is the threshold energy for the production of a particle of type s, and the limits on the E_s integration are the maximum and minimum energies that a particle of type s could have and still be able to produce a γ-ray of energy E_γ. The last quantity in equation (6–9), $f_{ds}(E_\gamma | E_s)$, is a distribution function over E_γ for γ-rays of energy E_γ produced via decay mode d by secondary particles of type s and energy E_s. Therefore,

$$\int dE_\gamma f_{ds}(E_\gamma | E_s) = 1 \tag{6–10}$$

For simplicity, we will assume that all collisions considered are those of high-energy cosmic-ray protons with hydrogen nuclei in the interstellar and intergalactic medium. The only other collisions of astrophysical significance are the p–α and α–p collisions, and we will assume here that these collisions are basically of the same character as the simpler and much more common p–p collisions, particularly in the energy region $E_p > 100$ GeV.

We will also consider here the space-averaged isotropic flux of cosmic γ-radiation, so as not to concern ourselves with the problem of variations in absolute intensity expected from various assumptions about the galactic and intergalactic cosmic-ray flux. For a discussion of these see, for example, Ginzburg and Syrovatskii (1964).

Thus, we will assume, as in chapter 5, that

$$I(E_p, \mathbf{r}) = I(E_p) \tag{6–11}$$

and

$$\int_0^{L_{\text{eff}}} dr\, n(\mathbf{r}) = \langle nL \rangle \tag{6–12}$$

In the following kinematic discussions, we will refer to the rest system of the decaying baryon by the abbreviation BARS (baryon rest system). We will also use the common relativistic convention of setting $c = 1$. Particle velocities (in units of c) are denoted by β, rest masses by M, and particle energies (in units of their respective rest masses (E/M) by γ.

411-892 O - 71 - 9

6-4a Neutral Sigma-Particle Decay

In the case of Σ^0 decay, we note that the energy of the decay γ-ray in the BARS is uniquely specified by the laws of conservation of momentum and energy. If we denote this energy by μ_Σ, it follows from equation (1–78) that

$$\mu_\Sigma = \frac{M_\Sigma^2 - M_\Lambda^2}{2M_\Sigma} = 0.0747 \text{ GeV} \tag{6–13}$$

The γ-ray energy in the ls is

$$E_\gamma = \gamma_\Sigma \mu_\Sigma (1 + \beta_\Sigma \cos \theta) \tag{6–14}$$

where θ is the angle between the γ-ray momentum vector in the BARS and the velocity vector of the BARS in the ls.

Because the decay is isotropic in θ, the resulting distribution of E_γ is uniform between the upper and lower limits allowed by equation (6–14), so that, by imposing the normalization conditions discussed previously, we find

$$f_{\gamma\Sigma}(E_\gamma | E_\Sigma) = \begin{cases} \dfrac{M_\Sigma}{2\mu_\Sigma (E_\Sigma^2 - M_\Sigma^2)^{1/2}} & \text{for } E_{\gamma 1} \leq E_\gamma \leq E_{\gamma 2} \\ 0 & \text{otherwise} \end{cases} \tag{6–15}$$

where

$$E_{\gamma 1} = \gamma_\Sigma \mu_\Sigma (1 - \beta_\Sigma) \qquad \text{and} \qquad E_{\gamma 2} = \gamma_\Sigma \mu_\Sigma (1 + \beta_\Sigma) \tag{6–16}$$

so that as $\beta_\Sigma \to 1$,

$$E_{\Sigma, \max}(E_\gamma) \to \infty$$

and

$$E_{\Sigma, \min}(E_\gamma) \to \frac{M_\Sigma}{2\mu_\Sigma} E_\gamma \tag{6–17}$$

provided the Σ^0 particles are created with an energy of the order of a gigaelectron volt or greater. We will find that this condition will be fulfilled in those cases that are of greatest interest for discussing the effects of Σ^0 decay on the cosmic γ-ray spectrum.

Incorporating equations (6–7), (6–15), and (6–17) into the general formula (6–9), as well as assumptions (6–11) and (6–12) and the branching ratio from table 6–3, we obtain

$$I_{\Sigma^0}(E_\gamma) = \frac{M_{\Sigma^0}}{4\mu_{\Sigma^0}} \langle nL \rangle \int_{E_{\text{th}\Sigma^0}}^{\infty} dE_p \, I_p(E_p) \int_{(M_{\Sigma^0}/2\mu_{\Sigma^0})E_\gamma}^{\infty} dE_{\Sigma^0} \sigma_{\Sigma^0}(E_p) \times \frac{\delta[E_{\Sigma^0} - \eta_{\Sigma^0}(E_p)]}{(E_{\Sigma^0}^2 - M_{\Sigma^0}^2)^{1/2}} \tag{6–18}$$

If we assume (as previously) a constant production cross section for $E_p > 25$ GeV and write $I_p(E_p)$ in the form

$$I_p(E_p) = K_p E_p^{-\Gamma} \tag{6-19}$$

where K_p and Γ are empirical constants, equation (6–18) can be integrated to give an approximate asymptotic spectrum for $E_\gamma > 10$ GeV. The result is

$$I_{\Sigma^0}(E_\gamma) \rightarrow K_{\Sigma^0} E_\gamma^{-\Gamma} \tag{6-20}$$

with

$$K_{\Sigma^0} \equiv \frac{K_p}{2\Gamma} \langle nL \rangle \sigma_{\Sigma^0} \left(\frac{2\chi \mu_{\Sigma^0}}{M_{\Sigma^0}} \right)^{\Gamma - 1} \tag{6-21}$$

6-4b The *i*-Process Decays

The baryons Σ^+, Λ, $N^*(1.410)$, and $N^*(1.688)$ decay by the *i*-process defined previously and thereby produce γ-rays. Because the *i*-process is a two-stage process, the determination of the distribution function $f_{di}(E_\gamma | E_i)$ requires an integration over an additional energy parameter. We will again, as in chapter 5, specify this parameter to be E'_γ. Equation (6–9) can then be expressed as (see derivation of equation (5–61)

$$I_i(E_\gamma) = C_i \int_{E\text{th},i}^{\infty} dE_p \, I(E_p) \int_{L_i}^{U_i} \frac{dE'_\gamma}{E'_\gamma} \int_{(M_i/2E'_\gamma)E_\gamma}^{\infty} dE_i \, \frac{\sigma_i(E_p)\delta[E_i - \eta_i(E_p)]}{(E_i^2 - M_i^2)^{1/2}} \tag{6-22}$$

where M_i is the mass of the isobar or hyperon considered;

$$C_i \equiv \frac{1}{2} \frac{R_i \langle nL \rangle \zeta_i}{\rho_i} \qquad \text{and} \qquad \zeta_i = 2 \tag{6-23}$$

with ρ_i defined by equation (5–55).

The relevant parameters needed to solve equation (6–22) for $N^*(1.410)$, $N^*(1.688)$, Σ^+, and Λ are given in table 6–4. If we assume, as before, that the production cross sections are constant above 25 GeV and that $I(E_p)$ can be written as $K_p E_p^{-\Gamma}$, equation (6–22) can be integrated to yield an

TABLE 6–4.—*Kinematic Parameters for* Λ, Σ^+, $N^*(1.410)$, *and* $N^*(1.688)$

Particle	μ_i, GeV	ρ_i	U_i, GeV	L_i, GeV	$C_i/\langle nL \rangle$	$(U_i/M_i)^{2.5}$
$N^*(1.688)$	0.586	0.339	0.579	0.007	0.737	6.89×10^{-2}
$N^*(1.410)$	.391	.262	.379	.012	.954	3.81×10^{-2}
Σ^+	.232	.159	.211	.022	1.60	1.51×10^{-2}
Λ	.170	.0929	.137	.033	1.78	0.58×10^{-2}

asymptotic approximation for $E_\gamma > 10$ GeV. The result is again of the form

$$I_i(E_\gamma) = K_i E_\gamma^{-\Gamma} \tag{6-24}$$

with

$$K_i \equiv \frac{2K_p C_i \sigma_i}{\Gamma^2} (2\chi)^{\Gamma-1} \frac{U_i^\Gamma - L_i^\Gamma}{M_i^\Gamma} \tag{6-25}$$

6-4c Gamma Rays From π^0-Mesons Produced by Pionization

We will now calculate the cosmic γ-ray spectrum predicted from the decay of kaons and neutral pions created by the so-called pionization or fireball processes. (See review article of Fujimoto and Hayakawa, 1967.) We have already derived the expression for the γ-ray spectrum produced from neutral pion decay (Eq. (1–100)). It then follows from assumptions (6–11) and (6–12) that

$$I_{\pi^0}(E_\gamma) = 2\langle nL\rangle \int_{E_{\mathrm{th}_{\pi^0}}}^{\infty} dE_p\, I(E_p) \int_{E_\gamma + (M_\pi^2/4E_\gamma)}^{\infty} dE_\pi \frac{\sigma(E_\pi | E_p)}{(E_\pi^2 - M_\pi^2)^{1/2}} \tag{6-26}$$

The function $\zeta_\pi(E_p)\sigma_\pi(E_p)$ is plotted in figure 5–9. In the high-energy asymptotic limit, we again assume $I(E_p) \simeq K_p E_p^{-\Gamma}$. We also assume $\sigma_\pi(E_\pi|E_p)$ to be of the approximate form

$$\sigma(E_\pi | E_p) = \sigma_0 E_p^a \delta(E_\pi - \chi_0 E_p^b) \tag{6-27}$$

with the coefficients σ_0 and χ_0 and the exponents a and b taken as constants. We then obtain from equation (6–26), for $E_\gamma > 5$ GeV, the asymptotic form

$$I_{\pi^0}(E_\gamma) = 2\langle nL\rangle \int_{E_{\mathrm{th}_{\pi^0}}}^{\infty} dE_p\, \sigma_0 E_p^a I(E_p) \int_{E_\gamma}^{\infty} dE_\pi \frac{\delta(E_\pi - \chi_0 E_p^b)}{(E_\pi^2 - M_\pi^2)^{1/2}} \tag{6-28}$$

which can be integrated to yield the solution

$$I_{\pi^0}(E_\gamma) = K_0 E_\gamma^{-g/b} \tag{6-29}$$

where

$$g \equiv (\Gamma + b) - (a + 1) \tag{6-30}$$

and

$$K_0 \equiv \frac{2}{g} \langle nL\rangle K_p \sigma_0 \chi_0^{[(g/b)-1]} \tag{6-31}$$

Pionization is a term that may be taken to include the various models that have been proposed to explain the bulk of pions produced in high-energy collisions. In these models, energy lost in the collision is con-

TABLE 6–5.—*Parameters for Determining γ-ray Spectra From Various Pionization Models* [a]

Model	Valid energy range	a	b	g/b		
				$\Gamma=2.5$	$\Gamma=2.7$	$\Gamma=3.2$
Fermi's model (Fermi, 1951).	All E_p.....	0.25	0.75	2.67	2.93	3.6
1-fireball model.....	$E_p < 150$ GeV....	.5	.5	3.0	3.4	NA
2-fireball model.....	$E_p > 10^3$ GeV....	.25	.75	NA	2.93	3.6
Landau's model.....	All E_p.....	.....	.....	(b)		

[a] See Fujimoto and Hayakawa (1967).

[b] Gamma-ray spectrum proportional to $E_\gamma^{-3.2}$, according to Lieber et al. (1965).

NA = Not applicable.

sidered to concentrate initially into one or more pion-emitting centers or fireballs. Studies indicate that the fireballs move relatively slowly in the cms compared to the baryons we have considered. Therefore, the pions arising from this process are, in general, not so energetic as *i*-process pions. Depending on the model, different multiplicity laws $\zeta(E_p)$ are predicted, all of which can be made to fit the data available in appropriate regions of E_p because of the large errors involved and the relatively slow variations of $\zeta(E_p)$ predicted over large ranges of E_p. The multiplicity laws yield the quantity a in equation (6–27). If we assume, as the data indicate, that, on the average, a constant fraction of energy goes into pionization independent of E_p, then

$$b = 1 - a \tag{6–32}$$

The exponent in equation (6–29), g/b, can then be determined for the various models, as shown in table 6–5. All the pionization spectra have steeper energy dependences (larger g/b) than the calculated *i*-process spectra (exponents equal Γ at high energy), reflecting the fact that pionization produces γ-rays of lower average energy than the *i*-process.

6–5 NUMERICAL CALCULATION OF THE ENERGY SPECTRUM OF GALACTIC GAMMA RAYS ABOVE 1 GeV

Equations (6–18), (6–22), and (6–26) were solved numerically (Stecker et al., 1968) assuming the cosmic-ray proton energy spectrum to be a broken power law of the form $K_p E_p^{-\Gamma}$, as shown in table 6–6.[3] The effect of α–p, p–α, and α–α interactions was taken into account by estimating,

[3] Table 6 in Stecker (1968a) is in error.

from the cross section and energy spectrum data given in figures 5–7 and 5–9, that p–α and α–p interactions contribute an additional flux of about 60 percent of that from p–p interactions and that α–α interactions contribute another 10 percent. Thus, we may define an effective cosmic-ray spectrum in energy per nucleon given by $K_{cr}E_{cr}^{-\Gamma}$, where $K_{cr}=1.7K_p$.

TABLE 6–6.—*Form of the Cosmic-Ray Spectrum* $I(E_{cr})=K_{cr}E_{cr}^{-\Gamma}$

Energy range, GeV	K_p	K_{cr}	Γ
10 to 10^2	$10^{-0.05}$	$10^{0.18}$	2.5
10^2 to 10^6	$10^{0.35}$	$10^{0.58}$	2.7
10^6 to $10^{8.5}$	$10^{3.35}$	$10^{3.58}$	[a] 3.2
$10^{8.5}$ to 10^{11}	$10^{-1.75}$	$10^{-1.52}$	[a] 2.6

[a] See Bradt et al., 1965.

The cross sections for the production of nucleon isobars and hyperons in p–p interactions are given in tables 6–1 and 6–2 for $E_p < 25$ GeV and were assumed to have the values in table 6–3 for $E_p > 25$ GeV.

The solution of equation (6–26) for $E_p < 150$ GeV is based on the one-fireball model. (See table 6–5.) It assumes a unique average cms pion energy independent of E_p (see ch. 5 and also Hayakawa et al., 1964) and also a multiplicity law of the form $\zeta(E_p) \sim E_p^{1/2}$. The upper limit of 150 GeV on E_p for the validity of the one-fireball model is in accordance with the treatment of Fujimoto and Hayakawa (1967). For $E_p > 500$ GeV, a two-fireball model may be taken to approximate the data more closely. As for the one-fireball model described above, equation (6–26) must be integrated numerically; the two-fireball model may be well represented by the asymptotic solution given by equation (6–29) with $a=0.25$ and $b=0.75$. (See Fujimoto and Hayakawa, 1967.) A smooth transition between the one-fireball and the two-fireball models was assumed to occur in the region $150 \leq E_p \leq 500$ GeV. It is found that the resulting solution is determined by the one-fireball model for $E_\gamma < 3.5$ GeV and by the two-fireball model for $E_\gamma > 10$ GeV.

Figure 6–1 shows the total γ-ray spectrum calculated with the use of equations (6–18), (6–22), (6–26), and (6–29), as just described as well as the results from chapter 5. Our results in figures 6–1 and 6–2 show that if we sum the contributions to the γ-ray spectrum from the pioniza-

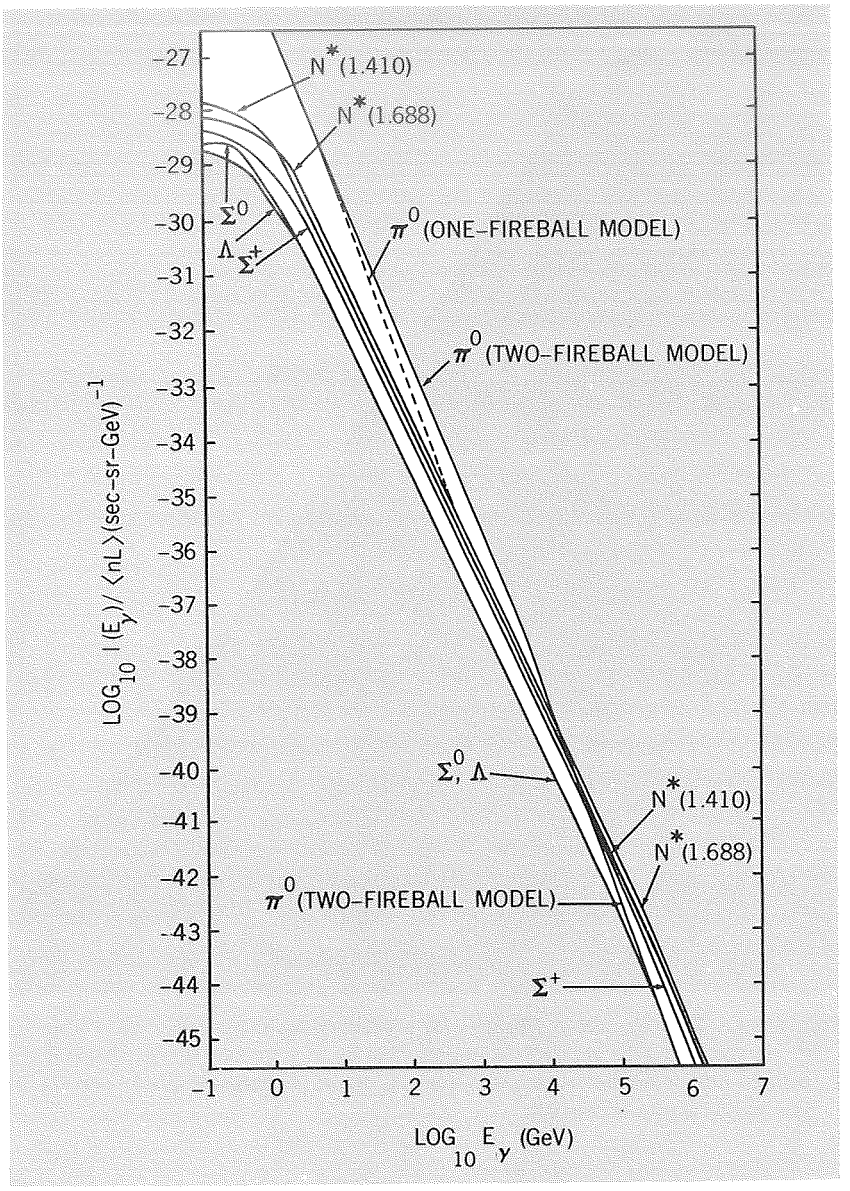

FIGURE 6–1.—Calculated γ-ray spectra from various secondary particles produced in galactic cosmic-ray interactions.

tion processes just described and from the *i*-process discussed in the previous section, we find that the characteristics of the spectrum for

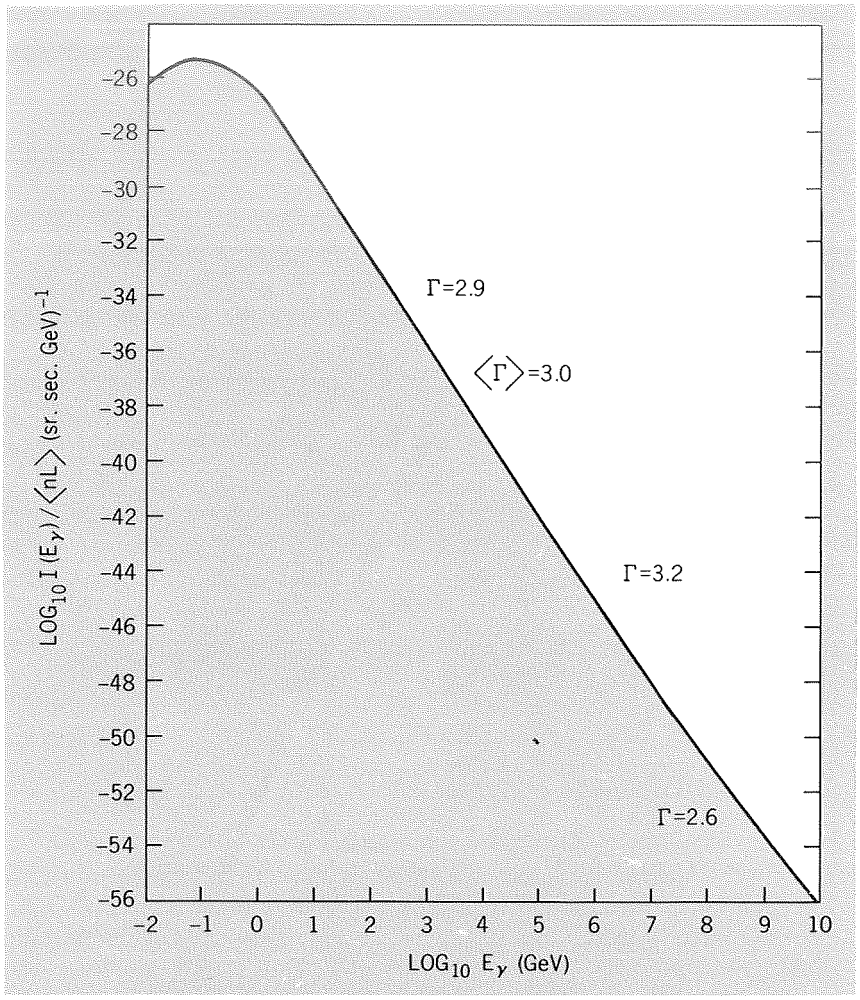

FIGURE 6–2. — Total calculated galactic γ-ray production spectrum as described in the text. The internal error in absolute intensities (due to uncertainties in experimental cross sections, cosmic-ray intensity, and branching ratios) is approximately 35 percent. The error in Γ is approximately 0.2.

$E_\gamma > 6000$ GeV may indeed be determined by the decays of various hyperons and baryon resonances.[4]

[4] For a discussion of the effect of hyperons and nucleon resonances in atmospheric cosmic-ray interactions and a comparison with the observed γ-ray and muon spectra as well as the muon charge ratio, see Pal and Peters (1964). Observational verification of the importance of the *i*-process in interactions where $E_p > 10^3$ GeV can be found in Kazuno (1964).

The characteristics of the γ-ray spectra given in figures 6–1 and 6–2 can be readily understood. The increase in the primary spectral index from 2.7 to 3.2 at 1000 TeV results in a corresponding increase in the spectral index of the *i*-process γ-ray spectra from 2.7 to 3.2 at about 200 TeV. However, the change in the primary spectrum produces a more pronounced steepening in the spectral index of the pionization γ-ray spectrum, increasing it from 2.9 to 3.6 at approximately 3 TeV. (See table 6–5.) The effect of these changes on the total γ-ray spectrum (*i*-process plus pionization) is a gradual increase in the spectral index from 2.9 to 3.2 between 3 and 300 TeV. The total calculated spectral index is approximately 2.9 between 0.1 and 1 TeV and 3.0 between 1 and 10 TeV, and is consistent with the present data on the γ-ray spectrum produced by atmospheric cosmic-ray collisions, as summarized by Fujimoto and Hayakawa (1967).

Equilibrium Spectra of Secondary Cosmic-Ray Positrons in the Galaxy and the Spectrum of Cosmic Gamma Rays Resulting From Their Annihilation

7-1 INTRODUCTION

The annihilation of cosmic-ray positrons has for some time been recognized as a potential source of cosmic γ-rays. Gamma-ray fluxes from cosmic positron annihilation have been estimated and discussed by various authors (Pollack and Fazio, 1963; Hayakawa et al., 1964; and Ginzburg and Syrovatskii, 1964). Pollack and Fazio (1963) have discussed the possible relationship between the present flux of 0.5-MeV γ-radiation from positron annihilation and the cosmic-ray intensity and galactic gas density 10^9 years ago. Ginzburg and Syrovatskii (1964) have pointed out that the intensity of the 0.5-MeV line may be a sensitive measure of the leakage rate of cosmic-ray positrons from the galaxy. These authors have also given an approximate formula for the calculation of the γ-ray spectrum from the annihilation of high-energy positrons.

It has therefore become apparent that the cosmic γ-ray spectrum from cosmic-ray positron annihilation may contain much potential information reflecting various astrophysical conditions in our own galaxy and in possible cosmic-ray sources, both galactic and extragalactic.

Cosmic-ray positrons may be produced in the galaxy either from the decay of secondary π^+-mesons via the decay chain

$$\begin{array}{l} \pi^+ \rightarrow \mu^+ + \nu_\mu \\ \qquad\quad \hookrightarrow e^+ + \nu_e + \bar{\nu}_\mu \end{array} \tag{7-1}$$

As was the case with the neutral pions discussed previously, the positive pions may be produced either in cosmic-ray interactions with the galactic gas or in matter-antimatter annihilations.

In addition to the positrons resulting from pion decay, lower energy positrons are produced in the galaxy, principally by cosmic-ray p—^{12}C, p—^{14}N, and p—^{16}O collisions at relatively low energy, which result in the production of radionuclei having β-ray-positron-emitting decay modes.

Since these interactions are nuclear transmutations rather than pion-producing interactions, they involve relatively low threshold energies (of the order of 10 MeV rather than 300 MeV). Moreover, the β-ray positrons are produced in the galaxy, principally by cosmic-ray p–^{12}C. whereas the spectrum of pion-decay positrons peaks at about 35 MeV and decreases rapidly toward lower energies. Thus, if there exists a large flux of low-energy galactic cosmic rays, these particles may provide the most copious source of low-energy cosmic-ray positrons. This source may then contribute significantly to an observable flux of positrons near the Earth at and below 1-MeV energy. Furthermore, because of their low energy, β-ray positrons are much more likely to stop and annihilate in the galaxy to produce 0.51-MeV γ-rays than are the positrons from the pion-decay process. Reversing the argument leads to the conclusion that the intensity of the 0.51-MeV positron-annihilation line in the galaxy may provide a sensitive measure of the galactic cosmic-ray flux below 1 GeV/nucleon.

A typical cosmic-ray positron may undergo one of three fates: it may escape from the galaxy, annihilate with an electron while at relativistic energy, or lose almost all of its energy before annihilation. One must, of course, consider that annihilations may occur either between free electrons and positrons or through the formation of intermediate bound states of positronium. All of the physical processes listed in this section must be considered in calculating the final positron annihilation γ-ray spectrum.

7–2 THE POSITRON PRODUCTION SPECTRUM FROM THE DECAY OF POSITIVE PIONS

Positron production arising from pion-producing cosmic-ray interactions followed by the decay process (7–1) has been discussed in many places in the literature (Hayakawa, 1963; Hayakawa and Okuda, 1962; Hayakawa et al., 1964; Ginzburg and Syrovatskii, 1964; Jones, 1963, 1965a; Pollack and Fazio, 1965; Scanlon and Milford, 1965; Ramaty and Lingenfelter, 1966a, b, 1968; and Perola, Scarsi, and Sironi, 1968). We present here a brief review of the kinematics of the decay along with the results of the most recent calculations by Ramaty and Lingenfelter.

The decay process (7–1), being a three-stage decay chain, will involve three intermediate integrations of the form of equation (1–14) in order to determine the positron production spectrum. The decay

$$\pi^+ \rightarrow \mu^+ + \nu_\mu \tag{7–2}$$

is a two-particle decay involving one massless particle (the neutrino),

so equation (1–78) is applicable. From equations (1–65) and (1–78), we obtain

$$E_\mu = \frac{E_\pi}{M_\pi}\left[\left(\frac{M_\pi^2 + M_\mu^2}{2M_\pi}\right) + \left(1 - \frac{M_\pi^2}{E_\pi^2}\right)^{1/2}\left(\frac{M_\pi^2 - M_\mu^2}{2M_\pi}\right)\cos\theta'\right] \tag{7–3}$$

or, using η and ρ,

$$E_\mu = E_\pi[\eta(M_\pi, M_\mu) + \beta_\pi\rho(M_\pi, M_\mu)\cos\theta'] \tag{7–4}$$

As was shown in chapter 1 (e.g., see eq. (1–147)), equation (7–4) can also be expressed as

$$E_\pi = \frac{M_\pi^2}{M_\mu^2}[\eta(M_\pi, M_\mu) + \tfrac{1}{2}\beta_\mu\kappa(M_\pi, M_\mu)\cos\theta']E_\mu \tag{7–5}$$

through the use of equation (1–42); equation (7–5) can be used to place limits on the energy range of pions which produce muons of energy E_μ. We thus obtain

$$f(E_\mu) = \int_{E_{\pi,\min}}^{E_{\pi,\max}} dE_\pi \frac{f(E_\pi)}{\kappa(M_\pi, M_\mu)(E_\pi^2 - M_\pi^2)^{1/2}} \tag{7–6}$$

where

$$E_{\pi,\substack{\max\\\min}} = \frac{M_\pi^2}{M_\mu^2}[\eta(M_\pi, M_\mu) \pm \tfrac{1}{2}\beta_\mu\kappa(M_\pi, M_\mu)]E_\mu \tag{7–7}$$

Equation (7–7) may be numerically approximated by

$$E_{\pi,\substack{\max\\\min}} = (1.36 \pm 0.36\beta_\mu)E_\mu \tag{7–8}$$

and, as $\beta_\mu \to 1$,

$$\begin{aligned} E_{\pi,\max} &\to \left(\frac{M_\pi}{M_\mu}\right)^2 E_\mu \simeq 1.72E_\mu \\ E_{\pi,\min} &\to E_\mu \end{aligned} \tag{7–9}$$

The decay

$$\mu^+ \to e^+ + \nu_e + \nu_\mu \tag{7–10}$$

is a three-body decay with a resultant broad energy spectrum of the positron in the rest system of the muon. Let us denote the normalized positron energy spectrum in the muon rest system by $D_\mu(E_e')$. It has been shown that

$$D_\mu(E_e') = \frac{4E_e'}{E^{*4}}(E_e'^2 - M_e^2)^{1/2}\left[3(E^* - E_e') + \frac{2}{3}\omega(4E_e' - 3E^*)\right] \tag{7–11}$$

where E^* is the maximum energy available to the electron in the decay,

$$E^* = \frac{M_\mu}{2}\left[1 + \frac{M_e^2}{M_\mu^2}\right] \simeq \frac{M_\mu}{2} \tag{7-12}$$

and $\omega \simeq 3/4$ is the Michel parameter (Michel, 1949).

From equations (1–42) and (1–49) we obtain the relation between E_μ and E_e' for a given value of E_e as

$$E_\mu = \frac{M_\mu}{M_e^2} E_e E_e'(1 + \beta_e \beta_e' \cos\theta') \tag{7-13}$$

which sets the limits on the energy range of muons which produce positrons of energy E_e.

Putting all of these results together in a manner similar to that used in chapter 1 for obtaining formulas for γ-ray production spectra, we obtain

$$q(E_{e^+}) = 2\pi n \int_{E_{\mathrm{th}_p}}^{\infty} dE_p I(E_p) \int_{M_e}^{E^*} \frac{dE_e' D(E_e')}{\sqrt{E_e'^2 - M_e^2}} \int_{(M_\mu/M_\pi^2)E_e E_e'(1-\beta_e\beta_e')}^{(M_\mu/M_\pi^2)E_e E_e'(1+\beta_e\beta_e')} dE_\mu$$
$$\times \int_{(M_\pi^2/M_\mu^2)(\eta-\beta_\mu\rho)E_\mu}^{(M_\pi^2/M_\mu^2)(\eta+\beta_\mu\rho)E_\mu} dE_\pi \frac{\sigma(E_\pi|E_p)}{(E_\pi^2 - M_\pi^2)^{1/2}} \tag{7-14}$$

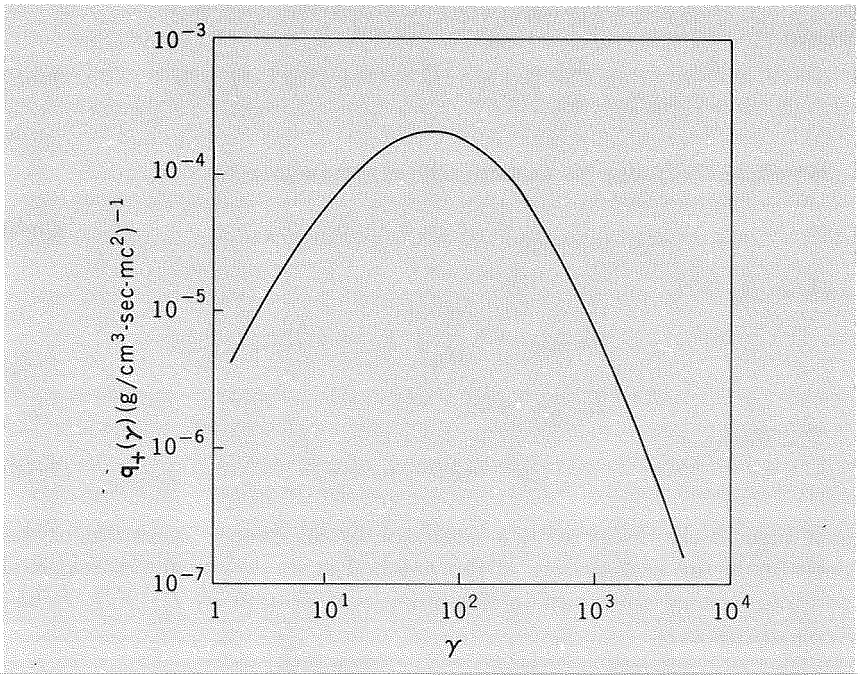

FIGURE 7–1.—The source spectrum of positrons produced from the decay of positive pions formed in cosmic-ray collisions.

It is of interest to note that most calculations of the positron production spectrum from pion decay have included the approximation of neglecting the muon recoil in the pion decay by setting $\beta_\mu \simeq \beta_\pi$. In this approximation, the right-hand integral in equation (7–14) is eliminated, and the muon and pion production functions obey the relation

$$\sigma_\mu(E_\mu|E_p) = \frac{M_\pi}{M_\mu}\,\sigma_\pi\left(\frac{M_\pi}{M_\mu}E_\mu\middle|E_p\right) \tag{7–15}$$

Ramaty and Lingenfelter (1966a) have shown that this approximation introduces little error into the calculation.

The most recent determination of the positron production spectrum from charged pion decay, as calculated by Ramaty, is shown in figure 7–1.

7–3 THE POSITRON PRODUCTION SPECTRUM FROM THE DECAY OF RADIONUCLEI

The production spectrum of radionuclei $q_r(E_r)$ is given by (Ramaty, Stecker, and Misra, 1970)

$$q_r(E_r) = 4\pi \sum_{i,k} \int dE_i\, I_i(E_i) n_k \sigma_{r,ik}(E_i) f_{r,ik}(E_r|E_i) \tag{7–16}$$

where E_i and E_r are the energies of the primary and secondary particles, respectively; I_i is the intensity of primary cosmic-ray nuclei of type i in interstellar space; n_k is the number density of interstellar gas atoms of type k; $\sigma_{r,ik}$ is the interaction cross section for production of a radionucleus of type r, and $f_{r,ik}(E_r|E_i)$ is the normalized energy distribution function for production of a nucleus with energy E_r in an interaction of energy E_i.

Among the variety of β-emitting nuclei which may be formed in galactic cosmic-ray interactions, only ^{11}C, ^{13}N, ^{14}O, and ^{15}O contribute significantly to positron production. The principal reactions and their threshold energies are given in table 7–1 along with their decay modes and maximum positron energies. The cross sections were summarized by Lingenfelter and Ramaty (1967) and by Audouze, Epherre, and Reeves (1967). The distribution functions $f_{r,ik}(E_r|E_i)$ are, in general, unknown. Their detailed form, however, is not important for the present problem since most of the positrons are emitted from nuclei decaying near rest. Thus, the positron production spectrum is determined mainly by the β-ray spectrum of the parent nuclei. Ramaty et al. (1970) assumed that in these p–CNO interactions, the kinetic energy per nucleon is equally distributed among all the secondary nuclei produced, so that

$$f_{r,ik}(E_r|E_i) = \delta\left[E_r - A_r\left(\frac{E_i - M_i - Q_{ik}}{A_i + A_k}\right) - M_r\right] \tag{7–17}$$

TABLE 7–1.—*Principal Reactions Leading to Production of β-Emitting Nuclei*

[See Audouze et al., 1967]

Reaction	σ, mb	Decay	Half-life	Maximum positron energy, MeV
$^{12}C(p, 3p2n)^{8}B$	?	$^{8}B(\beta^+)^{8}Be$	0.78 s	1.4
$^{12}C(p, p2n)^{10}C$	~3	$^{10}C(\beta^+)^{10}B$	19 s	1.9
$^{14}N(p, 2p3n)^{10}C$	?			
$^{16}O(p, 3p, 4n)^{10}C$	<10			
$^{12}C(p, pn)^{11}C$	~70	$^{11}C(\beta^+)^{11}B$	20.5 min	0.97
$^{14}N(p, 2p2n)^{11}C$	~30			
$^{16}O(p, 3p3n)^{11}C$	~10			
$^{12}C(p, n)^{12}N$	?	$^{12}N(\beta^+)^{12}C$	0.011 s	16.4
$^{14}N(p, p2n)^{12}N$	?			
$^{16}O(p, 2p3n)^{12}N$	?			
$^{14}N(p, pn)^{13}N$	~15	$^{13}N(\beta^+)^{13}C$	10.0 min	1.19
$^{16}O(p, 2p2n)^{13}N$	~10			
$^{14}N(p, n)^{14}O$	[a]~50	$^{14}O(\beta^+)^{14}N$	71 s	1.18, 4.14
$^{16}O(p, p2n)^{14}O$	<10			
$^{16}O(p, pn)^{15}O$	~50	$^{15}O(\beta^+)^{15}N$	2.06 min	1.74

?=Unknown and not included in estimate of positron production.

[a] This cross section has a value of about 10 mb at energies below 12 MeV but is negligible above 150 MeV.

where A_i and A_K are the mass numbers of the incident and target nuclei, respectively.

They assumed for the purposes of calculation that the ratios H:C:N:O in the interstellar gas are $1 : 3.4 \times 10^{-4} : 1.1 \times 10^{-4} : 5.8 \times 10^{-4}$, based on the composition of the solar atmosphere (Durgaprasad et al., 1968), which agree reasonably well with the universal abundances given by Suess and Urey (1956) and Cameron (1959).

The cosmic-ray energy spectrum and charge composition at solar minimum has been measured by a number of experimenters. The proton spectrum above 20 MeV was summarized by Gloeckler and Jokipii (1967), and the spectrum below 20 MeV is given by Fan et al. (1968). The CNO spectra above 50 MeV/nucleon were summarized by Meyer (1969). Because of the lack of data at lower energies, we have assumed that these spectra are of the form $E_i^{0.4}$, normalized to observations at higher energies.

The interstellar primary cosmic-ray intensities can be obtained from the solar minimum spectra through multiplication by a modulation function of the form

$$\mathscr{M}(R) = \begin{cases} \exp\ (R_r/R_0\beta) & \text{for } R < R_0 \\ \exp\ (R_r/R\beta) & \text{for } R > R_0 \end{cases} \tag{7-18}$$

where R and β are rigidity and velocity respectively, R_0 is a characteristic transition rigidity that depends on the distribution of interplanetary magnetic field irregularities, and R_r is a parameter which is space and time dependent and defines the total residual modulation. This modulation function was recently discussed by Ramaty and Lingenfelter (1969). They have shown that above a rigidity of 500 MV the observed cosmic-ray ^{2}H and ^{3}He spectra are consistent with those obtained from nuclear interactions in interstellar space, with $R_r \approx 350$ MV and a mean pathlength for galactic cosmic rays of $X \approx 4$ g/cm^2. Since there is no information on residual modulation at lower energies, we have to treat R_0 as a free parameter.

Since the lifetimes of the CNO β-emitters are short, the positron production spectrum q_+ can be obtained directly from the spectra q_r by taking into account the kinematics of the decay. Thus,

$$q_+(E_+) = \sum_r \frac{1}{2} \int_{M_e}^{E^*} \frac{dE'_+ P(E'_+)}{(E'^2_+ - M_e^2)^{1/2}} \int_{E_{r,\,\min}}^{E_{r,\,\max}} \frac{dE_r\, q_r(E_r)}{(E_r^2 - M_r^2)^{1/2}} \tag{7-19}$$

where E_r, E'_+, and E_+ are the total energies of the decaying isotope, the positron in the rest frame of the isotope, and the positron in the galactic rest frame, respectively; E^* is the maximum value of E'_+ and is given in table 7–1 for the various isotopes involved. The function $P(E'_+)$ is the normalized distribution function for positron production from beta-decay processes and is given by Fermi (1934) as

$$P(E'_+) \propto E'_+ (E'^2_+ - M_e^2)^{1/2} (E^* - E'_+)^2 \tag{7-20}$$

The limits $E_{r\,\min}^{\max}$ are found once again by using equations (1–42) and (1–49) and are given by

$$E_{r,\,\min}^{\max} = \frac{M_r}{M_e^2} E_+ E'_+ (1 \pm \beta_+ \beta'_+) \tag{7-21}$$

Using the data previously discussed, Ramaty et al. (1970) have numerically solved equations (7–16) and (7–19) for the solar minimum spectrum and for $R_r = 350$ MV with various values of R_0. As an extreme assump-

tion, they also used a power-law cosmic-ray spectrum of the form $T_i^{-2.5}$, with low-energy cutoffs T_c at 5, 15, and 100 MeV/nucleon.

The resultant production spectra together with the positrons that would result from pion decay are shown in figure 7–4. As can be seen, the CNO source becomes significant only if there are large fluxes of low-energy cosmic rays. The large positron production at low energies for $R_0 = 200$ MV and for the power-law spectrum comes primarily from ^{13}N and ^{14}O produced by low-energy protons via the reactions $^{16}O(p, 2p2n)^{13}N$ and $^{14}N(p, n)^{14}O$.

7-4 THE EQUILIBRIUM SPECTRUM OF SECONDARY GALACTIC POSITRONS FROM PION DECAY

In order to calculate plausible annihilation γ-ray spectra from our own galaxy, we will assume that the only source of galactic cosmic-ray positrons above a few MeV energy is the result of primary cosmic rays colliding with atoms of interstellar hydrogen and helium gas in the galaxy and producing positive pions which rapidly decay into positrons and neutrinos.

We further assume that these positrons have reached a quasi-equilibrium condition in the galaxy determined by leakage out of the halo, annihilation, and energy loss by ionization and coulomb interactions, bremsstrahlung, Compton collisions, and synchrotron radiation.

The positron equilibrium energy spectrum $n(E_+)dE_+$ then obeys the relation

$$\frac{d}{dt}\int_0^\infty dE_+\, n(E_+, t) = \int_0^\infty dE_+\, q(E_+, t) - \int_0^\infty dE_+\, r_\tau(E_+, t) \qquad (7\text{–}22)$$

where $q(E_+, t)$ is the generating source function of high-energy positrons (in this case, from the decay of mesons formed in high-energy interactions) and $r_\tau(E_+, t)$ is the total positron loss rate due to annihilation and leakage from the galaxy.

In the cosmic medium, energy loss mechanisms such as synchrotron radiation are at work, resulting in a continuous loss of energy per positron. We can take this effect into account by transforming equation (7–22) into

$$\int_0^\infty dE_+ \left[\frac{\partial}{\partial t} n(E_+, t) + \frac{\partial}{\partial E_+}\left(n(E_+, t)\frac{dE_+}{dt}\right)\right] = \int_0^\infty dE_+ \,[q(E_+, t) - r_\tau(E_+, t)] \qquad (7\text{–}23)$$

For convenience, we will now drop the subscript "+" and rewrite equation (7–23) in the differential form

$$\frac{\partial}{\partial t} n(E, t) + \frac{\partial}{\partial E}\,[n(E)r(E)] = q(E, t) - \frac{n(E, t)}{\tau_s(E, t)} \qquad (7\text{–}24)$$

with the loss term $r(E, t)$ rewritten in terms of a survival time $\tau_s(E, t)$ such that for an annihilation time τ_A and a leakage time τ_l,

$$\tau_s(E, t) = \frac{\tau_A(E, t)\tau_l(E, t)}{\tau_A(E, t) + \tau_l(E, t)} \tag{7-25}$$

and

$$r(E) \equiv \frac{dE}{dt} \tag{7-26}$$

The Green's function form of equation (7–24) is

$$\frac{\partial}{\partial t} G[E, t|E', t'] + \frac{\partial}{\partial E} [r(E, t)G[E, t|E', t']] + \frac{G[E, t|E', t']}{\tau_s(E, t)} = \delta(E - E')\delta(t - t') \tag{7-27}$$

In the case where $r(E|t) = r(E)$ and $n_{e-}(t) = n_{e-}$ independent of time, the Green's function for equation (7–27) has the structure

$$G[E, t|E', t'] = \frac{1}{|r(E)|} \exp\left[-\int_E^{E'} \frac{dE''}{\tau(E'')|r(E'')|}\right] \delta\left(t - t' - \int_E^{E'} \frac{dE''}{|r(E'')|}\right) \tag{7-28}$$

Thus, the solution for $n(E, t)$ is

$$n(E, t) = \frac{1}{|r(E)|} \int_E^{\infty} dE'\, q\left(E', t - \int_E^{E'} \frac{dE''}{|r(E'')|}\right) \exp\left[-\int_E^{E'} \frac{dE''}{\tau(E'')|r(E'')|}\right] \tag{7-29}$$

At this point, we will refer back to the basic formulas derived in chapter 2 for calculating the γ-ray spectra from positron annihilation. We will again find it useful to discuss these calculations in terms of the positron Lorentz factor, $\gamma = E/M_e$. Assuming a time-independent source $q_+(\gamma)$, we can then write equation (7–29) as

$$n(\gamma) = \frac{1}{|r(\gamma)|} \int_{\gamma}^{\infty} d\gamma'\, q_+(\gamma') \exp\left[-\int_{\gamma}^{\gamma} \frac{d\gamma''}{|r(\gamma'')|\tau_s(\gamma'')|}\right] \tag{7-30}$$

Equation (7–30) may then be used to obtain numerical solutions for $n(\gamma)$ and the positron equilibrium flux

$$I_+(\gamma) = \frac{c}{4\pi} \frac{n(\gamma)(\gamma^2 - 1)^{1/2}}{\gamma} \tag{7-31}$$

The survival time used will be given by

$$\frac{1}{\tau_s(\gamma)}=\frac{1}{\tau_A(\gamma)}+\frac{1}{\tau_l(\gamma)} \tag{7-32}$$

with $\tau_A(\gamma)$ and $\tau_l(\gamma)$ being the annihilation time and mean leakage time (or diffusion time) for positrons of energy γMc^2. From equation (2–22), we obtain

$$\frac{1}{\tau_A(\gamma)}=\frac{n_e\sigma_0 c}{\gamma}\left(\frac{\gamma-1}{\gamma+1}\right)^{1/2}\left\{\frac{\gamma^2+4\gamma+1}{\gamma^2-1}\ln\left[\gamma+(\gamma^2-1)^{1/2}\right]-\frac{\gamma+3}{(\gamma^2-1)^{1/2}}\right\} \tag{7-33}$$

The leakage time will be assumed to be inversely proportional to velocity so that

$$\frac{1}{\tau_l(\gamma)}=\frac{(\gamma^2-1)^{1/2}}{\gamma T_l} \qquad T_l=\text{constant} \tag{7-34}$$

Most of the interstellar gas in our galaxy is un-ionized with the exception of the so-called H-II regions near the very hot O and B stars, which are powerful sources of ionizing ultraviolet radiation. Allen (1963) gives the proportion of space near the galactic plane occupied by clouds of interstellar gas and dust as 7 percent and that occupied by ionized clouds (H-II regions) as 0.4 percent. We will therefore assume that the galactic gas is entirely neutral for the purposes of these calculations and take for the energy loss rate from ionization the expression (see Heitler, 1960; Morrison, 1961):

$$r_I(\gamma)=\frac{8}{3}\sigma_0 n_e c\,\frac{\gamma}{(\gamma^2-1)^{1/2}}\left\{22+\ln\left[\gamma(\gamma-1)(\gamma^2-1)\right]-1.695\left(\frac{\gamma^2-1}{\gamma^2}\right)-\frac{1.39}{\gamma}\right\} \tag{7-35}$$

The energy loss rate from bremsstrahlung may be taken as

$$r_B(\gamma)=7.3\times10^{-16}n_e\gamma \tag{7-36}$$

based on radiation lengths for hydrogen and helium given by Dovzhenko and Pomanskii (1964).

The loss rate from synchrotron radiation and Compton collisions may be taken as

$$r_{s+c}(\gamma)=(1.3\times10^{-9}H^2+3\times10^{-11}\rho_\gamma)\gamma^2 \tag{7-37}$$

where H is given in gauss and the radiation density ρ_γ is given in eV/cm^3 (Ramaty and Lingenfelter, 1966a).

The total positron energy-loss rate is taken to be the sum of equations (7–35) through (7–37), so that

$$r(\gamma) = r_I(\gamma) + r_B(\gamma) + r_{s+c}(\gamma) \tag{7–38}$$

We have now specified all the quantities needed for the numerical solution of equation (7–30). The solution to equation (7–30) then yields the function $n(\gamma)$, which can be used in equation (2–19) to obtain a numerical solution for the in-flight annihilation γ-ray spectrum (AGS) discussed in chapter 2. From equations (2–19) and (7–30), we obtain

$$Q(\eta) = 4H_+ \left(\frac{1}{2}\right) n_e{}^- \sigma_0 c \int_{G(\eta)}^{\infty} d\gamma \frac{\phi(\chi_0(\eta, \gamma), \gamma)}{\gamma(\gamma^2-1)^{1/2}|r(\gamma)|} \times \int_{\gamma}^{\infty} d\gamma' q_+(\gamma') \exp\left[-\int_{\gamma}^{\gamma'} \frac{d\gamma''}{|r(\gamma'')|\tau_s(\gamma'')}\right] \tag{7–39}$$

An interesting case to note in calculating the equilibrium positron spectrum $I_+(\gamma)$ is that for which the source $q_+(\gamma)$ is a source of low-energy positrons, as is the case with the positrons arising from β-decay as discussed in section 7–3. For those positrons, ionization losses predominate so that $r(\gamma) \simeq r_I(\gamma)$, which is proportional to the gas density. We may then reformulate equation (7–30) in a slightly different, but instructive, way.

The leakage lifetime τ_L can be expressed in terms of the mean amount of matter traversed by cosmic rays, $X = \rho c \beta \tau_L$. From cosmic-ray spallation studies, it is found that $X \approx 4 \text{g/cm}^2$.

Equation (7–31) for the equilibrium positron flux $I_+ = n_+ \beta c/4\pi$ can be written as

$$I_+(\gamma) = \frac{1}{4\pi} \frac{1}{K(\gamma)} \int_{\gamma}^{\infty} d\gamma' q_+(\gamma') \exp\left[-\frac{1}{X}\int_{\gamma}^{\gamma'} \frac{d\gamma''}{K(\gamma'')} \frac{1}{1 + X/X_A(\gamma'')}\right] \tag{7–40}$$

where $K(\gamma) = r(\gamma)/\rho\beta c$ (in cm^2/g) is the stopping power of protons in hydrogen, and X_A is an equivalent annihilation pathlength given by

$$X_A(\gamma) = 9.3(\gamma+1)\left[\frac{\gamma^2+4\gamma+1}{\gamma^2-1} \ln(\gamma + \sqrt{\gamma^2-1}) - \frac{\gamma+3}{\sqrt{\gamma^2-1}}\right]^{-1} \quad \text{g/cm}^2 \tag{7–41}$$

As can be seen, the positron intensity I_+ depends only on the interstellar cosmic-ray intensity (through the production function q_+) and on the pathlength X. Furthermore, at low positron energies, where the range of these particles is much smaller than X, I_+ depends only on the cosmic-ray intensity itself.

TABLE 7–2.—*Average Astrophysical Parameters for the Galactic Disk and Halo*

	n_e, cm^{-3}	H, μG	ρ_γ, eV/cm^3	T_l, 10^6 yr	L_{eff}, cm
Disk	0.5–1	6	0.45	2–4	3×10^{22}
Halo	$1–3\times10^{-2}$	3	0.65	100–300	5×10^{22}

In order to utilize equations (7–30) and (7–39) to determine the positron equilibrium flux and AGS in the galaxy, Stecker (1969a) chose typical average values for the quantities n_e, H, ρ_γ, and T_l for both the galactic disk and the galactic halo models. These values are given in table 7–2. The radiation density ρ_γ includes the contribution of 0.25 eV/cm^3 from the 2.7 K universal microwave field (Stokes, Partridge, and Wilkinson, 1967).

Using the values given in table 7–2 for the galactic halo model to integrate equations (7–30) and (7–39) numerically, Stecker (1969a) obtained typical galactic spectra from pion-decay positions for $I_+(\gamma)$ and $Q(\eta)$. The results are given in figures 7–2 and 7–3 for various values of mean pathlength X (g/cm^2) and corresponding T_l.[1] The flux of annihilation γ-radiation observed at the Earth, $I_A(\eta)$, is given by

$$I_A(\eta)=\frac{L_{\text{eff}}}{4\pi}Q(\eta) \tag{7–42}$$

where L_{eff} is the effective pathlength for γ-ray production.

For leakage times less than 10 million years, the equilibrium positron flux has roughly the same characteristics as the source spectrum of figure 7–1, and its magnitude is proportional to the leakage time. In the case of longer leakage times, the positrons are trapped in the galaxy for

[1] The relation between mean pathlength X and mean leakage time T_l is given by the equation $X=\rho cT_l$, where ρ is the mean density of the gas in the medium (Ramaty and Lingenfelter, 1966a). Assuming the galactic medium is 90 percent hydrogen and 10 percent helium, with X in g/cm^2, n_H in atoms/cm^3, and T_l in millions of years, this relation becomes $X\simeq 5n_HT_l$. Thus, for a halo model with $X=5$ g/cm^2 and $n_H=10^{-2}$ cm^{-3}, $T_l=10^8$ years; whereas for a disk model with $X=5$ g/cm^2 and $n_H=1$ cm^{-3}, $T_l=10^6$ years. We choose here to discuss the background γ-ray spectrum from a halo model of the galaxy, since it has been shown by Ramaty and Lingenfelter (1966b) that such a model gives a positron equilibrium spectrum, even in the disk, which is almost identical with that obtained for a disk-plus-halo model. The inclusion of a spatial diffusion term of the form $D_0\nabla^2N$ in equation (7–24) will have little effect for positrons with $\gamma<2\times10^4$. It may also be noted that a recent study by Anand, Daniel, and Stephens (1968) indicates that there is no large gradient of the cosmic-ray electron intensity between the disk and the halo for energies less than 10 GeV.

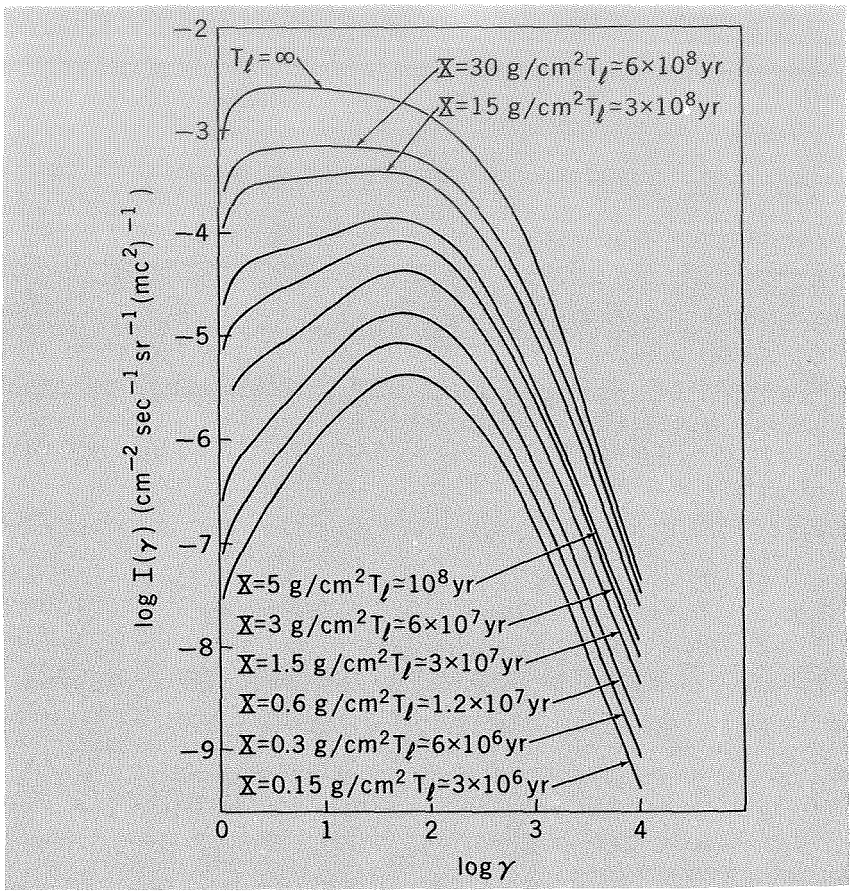

FIGURE 7–2. — Various positron equilibrium fluxes for the halo model of the galaxy given for various approximate mean pathlengths and mean leakage times (Stecker, 1969a).

a sufficient time for the energy loss processes, particularly ionization loss, to affect the spectrum by progressively flattening it below 30 MeV. Studies of spallating cosmic-ray nuclei yield a mean pathlength, $X = 4 \pm 1$ g/cm^2 for cosmic-ray nuclei. The curve in figure 7–2 corresponding to $X = 5$ g/cm^2 is in agreement with the cosmic-ray positron measurements of Hartman (1967). It may be noted that measurements of the galactic positron flux below 30 MeV would yield a more sensitive check on the galactic mean leakage time.

Figure 7–3 shows the annihilation γ-ray spectra obtained using the positron equilibrium fluxes of figure 7–2. The spectra shown are from annihilations in flight of positrons having energies greater than 5 keV. The AGS from positrons annihilating with energies below 5 keV will be discussed in the next section. It can be seen that the peaks of these

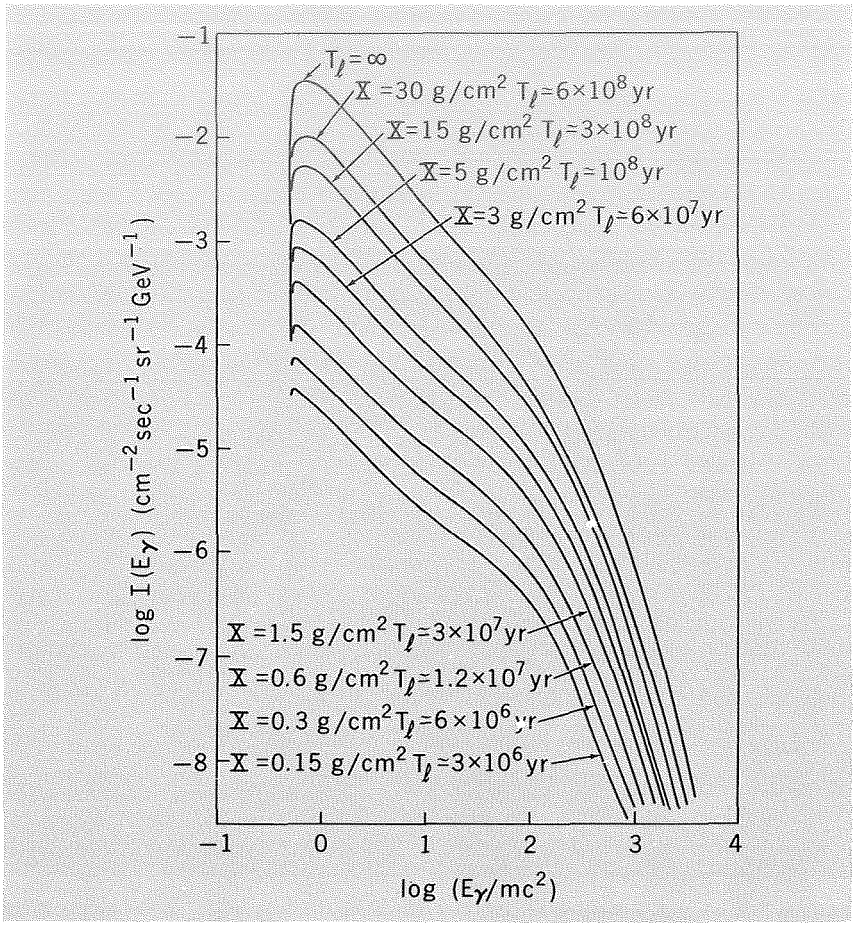

FIGURE 7–3. — The annihilation γ-ray flux spectra for the positron equilibrium fluxes given in figure 7–2 that result from annihilations in flight of positrons with energies greater than 5 keV (Stecker, 1969a).

spectra lie in the region $1/2 < \eta < 1$. This effect is due to a pileup of those γ-rays from the annihilation of relativistic positrons that are emitted in the backward direction in the cms. (See ch. 2.)

Using a value of 4 g/cm^2 for X and the formulas given in this chapter, Ramaty et al. (1970) calculated the total positron source spectrum and equilibrium flux in the galaxy from both pion-decay positrons and β-decay positrons. These spectra were calculated for various values of R_r and R_0 in equation (7–18) in order to convert from the cosmic-ray spectrum measured at the Earth to various possible galactic cosmic-ray spectra. As an extreme case, Ramaty et al. (1970) also considered power-law cosmic-ray spectra in kinetic energy per nucleon with an exponent of

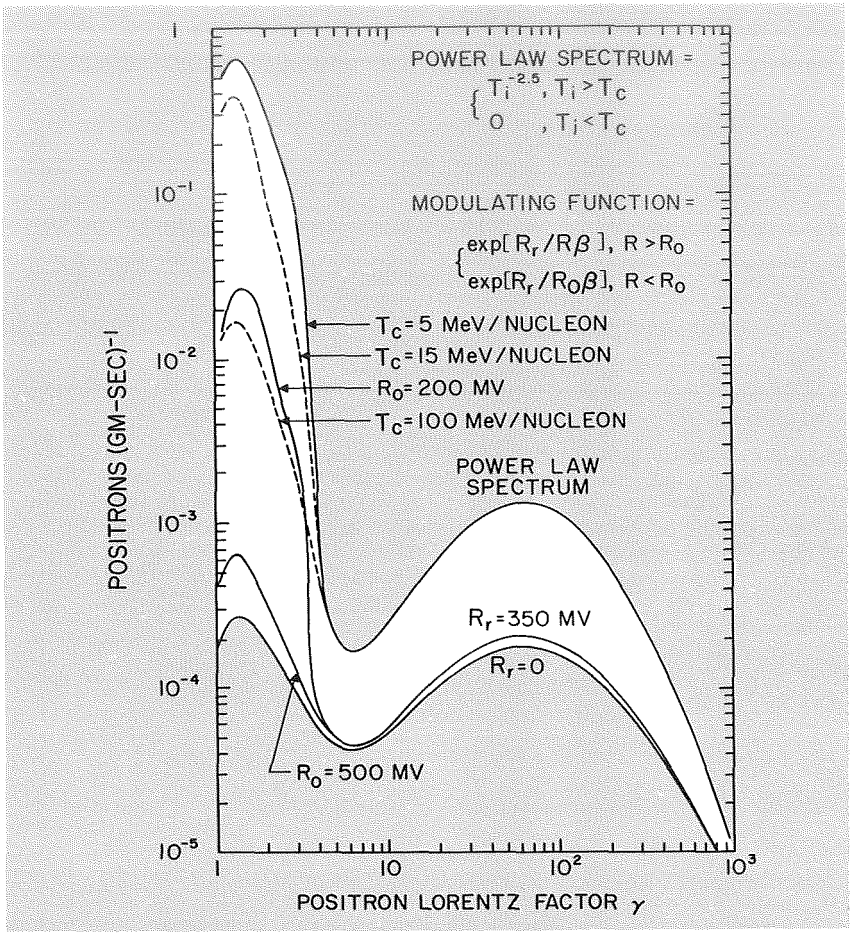

FIGURE 7–4.—Positron production spectra per gram of interstellar material calculated using a power-law cosmic-ray spectrum with various low-energy cutoffs, T_c, and demodulated solar minimum spectra with various values of R_r and R_0 (Ramaty et al., 1970).

-2.5 and various low-energy cutoffs, T_c. The source spectra calculated are shown in figure 7–4 and the resultant equilibrium spectra are shown in figure 7–5. As can be seen, the source spectra and equilibrium spectra of low-energy β-ray positrons are particularly sensitive to the various modulation parameters which determine the low-energy cosmic-ray flux. This is, of course, due to their low production threshold energy.

As can be seen, positrons with energies greater than about 2 MeV come principally from pion decay. At lower energies, the relative contribution of the β-emitters depends critically either on the value of R_0 (for $R_r = 350$ MV) or on the assumed low-energy cutoff (for a power-law spectrum).

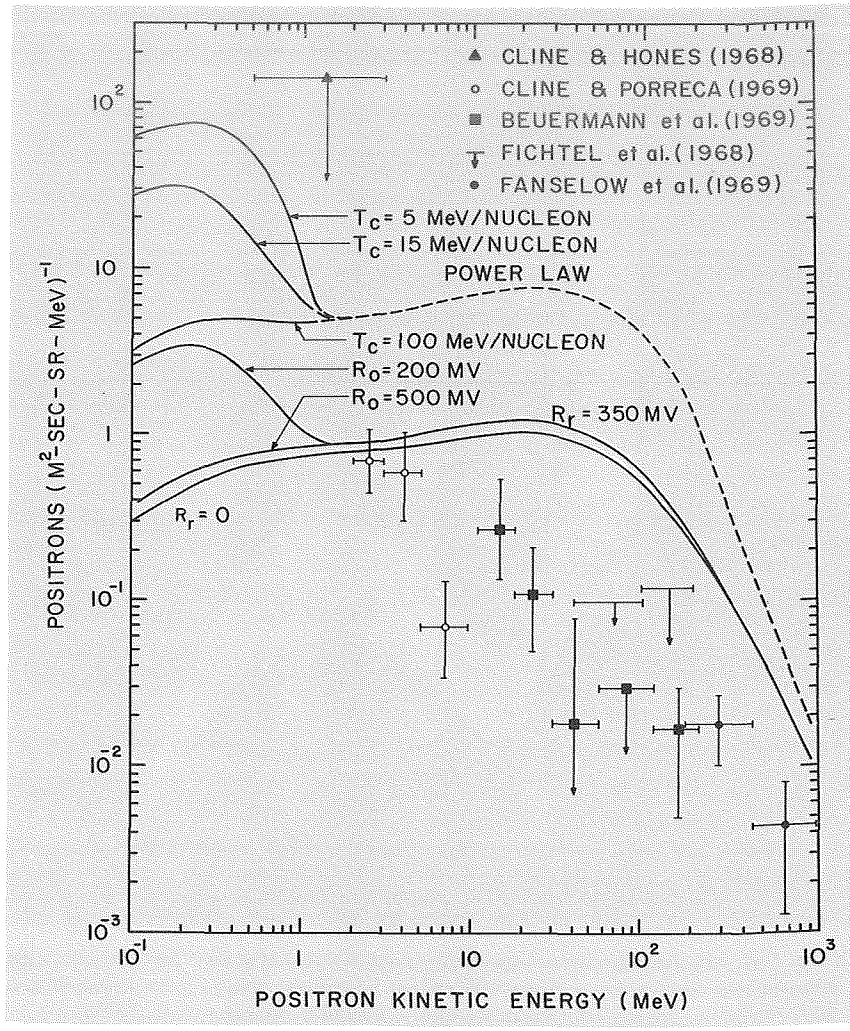

FIGURE 7–5.—Positron intensities in interstellar space together with the available positron measurements below 1 GeV (Ramaty et al., 1970).

TABLE 7–3.—*Cosmic-Ray Energy Density* (eV/cm³)

Solar minimum	$R_r = 350$ MV ($T \geq 5$ MeV/ Nucleon)		Power law		
	$R_0 = 500$ MV	$R_0 = 200$ MV	$T_c = 100$ MeV/ Nucleon	$T_c = 15$ MeV/ Nucleon	$T_c = 5$ MeV/ Nucleon
0.5.....	0.6	57	3.1	17	50

The energy densities of cosmic rays for the various spectra just discussed are given in table 7–3. As can be seen from figure 7–5 and table 7–3, unless the energy density in low-energy cosmic rays is of the order of a few tens of electron volts per cubic centimeter, most of the positron flux at ~ 1 MeV would come from pion decay rather than CNO β-decay and would be small compared to the upper limit given by Cline and Hones (1968). If spread uniformly over the galactic disk, such energy densities lead to serious difficulties regarding the stability of the galaxy (Parker, 1966). On the other hand, since the ranges of both low-energy protons and positrons are short (~ 0.1 g/cm^2), the ~ 1-MeV positron measurements sample only a small region of space which may not necessarily be representative of the galaxy as a whole.

For example, consider a 10-MeV proton; its range in hydrogen is 0.05 g/cm^2, which, for an ambient density of n atoms/cm^3, leads to a lifetime $t \approx 2 \times 10^5/n$ years. The net streaming distance corresponding to t is $a \approx (4/3\lambda\beta ct)^{1/2}$, where λ is the mean free path for diffusion. If $\lambda = 1$ pc, $a \approx 100/n^{1/2}$ pc. Since the rate of supernova explosions in the galaxy (volume $\approx 2 \times 10^{66}$ cm^3) is about 10^{-2} per year, in a spherical volume of radius $100/n^{1/2}$ pc a supernova would be expected to occur once every $2 \times 10^6 n^{3/2}$ years. For $n \gtrsim 1$ atom/cm^3, this time interval is much larger than the lifetime against ionization given before. Therefore, if these protons are produced in supernova explosions and not by more frequent events such as novae or flare stars, their intensities would exhibit sharp maxima close to the time of the explosion and decay to much lower values later on. According to Gold (1969), a supernova explosion may liberate as much as 10^{52} ergs. If 50 percent of this is in low-energy cosmic rays, the mean energy density for about $2 \times 10^5/n$ years over a sphere of radius $100/n^{1/2}$ pc would be $\sim 30\ n^{3/2}$ eV/cm^3. This is sufficient to produce a detectable flux of β-ray positrons. On a galactic scale, however, the same sources of low-energy cosmic rays occurring at a frequency of 10^{-2} per year would only produce an average energy density of $3/n$ eV/cm^3. For $n = 1$, this is somewhat large but not inconsistent with the overall energetics of the galaxy.

Since the large fluxes of low-energy cosmic rays are restricted to small volumes and short times, they do not conflict with observations that integrate over large distances, such as the temperature of H-I clouds, based on 21-cm observations, and the density of free electrons, based on the observed spectrum of nonthermal radio emission. (The connection of these quantities with low-energy cosmic rays was discussed by Balasubrahmanyan et al. (1968). The ~ 1-MeV positron measurements, however, by sampling only a small region of space corresponding to the range of the positrons of 0.2 g/cm^2 ($t \approx 10^5/n$ years, $a \approx 70/n^{1/2}$ pc), may provide evidence for local enhancement of low-energy cosmic-ray fluxes.

As can be seen from figure 7–5, given a reasonable solar modulation, the positron measurements above a few MeV are all consistent with the calculated spectra from the pion-decay process. Since the range of protons above pion production threshold is larger than 4 g/cm^2, these spectra represent mean values over time periods comparable to the positron leakage lifetime from the galaxy. The spatial and temporal inhomogeneities discussed previously, which would allow large but localized low-energy cosmic-ray fluxes, do not apply to this energy domain. The positron spectrum above a few MeV, obtained from a demodulated cosmic-ray distribution with $R_r = 350$ MV, would therefore be a good representation of the interstellar positron intensity.

7–5 THE NUMBER OF COSMIC-RAY POSITRONS ANNIHILATING NEAR REST

We now come to the problem of determining the AGS from cosmic-ray positrons annihilating near rest. Because some aspects of this determination seem deceptively simple, there has been a tendency to oversimplify this problem in the literature. For this reason, I will first list various aspects of the problem essential to an accurate analysis before proceeding to treat them.

(1) The most important source of the cosmic-ray positrons having energies greater than a few MeV is the decay of secondary charged pions. There are, however, sources of relatively low energy positrons (less than a few MeV) which, as we have seen, may have a greater probability of being trapped inside the galaxy until they annihilate near rest. These sources are the β-emitters, which are produced predominantly by low-energy cosmic-ray interactions involving carbon, nitrogen, and oxygen. Therefore, any observable 0.5-MeV line radiation from the galaxy may be primarily due to these β-emitters and an observation of the intensity of the 0.5-MeV line could supply information on the intensity of low-energy cosmic radiation in the galaxy.

(2) In considering annihilations near rest, one must consider the possibility of the intermediate formation of the bound electron-positron system; i.e., the positronium atom. At low energies, the cross section for positronium formation becomes much greater than the cross section for free annihilation.

(3) Once formed in interstellar space, a positronium atom will annihilate into three photons 75 percent of the time. This situation, as we have seen in chapter 2, contrasts sharply with the case of free annihilations, where three-photon annihilations occur with a prob-

ability of less than 1/2 percent. Therefore, the three-photon annihilation process, which produces a continuous spectrum from 0 to 0.5 MeV, must be considered along with the two-photon line annihilations. Their relative importance depends directly on the fraction of positrons which ultimately form positronium.

The positrons which annihilate near rest most likely come from two sources:

(1) Positrons from the decay of secondary charged pions which were created at low enough energies to be trapped for a sufficiently long time in the galaxy to lose essentially all their energy before either annihilating in flight or escaping from the galaxy.
(2) Positrons from the decay of β-emitting nuclei formed in collisions of low-energy cosmic rays involving nuclei of carbon, nitrogen, and oxygen.

The fraction of the original positron flux from the decay of secondary pions which annihilate near rest, f_+, is given by

$$f_+ = \frac{\int_1^\infty d\gamma\, q_+(\gamma)\, \exp\left[-\int_1^\infty \frac{d\gamma'}{|r(\gamma)|\tau_s(\gamma')}\right]}{\int_1^\infty d\gamma\, q_+(\gamma)} \tag{7-43}$$

This fraction was calculated numerically (Stecker, 1969a) using equations (7–32) through (7–38) and is given in table 7–4 and figure 7–6 for various possible mean leakage times T_l. Table 7–4 also gives the corresponding values of $Q_{\text{rest},\pi}$, the total number of positrons from pion decay per gram per second annihilating below 5 keV for the halo model of table 7–2 $Q_{\text{rest},\pi}$ being defined by the numerator of equation (7–43).

TABLE 7–4.—*Annihilations Near Rest* ($T_+ \leq 5$ *KeV*)

T_l, 10^6 yr	f_+, %	$Q_{\text{rest},\pi}$ g^{-1}-s^{-1}
∞	80	4.8×10^{-2}
600	20	1.2×10^{-2}
300	9.3	5.6×10^{-3}
100	1.6	9.6×10^{-4}
60	.61	3.7×10^{-4}
30	.14	8.4×10^{-5}
10	.022	1.3×10^{-5}
6	.0065	3.9×10^{-6}
3	.0025	1.5×10^{-6}

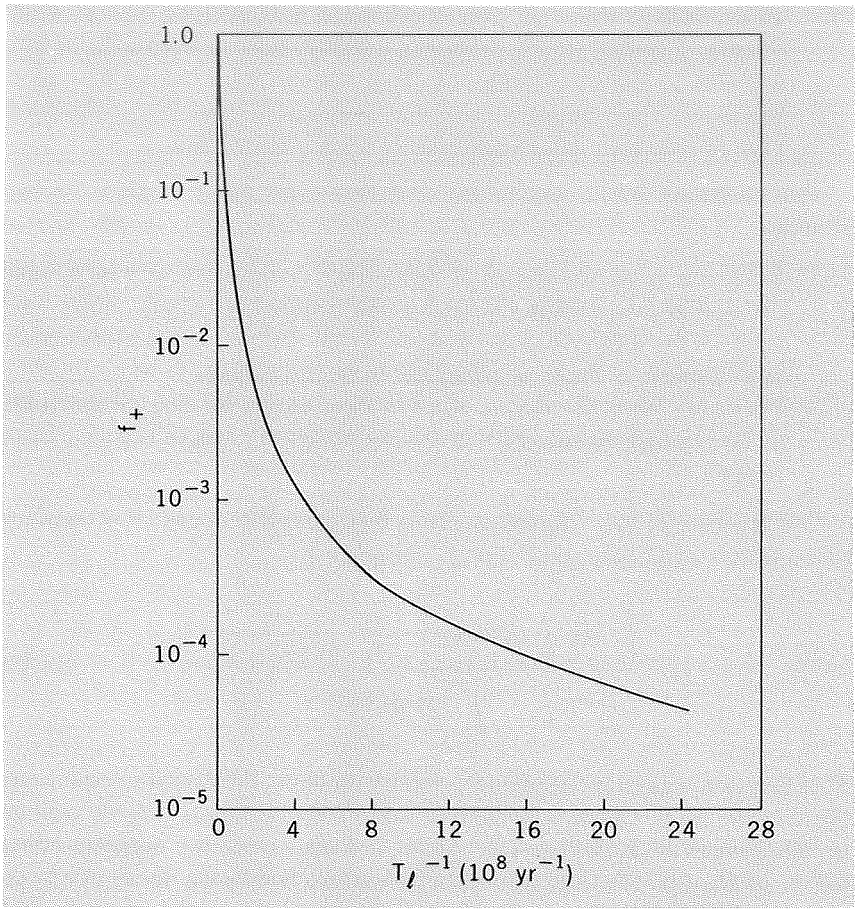

FIGURE 7–6. – The fraction of pion-produced positrons which annihilate at energies less than 5 keV as a function of mean leakage time (Stecker, 1969a).

In the case of an infinite leakage time (all positrons being trapped and annihilating in the galaxy), we find that 80 percent of the positrons produced annihilate near rest, a figure which is in perfect agreement with that given by Heitler (1960) as an asymptotic value for the annihilation of ultrarelativistic positrons when the dominant energy loss comes from ionization. However, for the leakage time usually considered as plausible for the galactic halo (10^8 years, corresponding to $X \simeq 5$ g/cm^2), only 1 to 2 percent of these positrons annihilate near rest.

Ramaty et al. (1970) made use of equation (7–43) to calculate the total number of positrons that annihilate near rest, including the contribution of β-ray positrons as well as pion-decay positrons. They used the various source spectra given in figure 7–4 for $q_+(\gamma)$. Their results for

TABLE 7–5. — *Total Positron Annihilation Rates* $Q_T(g^{-1}\text{-}s^{-1})$

Solar minimum	$R_r = 350$ MV		Power law		$I_+ = 2\times10^{-2}$ $cm^{-2}\text{-}s^{-1}\text{-}sr^{-1}$	
	$R_0 = 500$ MV	$R_0 = 200$ MV	$T_c = 100$ MeV/ Nucleon	$T_c = 5$ MeV/ Nucleon	Mean	Maximum
1.1×10^{-3}	1.8×10^{-3}	4.3×10^{-2}	3.3×10^{-2}	1.3×10^{-1}	$\frac{2.2\times10^{-2}}{n^{5/2}}$	0.5

the various assumed low-energy cosmic-ray spectra and for $X = 4$ g/cm are given in table 7–5. As an extreme case, they computed the annihilation rates that would result from an interstellar positron flux of the same order as the upper limit given by Cline and Hones (1968).

Using a total positron intensity of 2×10^{-2} particles of 1 MeV/cm²-s-sr, they also computed a maximum annihilation rate corresponding to a positron lifetime against ionization of $10^5/n$ years and a mean rate corresponding to an average time between supernova explosions of $5\times10^6 n^{3/2}$ years in a spherical volume of radius $70/n^{1/2}$ pc as discussed in section 7–4. These rates are also given in table 7–5.

7–6 GALACTIC POSITRONIUM FORMATION

The cross section for positronium formation by fast positrons in atomic hydrogen has been calculated by Cheshire (1964) and will be used as an approximation for the interstellar medium. The ratio of positronium formation to free annihilation is only significant at nonrelativistic energies and may be approximated by

$$\frac{\sigma_{pos}(\gamma)}{\sigma_A(\gamma)} \equiv S(\gamma) = \begin{cases} 0 & (\gamma-1) > 10^{-2} \\ 10^{-6}(\gamma-1)^{-3} & 10^{-4} < (\gamma-1) < 10^{-2} \\ 10^{-2}(\gamma-1)^{-2} & \text{for } 2.5\times10^{-5} < (\gamma-1) < 10^{-4} \\ 6.4\times10^{11}(\gamma-1) & 10^{-5} < (\gamma-1) < 2.5\times10^{-5} \\ 0 & (\gamma-1) < 10^{-5} \end{cases} \tag{7–44}$$

At energies of the order of the hydrogen binding energy, the probability for positronium formation in the ground state has been estimated to be between 0.25 and 0.50 and the probability for positronium formation in excited states is small (Deutsch, 1953).

Equation (7–44) was used by Stecker (1969a) to determine the amount of positronium being formed by positrons combining with electrons as a function of energy. The result of this calculation is shown in figure 7–7.

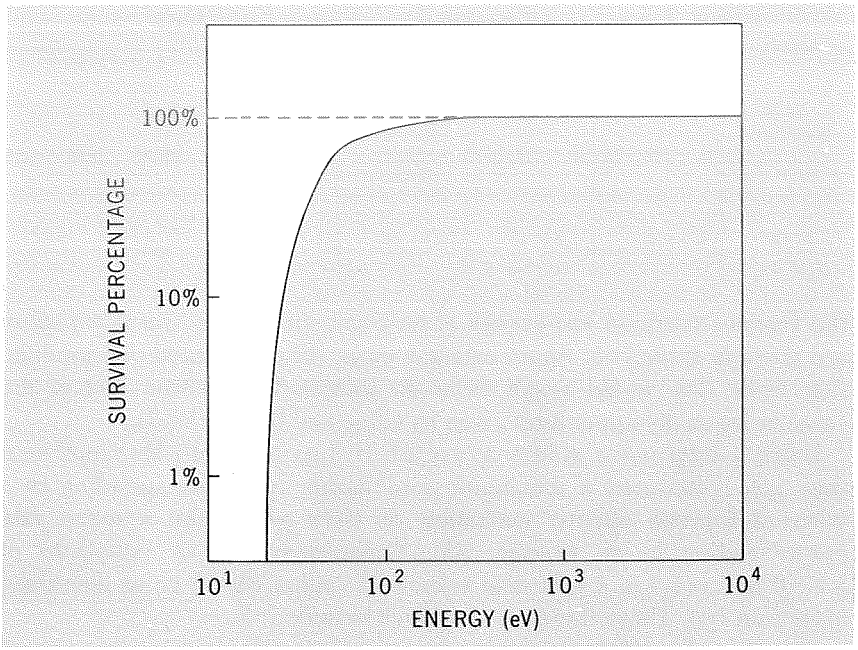

FIGURE 7–7. – The percentage of positrons which, having survived to reach an energy of 10 keV, survive to reach lower energies. The dashed line indicates the survival fraction found when only free annihilations are considered; the solid line indicates the survival fraction when positronium formation is also taken into account (Stecker, 1969a).

This figure shows the percentage of positrons which, having survived to reach a 10-keV kinetic energy, survive to reach lower energies. The dashed line indicates the survival fraction for free annihilation only; the solid line indicates the survival fraction when positronium formation is taken into account. Figure 7–7 shows that almost all of the positrons annihilating near rest do so through intermediate positronium formation with an average energy of about 35 eV.

7–7 THE INTENSITY OF THE POSITRON ANNIHILATION LINE AT 0.51 MeV

It follows from the results of the last section and from the discussion in chapter 2 that galactic cosmic-ray positrons annihilate primarily from an S state of positronium with 75 percent of these annihilations producing a three-photon continuum rather than a two-photon line at 0.51 MeV. Therefore, on the average, one 0.51-MeV photon is produced for every two positrons which annihilate. Thus, the intensity of 0.51-MeV γ-rays

observed along the line of sight as a function of galactic coordinates is given by

$$I_{0.51}(l^{II}, b^{II}) = \frac{Q_{T,\,\mathrm{rest}} M(l^{II}, b^{II})}{8\pi} \tag{7-45}$$

where $M(l^{II}, b^{II})$ in g/cm^2 is the amount of interstellar gas in the direction of observation.[2] Equation (7–45) was used by Ramaty et al. (1970) to determine possible intensities of the 0.51-MeV annihilation line in different directions in the galaxy based on the values of $Q_{T,\,\mathrm{rest}}$ given in table 7–5. The results of this calculation and their implications will be given in the next chapter, where we will complete our discussion of galactic γ-ray production.

[2] The symbols l^{II} and b^{II} denote galactic longitude and latitude respectively.

411-892 O - 71 - 11

The Production of Gamma Rays in the Galaxy

In this chapter we will briefly discuss four other mechanisms for galactic γ-ray production; viz, Compton interactions, bremsstrahlung, synchrotron radiation, and photomeson production. The results of these discussions, together with the results of chapters 5, 6, and 7, will then be summarized and applied to estimate γ-ray production spectra in various parts of the galaxy.

8–1 GAMMA-RAY PRODUCTION SPECTRA FROM COMPTON INTERACTIONS

The Compton effect has been treated extensively in the literature of high-energy astrophysics from three points of view: As an interaction in which cosmic-ray electrons lose energy (Feenberg and Primikoff, 1948, and Donahue, 1951; see also ch. 7); as an interaction in which γ-rays lose energy to electrons of thermal energy (e.g., see ch. 4); and as an interaction capable of producing high-energy γ-rays when thermal photons interact with cosmic-ray electrons. This last process, which we will now briefly discuss, has long been considered to be a potentially important source of cosmic γ-rays, first by interactions with starlight photons (Feenberg and Primikoff, 1948; Felten and Morrison, 1963) and later by interactions with the universal blackbody radiation (Felten, 1965; Gould, 1965; Hoyle, 1965; Fazio, Stecker, and Wright, 1966; and Felten and Morrison, 1966). The Compton process is the relativistic form of Thompson scattering. It is the scattering of a photon off an electron. Such a scattering is shown in figure 8–1 in both the laboratory frame and the rest frame of a cosmic-ray electron (Felten, 1966). We will use Felten's notation, with quantities in the electron rest system primed and laboratory quantities unprimed. Quantities referred to before the interaction will have no subscript and those referred to after the interaction will have the subscript 1. The cosmic-ray electron in the ls is assumed to have an energy $E=\gamma mc^2$. Using the formulas derived in

chapter 1 and referring to figure 8–1, we find

$$\epsilon' = \gamma\epsilon(1 + \beta \cos \alpha) \tag{8–1}$$

$$\epsilon_1 = \gamma\epsilon_1'(1 - \beta \cos \alpha_1') \tag{8–2}$$

$$\epsilon_1' = \frac{\epsilon'}{1 + \dfrac{\epsilon'}{mc^2}(1 - \cos \theta')} \tag{8–3}$$

and

$$\tan \alpha' = \frac{\sin \alpha}{\gamma(\cos \alpha + \beta)} \tag{8–4}$$

Combining equations (8–1) through (8–3), we then find

$$\epsilon_1 = \frac{\gamma^2\epsilon(1 + \beta \cos \alpha)(1 - \beta \cos \alpha_1')}{1 + \dfrac{\gamma\epsilon}{mc^2}(1 + \beta \cos \alpha)(1 - \cos \theta')} \tag{8–5}$$

For the applications of principal concern here, we will have the condition $\gamma\epsilon \ll mc^2$, so that the Compton cross section (Heitler, 1960)

$$\sigma_c \rightarrow \sigma_T = \frac{8}{3}\pi r_0^2 = 6.65 \times 10^{-25} \text{ cm}^2 \tag{8–6}$$

and, from equation (8–5),

$$\epsilon_1 \sim \gamma^2\epsilon \qquad (\gamma\epsilon \ll mc^2) \tag{8–7}$$

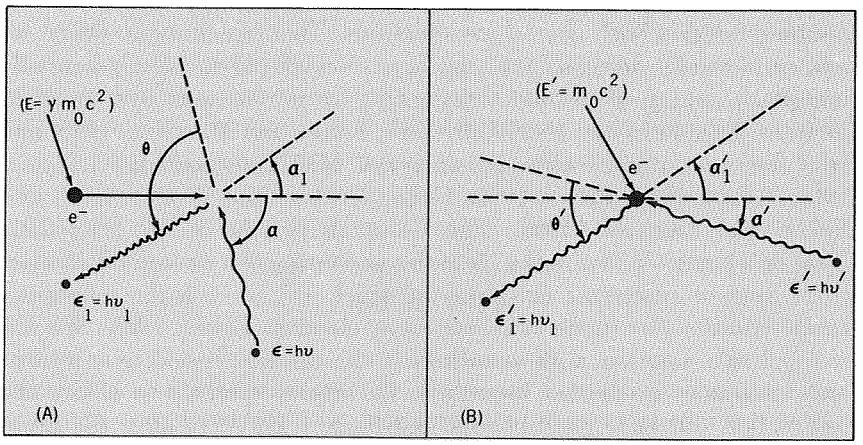

FIGURE 8–1.—A photon-electron collision, viewed in two reference frames (Felten, 1966). (*a*) Cosmic frame *S*. (*b*) Electron rest frame *S*′.

In the other extreme (Heitler, 1960) we must use the Klein-Nishina formula for the cross section, which has the asymptotic form

$$\sigma_c \to \pi r_0^2 \left(\frac{mc^2}{\epsilon}\right)\left[\frac{1}{2}+\ln\left(\frac{2\epsilon}{mc^2}\right)\right] \qquad (\gamma\epsilon \gg mc^2) \tag{8-8}$$

and we also find from equation (8–5) that

$$\epsilon_1 \sim \gamma mc^2 \sim E \qquad (\gamma\epsilon \gg mc^2) \tag{8-9}$$

Under the condition $\gamma\epsilon \ll mc^2$, the differential cross section for the production of a γ-ray of energy $E_\gamma = \epsilon_1$ by Compton scattering is given by (Ginzburg and Syrovatskii, 1964)

$$\sigma(E_\gamma|\epsilon, E) = \frac{\pi r_0^2}{4}\frac{(mc^2)^4}{\epsilon^2 E^3}\left\{2\frac{E_\gamma}{E} - \frac{(mc^2)^2 E_\gamma^2}{\epsilon E^3} + \frac{4E_\gamma}{E}\ln\frac{(mc^2)^2 E_\gamma}{4\epsilon E^2} + \frac{8\epsilon E}{(mc^2)^2}\right\} \tag{8-10}$$

and the mean energy of the γ-ray produced is given by

$$\langle E_\gamma\rangle = \frac{4}{3}\gamma^2\langle\epsilon\rangle \tag{8-11}$$

for an initial photon density distribution $n_{\rm ph}(\epsilon)$, where

$$\langle\epsilon\rangle = \frac{\int d\epsilon\, \epsilon\, n_{\rm ph}(\epsilon)}{\int d\epsilon\, n_{\rm ph}(\epsilon)} \tag{8-12}$$

The total γ-ray production spectrum is, of course, given by

$$I(E_\gamma) = \int d\mathbf{r} \int dE\, I_e(E, \mathbf{r}) \int dE\, n_{\rm ph}(\epsilon, \mathbf{r})\sigma(E_\gamma|\epsilon, E) \tag{8-13}$$

In the case where the cosmic-ray electrons have an energy distribution of the power-law form

$$I_e(\epsilon) = K_e E^{-\Gamma} \tag{8-14}$$

it is found that (Ginzburg and Syrovatskii, 1964)

$$\int dE\, I_e(E)\sigma(E_\gamma|\epsilon, E) = 2^\Gamma \frac{\Gamma^2+4\Gamma+11}{(\Gamma+1)(\Gamma+3)^2(\Gamma+5)} \times 8\pi r_0^2 K_e (mc^2)^{1-\Gamma}\epsilon^{(\Gamma-1)/2}E_\gamma^{(\Gamma+1)/2} \tag{8-15}$$

For the important case of interactions with the blackbody radiation, where

$$n_{\rm ph}(\epsilon) = \frac{8\pi}{h^3c^3}\frac{\epsilon^2}{e^{\epsilon/kT}-1} \tag{8-16}$$

we find that

$$\left\langle \frac{4}{3}\epsilon \right\rangle \simeq 3.6\ kT \simeq 3.1 \times 10^{-13} T \qquad \text{GeV} \tag{8-17}$$

The radiation density

$$\rho_\gamma = \int d\epsilon\ n_{\text{ph}}(\epsilon) \simeq 4.75 \times 10^{-12} T^4 \qquad \text{GeV/cm}^3 \tag{8-18}$$

and the expression (8–13) for the resultant γ-ray intensity reduces to

$$I(E_\gamma) = f(\Gamma)\,\frac{2}{3}\,\sigma_T L_{\text{eff}} \rho_\gamma (mc^2)^{1-\Gamma} \left(\frac{4}{3}\langle\epsilon\rangle\right)^{(\Gamma-3)/2} K_e E_\gamma^{-(\Gamma+1)/2} \tag{8-19}$$

which, in numerical form, becomes

$$I(E_\gamma) \simeq 6.22 \times 10^{-21} L_{\text{eff}} [10^{-2.962\Gamma} f(\Gamma)] K_e T^{(\Gamma+5)/2} E_\gamma^{-(\Gamma+1)/2} \qquad (\text{cm}^2\text{-s-sr-GeV})^{-1} \tag{8-20}$$

where L_{eff} is the effective pathlength for γ-ray production and

$$f(\Gamma) = 4.74(1.05)^\Gamma \frac{\Gamma^2 + 4\Gamma + 11}{(\Gamma+1)(\Gamma+3)^2(\Gamma+5)} \Gamma\left(\frac{\Gamma+5}{2}\right) \zeta\left(\frac{\Gamma+5}{2}\right) \tag{8-21}$$

$\Gamma(x)$ is the well-known gamma function and $\zeta(x)$ is the Riemann function

$$\zeta(x) = \sum_{n=1}^{\infty} \frac{1}{n^x} \tag{8-22}$$

In particular, Ginzburg and Syrovatskii give the values for $f(\Gamma)$ listed in table 8–1.

Thus, we find that for most applications of importance to high-energy astrophysics, where $2 \lesssim \Gamma \lesssim 3.5$, $f(\Gamma) \simeq 1$.

TABLE 8-1. —*Approximate Values of the Function* f(Γ) *in Equation (8–21)*

Γ	$f(\Gamma)$
1	0.84
2	.86
3	.99
4	1.4

As a check on equation (8–19), one can make the approximation for $\gamma\epsilon \ll mc^2$ that

$$\sigma(E_\gamma|\epsilon E) \simeq \sigma_T \delta\left(E_\gamma - \frac{4}{3}\langle\epsilon\rangle \frac{E^2}{(mc^2)^2}\right) \tag{8–23}$$

Then

$$I(E_\gamma) = n_{\rm ph}\sigma_T L_{\rm eff} \int dE\ K_e E^{-\Gamma} \delta\left(E_\gamma - \frac{4}{3}\langle\epsilon\rangle \frac{E^2}{(mc^2)^2}\right)$$

$$= n_{\rm ph}\sigma_T L_{\rm eff} K_e \left[\left(\frac{3}{4}\right)^{1/2} E_\gamma^{1/2} \langle\epsilon\rangle^{-1/2} mc^2\right]^{-\Gamma} \frac{dE}{dE_\gamma}$$

$$= \frac{1}{2}\, n_{\rm ph}\sigma_T L_{\rm eff} K_e (mc^2)^{1-\Gamma} \left(\frac{4}{3}\langle\epsilon\rangle\right)^{(\Gamma-1)/2} E_\gamma^{(\Gamma+1)/2}$$

$$= \frac{2}{3}\, \sigma_T L_{\rm eff} \rho_\gamma (mc^2)^{(1-\Gamma)} \left(\frac{4}{3}\langle\epsilon\rangle\right)^{(\Gamma-3)/2} K_e E_\gamma^{(\Gamma+1)/2} \tag{8–24}$$

which, for $f(\Gamma) \simeq 1$, is in excellent agreement with equation (8–19). The small numerical discrepancy between equations (8–19) and (8–24) arises because of the Bose-Einstein distribution in photon energies for a thermal photon field.

8–2 GAMMA-RAY PRODUCTION SPECTRA FROM BREMSSTRAHLUNG INTERACTIONS

Bremsstrahlung, which is a German word meaning "breaking radiation," is the radiation emitted by a charged particle accompanying deceleration. The cross sections for γ-ray production from bremsstrahlung are derived in Heitler's book (Heitler, 1960). In the case of bremsstrahlung from nonrelativistic electrons radiating in the field of a target nucleus, the cross section for production of a γ-ray of energy E_γ by an electron of energy E in the field of an atomic nucleus of charge Z is given by

$$\sigma_b(E_\gamma|E) \equiv \sigma_b(E, E_\gamma) f_b(E_\gamma|E) \tag{8–25}$$

where $f_b(E_\gamma|E)$ is again the normalized distribution function for γ-ray production; and where, in terms of kinetic energy $T = E - mc^2$,

$$\sigma_b(E, E_\gamma) = \frac{\alpha Z^2}{\pi}\, \sigma_T \left(\frac{mc^2}{T}\right) \ln\left\{\frac{[(T)^{1/2} + (T - E_\gamma)^{1/2}]^2}{E_\gamma}\right\} \left(\frac{T}{E_\gamma}\right)$$

$$\text{for } 2\pi Z\alpha \ll \beta \ll 1 \tag{8–26}$$

The cross section for bremsstrahlung by relativistic electrons is given by

$$\sigma_b(E, E_\gamma) = \frac{4\alpha Z^2}{\pi} \sigma_T \ln\left(\frac{2E}{mc^2} - \frac{1}{3}\right)\left(\frac{E}{E_\gamma}\right)$$

$$\text{for } mc^2 \ll E \ll \alpha^{-1} Z^{-1/3} mc^2 \qquad (8\text{–}27)$$

In the ultrarelativistic case, where the cross section is calculated by taking into account the screening of the charge of the atomic nucleus by atomic electrons, the resultant cross section is given by

$$\sigma_b(E, E_\gamma) = \frac{4\alpha Z^2}{\pi} \sigma_T \ln\left(183 Z^{-1/3} + \frac{1}{18}\right)\left(\frac{E}{E_\gamma}\right)$$

$$\text{for } E \gg \alpha^{-1} Z^{-1/3} mc^2 \qquad (8\text{–}28)$$

Of course, in the case of an ionized gas, equation (8–27), derived for the case where screening effects are unimportant, is applicable at all relativistic energies. The cross sections given in equations (8–26) to (8–28) may be corrected for the additional contribution from interactions between cosmic-ray electrons and atomic electrons by the replacement $Z^2 \rightarrow Z(Z+1)$.

Another case which may be of astrophysical interest for γ-ray production is that of bremsstrahlung from nonrelativistic protons, as has been pointed out by Boldt and Serlemitsos (1969). In this case, it is the electron which is at rest and the proton which is the energetic particle in the ls. The appropriate cross section for this interaction, which corresponds to equation (8–26) for cosmic-ray electrons, is then

$$\sigma_b(E_p, E_\gamma) = \frac{\alpha}{\pi} \sigma_T \left(\frac{M_p c^2}{T_p}\right)$$

$$\ln\left\{\frac{\left[\sqrt{(m_e/M_p)T_p} + \sqrt{(m_e/M_p)T_p - E_\gamma}\right]^2}{E_\gamma}\right\}\left[\frac{(m_e/M_p)T_p}{E_\gamma}\right] \qquad (8\text{–}29)$$

It is immediately obvious from equations (8–27) and (8–28) that for relativistic particles, the bremsstrahlung cross sections have little or no dependence, except for a linear one, on E. Indeed, equation (8–28) may be written in the form

$$\sigma_b(E, E_\gamma) \simeq \frac{\langle M \rangle}{\langle X \rangle}\left(\frac{E}{E_\gamma}\right) \qquad (8\text{–}30)$$

where $\langle M \rangle$ is the average mass of the target atoms in grams and $\langle X \rangle$ is the average radiation length for the gas in grams per square centi-

meter. The average radiation length for interstellar matter is

$$X \simeq 65 \text{ g/cm}^2 \tag{8-31}$$

based on the values given for pure hydrogen and pure helium by Dovshenko and Pomanskii (1964):

$$X_{\text{H}} = 62.8 \text{ g/cm}^2 \tag{8-32}$$

$$X_{\text{He}} = 93.1 \text{ g/cm}^2 \tag{8-33}$$

To a good approximation, especially in the case of relativistic bremsstrahlung (Heitler, 1960), the normalized distribution of γ-rays produced may be taken to be a square distribution given by

$$f(E_\gamma|E) \begin{cases} E^{-1} & \text{for } 0 \leq E_\gamma \leq E \\ 0 & \text{otherwise} \end{cases} \tag{8-34}$$

so that the γ-ray production spectrum is given by

$$I_b(E_\gamma) = \frac{\langle M \rangle}{\langle X \rangle} \left[\int_{E_\gamma}^{\infty} dE \, I_e(E) \right] E_\gamma^{-1}$$

$$= \frac{1}{\langle X \rangle} \int d\mathbf{r} \langle \rho(\mathbf{r}) \rangle \frac{I_e(>E_\gamma)}{E_\gamma} \tag{8-35}$$

where $\rho(\mathbf{r})$ is the matter density of the gas in grams per cubic centimeter. For bremsstrahlung between cosmic-ray electrons and interstellar gas, we may use equation (8–31) to write equation (8–35) in the form

$$I_b(E_\gamma) = 3.4 \times 10^{-26} \langle nL \rangle \frac{I(>E_\gamma)}{E_\gamma} \tag{8-36}$$

8–3 GAMMA-RAY PRODUCTION SPECTRA FROM SYNCHROTRON RADIATION

Synchrotron radiation, or magnetic bremsstrahlung, is the radiation emitted by a relativistic particle spiraling in a magnetic field. Its mathematical description has been given by Schwinger (1949). An electron suffers energy losses by synchrotron radiation at a rate

$$\left(\frac{dE}{dt} \right)_{\text{sync}} = -\frac{4}{3} \sigma_T c \gamma^2 \rho_H \tag{8-37}$$

where the magnetic energy density ρ_H is

$$\rho_H = H^2/8\pi \tag{8-38}$$

This rate can be compared with the energy loss rate suffered by an electron through Compton interactions with a photon field of energy density ρ_γ. That rate is

$$\left(\frac{dE}{dt}\right)_{\text{compt}} = -\frac{4}{3}\sigma_T c\gamma^2\rho_\gamma \tag{8-39}$$

The equivalence of equations (8–37) and (8–39) is not accidental, but can be shown to be a direct consequence of electromagnetic theory (Jones, 1965b).

The photons emitted as synchrotron radiation have a characteristic frequency given by

$$\omega_c = \frac{3}{2}\gamma^2\left(\frac{eH}{mc}\right) \tag{8-40}$$

The synchrotron effect can be thought of as the interaction of the electron with "virtual" photons of the magnetic field. Denoting these photons by the subscript v, it is found (Jones, 1968) that they have an average energy

$$\epsilon_v = \frac{8}{5\pi\sqrt{3}}\left(\frac{\hbar}{mc}\right)eH \tag{8-41}$$

and a number density

$$n_v = \frac{H^2}{8\pi\epsilon_v} \tag{8-42}$$

The resultant γ-rays have a characteristic energy found from equation (8–40) to be

$$E_{\gamma,c} = \frac{3}{2}\gamma^2\left(\frac{\hbar}{mc}\right)eH \tag{8-43}$$

Equation (8–43) expresses the same type of energy dependence on the electron energy, $E = \gamma mc^2$, as did equation (8–11) for Compton γ-rays. If we take a power-law spectrum of the form

$$I_e(E) = K_e E^{-\Gamma} \tag{8-44}$$

we will again get the same power-law dependence for the resultant synchrotron radiation as we did for the Compton radiation in the deriva-

tion of equation (8–24), viz,

$$I_{\text{sync}}(E_\gamma) \propto E_\gamma^{-(\Gamma+1)/2} \tag{8–45}$$

Ginzburg and Syrovatskii (1965) give the exact formula for $I_{\text{sync}}(E_\gamma)$ in a form suitable for calculation. The γ-ray spectrum, numerically modified from the form given by Ginzburg and Syrovatskii and expressed in gigaelectron volt units, is

$$I_{\text{sync}}(E_\gamma) = 9.46 \times 10^{-10}(8.15 \times 10^{-6})^{\Gamma} a(\Gamma) L_{\text{eff}} \times K_e H^{(\Gamma+1)/2} E^{-(\Gamma+1)/2} \quad (\text{cm}^{-2}\text{-s}^{-1}\text{-sr}^{-1}\text{-GeV}^{-1}) \tag{8–46}$$

with the coefficient $a(\Gamma)$ given by table 8–2.

A relativistic electron of energy E in gigaelectron volts, spiraling in a magnetic field of amplitude H, in gauss, will produce a characteristic spectrum of γ-rays having a peak at

$$E_{\gamma, m} = 1.9 \times 10^{-11} H_\perp E^2 \quad \text{GeV} \tag{8–47}$$

where $H_\perp$ is the component of the field perpendicular to the circular component of motion of the electron.

It follows from equation (8–47) that in a field of $H_\perp = 5 \times 10^{-6}$ G, which is of the order of the fields found in interstellar space, it takes a 10^8-GeV electron to produce a 1-GeV γ-ray. If we consider for comparison Compton interactions with starlight photons of roughly the same energy density and having energies of about 1 eV per photon, it only requires a 14-GeV electron to produce a 1-GeV γ-ray. Such electrons are at least 15 orders of magnitude more plentiful than are 10^8-GeV electrons, if indeed the latter exist at all; so it may readily be seen that for almost all cases of astrophysical interest at present, synchrotron radiation may be regarded as a negligible source of γ-rays.[1]

TABLE 8–2.—*The Coefficient* a(Γ) *in Equation (8–46)*

[Ginzburg and Syrovatskii, 1965]

Γ	$a(\Gamma)$
2.5	0.085
2.6	.083
3	.074
4	.072

[1] A possible important exception may be for point sources possessing strong magnetic fields, such as pulsars.

8–4 GAMMA RADIATION FROM PHOTOMESON PRODUCTION INTERACTIONS

We will mention here, in passing, the mechanism for production of γ-rays from the decay of neutral pions produced by interactions of ultra-high-energy cosmic rays; i.e., via interactions such as

$$\gamma + p \rightarrow p + \pi^0 \quad (8\text{–}48)$$
$$\pi^0 \rightarrow 2\gamma$$

where the threshold for interactions with starlight photons is of the order of 10^8 GeV. Hayakawa (1963) suggested that this interaction may be important for γ-ray production at energies above 10^6 GeV if the ultra-high-energy cosmic rays are universal. This is no longer thought to be the case, since, as we have seen in chapter 4, γ-rays of such energies cannot propagate more than 3×10^{22} cm, or about 3×10^{-6} of the visible radius of the universe, because of interactions with the universal blackbody radiation. In addition, there is considerable doubt as to the universality of ultra-high-energy cosmic rays (Stecker, 1968).

8–5 POSSIBLE IMPLICATIONS OF PRESENT OBSERVATIONS OF GALACTIC GAMMA RAYS

In this section, an attempt will be made to relate some of the theoretical calculations on galactic γ-ray production to the present observations and to thereby construct a plausible model for γ-ray production in our galaxy which is consistent with the present data. Unfortunately, it is necessary at this writing to preface this section with a caveat. We are now just on the threshold of establishing the field of observational γ-ray astronomy. It has become apparent that in order to detect diffuse fluxes of cosmic γ-rays above the atmospherically produced background, it is necessary to make use of satellite-borne detectors. Such detectors are just now at the stage of development where they have attained the sensitivity necessary for cosmic γ-ray detection. Instruments now in the development and planning stages will eventually provide a vast improvement in resolution and sensitivity. The data used here should be considered to be preliminary and subject to change. Thus, the interpretation of these data, as presented here, may require future modification.

We may mark the birth of observational γ-ray astronomy with the detection of cosmic γ-rays above 100-MeV energy by Clark, Kraushaar, and Garmire (1968). (See appendix.) Their results indicated that cosmic γ-radiation is strongly anisotropic, being most intense in the galactic plane and particularly at the galactic center. (See figs. 8–2 and 8–3.)

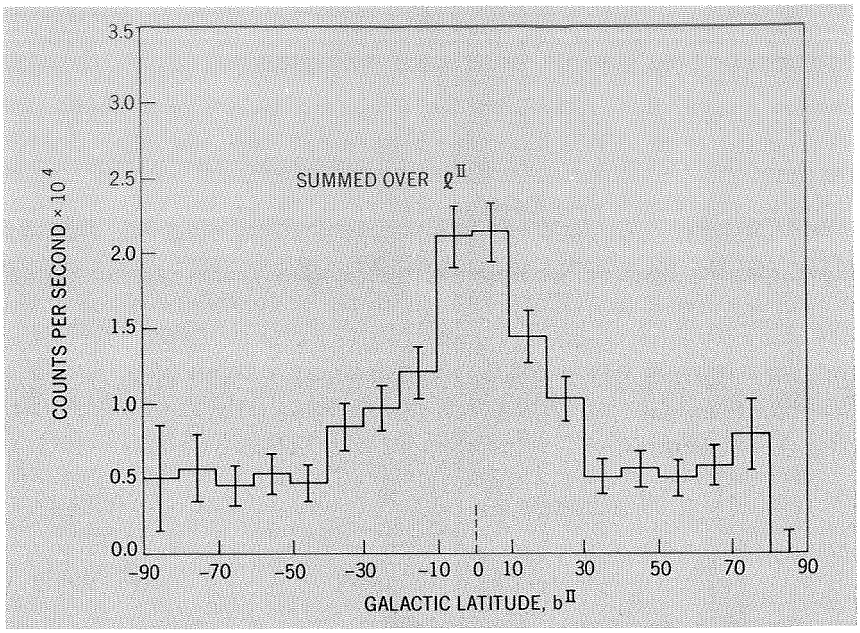

FIGURE 8–2. — Dependence of γ-ray intensity on galactic latitude b^{II} (data summed over all galactic longitudes l^{II}; Clark et al., 1969).

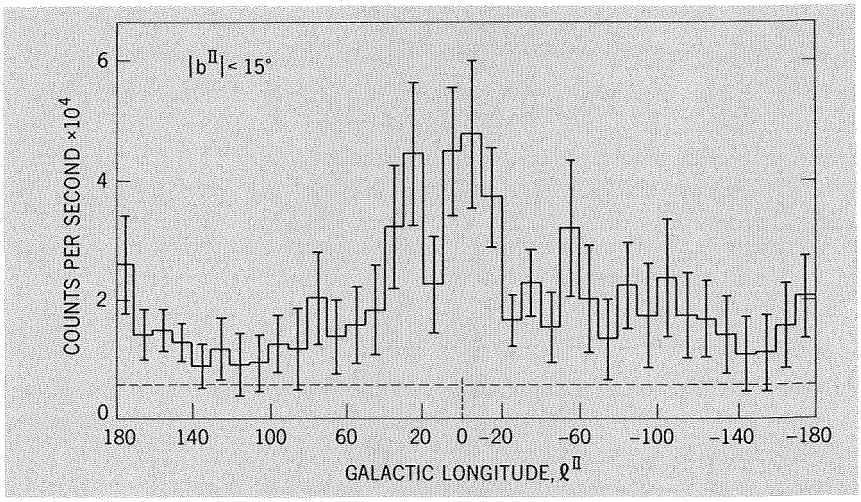

FIGURE 8–3. — Dependence of γ-ray intensity (within 15° galactic latitude of the galactic disk) on galactic longitude l^{II} (Clark et al., 1969).

The detection of this anisotropy itself is a strong indication that a large fraction of the γ-rays detected were of galactic origin. Fichtel, Kniffen, and Ögelman (1969) appear also to have detected the source at the galactic center. Sood (1969); Valdez, Frier, and Waddington (1969); and Hutchinson et al. (1969) have also reported an apparent anisotropy in detected γ-rays toward the galactic plane; although Frye et al. (1969) failed to detect such an anisotropy.

The absolute intensities of the γ-ray line source from the galactic plane and the peak in the intensity distribution at the galactic center remain somewhat in doubt (by probably not more than a factor of 2); and the intensities originally reported by Clark et al. (1968, 1969) have now been revised downward by approximately a factor of 2, due to a recalibration of the sensitivity of their detector (Clark et al., 1970). We shall utilize these revised intensities in our discussion in this section.

There appears to be a γ-ray flux from the galactic center above 100 MeV having a line intensity of $\sim 2 \times 10^{-4}$ cm^{-2}-s^{-1}-rad^{-1}. Gamma rays coming from the region of the galactic disk have a line intensity of 0.5×10^{-4} cm^{-2}-s^{-1}-rad^{-1}. Clark et al. suggested that these fluxes, first reported to be an order of magnitude higher than those predicted from various diffuse production mechanisms, may originate mainly in unresolved discrete sources (a suggestion which was further explored by Ögelman, 1969). However, they were careful to point out that large amounts of undetected hydrogen may also account for these fluxes.

From 21-cm radio observations of the galaxy, it has been found that the average value of the product of mean density and linear extension (usually denoted as $\langle nL \rangle$ for emitting atomic hydrogen in the galactic disk, spread out over the 15° resolution cone of the detector aboard the OSO–3 satellite is approximately 3×10^{21} cm^{-2}. This value corresponds to a mean density in the disk itself of approximately 0.7 cm^{-3} (Kerr and Westerhout, 1965). If the atomic hydrogen seen in emission were to be considered the full content of hydrogen gas in the galaxy, the resultant γ-ray production from π^0-decay, according to the results of chapter 5 (fig. 5–10), would produce a flux of γ-rays of energy greater than 100 MeV of $\sim 3 \times 10^{-5}$ cm^{-2}-s^{-1}-rad^{-1}, and the fluxes estimated from other production mechanisms in the galactic disk would be considerably lower.

The author (Stecker, 1969b) attempted to account for the fluxes originally reported by Clark et al. (1968) by suggesting that these γ-rays result from the decay of neutral pions produced in cosmic-ray interactions with the total nucleon content of interstellar gas, much of which was hypothesized to be in the form of molecular hydrogen. Arguments were given, based on recent results from other branches of astronomy dealing with the study of the interstellar medium, to support this hypothesis. This paper was closely followed by a detailed presentation of the OSO–3

results by Clark et al. (1969) at the 37th IAU Symposium in Rome showing that the γ-ray spectrum from the galactic disk closely matched that of the horizon-albedo γ-ray spectrum from the Earth, arising mainly from the decay of neutral pions produced by cosmic-ray interactions with the Earth's atmosphere. This gives tentative, but not conclusive, support to the pion-decay hypothesis for the origin of galactic γ-rays. Stronger support for the pion-decay hypothesis has recently been communicated by Fichtel and Kniffen (private communication) who have found that in the galactic-center region, $I(E_\gamma > 50\,\text{MeV}) < 1.5I\,(E_\gamma > 100$ MeV). (See also Kniffen and Fichtel (1970).)

To explain the γ-ray intensity originally quoted by Clark et al. (1968), using the pion-decay hypothesis, a mean gas density in the galactic disk of the order of 5 nucleons/cm^3 was required, a value close to the upper limit allowed by galactic dynamics (Parker, 1968). However, due to a recent recalibration of the sensitivity of the OSO–3 detector, the γ-ray fluxes originally given by Clark et al. (1968) have been revised downward by a factor of ~ 2 (Clark et al., 1970). A total nucleon density of the order of 2 cm^{-3} will provide a γ-ray flux in the galactic disk within the accuracy of the revised observational value under the assumption of a uniform cosmic-ray intensity in the galactic disk. Since 21-cm observations indicate a mean density of atomic hydrogen in the galactic disk of the order of 1 cm^{-3}, the γ-ray observations indicate that

$$\langle n_{\text{H-I, cool}} + 2n_{\text{H}_2} \rangle \simeq \langle n_{\text{H-I, emission}} \rangle \tag{8–49}$$

under the assumption of a fairly uniform cosmic-ray intensity in the galaxy.

A considerable quantity of molecular hydrogen in the interstellar medium had been considered a likely possibility until Stecher and Williams (1967) found an effective mechanism for its photodestruction. It now appears that in the presence of an average interstellar radiation field, the amount of molecular hydrogen expected to be present will be negligible. Recent rocket measurements appear to support this conclusion (Carruthers, 1968; Smith, 1969). In dark clouds, however, the rate of molecular hydrogen formation is expected to exceed the photodestruction rate; and essentially all the hydrogen is expected to exist in molecular form. Recent observations of dark clouds (Hollenbach and Salpeter, 1970, and Garzoli and Varsavsky, 1966) show an anticorrelation between atomic hydrogen and dust which may indicate that the hydrogen in these clouds has been converted into molecular form.

Kerr and Westerhout (1965) have argued that the hydrogen contained in cool, optically thick interstellar clouds can be expected to equal that seen in 21-cm emission, which is a more smoothly distributed component

of gas at a considerably higher temperature. Additional theoretical support for the model on the basis of dynamical stability arguments has also been given (Parker, 1968). In addition, the galactic longitude distribution obtained for interstellar hydrogen from 21-cm emission measurements alone appears to be far more isotropic than our concept of the Sun's position in the galaxy would indicate, which again suggests that a significant fraction of interstellar gas must be present in optically thick clouds within 10 kpc of the galactic center (Kerr and Westerhout, 1965). This argument is further strengthened by the fact that the gas-to-dust ratio in the interstellar medium appears to be constant, together with the observation of 27 magnitudes of extinction toward the galactic center (Becklin and Neugebauer, 1968) which implies that there is a large quantity of interstellar gas in that direction.

Gould and Salpeter (1963) and Gould, Gold, and Salpeter (1963) have pointed out that the observed spatial distribution of K-giant stars as a function of perpendicular distance from the galactic plane suggests a much stronger gravitational field for the galaxy than can be accounted for by stars and observed atomic hydrogen in the disk. A mean gas density of 5 cm^{-3} in the disk would be required to produce the observed K-giant distribution.

From an analysis of the observed distribution of atomic hydrogen gas and δ-Cephei variables, Dorschner, Gürtler, and Schmidt (1965) have come to the same conclusion, suggesting that 80 percent of the interstellar gas is in the form of molecular hydrogen. They show that the unseen mass necessary to produce the galactic gravitational field would have to be very strongly concentrated toward the galactic plane and therefore would not likely be composed of stars.

From studies of the spin temperature of interstellar hydrogen from 21-cm line spectra, Mebold (1969) has recently concluded that the total mass of interstellar hydrogen has been considerably underestimated from emission-line studies and that there exists a large quantity of gas which is in a condition favorable for star formation; viz, in the form of cool, dense clouds.

Werner and Harwit (1968) have observed a faint infrared emission feature which they have interpreted to be evidence for the existence of substantial amounts of molecular hydrogen in a dark cloud in Orion. The number of molecules along the line of sight is given as $\gtrsim 10^{21}$ cm^{-2}. Such clouds, although inherently difficult to observe, may be quite common in the galactic disk.

Since molecules such as NH_3, OH, H_2O, and CH_2O exist in detectable quantities, it would indeed be surprising if the H_2 molecule, made entirely of the most abundant element in the universe, did not exist in appreciable quantities. Indeed, Heiles (1968) has suggested that the

primary mechanism for the formation of OH molecules in dark clouds is based on the reaction

$$H_2 + O \rightarrow OH + H \qquad (8\text{–}50)$$

(Caroll and Salpeter, 1966) in which the H_2 molecule plays a fundamental role.

Studies of external galaxies have indicated that regions containing young stars (regions of active star formation) do not coincide in many cases with the regions of maximum atomic hydrogen density as seen in 21-cm emission. This would not be at all surprising if star formation occurred mainly in cool, dense, unobserved clouds, as suggested by Mebold (1969).

Most recently, Carruthers (1970) has made a direct observation of the H_2 Lyman resonance absorption bands in the far-ultraviolet spectrum of the star ξ Persei. His results indicate that, at least in this direction, nearly half of the total interstellar hydrogen exists in molecular form. Theoretical calculations by Hollenbach and Salpeter (*Astrophysical Journal*, in press) indicate approximately 100 percent efficiency for formation of molecular hydrogen on dust grains in neutral hydrogen (H-I) regions in the galaxy.

Thus, the pion-decay hypothesis for the origin of the disk component of galactic γ-radiation (under the assumption of a total mean nucleon density of interstellar gas of ~ 2 cm^{-3}) provides a natural and adequate explanation for both the intensity and spectral characteristics of this radiation as observed by Clark et al. (Stecher and Stecker, 1970). The intensity distribution of this component as a function of galactic longitude shows only one statistically significant peak; viz, the peak at the galactic center. Observations made by detectors with better sensitivity and resolution should enable γ-ray astronomers to map the disk component for γ-ray "hot spots," which should reflect the true distribution of the total content of interstellar gas, independent of temperature and optical opacity conditions in various regions of the galaxy. However, we are at present limited to a general discussion of the intensity of the disk component with the possibility of an additional source component at the galactic center. The peak in the γ-ray intensity at the galactic center, which has a line strength of $\sim 2 \times 10^{-4}$ cm^{-2}-s^{-1}-rad^{-1} above 100 MeV, as determined both by the revised OSO–3 measurements and by Fichtel et al. (1969) requires further discussion. Approximately half of these γ-rays can be explained as due to the decay of neutral pions produced in cosmic-ray interactions with the galactic gas (the disk component we have been discussing) on the assumption that the cosmic-ray intensity is uniform throughout the galaxy. An increase in cosmic-ray intensity

toward the galactic center by an additional factor of ~ 2 could thus account for the increased flux in the galactic center region. Alternatively we could introduce a "two-component" model for galactic γ-rays in which γ-rays from a production mechanism other than pion decay contribute an additional flux to that produced by the general disk component. We would thus classify the galactic center as a γ-ray source. There may be such a source of γ-rays produced by Compton interactions of cosmic-ray electrons with the intense infrared radiation field located at the galactic center and detected at 100μ by Hoffman and Frederick (1969). Hoffman and Frederick have found this source to extend $\lesssim 2°3'$ in galactic latitude and $\gtrsim 6°5'$ in galactic longitude and to have a brightness temperature of 16 K. The source has been suggested by Lequeux (1970) to be produced by reradiation of intense starlight in the central region of the galaxy by interstellar grains produced in the atmospheres of red giant stars (Donn et al., 1968), with such grains being an order of magnitude more numerous in the galactic center region than in the disk. Using the infrared intensities given by Hoffman and Frederick, we find that cosmic-ray electrons with the same spectrum as that observed at the Earth can produce a γ-ray flux of 2×10^{-5} to 7×10^{-5} $cm^{-2}\text{-}s^{-1}\text{-}rad^{-1}$ above 100 MeV by Compton interactions, which is the same order of magnitude as the estimated flux from the disk component in the galactic center region. A hypothetical γ-ray spectrum from the galactic center is shown in figure 8–4. It is impossible at this time to determine theoretically whether pion decay or Compton interactions would be expected to play the major role in the production of γ-rays at the galactic center under the assumptions of the two-component model presented here.[2] The situation is further complicated by the possibility of increased fluxes of both cosmic-ray electrons and nucleons at the galactic center, although there is no need to postulate the existence of such fluxes in order to account for the observed γ-radiation. It is also unnecessary to postulate the existence of an 8 K graybody infrared radiation field of galactic extent, a hypothesis which was invoked by Shen (1969) and Cowsik and Pal (1969) based on a measurement of Shivanandan, Houck, and Harwit (1968). In order to account for the originally quoted OSO–3 measurements, however, the proposed existence of this 13 eV/cm^3 radiation field poses serious theoretical problems pertaining to its origin and role in the galactic energy balance and its effect on cosmic-ray electrons (Anand, Daniel, and Stephens, 1969) and ultra-high-energy cosmic rays

[2] However, the recent measurements by Fichtel and Kniffen would appear to limit the Compton interaction flux to about 50 percent of the total flux from the galactic center above 100 MeV as in the model shown in figure 8–4.

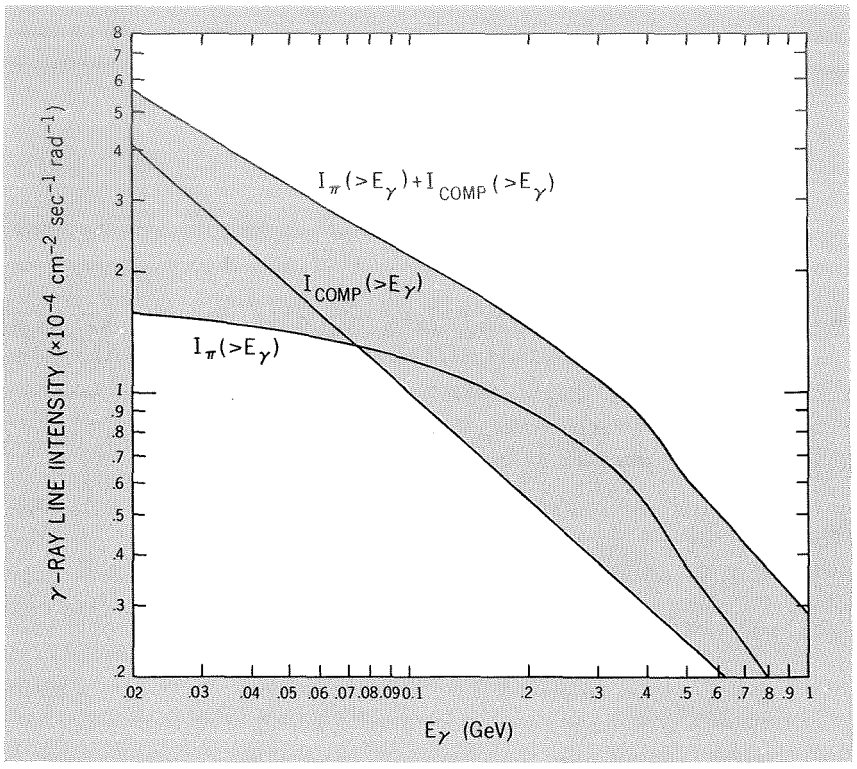

FIGURE 8–4. – A possible γ-ray spectrum from the galactic center based on the two-component source model (pion decay and Compton interactions), as discussed in the text.

(Encrenaz and Partridge, 1969).[3] The 8 K hypothesis is also in conflict with measurements of the spin temperatures of various molecules in the interstellar medium (Bartolot, Clauser, and Thaddeus, 1969; Thaddeus and Clauser, 1966; and Evans, Cheung, and Sloanaker, 1970) and most recently has been directly contradicted by a new infrared measurement by McNutt and Feldman (1970).[4]

Based on the discussion we have just presented, Stecher and Stecker (1970) reached some tentative conclusions regarding the origin of galactic γ-rays.

(1) Gamma rays originating in the galactic disk most likely result from the decay of neutral pions produced in interstellar cosmic-ray

[3] It has also recently been found to conflict with measured upper limits of hard X-ray emission from the galactic plane (Blecker and Deerenberg, 1970).

[4] Shivanandan (1970) has reported that due to a recent recalibration of their detector, the flux originally reported by Shivanandan et al. (1968) should be reduced by a factor of ~ 4 and that the revised flux should be considered an upper limit.

interactions. The excess originating in the galactic center region can be produced by a combination of the pion-decay process and Compton interactions between cosmic-ray electrons and infrared radiation.

(2) The explanations offered above obviate the necessity for invoking strong γ-ray point sources, large gradients in the galactic cosmic-ray flux, or 8 K graybody radiation fields of galactic extent in order to explain the revised γ-ray observations.

8-6 POSITRON-ANNIHILATION GAMMA RAYS AT 0.51 MeV FROM THE GALACTIC PLANE AND THE GALACTIC CENTER

We have seen in chapter 7 that positrons annihilate primarily from an S-state of positronium, with 75 percent of these annihilations producing a three-photon continuum rather than a two-photon line at 0.51 MeV. Therefore, on the average, one 0.51-MeV photon is produced for every two positrons which annihilate. Thus, the intensity of 0.51-MeV γ-rays observed along the line of sight as a function of galactic coordinates is given by

$$I_{0.51}(l^{\text{II}}, b^{\text{II}}) = \frac{Q_{T,\,\text{rest}} M(l^{\text{II}}, b^{\text{II}})}{8\pi} \tag{8-51}$$

where $M(l^{\text{II}}, b^{\text{II}})$ in grams per square centimeter is the amount of interstellar gas in the direction of observation. The resultant γ-ray intensities for various directions of observation are given in table 8–3. The values of $M(l^{\text{II}}, b^{\text{II}})$ obtained from 21-cm observations are taken from Ginzburg and Syrovatskii (1964). The values of $M(l^{\text{II}}, b^{\text{II}})$ designated by "missing-mass hypothesis" are based on the discussion of the last section, as needed to explain the recent observations of 100-MeV γ-rays from the galaxy as being due to bremsstrahlung and π° production.

The results of Metzger et al. (1964) indicate that the background continuum X-rays have a flux of about 6×10^{-5} cm^{-2}-s^{-1}-sr^{-1}-keV^{-1} at 0.51 MeV. Thus, an instrument with a resolution of 5 keV (the predicted width of the 0.51-MeV line) would be able to measure a line imposed on that continuum with a flux of about 3×10^{-4} cm^{-2}-s^{-1}-sr^{-1}.

Thus, $I_{0.51}(l^{\text{II}}, b^{\text{II}})$ must be greater than 3×10^{-4} cm^{-2}-sr^{-1}-s^{-1} in order to be observable above the X-ray background continuum by a detector with an energy resolution of 5 keV, which is the theoretical width of the 0.51-MeV line. This intensity is therefore a reasonable lower limit on the 0.51-MeV line intensity, which must be present in order for the annihilation line to be detected. By comparing this lower limit with the calculated intensities given in table 8–3, we see that the annihilation radiation could only be detected in the direction of the galactic center,

TABLE 8–3.—*Resultant γ-Ray Intensities for Various Directions of Observation*

	Solar minimum	$R_r = 350$ MV		Power law		$I_+ = 2\times10^{-2}$ cm^{-2}-s^{-1}-sr^{-1}	
		$R_0 = 500$ MV	$R_0 = 200$ MV	$T_c = 100$ MeV/ Nucleon	$T_c = 5$ MeV/ Nucleon	Mean	Maximum
Average (including halo) (21-cm) $\frac{1}{4\pi}\int dl^{II}\sin b^{II} db^{II} M(l^{II}, b^{II}) \simeq 1.6\times10^{-3}$	7.0×10^{-8}	1.1×10^{-7}	2.8×10^{-6}	2.1×10^{-6}	8.3×10^{-6}	$\frac{1.4\times10^{-6}}{n^{5/2}}$	3.2×10^{-5}
Anticenter (21-cm) $M(\pi, 0)\simeq 1.2\times10^{-2}$	5.6×10^{-7}	8.6×10^{-7}	2.1×10^{-5}	1.6×10^{-5}	6.2×10^{-5}	$\frac{1.0\times10^{-5}}{n^{5/2}}$	2.4×10^{-4}
Galactic center (21-cm) $M(0,0)\simeq 6\times10^{-2}$	2.7×10^{-6}	4.3×10^{-6}	1.0×10^{-4}	7.9×10^{-5}	3.1×10^{-4}	$\frac{5.3\times10^{-5}}{n^{5/2}}$	1.2×10^{-3}
Disk average (missing-mass hypothesis) $\frac{1}{2\pi}\int dl^{II} M(l^{II}, 0) \simeq 3\times10^{-2}$	1.4×10^{-6}	2.2×10^{-6}	5.0×10^{-5}	4.0×10^{-5}	1.6×10^{-4}	$\frac{2.7\times10^{-5}}{n^{5/2}}$	6.0×10^{-4}
Galactic center (missing-mass hypothesis) $M(0, 0) \simeq 0.1$	4.4×10^{-6}	7.0×10^{-6}	1.7×10^{-4}	1.3×10^{-4}	5.0×10^{-4}	$\frac{8.5\times10^{-5}}{n^{5/2}}$	2×10^{-3}

and, with the "missing-mass hypothesis," possibly also as a disk average. The calculated γ-ray fluxes, however, were obtained by assuming that the primary cosmic-ray intensities are spread uniformly along the line of sight over which the annihilation is formed. Such an assumption requires a mean cosmic-ray energy density of ~ 50 eV/cm^3 in order to produce a detectable annihilation line for the demodulated cosmic-ray spectrum with $R_r = 350$ MV and $R_0 = 200$ MV and for the power-law distribution. This energy density is at least an order of magnitude higher than that allowed by the general dynamics of the interstellar medium (Parker, 1966). The energy requirements for the power-law spectrum with $T_c = 100$ MeV/nucleon are smaller and therefore not necessarily inconsistent with the energy arguments mentioned above. A primary cosmic-ray spectrum of this form, however, conflicts with the ^{2}H and ^{3}He calculations (Ramaty and Lingenfelter, 1969) and possibly with the positron measurements in the 10 to 10^3 MeV region. (See fig. 7–5.) Therefore, it is probably not a good representation of the overall galactic cosmic-ray distribution.

We conclude that the 0.51-MeV annihilation γ-ray intensity produced by positrons from both pion and CNO beta emitters for a homogeneous disk model most probably will be smaller than the observed X-ray background and hence be unobservable.

As can be seen from table 8–3, however, if the 1-MeV positron measurement of Cline and Hones (1969) is regarded as a real flux rather than as an upper limit and is spread uniformly along the line of sight, the annihilation line would be observable both toward the galactic center and as a disk average. However, if these 1-MeV positrons are produced in supernova explosions and exhibit spatial and temporal inhomogeneities corresponding to their short ranges, the resultant γ-ray flux would again be below the X-ray background and would be unobservable.

Since the galactic center is known to be an intense source of high-energy γ-rays, and since the energy arguments that we have used do not necessarily hold for that region, the galactic center may be a detectable source of 0.51-MeV γ-rays. It may thus be more profitable to look for this radiation with a high-spatial-resolution detector than to look for a diffuse galactic flux. This argument is valid even if a diffuse flux is detectable, since, as can be seen from table 8–3, such a flux would still be more intense toward the galactic center.

3

Extragalactic Gamma Rays and Cosmology

INTRODUCTION TO RELATIVISTIC COSMOLOGY

9-1 INTRODUCTION

In the general theory of relativity, Einstein set out to identify the gravitational field with the geometry of space time itself. Using differential geometry, he derived an equation which identified the curvature of space time with the matter-energy density contained in it. Expressed in tensor form, the Einstein field equations are written

$$G_{\mu\nu}-\tfrac{1}{2}(Gg_{\mu\nu}-2\Lambda g_{\mu\nu})=8\pi\gamma T_{\mu\nu} \tag{9-1}$$

where $G_{\mu\nu}$ is the Einstein-Ricci tensor, G is its trace, $g_{\mu\nu}$ is the metric tensor which is defined by the equation

$$ds^2=g_{\mu\nu}\,dx_\mu\,dx_\nu \tag{9-2}$$

μ and ν are tensor indices which take on four values (one timelike, three spacelike), Λ is the cosmological constant, γ is the gravitational constant, and $T_{\mu\nu}$ is the energy-momentum tensor given by

$$T_{\mu\nu}=\left(\frac{p}{c^2}+\rho\right)\beta_\mu\beta_\nu+\frac{p}{c^2}\,g_{\mu\nu} \tag{9-3}$$

for a macroscopic body. In equation (9–1), p is the pressure, ρ the mass density, and β_μ and β_ν are components of the comoving velocity vector within the mass.

For an isotropic and homogeneous universe, the metric tensor has the Robertson-Walker form in dimensionless spherical coordinates; i.e.,

$$g_{\mu\nu}=\begin{pmatrix} c & 0 & 0 & 0 \\ 0 & -R(t)(1-k\eta^2)^{-1/2} & 0 & 0 \\ 0 & 0 & -R(t)\eta & 0 \\ 0 & 0 & 0 & -R(t)\eta\sin\theta \end{pmatrix} \tag{9-4}$$

where η is a dimensionless radial coordinate. Thus

$$ds^2 = c^2\,dt^2 - R^2(t)\left[(1-k\eta^2)^{-1}\,d\eta^2 + \eta^2(d\theta^2 + \sin^2\theta\,d\phi^2)\right] \tag{9–5}$$

where $R(t)$ is a time-dependent scale factor to be determined by solving the field equations (eq. (9–1)), and k is the curvature constant which has the values -1, 0, and $+1$.

Using the Robertson-Walker metric, equation (9–1) simplifies into the relations

$$\frac{\dot{R}^2}{R^2} + \frac{2\ddot{R}}{R} + \frac{8\pi\gamma p}{c^2} = -\frac{kc^2}{R^2} + \Lambda c^2 \tag{9–6}$$

and

$$\frac{\dot{R}^2}{R^2} - \frac{8\pi\gamma\rho}{3} = -\frac{kc^2}{R^2} + \frac{\Lambda c^2}{3} \tag{9–7}$$

In the present state of the universe, $\rho \gg p/c^2$, and equations (9–6) and (9–7) are usually solved for the zero-pressure approximation.

The Robertson-Walker line element given in equation (9–5) can also be written in the form

$$ds^2 = c^2\,dt^2 - R^2(t)\,du^2 \tag{9–8}$$

where

$$du^2 = \frac{d\eta^2}{1-k\eta^2} + \eta^2(d\theta^2 + \sin^2\theta\,d\phi^2) \tag{9–9}$$

The dimensionless length measured along the radial direction is then given by

$$u = \int_0^{\eta} \frac{d\eta}{(1-k\eta^2)^{1/2}} = \begin{cases} \sin^{-1}\eta & \text{for } k=+1 \\ \eta & \text{for } k=0 \\ \sinh^{-1}\eta & \text{for } k=-1 \end{cases} \tag{9–10}$$

Photons travel along geodesics which obey the same relation as in special relativity; viz,

$$ds^2 = 0 \tag{9–11}$$

which, from equation (9–8), is equivalent to the condition

$$u = c\int_{t_e}^{t_r} \frac{dt}{R(t)} \tag{9–12}$$

with t_e being the time when the photon was emitted and t_r being the time when the photon was received.

The emitting and receiving points are embedded in the metric so that the distance between them is changing by the scale factor $R(t)$; the dimensionless metric distance u is a constant. If we therefore consider

two successive wave crests of a light ray as being emitted at times t_e and $t_e+\Delta t_e$, respectively, and received at times t_r and $t_r+\Delta t_r$, then

$$\int_{t_e}^{t_r}\frac{dt}{R(t)}=\int_{t_e+\Delta t_e}^{t_r+\Delta t_r}\frac{dt}{R(t)}=u=\text{constant} \tag{9–13}$$

Thus

$$\int_{t_e+\Delta t_e}^{t_r+\Delta t_r}\frac{dt}{R(t)}-\int_{t_e}^{t_r}\frac{dt}{R(t)}=\int_{t_r}^{t_r+\Delta t_r}\frac{dt}{R(t)}-\int_{t_e}^{t_e+\Delta t_e}\frac{dt}{R(t)}$$

$$=\frac{\Delta t_r}{R(t_r)}-\frac{\Delta t_e}{R(t_e)}=0 \tag{9–14}$$

or

$$\frac{\Delta t_r}{R(t_r)}=\frac{\Delta t_e}{R(t_e)}$$

Since the wavelength of the emitted wave is $c\Delta t_e$ and that of the wave when received is $c\Delta t_r$, from equation (9–14) it follows that the wavelength is shifted by the amount

$$z\equiv\frac{\lambda_r-\lambda_e}{\lambda_e}=\frac{\Delta\lambda}{\lambda}=\frac{R(t_r)-R(t_e)}{R(t_e)}$$

or

$$\frac{R(t_r)}{R(t_e)}=1+z \tag{9–15}$$

We have observed this shift in the spectral lines of distant galaxies as always being toward longer wavelengths, so that $R(t_r)>R(t_e)$. From this evidence, it has been deduced that our universe is expanding with time.

9–2 GAMMA-RAY FLUXES

Let us now consider the effect of cosmological factors in calculating γ-ray fluxes emitted at large redshifts, z. The number of photons received per second is reduced by a factor $R(t_e)/R(t_r)$ from the number produced per second at time t_e. We consider here γ-rays produced in particle collisions between two components having densities $n_a(t_e)$ and $n_b(t_e)$, respectively. We specify the differential photon intensity produced per collision as

$$G(E_\gamma) \qquad (\text{cm}^2\text{-s-sr-GeV-cm}^{-6})^{-1}$$

Then the differential photon flux received at t_r is given by

$$dF_r=\frac{4\pi n_a(t_e)n_b(t_e)G(E_{\gamma,e})\,dE_{\gamma,e}\,dV_e\,dt_e}{4\pi R^2(t_r)\eta^2} \tag{9–16}$$

where the numerator represents the photon flux emitted at t_e, and the denominator indicates the fact that at t_r this flux is evenly distributed over a spherical wavefront of radius $R(t_r)$.

We now define the dimensional length

$$dl = R(t)\ du \tag{9–17}$$

so that the volume element

$$dV_e = dl[R^2(t_e)\eta^2\ d\Omega] \tag{9–18}$$

Since

$$dt_e = \frac{R(t_e)}{R(t_r)}\ dt_r$$

and

$$dE_{\gamma,e} = \frac{R(t_r)}{R(t_e)}\ dE_{\gamma,r} \tag{9–19}$$

because the energy of a γ-ray is inversely proportional to its wavelength, we may substitute equations (9–18) and (9–19) into equation (9–17) and obtain

$$dF_r = n_a(t_e)\, n_b(t_e) G\left[\frac{R(t_r)}{R(t_e)}\ E_{\gamma,r}\right] \times \frac{4\pi R^2(t_e)\eta^2\ d\Omega\ dl\ dE_{\gamma,r}\ dt_r}{4\pi R^2(t_r)\eta^2} \tag{9–20}$$

Dropping the subscript r from equation (9–20), since γ-rays are measured only when they are received, we may reduce equation (9–20) to

$$\frac{dF}{d\Omega\ dt\ dE_\gamma} \equiv dI = \frac{n_a(z) n_b(z) G[(1+z)E_\gamma] dl}{(1+z)^2}$$

$$= \frac{n_a(z) n_b(z) G[(1+z)E_\gamma]}{(1+z)^2}\left(\frac{dl}{dz}\right) dz \tag{9–21}$$

by using the relation (9–15).

9–3 DERIVATION OF *dl/dz*

Equation (9–21) is quite useful in evaluating the metagalactic γ-ray spectra from various high-energy interactions. The results are obtained from numerical integration of the relation

$$I(E_\gamma) = \int_0^{z_{\max}} dz\ n_a(z) n_b(z)\ \frac{G[(1+z)E_\gamma]}{(1+z)^2}\left(\frac{dl}{dz}\right) \tag{9–22}$$

Therefore, in order to utilize equation (9–22), we must determine the

factor dl/dz by solving the field equations (9–6) and (9–7) for particular cases. As we shall discuss later, the two most important cases to consider are the Einstein-de Sitter model and the low-density model. We shall now evaluate dl/dz for these models and for the more general case.

9–3a The Einstein-de Sitter Model

This model corresponds to a Euclidean three-space with $k = \Lambda = p = 0$. Equation (9–7) then reduces to

$$\frac{\dot{R}^2}{R^2} = \frac{8\pi\gamma\rho}{z} \tag{9–23}$$

In this case, our space is a Euclidean three-sphere containing a constant mass-energy M, so that

$$\rho \sim \frac{M}{R^3} \tag{9–24}$$

From equations (9–23) and (9–24) we find

$$R(t) \sim t^{2/3} \tag{9–25}$$

In these equations, it is common to define the Hubble parameter

$$H \equiv \frac{\dot{R}}{R} \tag{9–26}$$

so that from equations (9–25) and (9–26), we obtain

$$H = \tfrac{2}{3} t^{-1} \tag{9–27}$$

It is also common to label quantities associated with the present epoch ($z = 0$) by a subscript 0. The quantity H_0 is then referred to as the Hubble constant. From equations (9–15), (9–25), and (9–27), we then find

$$R(z) = \frac{R_0}{1+z}$$

and (9–28)

$$t(z) = \frac{t_0}{(1+z)^{3/2}}$$

From equations (9–8), (9–11), and (9–17), we obtain

$$\frac{dl}{dz} = -c\frac{dt}{dz} \tag{9–29}$$

and from equations (9–27), (9–28), and (9–29), we obtain

$$\frac{dl}{dz} = \frac{cH_0^{-1}}{(1+z)^{3/2}} \tag{9–30}$$

9-3b The Low-Density Model

This model holds when $\Lambda = 0$ and $\frac{8\pi\gamma\rho R^2}{3c^2} \ll 1$. Thus, equation (9–7) reduces to

$$\frac{\dot{R}^2}{R^2} = -\frac{kc^2}{R^2} \tag{9–31}$$

For a physical solution, we must specify $k = -1$ (negative curvature) and, therefore, $\dot{R} =$ constant and $R = Kt$, where $K =$ constant. Therefore

$$t(z) = \frac{t_0}{1+z}$$

$$H(z) = H_0(1+z) \tag{9–32}$$

$$H_0 = t_0^{-1}$$

and

$$\frac{dt}{dz} = -\frac{t_0}{(1+z)^2}$$

From equations (9–29) and (9–32), we then find

$$\frac{dl}{dz} = \frac{cH_0^{-1}}{(1+z)^2} \tag{9–33}$$

9-3c Other Models With $\Lambda = p = 0$

For models of a more general form with $\Lambda = p = 0$, but where $k \neq 0$ and $\rho \neq 0$, it is useful to define a new parameter

$$\Omega \equiv -\frac{2}{H_0^2}\frac{\ddot{R}_0}{R_0} \tag{9–34}$$

which provides a measure of the gravitational deceleration of the universal expansion caused by the presence of matter of density ρ. By subtracting equation (9–7) from equation (9–6), we find that this deceleration is directly proportional to ρ and is given by

$$\Omega = \frac{8\pi\gamma}{3H_0^2}\rho_0 \tag{9–35}$$

From equations (9–15), (9–29), and (9–34), we then find

$$\frac{dl}{dz} = \frac{c}{(1+z)H(z)} \tag{9–36}$$

From equations (9–7) (in the case where $\Lambda = 0$), (9–26), and (9–35), it follows that $H(z)$ is given by

$$H = \left[\frac{8\pi\gamma\rho}{3} - \frac{kc^2}{R^2}\right]^{1/2}$$

$$= \left[H_0^2\Omega(1+z)^3 - \frac{kc^2}{R_0^2}(1+z)^2\right]^{1/2} \tag{9–37}$$

since

$$\rho = \frac{\text{const}}{R^3} = \rho_0(1+z)^3 \tag{9–38}$$

Substituting equation (9–37) into equation (9–36), we then find that

$$\frac{dl}{dz} = \frac{c}{H_0(1+z)^2}\left[(1+z)\Omega - \frac{kc^2}{R_0^2H_0^2}\right]^{-1/2} \tag{9–39}$$

But, from equation (9–37) for $t = t_0$, we obtain the identity

$$-\frac{kc^2}{R_0^2H_0^2} = 1 - \Omega \tag{9–40}$$

so that by substituting equation (9–40) into equation (9–39), we find an expression for dl/dz in the useful form

$$\frac{dl}{dz} = \frac{c}{H_0(1+z)^2(1+\Omega z)^{1/2}} \tag{9–41}$$

Equation (9–41) reduces to equation (9–30) in the case where $\Omega = 1$ and to equation (9–33) when $\Omega \to 0$.

If we specify the value of $\sim 10^{28}$ cm for c/H_0 (which is determined from astronomical observations for $z \lesssim 3 \times 10^{-3}$ to only ± 50 percent), and if we express ρ_0 in terms of an atomic density of n_0 atoms/cm^3, we may use equation (9–35) to define a critical density n_c such that

$$n_c = \frac{3H_0^2}{8\pi\gamma} \simeq 10^{-5}\ \text{cm}^{-3} \tag{9–42}$$

and

$$\Omega = n_0/n_c \tag{9–43}$$

It then follows from equations (9–40) and (9–43) that if the mean density of the universe is greater than n_c, the universe will have a positive curvature; if $n_0 < n_c$, the universe will have a negative curvature, and in the case where $n_0 = n_c$, we have a Euclidean universe of zero curvature (the Einstein-de Sitter model we considered earlier).

We will not consider here models of a still more general nature where $\Lambda \neq 0$, since there is at present no empirical need to do so. However, it is interesting to note in passing that models with $\Lambda \neq 0$ can lead to states of metastable equilibrium in which the universe can maintain a static phase at a fixed value of R for an indefinite period of time. This static model of the universe is known as the Lemaitre model.

The Cosmic Gamma-Ray Spectrum From Secondary Particle Production Outside the Galaxy

In chapters 5 and 6 we made use of recent accelerator and cosmic-ray data to determine the details of the cosmic γ-ray spectrum from the secondary particles produced by cosmic-ray collisions in the galaxy. Here, we will make use of the cosmological formulas derived in chapter 9 in order to determine the cosmic γ-ray spectrum from secondary particles produced by cosmic-ray collisions in extragalactic space. This spectrum will differ from the galactic (or local) γ-ray spectrum because most of the generating collisions take place at large distances where we are looking back to a time when the universe was more compact and collisions were more frequent. These "early" γ-rays will be of lower energy due to the progressive redshift of the general cosmic expansion. Using the formulas derived in chapter 9, we take account of time-dilatation, volume-diminution, redshift, and curvature effects which become important at large redshifts.

In chapter 9, we obtained the important relation between redshift and radius of the universe, given by equation (9–15)

$$\frac{R(t_r)}{R(t_e)} = 1+z$$

where t_e is the time when the γ-ray was emitted and t_r is the time when the γ-ray is received (detected).

It follows from equation (9–15) that in a universe where most of the energy density is in the form of matter,

$$\frac{n(t_e)}{n(t_r)} = (1+z)^3 \qquad (10\text{–}1)$$

$$\frac{T_\gamma(t_e)}{T_\gamma(t_r)} = (1+z) \qquad (10\text{–}2)$$

and

$$\frac{n_\gamma(t_e)}{n_\gamma(t_r)} = (1+z)^3 \qquad (10\text{–}3)$$

where $n(t)$, $T_\gamma(t)$, and $n_\gamma(t)$ are the average particle density of matter, and the temperature and photon density of cosmic blackbody radiation in the universe. Let $G_g(E_\gamma)$ be the γ-ray spectrum generated by the galactic cosmic-ray spectrum, $I_g(E_p)$, in traveling a unit particle length (1 cm^{-2}) through the intergalactic medium. (This spectrum is the same as the quantity $I(E_\gamma)/\langle nL\rangle$ calculated in chs. 5 and 6.)

We now assume that some ubiquitous generating mechanism causes cosmic rays to be produced throughout the universe with the same power law as observed at the Earth, so that the metagalactic cosmic-ray spectrum differs only in absolute intensity from the galactic cosmic-ray spectrum. It follows that the form of the cosmic γ-ray spectrum anywhere in the metagalaxy, when observed in the comoving frame at that point, will be the same as the form of $G_g(E_\gamma)$. We may then write down an expression for the integrated metagalactic γ-ray flux in any direction as

$$I_\pi(E_\gamma) = \int_0^{z_{\max}} dz\, n(z) \frac{I_c(z)}{I_g} \frac{G_g[(1+z)E_\gamma]}{(1+z)^2} e^{-\tau(E_\gamma, z)} \frac{dl}{dz} \qquad (10\text{–}4)$$

with the derivation of equation (10–4) being similar to the derivation of equation (9–22) in the previous chapter. Here we have used the symbol I_g to represent the total intensity of galactic cosmic rays of energies above the pion-production threshold in order to normalize the generating spectrum G_g and to relate $I_\pi(E_\gamma)$ to the extragalactic cosmic-ray intensity $I_c(z)$. We have also included in equation (10–4) an added exponential factor to account for absorption of γ-rays, which may become important at high redshifts under certain conditions which we will discuss later. The following evaluation of equation (10–4) is based on a calculation by the author (Stecker, 1969c).

We will assume, for the purposes of calculating $I_\pi(E_\gamma)$, that at some early epoch, corresponding to $z \geq z_{\max}$, conditions were unsuitable for the acceleration of cosmic rays. We will consider $z_{\max}$ to correspond to the epoch of galaxy formation and consider two possible models for the origin of a metagalactic cosmic-ray flux. For model I, we will assume that the extragalactic cosmic-ray flux arises through leakage from the halos of radio galaxies from $z = z_{\max}$ to $z = 0$. For model II, we will assume that this flux was created primarily in a burst at the time of galaxy formation. For $z_{\max}$, we will also consider two extremes. One extreme is $z_{\max} = 10^2$, which corresponds to the earliest epoch when galaxy formation could probably occur. At $z = 10^3$, the blackbody temperature of the universe was of the order of 10^3 to 10^4 K, cool enough for ionized hydrogen to combine to form a neutral gas. According to Peebles (1965), $z = 10^3$ also corresponds to the epoch when gas clouds may have begun to form gravitationally bound systems.

The other extreme for z_{max} which we may consider corresponds to the highest redshift yet observed for a quasar; viz, 2.2.[1] This is, of course, an extreme which is limited by technique rather than by any physical criteria, and it is included mainly for purposes of discussion. We will also consider various intermediate values for z_{max} of 4, 9, and 40. (Doroshkevich, Zeldovich, and Novikov (1967) suggest that galaxy formation took place at $z = 10$ to 20, whereas Weymann (1967) suggests $z = 10^2$.)

It is important to note here that the upper limit z_{max} may be effectively restricted, not by the epoch of galaxy formation, but by attenuation of the metagalactic cosmic-ray flux due to the collisions themselves. The cross section for inelastic cosmic-ray p–p collisions is of the order of 30 mb. Therefore, the lifetime of the metagalactic cosmic rays against collisional losses is given by

$$T_c = \frac{1}{n\sigma c} = \frac{1}{n_0 \sigma c (1+z)^3}$$

$$\simeq 10^{15} n_0^{-1} (1+z)^{-3} \text{ s} \qquad (10\text{–}5)$$

The lifetime of the universe at a redshift z is

$$T_u \simeq 3 \times 10^{17} (1+z)^{-3/2} \text{ s} \qquad (10\text{–}6)$$

for an Einstein-de Sitter model, where $n_0 \simeq 10^{-5}$ cm^3.

Cosmic rays cannot accumulate in the metagalaxy if the ratio $T_c/T_u < 1$. Therefore, the condition $T_c/T_u = 1$ defines a critical value for an Einstein-de Sitter model of $z_{max} \sim 10^2$ beyond which a further buildup of metagalactic cosmic rays cannot occur. With these limitations on z in mind, we will now consider the various ideal models for describing the metagalactic cosmic-ray flux.

For model I, we assume a constant leakage rate so that the total number of cosmic rays in the metagalaxy is proportional to the time elapsed since galaxy formation. It follows from equation (10–6) that for an Einstein-de Sitter model this time is given by

$$\tau_g \simeq 10^{10} [(1+z)^{-3/2} - (1+z_{max})^{-3/2}] \quad \text{years} \qquad (10\text{–}7)$$

The cosmic-ray density will then increase with redshift according to the relation

$$\frac{I'(z)}{I_g} \sim (1+z)^3 [(1+z)^{-3/2} - (1+z_{max})^{-3/2}] \qquad (10\text{–}8)$$

[1] This number has since grown.

However, the cosmic rays which produce the neutral pions necessary for γ-ray production are only those above a threshold kinetic energy $E_{th} - M_p$ of about 300 MeV. We must therefore determine

$$I(z) = I'(E > E_{th}|z) \tag{10-9}$$

For a power-law cosmic-ray spectrum of the form

$$I(>E) \sim E^{-1.5} \tag{10-10}$$

as is approximately valid in the energy region where most pions are produced (see ch. 5), it follows from the redshift relation that

$$\begin{aligned} I(E > E_{th}|z) &= I'\left(E > \frac{E_{th}}{(1+z)}\right) \\ &= I'(z)\left[\frac{1+z}{1+z_{max}}\right]^{1.5} \end{aligned} \tag{10-11}$$

so that we must use an effective flux of

$$\frac{I(z)}{I_g} \sim (1+z)^3 \left[\frac{1+z}{1+z_{max}}\right]^{1.5} [(1+z)^{-3/2} - (1+z_{max})^{-3/2}] \tag{10-12}$$

For model II, we assume that the metagalactic cosmic rays were created in a burst at the time of galaxy formation. We thus find for this model that

$$\frac{I(z)}{I_g} \sim (1+z)^3 \left[\frac{1+z}{1+z_{max}}\right]^{1.5} \tag{10-13}$$

Using the models defined by equations (10–12) and (10–13), together

TABLE 10–1.—*Value of* I_0/I_g *for* $n_0 = 10^{-5}$ cm^{-3}

[Stecker, 1969c]

Model	z_{max}				
	2.2	4	9	40	100
Constant-leakage model	1.8×10^{-1}	1.3×10^{-1}	7.0×10^{-2}	3.2×10^{-2}	2.8×10^{-2}
Burst model	2.6×10^{-2}	9.0×10^{-3}	2.2×10^{-3}	3.0×10^{-4}	1.1×10^{-4}

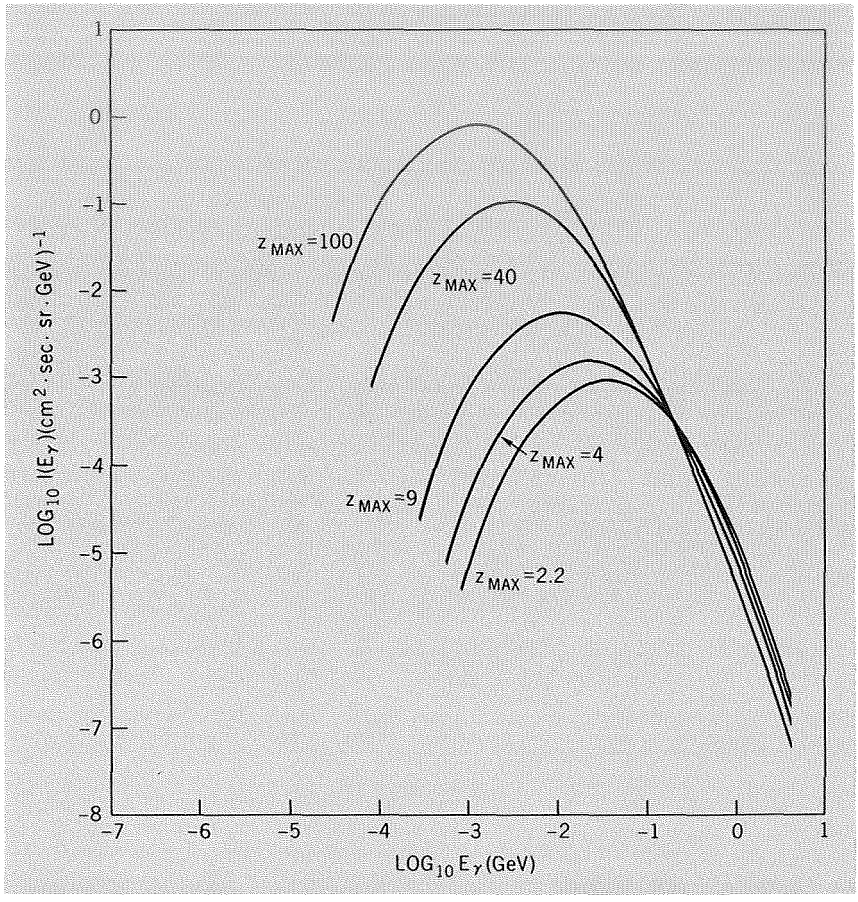

FIGURE 10–1.—Differential spectrum for leakage model (model I) (Stecker, 1969c).

with the value for dl/dz given by equation (9–30), Stecker (1969c) used equation (10–4) to calculate the extragalactic γ-ray spectra produced by cosmic-ray models I and II. These results were normalized by requiring the integral γ-ray spectrum above 100 MeV to be equal to 1.1×10^{-4} cm^{-2}-s^{-1}-sr^{-1}, according to the results of Clark et al. (1968) measured by the detector aboard the OSO–3 satellite.[2] As has been noted previously, such a normalization makes possible the determination of upper limits on the value I_0/I_g; i.e., the present metagalactic intensity of cosmic-ray nucleons. These upper limits are given in table 10–1.

The γ-ray fluxes thus calculated are given in figures 10–1 to 10–4. Figure 10–5 shows the γ-ray flux expected from the galactic halo in the

[2] This value has now been determined by Clark et al. (1970) to be approximately a factor of 2 to 4 too high.

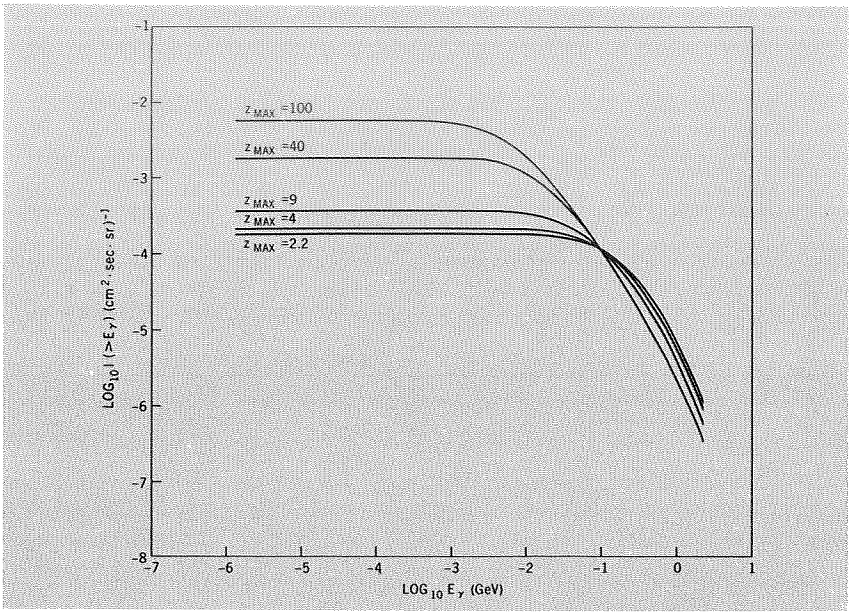

FIGURE 10–2.—Integral spectrum for leakage model (model I) (Stecker, 1969c).

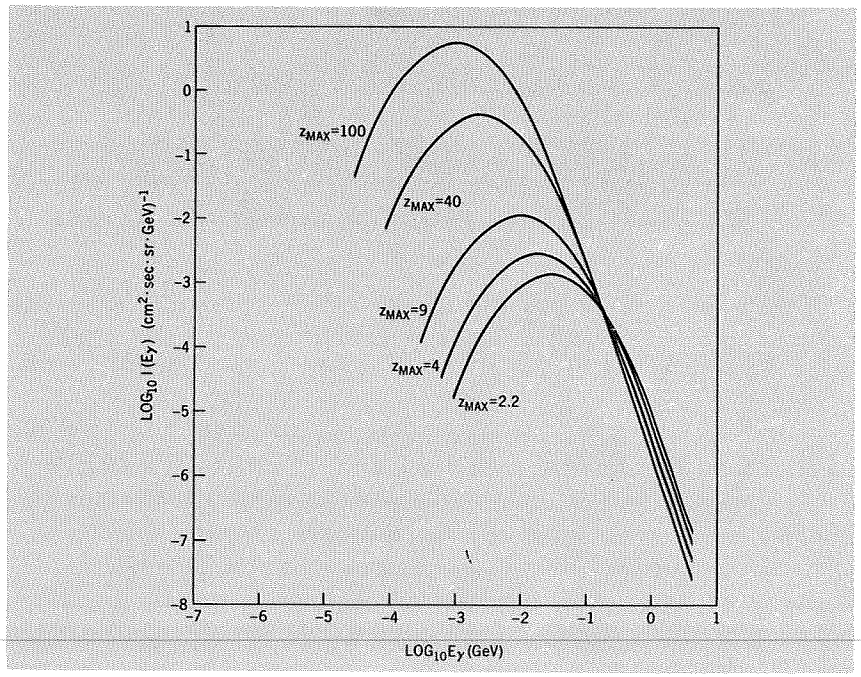

FIGURE 10–3.—Differential spectrum for burst model (model II) (Stecker, 1969c).

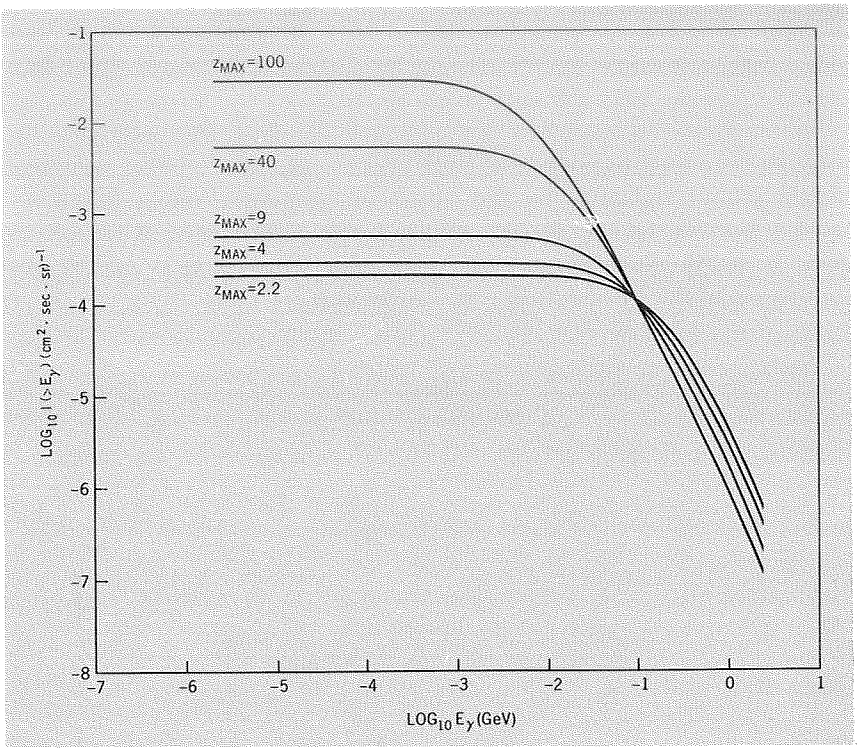

FIGURE 10–4.—Integral spectrum for burst model (model II) (Stecker, 1969c).

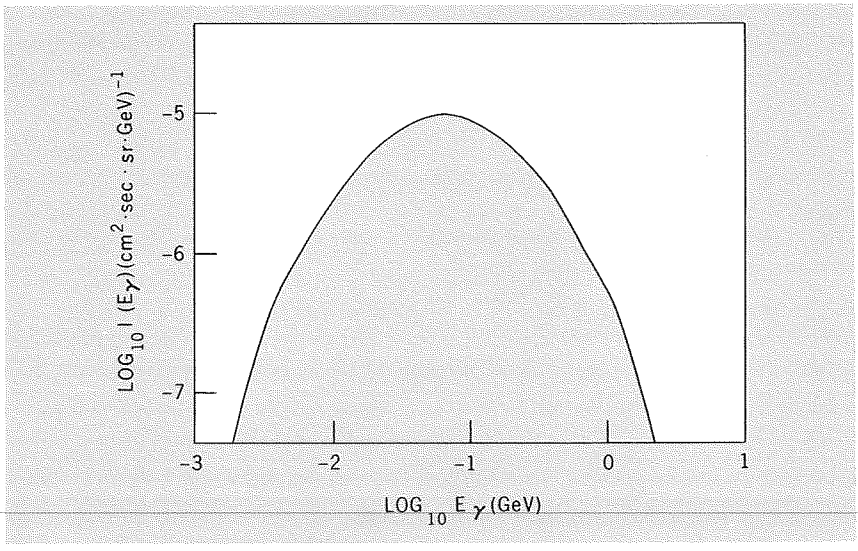

FIGURE 10–5.—Differential spectrum for the galactic halo ($\langle nL \rangle = 3 \times 10^{20}$ cm^{-2}).

direction of the pole, based on the results of chapters 5 and 6 and taking $\langle nL \rangle = 3 \times 10^{20}$ cm$^{-2/3}$. It can be seen that the local γ-ray flux from the galactic halo will not explain the data of Clark et al. and should be unimportant compared to the extragalactic flux. The extragalactic γ-ray spectra tend to peak near $7 \times 10^{-2}/(1+z_{max})$ GeV, being weighted toward higher redshifts by the effect of greater densities at earlier epochs. Because of the density effect, a cosmic-ray burst at large redshifts is much more effective in producing γ-rays than a continuous production of the same number of cosmic rays.

---

[3] Thus $I_{pole}(E_\gamma) = 3 \times 10^{20}\, G_g(E_\gamma)$.

Cosmic Gamma Rays From Extragalactic Proton-Antiproton Annihilations

11-1 INTRODUCTION

The existence or nonexistence of antimatter in the universe is a question of importance in the fields of cosmology and particle physics (Alfvén, 1965). Recently, Harrison (1967) has proposed the existence of large amounts of antimatter in the universe in order to account for the condensation of matter into galaxies. The only practical way of determining the existence of such antimatter is by the detection of the γ-radiation produced when antimatter and matter annihilate into mesons having γ-ray-producing decay modes. The γ-ray spectra from such annihilations are presented here. They are based on the results of recent accelerator experiments on antiproton annihilation as discussed in chapter 3 and also include cosmological distortions of local annihilation γ-ray spectra.

11-2 THE LOCAL ANNIHILATION GAMMA-RAY SPECTRUM

The annihilation γ-ray spectrum (AGS) for $p-\bar{p}$ interactions involving kinetic energies less than 286 MeV (the threshold for nonannihilation pion production) is given by the expression

$$I_A(E_\gamma) = \frac{B}{4\pi} \int dv\, v f(v) \sum_s \int dE_s\, \sigma_s(E_s|v) \sum_d \zeta_{\gamma d} R_{\gamma d} f_{ds}(E_\gamma|E_s) \quad (11\text{–}1)$$

as shown in chapter 3, where v is the relative velocity of the proton and antiproton, $f(v)$ is the normalized distribution function over this velocity, s is an index representing the particular type of particle produced in the annihilation, $\sigma_s(E_s|v)$ is the cross section times multiplicity of particles of type s and energy E_s produced in a collision of velocity v, and the index d specifies a specific decay mode with a branching ratio $R_{\gamma d}$ which produces $\zeta_{\gamma d}$ γ-rays with a normalized energy distribution $f(E_\gamma|E_s)$.

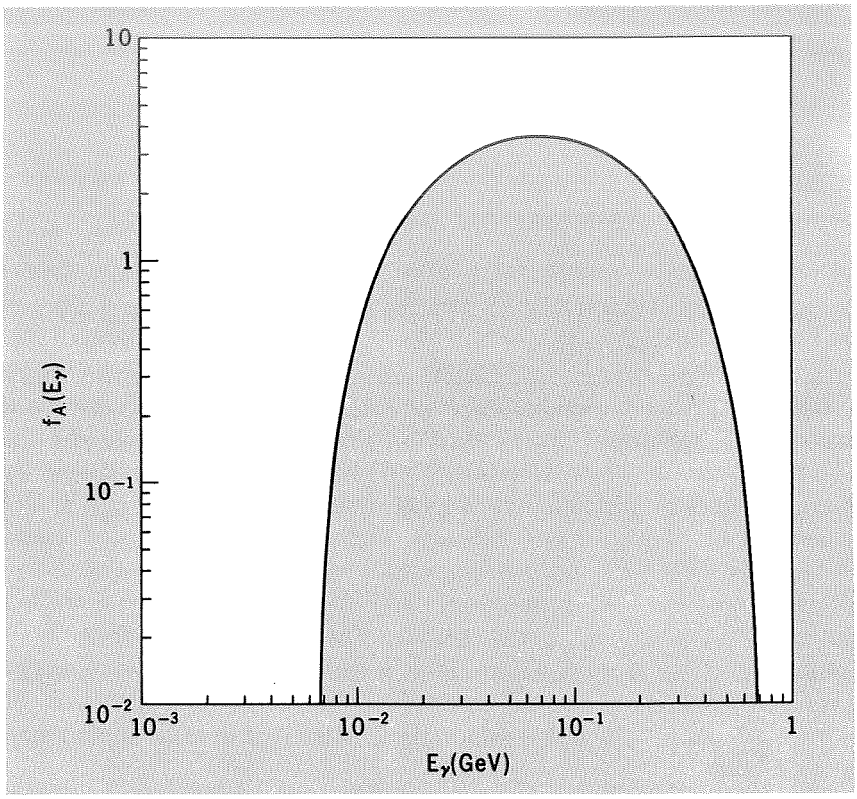

FIGURE 11–1.—The normalized local differential γ-ray spectrum from $p-\bar{p}$ annihilation.

The quantity B is defined as the product of interacting proton and antiproton densities integrated over a line-of-sight pathlength l; i.e.,

$$B = \int_0^{l_{\max}} dl\; n_p(l) n_{\bar{p}}(l) \tag{11–2}$$

Based on the calculations of Morgan and Hughes (1969), we showed in chapter 3 that $(E_s|v)$ can be represented as having a power-law velocity dependence using three different exponents given by equation (3–31) for three different temperature ranges given in equation (3–30). Using equations (3–47) and (3–48), we may thus write

$$I_A(E_\gamma) = \frac{B}{4\pi}\, \sigma_{\text{III}} c \zeta_\gamma \left[\frac{2}{\pi^{1/2}}\, \Gamma(1.68) \left(\frac{2kT}{mc^2}\right)^{0.18}\right] f_A(E_\gamma)$$
$$\text{for } 10\text{ K} \leqslant T \leqslant 10^4\text{ K} \tag{11–3}$$

and

$$I_A(E_\gamma) = \frac{B}{4\pi}\,\sigma_\Pi c\zeta_\gamma \left(\frac{2mc^2}{\pi kT}\right)^{1/2} f_A(E_\gamma) \qquad \text{for } 10^4\ \text{K} \lesssim T \lesssim 10^{11}\ \text{K} \quad (11\text{–}4)$$

The local annihilation spectrum $f_A(E_\gamma)$, as calculated in chapter 3, is shown in figure 11–1.

11-3 REDSHIFTED SPECTRA

For cosmological γ-ray production

$$B \rightarrow \int dz\, n_p(z) n_{\bar{p}}(z)\, \frac{dl}{dz} \quad (11\text{–}5)$$

where, from equation (9–41),

$$\frac{dl}{dz} = \frac{c}{H_0(1+z)^2(1+\Omega z)^{1/2}}$$

Taking (from equation 9–38)

$$n_p(z) = n_{p,0}(1+z)^3$$

and (11–6)

$$n_{\bar{p}}(z) = n_{\bar{p},0}(1+z)^3$$

and defining

$$B_0 \equiv \left(\frac{c}{H_0}\right) n_{p,0} n_{\bar{p},0} \quad (11\text{–}7)$$

we find by using equation (9–21) that

$$I_A(E_\gamma) = \frac{B_0 \sigma_i c^{\delta_i}}{2\pi^{3/2}} \left(\frac{2k}{m}\right)^{\left(\frac{1-\delta_i}{2}\right)} \Gamma\left(2 - \frac{\delta_i}{2}\right)$$

$$\times \int dz [T(z)]^{\left(\frac{1-\delta_i}{2}\right)} \frac{(1+z)^2}{(1+\Omega z)^{1/2}}\, G_A[(1+z)E_\gamma] e^{-\tau(E_\gamma, z)} \quad (11\text{–}8)$$

where $i = \text{II, III}$; $\sigma_{\text{II}} = 2$; $\delta_{\text{III}} = 0.64$; $\sigma_{\text{II}} = 1.1 \times 10^{-27}\ \text{cm}^2$; $\sigma_{\text{III}} = 2.6 \times 10^{-18}\ \text{cm}^2$; $G_A(E_\gamma) \equiv \zeta_\gamma f_A(E_\gamma)$ where $f_A(E_\gamma)$ is shown in figure 11–1; and T_m is the matter temperature of the universe, which is a function of z.

At the earliest stages in the evolution of the universe, when the matter in the universe was in thermal equilibrium with the universal blackbody radiation due to Compton interactions between thermal photons and electrons, T_m was equal to T_r (the temperature of the radiation field). Zeldovich, Kurt, and Syunyaev (1969) have shown that even though the intergalactic gas has cooled to the 50-percent neutral point by the time corresponding to a redshift of 1200 to 1300, the small fraction of ionized material left at lower redshifts is enough to sustain temperature equilibrium between matter and the radiation field until a redshift of 150 to 200.

The photon density of a radiation field at temperature T_0 is given from the Planck formula as

$$n_{r,0}(\epsilon, T_0)\,d\epsilon = \frac{8\pi}{h^3c^3}\,\frac{\epsilon^2\,d\epsilon}{\exp\left[\dfrac{\epsilon}{kT_{r,0}}\right]-1} \tag{11-9}$$

At a redshift $z \neq 0$, this distribution is given by

$$n_r(z, \epsilon)\,d\epsilon = \frac{8\pi}{h^3c^3}\,\frac{(1+z)^3\epsilon^2\,d\epsilon}{\exp\left[\dfrac{(1+z)\epsilon}{kT_{r,0}}\right]-1}$$

$$= (1+z)^3 n_{r,0}[\epsilon, T_r(z)]\,d\epsilon \tag{11-10}$$

where

$$T_r(z) \equiv (1+z)T_{r,0} \tag{11-11}$$

Thus, we find that the redshifted Planckian maintains its form with the parameter $T(z)$ in the exponent given by equation (11–11). The photon density redshifts in the same manner as matter density as given by equation (10–1). The energy density in the radiation field then redshifts as

$$\rho_r = \rho_{r,0}(1+z)^4 \tag{11-12}$$

in accord with the definition of $T_r(z)$ given by equation (11–11) and the relation $\rho \sim T^4$.

We therefore find that

$$T_m(z) = T_r(z) = T_{r,0}(1+z) \qquad \text{for } z \gtrsim 150 \text{ to } 200 \tag{11-13}$$

At lower redshifts, when the matter has thermally decoupled from the radiation field, the momentum distribution of the atoms in the intergalactic gas is given by the Maxwellian,

$$n_0(p, T_{m,0})\,dp = \text{const} \times p^2 e^{-p^2/2mkT_{m,0}}\,dp \tag{11-14}$$

These atoms lose momentum through collisions due to the effect of the overall adiabatic expansion of the universe; their resultant momentum change is

$$p(z) = p_0 \frac{R_0}{R(z)} = p_0(1+z) \tag{11-15}$$

Substituting equation (11–15) into equation (11–14), we then find

$$n_m(z, p)dp = (1+z)^3 n_{m,0}[p, T_m(z)]dp \tag{11-16}$$

with

$$T_m(z) = T_{m,0}(1+z)^2 \tag{11-17}$$

From equation (11–16), it is immediately evident that the total number of atoms, $\sim nR^3$, is conserved during the expansion, as must be the case.

We thus find that

$$T_m(z) = T_{m,0}(1+z)^2 \qquad \text{for } z \lesssim 150 \text{ to } 200 \tag{11-18}$$

with

$$T_m(150 \text{ to } 200) \simeq T_r(150 \text{ to } 200) \tag{11-19}$$

The adiabatic expansion concept may be used to link the derivations of equations (11–11) and (11–17) for the temperature-redshift relations. In an adiabatic expansion, it is well known that

$$TV^{(\gamma-1)} = \text{constant} \tag{11-20}$$

where the quantity γ here is the ratio of specific heat at constant pressure to that at constant temperature and V is the volume of the gas (in this case the volume of the universe) which from equation (9–15) is given by

$$V(z) = V_0(1+z)^{-3} \tag{11-21}$$

For photons and monatomic gases at relativistic temperatures ($pc \simeq E$), $\gamma = 4/3$, whereas for nonrelativistic gases, $\gamma = 5/3$. Thus, from equations (11–21) and (11–20) we immediately obtain equation (11–11) for photons and relativistic gases and equation (11–17) for nonrelativistic gases.

Equations (11–11) and (11–17) may then be used in equation (11–8) to evaluate $I_A(E_\gamma)$.

It is of interest to note that since $f_A(E_\gamma)$ is nonvanishing only within a restricted energy range (given by eq. (3–76)), there exists an energy region

$$E_\gamma \lesssim 5 \text{ MeV} \tag{11-22}$$

TABLE 11–1.—*Exponents of Cosmological Power-Law Annihilation γ-Ray Spectra*

Ω	z	$E_{\gamma 0} \simeq \frac{70 \text{ MeV}}{(1+z)}$	δ	$\alpha+1$
1	0–150	500 keV–70 MeV	0.64	2.86
	150–1000	70 keV–500 keV	0.64	2.68
	10^3–10^8	< 70 keV	2	2.00
$\simeq 0$	0–150	500 keV–70 MeV	0.64	3.36
	150–1000	70 keV–500 keV	0.64	3.18
	10^3–10^8	< 70 keV	2	2.50

where the integral in equation (11–8) is independent of the form of $f_A(E_\gamma)$ and the resultant spectrum has a power-law form when absorption may be neglected. In actuality, the power-law form of the spectrum is a valid approximation even over a wider energy range, where a change of the limits of integration over $f_A(E_\gamma)$ does not significantly affect the value of the integral. In this case, we find

$$I_A(E_\gamma) = 2B_0\sigma_\pi\zeta_\pi cKE_\gamma^{-(\alpha+1)} \sim E_\gamma^{-(\alpha+1)} \tag{11–23}$$

where

$$K \equiv \int_{5 \text{ MeV}}^{919 \text{ MeV}} dE_\gamma E_\gamma^\alpha f_\gamma(E_\gamma) \tag{11–24}$$

and α is the exponent of the total power-law dependence of the integrand on $(1+z)$; i.e.,

$$I_A(E_\gamma) \sim \int dz(1+z)^\alpha f_A[(1+z)E_\gamma] \tag{11–25}$$

For an Einstein-de Sitter universe, $\Omega = 1$, whereas for a low-density Friedman universe, $\Omega \simeq 0$. Thus, we find the power-law production spectra with exponents given in table 11–1 for the various ranges of γ-ray energies at $z = 0$.

Extragalactic Gamma Rays From Compton Interactions and Bremsstrahlung

12-1 COSMOLOGICAL GAMMA RAYS FROM COMPTON INTERACTIONS

We next take into account the cosmological effects in computing the extragalactic γ-ray spectrum from Compton interactions between cosmic-ray electrons and photons of the universal blackbody radiation field in intergalactic space. The local ($z = 0$) spectrum is given from equation (8–19) as

$$I_{c,0}(E_\gamma) = \tfrac{2}{3}\sigma_T c H_0^{-1} f(\Gamma)\,(mc^2)^{1-\Gamma}\,(3.6k)^{(\Gamma-3)/2}\,K_{e,0}\rho_{r,0} \times T_{r,0}^{(\Gamma-3)/2} E_\gamma^{-(\Gamma+1)/2} \qquad (12\text{–}1)$$

for Compton γ-rays produced by cosmic-ray electrons having a power-law energy spectrum of the form

$$I(E_e) = K_{e,0} E_e^{-\Gamma} \qquad (12\text{–}2)$$

We have shown that, under the conditions where equation (12–2) is valid over all redshifts from 0 to $z_{\max}$ and where electron energy losses other than those from the universal expansion are neglected, the transformation from $K_{e,0}$ to $K_e(z)$ is given by

$$\begin{aligned} K_e(z) &= K_{e,0}(1+z)^3(1+z)^{\Gamma-1} \\ &= K_{e,0}(1+z)^{\Gamma+2} \end{aligned} \qquad (12\text{–}3)$$

where the first factor of $(1+z)^3$ represents the density effect and the factor of $(1+z)^{\Gamma-1}$ represents the transformation of the power-law energy spectrum from a burst of relativistic cosmic-ray electrons occurring at $z_{\max} \geq z$.

Substituting equations (11–12), (11–13), and (12–3) into the general formula (9–22), we find

$$I_c(E_\gamma, z_{\max}) = I_{c,0}(E_\gamma) \int_0^{z_{\max}} dz\, \frac{(1+z)^\Gamma}{(1+\Omega z)^{1/2}} \qquad (12\text{–}4)$$

Under these conditions, the power-law form for the Compton γ-ray

spectrum is maintained but the cosmological flux is enhanced by a factor given by the integral over z in equation (12–4).

However, Brecher and Morrison (1967) showed that the true situation is not as simple as that given by equation (12–4) under the conditions when the high-energy end of the electron spectrum is steepened owing to energy losses from the Compton interactions themselves. Since the blackbody radiation density is proportional to $(1+z)^4$, electrons lose energy primarily from Compton interactions, with the energy loss rate given by

$$\left(\frac{d\gamma}{dt}\right)_c = -\frac{4}{3}\frac{\sigma_T c \rho_r}{m_e c^2}\gamma^2 = \frac{(1+z)^4}{\tau_0}\gamma^2 \tag{12–5}$$

with

$$\tau_0 \equiv \frac{3m_e c^2}{4\sigma_T c \rho_{0,\,r}} \simeq 7.7 \times 10^{19}\ \text{s} \tag{12–6}$$

The energy loss from the universal expansion is given by

$$\left(\frac{d\gamma}{dz}\right)_{\text{exp}} = \frac{\gamma}{1+z} \tag{12–7}$$

From equations (12–5) and (9–41), we obtain

$$\left(\frac{d\gamma}{dz}\right)_c = \left(\frac{d\gamma}{dt}\right)_c \left(\frac{dt}{dz}\right) = \frac{(1+z)^2\gamma^2}{H_0\tau_0(1+\Omega z)^{1/2}} \tag{12–8}$$

The two energy loss rate terms are equal at the critical energy, $E_c = \gamma_c m_e c^2$, where

$$\gamma_c = \frac{H_0\tau_0(1+\Omega z)^{1/2}}{(1+z)^3} \simeq \frac{256(1+\Omega z)^{1/2}}{(1+z)^3} \tag{12–9}$$

or

$$E_c \simeq 0.13\frac{(1+\Omega z)^{1/2}}{(1+z)^3} \quad \text{GeV} \tag{12–10}$$

For $E < E_c$, the electron spectrum maintains its power-law form since these electrons lose their energy through the universal expansion; equation (12–3) is therefore valid. However, for $E > E_c$, the equilibrium electron flux is given by the solution of equation (7–24) under the conditions when Compton losses dominate. Under these conditions, equation (7–24) reduces to the form (Brecher and Morrison, 1967)

$$\frac{\partial}{\partial\gamma}\left[K_e\gamma^{-\Gamma'}\frac{(1+z)^4\gamma^2}{\tau_0}\right] = k_q\gamma^{-\Gamma} \tag{12–11}$$

where $k_q\gamma^{-\Gamma}$ is the original (injection) electron spectrum and Γ' is the exponent of the resulting equilibrium electron spectrum. It follows from

equation (12–11) that

$$\Gamma' = \Gamma + 1 \tag{12–12}$$

and

$$K_e = \frac{k_q \tau_0}{\Gamma (1+z)^4} \tag{12–13}$$

so that the equilibrium electron spectrum is depleted by a factor proportional to $(1+z)^4$ by Compton interactions with the universal radiation field and, in addition, the exponent of the electron spectrum is steepened by one power of E_e.

This steepening in the electron spectrum corresponds to a change of $\frac{1}{2}$ in the exponent of the Compton γ-ray spectrum at an energy

$$E_{\gamma, c} = \left\langle \frac{4}{3} \epsilon_0 \right\rangle \gamma_c^2 = 33 \left[\frac{(1+\Omega z)}{(1+z)^5} \right] \quad \text{eV} \tag{12–14}$$

Thus, the Compton γ-rays are expected to be produced by the steepened electron spectrum at all γ-ray energies. From equation (12–13), Brecher and Morrison conclude that unless there is a large evolutionary factor in the electron production spectrum, i.e., $k_q \sim (1+z)^m$, where $m \gtrsim 4$, there will be no significant enhancement of Compton γ-rays at large redshifts over those produced at the present epoch.

12-2 COSMOLOGICAL GAMMA RAYS FROM BREMSSTRAHLUNG INTERACTIONS

The local γ-ray spectrum from relativistic bremsstrahlung interactions is given by equation (8–36) as

$$I_{b,0}(E_\gamma) = 3.4 \times 10^{-26} n_0 c H_0^{-1} \frac{I_e(E_e > E_\gamma)}{E_\gamma} \tag{12–15}$$

Making use of equations (9–22) and (12–3), we obtain for the cosmological bremsstrahlung production spectrum

$$\begin{aligned} I_b(E_{\gamma 0}, z_{\max}) &= \frac{3.4 \times 10^{-26} n_0 c H_0^{-1} K_{e,0}}{\Gamma - 1} \\ &\quad \times \int_0^{z_{\max}} dz \, \frac{(1+z)^3 (1+z)^{\Gamma+2} [(1+z) E_{\gamma 0}]^{-\Gamma}}{(1+z)^4 (1+\Omega z)^{1/2}} \\ &= \frac{3.4 \times 10^{-3} \Omega}{\Gamma - 1} K_{e,0} E_{\gamma 0}^{-\Gamma} \int_0^{z_{\max}} dz \, \frac{(1+z)}{(1+\Omega z)^{1/2}} \\ &= \frac{6.8 \times 10^{-3}}{\Gamma - 1} K_{e,0} E_{\gamma 0}^{-\Gamma} \left[\left(1 + \frac{z}{3} - \frac{2}{3\Omega} \right) (1+\Omega z)^{1/2} \right. \\ &\quad \left. - \left(1 - \frac{2}{3\Omega} \right) \right] \end{aligned} \tag{12–16}$$

411-892 O - 71 - 14

In particular, for the Einstein-de Sitter universe where $\Omega = 1$,

$$I_b(E_{\gamma 0}, z_{\max}) = \tfrac{2}{3} I_{b,0}(E_{\gamma 0})[(1+z_{\max})^{3/2} - 1] \qquad (12\text{–}17)$$

and for the low-density model where $\Omega z \ll 1$,

$$I_b(E_{\gamma 0}, z_{\max}) = \tfrac{1}{2} I_{b,0}(E_{\gamma 0})[(1+z_{\max})^{2} - 1] \qquad (12\text{–}18)$$

Equations (12–16) through (12–18) are, of course, valid only in the energy range $E_\gamma < E_c$, with $E_c(\Omega, z)$ given by equation (12–10) corresponding to the energy range for electrons where they are undepleted by Compton interactions over a time scale corresponding to the age of the universe at a redshift z.

Stecker and Silk (1969), using a galactic cosmic-ray electron flux (Tanaka, 1968) given by

$$I_g = 1.26 \times 10^{-2} E_e^{-2.6} \qquad (\text{cm}^2\text{-s-sr-GeV})^{-1} \qquad (12\text{–}19)$$

have calculated the ratio I_0/I_g, where I_0 is the present flux of extragalactic electrons needed to produce the observed flux of isotropic γ-rays in the 0.1- to 1-MeV energy range under the assumption that these γ-rays are produced as the result of bremsstrahlung of extragalactic cosmic-ray electrons. They also calculated the fluxes of extragalactic protons needed to produce by π^0-decay the γ-ray flux above 100 MeV of 1.1×10^{-4} $(\text{cm}^2\text{-s-sr})^{-1}$ originally reported by Clark et al. (1968).

The resultant γ-ray spectra from bremsstrahlung and inelastic strong interactions were calculated for two cosmological models (viz, an Einstein-de Sitter (flat) universe with $n_0 = 10^{-5}$ cm^{-3} and an open universe with $n_0 = 10^{-7}$ cm^{-3}) and three models of cosmic-ray production (viz, a burst model where all the cosmic rays were produced at some initial epoch, a constant leakage model where cosmic rays have leaked out of radio sources at a constant rate since $t(z_{\max})$, and an evolving source model as suggested by Longair (1966) where the cosmic-ray production rate varies as $(1+z)^3$). These models have been discussed previously in chapter 10. The characteristics of the γ-ray spectra from these various processes are outlined in table 12–1. The values of I_0/I_g obtained for extragalactic cosmic-ray electrons and protons are shown in figures 12–1 and 12–2. They are plotted as functions of $(1+z_{\max})$, as needed to explain the observations.

The cosmic γ-ray (or X-ray) spectrum from nonrelativistic bremsstrahlung interactions of electrons has been calculated by Silk and McCray (1969). They calculated the bremsstrahlung spectrum of nonrelativistic electrons by using equation (8–26), taking into account the energy losses of the lower energy electrons by coulomb interactions in calculating the equilibrium spectrum of extragalactic electrons as a function of redshift. Their resultant electron spectrum is shown in figure 12–3. Figure 12–4 shows their calculated X-ray spectrum together with some of the recent observations of isotropic X-ray fluxes.

TABLE 12–1.—*Characteristics of Predicted Extragalactic γ-Ray Spectra From Various Processes in Given Energy Regions*

	< 0.5 MeV	1 to 100 MeV	> 100 MeV
Compton	Power-law spectrum of form $E^{-\Gamma}$ where $\Gamma = (\beta+1)/2$ and β is the index of the cosmic-ray electron spectrum. In particular, $\Gamma=2.3$ for $\beta = 3.6$ as discussed by Felten and Morrison (1966).	$\sim E^{-2.3}$	$\sim E^{-2.3}$
Bremsstrahlung	Power-law spectrum of form $E^{-\Gamma}$ where $\Gamma = \beta$ and $\beta \simeq 2.6$ in an open universe.	Power-law spectrum of form $E^{-\Gamma}$, where $\Gamma = \beta$ and $\beta \simeq 2.6$. (See text.)	$\sim E^{-3.6}$
Inelastic strong interactions	Negligible contribution; power law of form $\sim E^{+\Gamma}$ where $\Gamma \simeq 3$.	Spectrum peaks in this energy region at $\simeq 70\ \mathrm{MeV}(1+z_{max})^{-1}$.	$\sim E^{-3}$
Annihilation	Power-law production spectrum of form $E^{-\Gamma}$, where $\Gamma \simeq 2.68$ for flat universe and $\Gamma = 3.18$ for open universe. Absorption effects become important in this energy range. (See ch. 13.)	Power law of form $E^{-\Gamma}$, where $\Gamma \simeq 2.86$ for flat universe and $\Gamma \simeq 3.36$ for open universe.	Power law becomes steeply falling spectrum with no flux above 919 MeV.

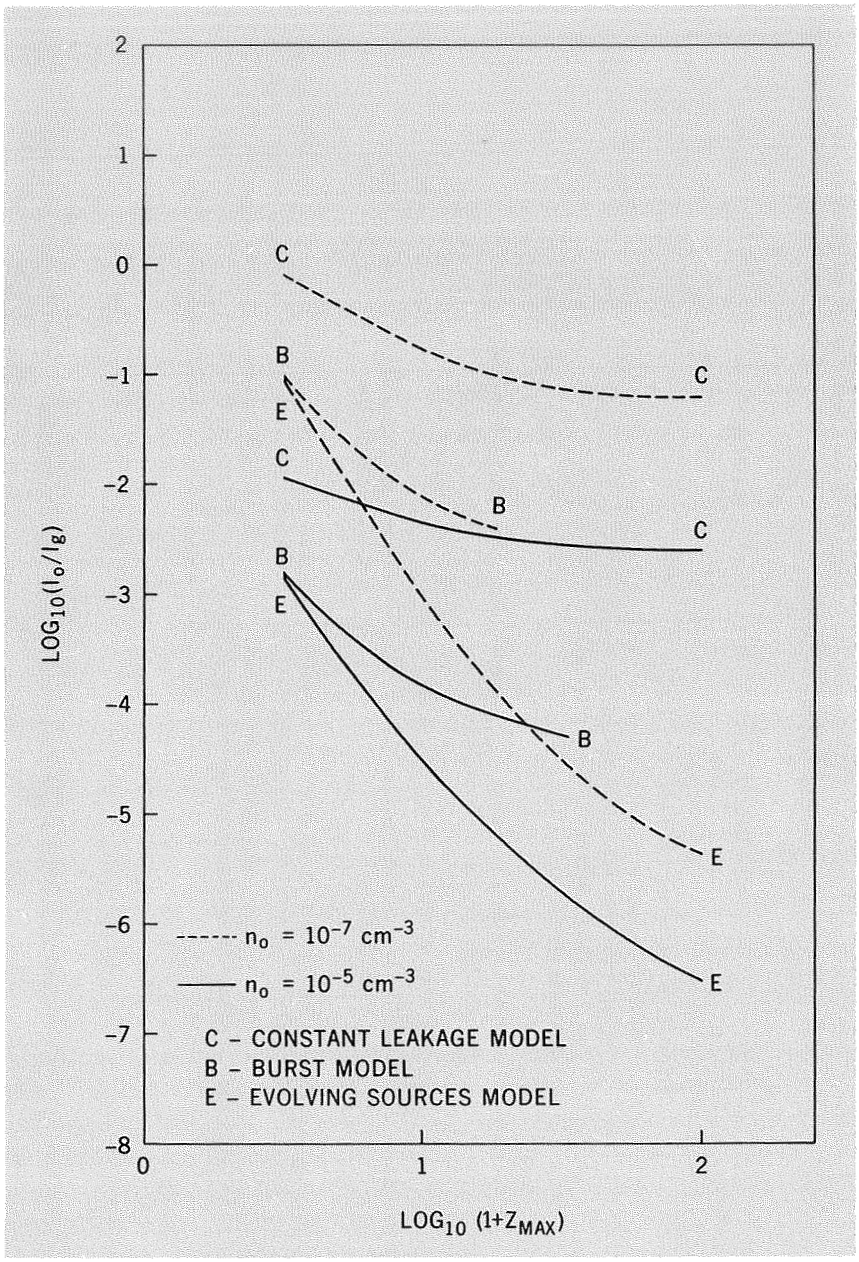

FIGURE 12–1.—Extragalactic electron intensities (Stecker and Silk, 1969).

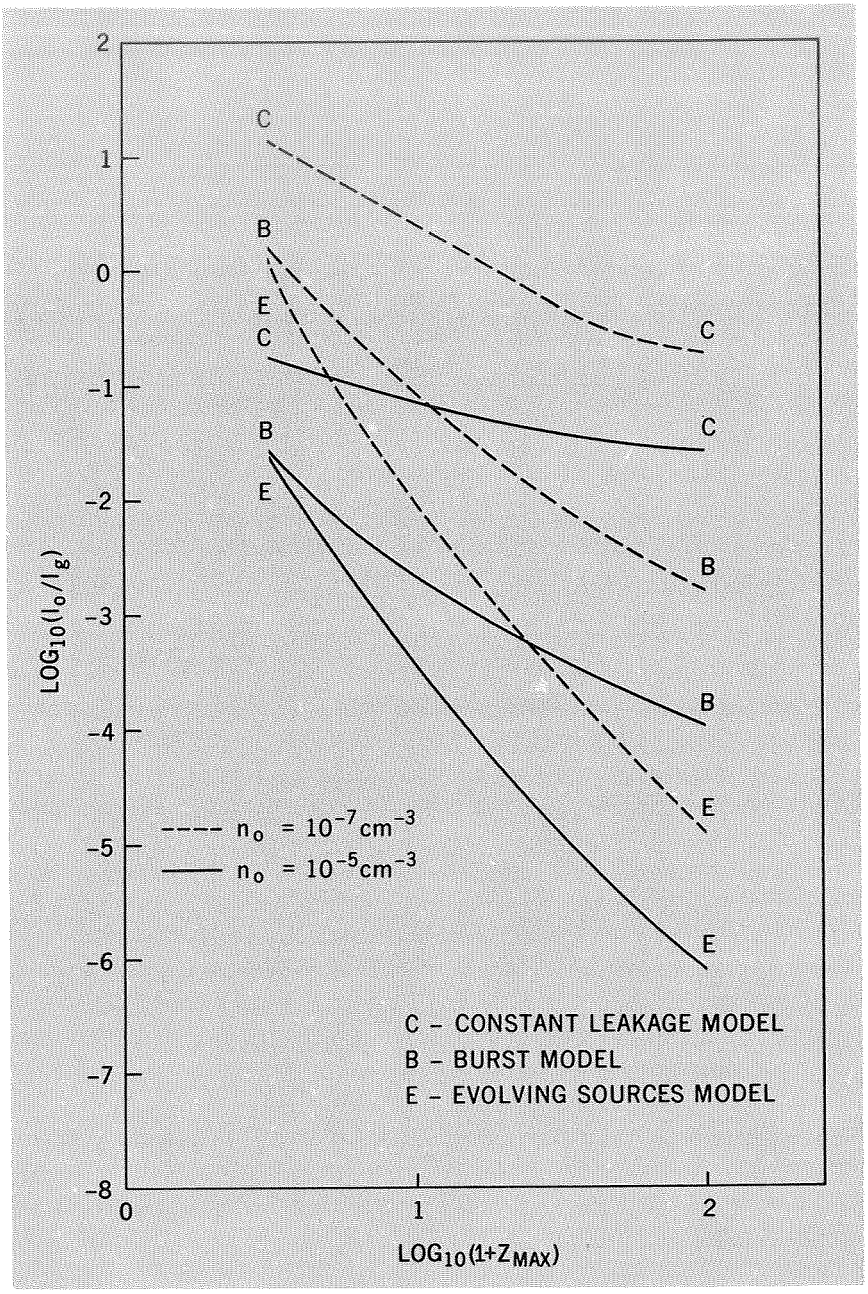

FIGURE 12–2.—Extragalactic proton intensities (Stecker and Silk, 1969).

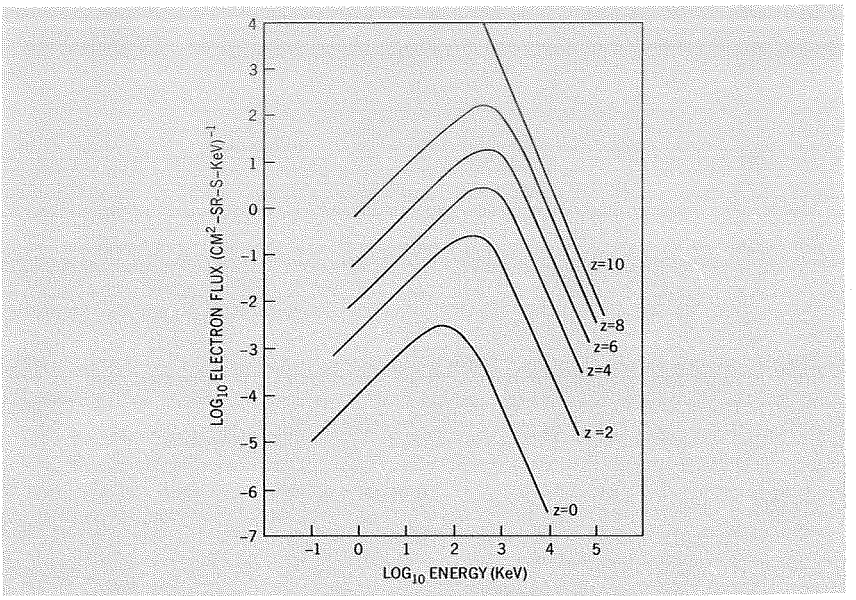

FIGURE 12–3.—Relaxation of a power-law cosmic-ray electron spectrum in an expanding universe with an ionized intergalactic medium ($n_0 = 10^{-7}$ cm^{-3}) (Silk and McCray, 1969).

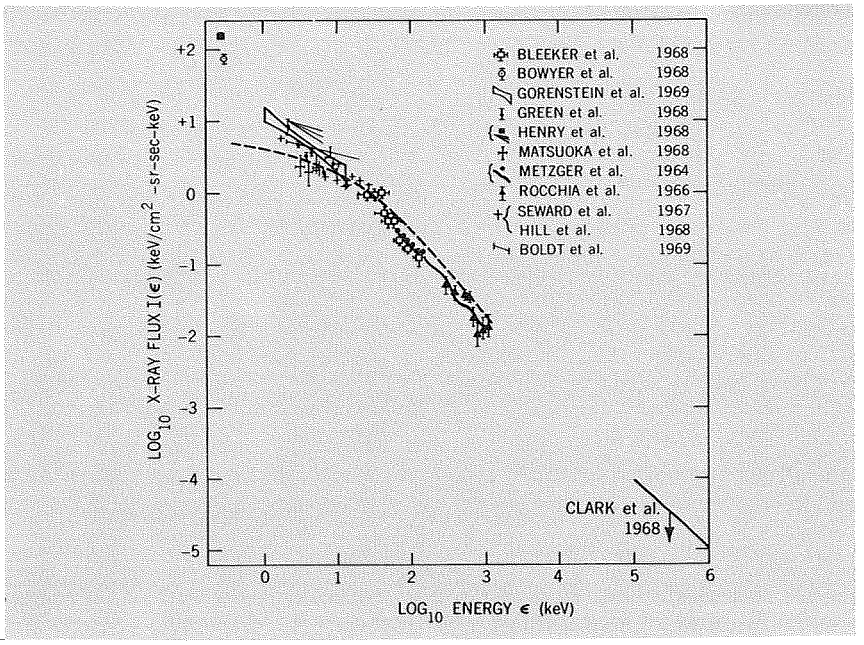

FIGURE 12–4.—Diffuse X-ray observations compared with calculated flux from burst model (dashed curve). The 0.25-keV point of Henry et al. (1968) has no correction for interstellar absorption (Silk and McCray, 1969).

Gamma-Ray Absorption Processes at High Redshifts

In chapter 4, we discussed in detail the processes which result in the absorption of cosmic γ-rays. In that chapter, we pointed out that there are three main absorption processes of importance under the conditions in interstellar and intergalactic space: Pair-production interactions of cosmic γ-rays with the universal blackbody radiation field, Compton interactions of cosmic γ-rays with electrons in the interstellar or intergalactic gas, and pair-production interactions of cosmic γ-rays with atoms of the interstellar or intergalactic gas. In this chapter, we will show how the effectiveness of these absorption processes is enhanced at high redshifts due to increased photon and matter densities at these redshifts when the universe was in a more compact state. We will also derive the energy dependences of these absorption processes, taking cosmological factors into account as discussed in chapter 9.

13-1 ABSORPTION BY PAIR-PRODUCTION WITH PHOTONS OF THE UNIVERSAL RADIATION FIELD

We begin our discussion by considering the absorption of cosmic γ-rays by pair-production interactions with photons of the universal blackbody radiation field. These interactions are primarily of the form

$$\gamma + \gamma \rightarrow e^+ + e^- \tag{13-1}$$

Detailed calculations of the γ-ray absorption coefficient $\kappa_{\gamma\gamma}(E_\gamma)$ for this process have been made by Gould and Schréder (1967a, b) and have been discussed in chapter 4. This absorption coefficient, which represents the probability per unit pathlength l that a γ-ray will be destroyed by the pair-production process (13-1) can be expressed for γ-rays interacting with a blackbody radiation field of temperature T as

$$\kappa_{\gamma\gamma}(E_\gamma) \simeq \frac{\alpha^2}{2\pi^{1/2}\Lambda}\left(\frac{kT}{mc^2}\right)^3 e^{-\nu}\nu^{1/2} \tag{13-2}$$

where

$$\nu \equiv \frac{(mc^2)^2}{kTE_\gamma} \gg 1 \tag{13-3}$$

$\alpha \simeq 1/137$ being the fine structure constant ($e^2/\hbar c$), $\Lambda = \hbar/mc = 3.86\times10^{-11}$ cm, and k being the Boltzmann constant.

In the other extreme,

$$\kappa_{\gamma\gamma}(E_\gamma) \simeq \frac{\pi\alpha^2}{3\Lambda}\left(\frac{kT}{mc^2}\right)^3 \nu \ln\left(\frac{0.117}{\nu}\right) \qquad \nu \ll 1 \tag{13-4}$$

For cosmological applications, we must take into account the redshift dependences of T and E_γ in an expanding universe,

$$T = T_0(1+z)$$

and (13-5)

$$E_\gamma = E_{\gamma 0}(1+z)$$

where the subscript zero refers to presently observed ($z=0$) quantities, so that $T_0 = 2.7$ K.

Taking the z-dependences into account, we then find that equation (13-2) is applicable in the energy range

$$E_\gamma \ll \frac{1.12\times10^6 \text{ GeV}}{(1+z)^2} \tag{13-6}$$

The optical depth of the universe to γ-rays is then given by

$$\tau(E_\gamma, z_{\max}) = \int_0^{l_{\max}(z_{\max})} dl\ \kappa_{\gamma\gamma}(E_\gamma, z)$$

$$= \int^{z_{\max}} dz\ \kappa_{\gamma\gamma}(E_\gamma, z)\left(\frac{dl}{dz}\right) \tag{13-7}$$

where, from equations (9-41) and (9-42),

$$\frac{dl}{dz} = \frac{10^{28} \text{ cm}}{(1+z)^2(1+10^5 n_0 z)} \tag{13-8}$$

n_0 being the present mean atomic density of all the matter in the universe. We will consider here two types of model universes: a "flat" or Einstein-de Sitter model with $n_0 = 10^{-5}$ cm^3 and an "open" model with $n_0 \ll 10^{-5} z$.

For the flat model, equation (13–7) reduces to

$$\tau(E_{\gamma 0}, z_{\max}) = 3.9 \times 10^8 E_{\gamma 0}^{-1/2} \int_0^{z_{\max}} dz \exp\left[\frac{-1.12 \times 10^6}{(1+z)^2 E_{\gamma 0}}\right] (1+z)^{-1/2} \tag{13–9}$$

with $E_{\gamma 0}$ in GeV.

For $z_{\max} \gg 1$, equation (13–9) can be further simplified to yield

$$\tau(E_{\gamma 0}, z_{\max}) \simeq 1.7 \times 10^2 E_{\gamma 0}^{1/2} (1+z_{\max})^{1/2} \exp\left[\frac{-1.12 \times 10^6}{(1+z_{\max})^2 E_{\gamma 0}}\right] \tag{13–10}$$

A numerical solution found by setting equation (13–7) for $\tau(E_{\gamma 0}, z_{\text{crit}}) = 1$, which defines the critical redshift where the universe becomes opaque to γ-rays of energy $E_{\gamma 0}$, can be well approximated by the expression

$$1 + z_{\text{crit}} \simeq 2.60 \times 10^2 E_{\gamma 0}^{-0.484} \tag{13–11}$$

For the open model, we find

$$\tau(E_{\gamma 0}, z_{\max}) = 3.9 \times 10^8 E_{\gamma 0}^{-1/2} \int_0^{z_{\max}} dz \exp\left[-\frac{1.12 \times 10^6}{(1+z)^2 E_{\gamma 0}}\right] \tag{13–12}$$

For $z_{\max} \gg 1$, equation (13–12) may be approximated by

$$\tau(E_{\gamma 0}, z_{\max}) \simeq 1.7 \times 10^2 E_{\gamma 0}^{1/2} (1+z_{\max}) \exp\left[-\frac{1.12 \times 10^6}{(1+z_{\max})^2 E_{\gamma 0}}\right] \tag{13–13}$$

Thus, there is no significant difference between the opacities of the open and flat model universes. This being the case, we may invert equation (13–11) to obtain an expression for the predicted cutoff energy E_c above which γ-rays originating at a redshift $z_{\max}$ cannot reach us. This relation is then given by

$$E_c \simeq \left(\frac{2.60 \times 10^2}{1+z_{\max}}\right)^{2.06} \tag{13–14}$$

and is graphed in figure 13–1.

In the other extreme, $\nu \ll 1$, we find that as we consider higher and higher energies, the universe will not become transparent to γ-rays again until we reach an energy E_{tr}, where the optical depth $\tau(E_{\text{tr}}, z_{\max})$ again falls to unity. The expression for the optical depth when $\nu \ll 1$ is given

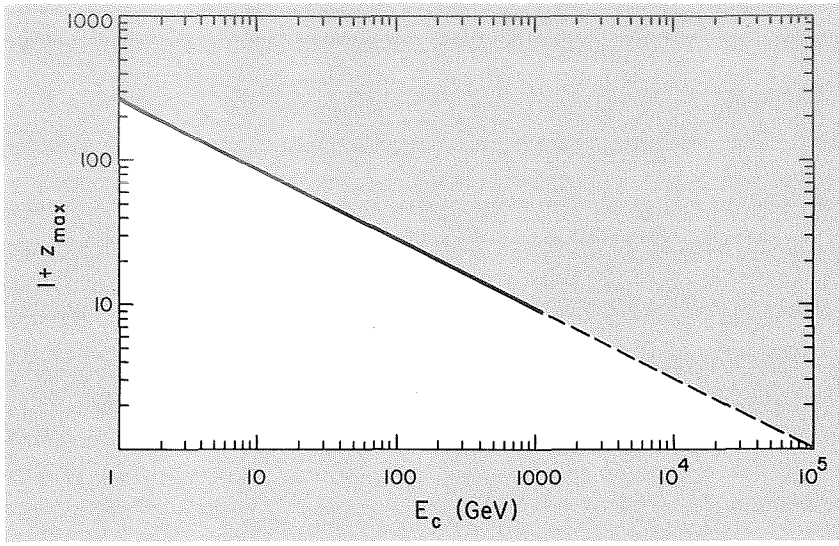

FIGURE 13–1.—Cutoff energy versus redshift for cosmological γ-rays (Fazio and Stecker, 1970)

for a flat universe by

$$\tau(E_{\gamma 0}, z_{\max}) \simeq 4.4\times 10^{13} E_{\gamma 0}^{-1} \int_0^{z_{\max}} dz(1+z)^{-3/2}$$
$$\simeq 8.8\times 10^{13} E_{\gamma 0}^{-1} \qquad (z_{\max} \gg 1) \qquad (13\text{–}15)$$

and for an open universe by

$$\tau(E_{\gamma 0}, z_{\max}) \simeq 4.4\times 10^{13} E_{\gamma 0}^{-1} \int_0^{z_{\max}} dz(1+z)^{-1} \simeq 4.4\times 10^{13} E_{\gamma 0}^{-1} \ln(1+z_{\max}) \qquad (13\text{–}16)$$

In both cases we find that $E_{\rm tr} > 10^{13}$ GeV so that we may safely assume that the universe, due to the blackbody radiation field, is essentially opaque to γ-rays of all energies greater than E_c.

13–2 GAMMA-RAY ABSORPTION BY PAIR-PRODUCTION AND COMPTON INTERACTIONS WITH INTERGALACTIC GAS

Gamma-ray absorption by pair-production and Compton interactions with intergalactic gas at high redshifts has been examined by Rees (1969a, b) and by Arons and McCray (1969). Our discussion here essentially follows theirs. The absorption cross section for Compton interac-

tions is given in equations (4–19) and (4–20); that for pair-production, in equation (4–23). These absorption processes are discussed in chapter 4, and the cross sections are graphed in figure 4–2. The total absorption cross section above 100-MeV energy is roughly constant and equals 1.8×10^{-26} cm^2. For the case of a constant absorption cross section, the optical depth as a function of redshift $z_{\max}$ is given by equations (13–7) and (13–8) as

$$\tau(z_{\max}) = \int_0^{z_{\max}} dz\, n(z)\sigma \left(\frac{dl}{dz}\right)$$

$$= n_0 \sigma c H_0^{-1} \int_0^{z_{\max}} \frac{(1+z)}{(1+\Omega z)^{1/2}}$$

$$= \frac{2}{3}\tau_c \Omega \left[\left(3+z-\frac{2}{\Omega}\right)(1+\Omega z)^{1/2} - \left(3-\frac{2}{\Omega}\right) \right] \qquad (13\text{–}17)$$

where

$$\tau_c \equiv n_c \sigma c H_0^{-1} = 1.8 \times 10^{-3} \qquad (13\text{–}18)$$

a result which was first obtained by Gunn and Peterson (1965).

For an Einstein-de Sitter universe ($\Omega = 1$)

$$\tau(z_{\max}) = \frac{2}{3}\tau_c [(1+z_{\max})^{3/2} - 1] \qquad (13\text{–}19)$$

and for a low-density universe ($\Omega z \ll 1$)

$$\tau(z_{\max}) = \frac{\Omega}{2}\tau_c [(1+z_{\max})^2 - 1] \qquad (13\text{–}20)$$

Possible Interpretation of Isotropic Gamma-Ray Observations

By comparing the theoretical calculations of isotropic γ-ray spectra from intergalactic secondary particle production (ch. 10), matter-antimatter annihilation (ch. 11), bremsstrahlung, and Compton interactions (ch. 12), we find that extragalactic bremsstrahlung and Compton interactions may be possible alternative explanations of the observed isotropic X-ray spectrum below 1 MeV. Both processes produce power-law X-ray spectra with exponents in the range from 2.4 to 2.6 from interactions involving cosmic-ray electrons having spectra similar to that of galactic electrons. However, as we showed in chapter 12, the bremsstrahlung X-rays are produced by electrons in the energy range where they are unattenuated by Compton interactions, whereas the Compton-produced X-rays result from interactions of higher energy electrons with a steeper energy spectrum, which have been attenuated by Compton interactions. Thus, as we showed in chapter 12, we can get cosmological enhancement of the bremsstrahlung X-ray spectrum at high redshifts, but such is not the case with Compton-produced X-rays.

The recent observations of Vette et al. (1969, 1970) have now provided measurements of background γ-rays with energies up to 6 MeV. (See appendix.) These data, providing the first measurements in this energy range, have already yielded valuable information. Their preliminary results are shown in figure 14–1. These measurements are consistent with the well-known power-law X-ray spectrum below 1 MeV. However, they indicate a marked departure from the power law above 1 MeV. For example, the 6-MeV point is an order of magnitude higher than what would be expected on the basis of a power-law extrapolation of the X-ray data. Also included in the figure are an upper limit set by a balloon flight of the University of Rochester group and updated by a recent recalibration and an upper limit at 10 MeV set by a balloon flight of the Naval Research Laboratory Nucleonics Division (Share, 1970). The OSO–3 point shown in the figure is based on the recent recalibration of Clark et al. (1970). The solid $p-p$ line for $z_{max}=100$ is the same as that

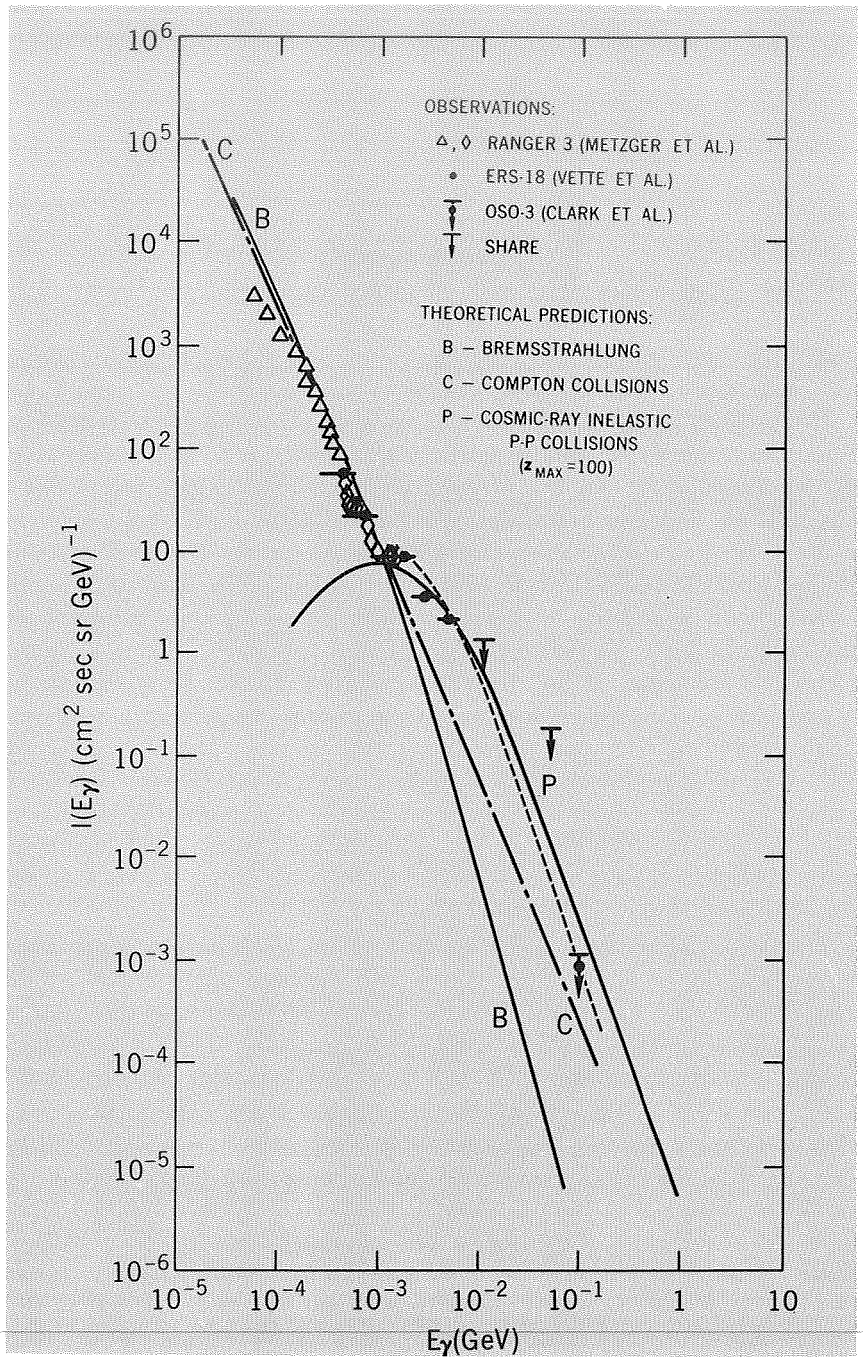

FIGURE 14–1.—Extragalactic high-energy photon spectra.

calculated in chapter 10 (Stecker, 1969c) for collisions involving cosmic rays with a power-law spectrum of exponent -2.5. The dashed line indicates the γ-ray spectrum generated by cosmic rays with a power-law spectrum of exponent -2.7. The data above 1 MeV, with the data of Clark et al. being interpreted as a real flux, fit the shape of the theoretical γ-ray spectrum from cosmic-ray p–p interactions integrated to a maximum redshift of ~ 100 for a burst or evolving source model where cosmic-ray production was higher in the past. They do not seem consistent with other theoretical spectra for energies above 1 MeV. Vette et al. (1970) have interpreted their results to indicate a new component of the cosmic γ-ray spectrum above 1 MeV which they find to be consistent with the theoretical interpretation presented here. In addition, Clark et al. (1969) have reported qualitative results indicating that the isotropic component of cosmic γ-radiation above 100 MeV has a softer spectrum than the galactic component. This result is also in agreement with the theoretical predictions presented previously.

These suggestive results make it even more imperative to obtain other γ-ray observations in the 1- to 100-MeV region in order to confirm the present data and to extend the range of the measurements. However, on the basis of these first results, we can present the following interpretation.

Comparison of the predicted spectra with the γ-ray observations indicates that extragalactic γ-radiation may be due to the decay of neutral pions produced in inelastic collisions of extragalactic cosmic-ray protons and gas. The peak in the resultant γ-ray spectrum, which normally occurs at ~ 70 MeV, is redshifted down to $\sim$ 1-MeV energy. This effect is due to the increased collision rate at larger redshifts, when our expanding universe was in a more compact state, as well as to increased cosmic-ray production at large redshifts. A cosmic-ray production rate which is constant over all redshifts will not account for the new observations. The assumption of various time-dependence models for cosmic-ray production leads to differing requirements for the present metagalactic cosmic-ray flux needed to produce the observed γ-rays. (See fig. 12–3.) The maximum redshift needed to fit the observations is ~ 100, which corresponds to an epoch when the age of the universe was 10^7 to 10^8 years and the temperature of the universal radiation field was ~ 270 K. This may correspond to the epoch when objects of galactic mass were beginning to form from the metagalactic medium (Weymann, 1967). There is mounting evidence that radio sources were more active (or prevalent) at earlier epochs (Longair, 1966; Rowan-Robinson, 1968; Schmidt, 1968) and it is plausible to speculate that in these sources, where electrons are accelerated to cosmic-ray energies, protons may also

be accelerated to these energies.[1] Whereas electrons have short lifetimes at high redshifts due to Compton interactions with the universal radiation field, possibly restricting their radio-emission stage to redshifts of ~ 10 or less, the protons do not undergo significant depletion from Compton interactions. Thus, the sources producing γ-rays at redshifts of ~ 100 will not be visible as radio sources. They may also be unobservable in the optical (Gunn and Peterson, 1965) and X-ray regions (Rees, 1969, and Arons and McCray, 1969), since a dense intergalactic medium becomes opaque to X-rays at redshifts < 10. Thus our best chance of studying these sources comes from γ-ray observations; and their study should be of prime importance to the young field of γ-ray astronomy.

I will henceforth refer to these primordial cosmic-ray sources as "protars." It seems reasonable to speculate that protars may be early stages in the evolution of quasars and galaxies; i.e., of objects of high mass that are in the initial stages of condensing out of the metagalactic medium. The subsequent release of gravitational energy coupled with the generation of strong magnetic fields during the contraction could then provide energy for the acceleration of cosmic rays.

Although most theoretical arguments favor a present intergalactic gas density of 10^{-7} to 10^{-5} cm^{-3}, studies of the spectra of quasars having redshifts of ~ 2 have indicated a neutral hydrogen density $\lesssim 10^{-11}$ cm^{-3} (Burbidge and Burbidge, 1967). This fact argues for a strongly ionized intergalactic medium. In addition, soft X-ray observations by Henry et al. (1968) have produced evidence of a hot intergalactic plasma with a density of 10^{-6} to 10^{-5} cm^{-3}. Recent comparisons of radio observations with theoretical models of free-free emission spectra from ionized intergalactic gas (Payne, 1969) have indicated that the intergalactic medium could have become ionized at some redshift $\lesssim 100$. Cosmic rays from protars would provide a natural source for heating the intergalactic medium at this epoch. It can be shown (Weymann, 1967) that once the ionization occurs, the medium would then remain ionized due to subsequent cosmic-ray heating up to the present epoch. Rees (1969b) has recently argued for an intergalactic gas remaining neutral at redshifts between ~ 2 and ~ 1000.

Cosmic rays from protars that have energies of ~ 300 MeV (the threshold for neutral pion production) at a redshift of ~ 100 would have their energy reduced to ~ 100 keV at a redshift of ~ 2 and would be about 50 times more effective in heating the intergalactic gas. Therefore, cosmic rays from protars existing out to redshifts of ~ 100 could cause a delayed ionization of the intergalactic medium effective at much lower redshifts.

---

[1] Other possible implications have been suggested by the author (Stecker, 1971).

It should be pointed out that the redshifts of ~ 100 proposed here for the protars may indicate that they are near the limit of observability for γ-ray observations. Rees (1969a) and Arons and McCray (1969) have independently considered the absorption of γ-rays by intergalactic gas due to Compton interactions and pair production. In an Einstein-de Sitter universe with a gas density of 10^{-5} cm^{-3}, the γ-ray absorption coefficient varies as the 3/2 power of redshift. For a high-density universe and a redshift of $z=100$, we find from equation (13–17) that the optical depth is ~ 1.2 for γ-rays with present energies between 1 and 100 MeV.

Thus, for a high-density universe, the γ-rays reaching us may be partially depleted by absorption effects. Of course, for models with $n_0 < 10^{-5}$ cm^{-3}, absorption effects are negligible at $z=100$.

It has been shown in chapter 13 that the γ-ray opacity due to interactions with the universal blackbody radiation for $z \lesssim 100$ is negligible for $E \leqslant E_c = 7.1$ GeV. However, above this energy absorption effects become important and steepen the resultant γ-ray spectrum. The spectrum above 7.1 GeV, instead of being an integral over the range $0 \leqslant z \leqslant 100$, becomes an integral over the range $0 \leqslant z \leqslant z_{\text{crit}}$, with z_{crit} given by equation (13–11).

Thus, for $z_{\max} \gg 1$, assuming that $z_{\text{crit}} = 260\, E_\gamma^{-1/2}$, considering a burst model for cosmic-ray protons (see ch. 10), and taking $G(E_\gamma) \sim E_\gamma^{-3}$ above 10 GeV, we find from equation (9–22)

$$I(E_\gamma) \sim E_\gamma^{-3} \int_0^{260E_\gamma^{1/2}} dz(1+z)^m \sim E_\gamma^{-\left(3+\frac{m+1}{2}\right)} \qquad (14\text{–}1)$$

where $m=0$ in the case of an Einstein-de Sitter universe and $m=\frac{1}{2}$ in the case of a low-density universe. Thus, for an Einstein-de Sitter model, the exponent in the cosmological γ-ray spectrum should increase by a factor of $\Delta\Gamma_\gamma \simeq \frac{1}{2}$, and for a low-density universe the increase is $\Delta\Gamma_\gamma \simeq \frac{3}{4}$.

It should also be noted that in a high-density model at redshifts of the order of 100, cosmic-ray attenuation by nuclear collisions will also become important. (See ch. 10.) Thus, we must increase somewhat the cosmic-ray production requirements for the high-density model. However, for present densities less than 0.5×10^{-5} cm^{-3}, attenuation is negligible.

Taking absorption effects into account, and considering models where the present gas density is 10^{-7} to 10^5 cm^{-3}, we can conclude that if the protar hypothesis is correct, protars have filled intergalactic space with remnant cosmic rays having a present density of 10^{-5} to 10^{-3} the galactic value; i.e., 10^{-17} to 10^{-15} erg/cm^3.

411-892 O - 71 - 15

References

Alfvén, H. 1965. *Rev. Mod. Phys., 37,* 652.

Allen, C. W. 1963. *Astrophysical Quantities.* 2d ed. London: Athlone Press.

Anand, K. C., Daniel, R. R., and Stephens, S. A. 1968. *Proc. Indian Acad. Sci., 68,* 219.

Anand, K. C., Daniel, R. R., and Stephens, S. A. 1969. *Nature, 224,* 1290.

Anderson, E. C. See Metzger et al., 1964.

Anderson, E. W., Blesser, E. J., Collins, G. B., Fujii, T., Menes, J., Turkot, F., Carrigan, R. A., Edelstein, R. M., Hien, N. C., McMahon, T. J., and Nadelhaft, I. 1966. *Brookhaven National Laboratories Rpt. No. 10136.*

Arons, J., and McCray, R. 1969. *Astrophys. J. Lett., 158,* L91.

Arnold, J. R. See Metzger et al., 1964.

Astbury, A. See Blair et al., 1966.

Audouze, J., Epherre, M., and Reeves, H. 1967. *High Energy Nuclear Interactions in Astrophysics* (B. S. P. Shen, ed.). New York: Benjamin.

Bachman, A. H. See Baltay et al., 1964.

Balasubrahmanyan, V. K. E., Boldt, E., Palmiera, R. A. R., and Sandri, G. 1968. *Can. J. Phys., 46,* S633.

Baltay, C., Ferbel, T., Sandweiss, J., Taft, H. D., Culwick, B. B., Fowler, W. B., Gailloud, M., Kopp, J. K., Louttit, R. I., Morris, T. W., Sanford, J. R., Schutt, R., Stonehill, D. L., Stump, R., Thorndike, A. M., Webster, M. S., Willis, W. J., Bachman, A. H., Baumel, P., and Lea, R. M. 1964. *Proc. Int. Conf. on Nuclear Structure.* Stanford: Stanford University Press. 267–287.

Baradzei, L. T., Rubtzov, V. I., Smorodin, Y. A., Solovyev, M. V., and Tolkachev, B. V. 1962. *J. Phys. Soc. Japan, 17,* Suppl. A–III, 433.

Barbaro-Galtieri, A. See Rosenfeld et al., 1965.

Barkas, W. H. See Rosenfeld et al., 1965.

Bartke, J., Cooper, W. A., Czapp, B., Filthuth, H., Goldschmidt-Clermont, Y., Montanent, L., Morrison, D. R. O., Nilsson, L., Peyron, C. H., and Sosnowski, R. 1963. *Nuovo Cimento, 29,* 8.

Bartolot, V. J., Clauser, S. F., and Thaddeus, P. 1969. *Phys. Lett., 22,* 307.

Bastien, P. L. See Rosenfeld et al., 1965.

Batson, A. P., Culwick, B. B., Klepp, H. B., and Riddiford, L. 1959. *Proc. Roy. Soc., A251,* 233.

Baumel, P. See Baltay et al., 1964.

Becklin, E. E., and Neugebauer, G. 1968. *Astrophys. J., 151,* 145.

Bertolini, E. See Focardi et al., 1965.

Blair, I. M., Taylor, A. E., Chapman, W. S., Kalmus, P. I. P., Litt, J., Miller, M. C., Scott, D. B., Sherman, H. J., Astbury, A., and Walker, T. G. 1966. *Phys. Rev. Lett., 17,* 789.

Bleeker, J. A. M., and Deerenberg, A. J. M. 1970. *Nature,* 227, 470.

Blesser, E. J. See Anderson et al., 1966.
Böckmann, K., Nellen, B., Paul, E., Wigini, B., Borecka, I., Diaz, J., Heeren, V., Liebermeister, V., Lohrmann, E., Raubold, E., Söding, P., Wolff, S., Kidd, J., Mandelli, L., Mosca, L., Pelosi, V., Ratti, S., and Tallone, L. 1966. *Nuovo Cimento, 42A*, 954.
Boldt, E. See Balasubrahmanyan et al., 1968.
Boldt, E., and Serlemitsos, P. 1969. *Astrophys. J., 157*, 557.
Borecka, I. See Bockmann et al., 1966.
Bradt, H., Clark, G., LaPointe, M., Domingo, V., Escobar, I., Kamata, K., Murakumi, K., Suga, K., and Toyoda, Y. 1965. *Proc. Int. Conf. Cosmic Rays*, London 2, 715.
Brecher, K., and Morrison, P. 1967. *Astrophys. J. Lett., 150*, L61.
Burbidge, E. M. See Burbidge and Burbidge, 1967.
Burbidge, G., and Burbidge, E. M. 1967. *Quasi Stellar Objects*. San Francisco: W. H. Freeman & Co., 46.
Burbidge, G. R. See Gould and Burbidge, 1965, 1967.
Button, J., Eberhard, P., Kalbfleisch, G. R., Lannutti, J., Lynch, G. R., Maglić, B. C., Stevenson, M. L., and Xuong, N. H. 1961. *Phys. Rev., 121*, 1788.
Byram, E. T. See Henry et al., 1968.
Cameron, A. G. W. 1959. *Astrophys. J., 129*, 676.
Caroll, T. D., and Salpeter, E. E. 1966. *Astrophys. J., 143*, 609.
Carrigan, R. A. See Anderson et al., 1966.
Carruthers, G. R. 1968. *Astrophys. J., 151*, 269.
Carruthers, G. R. 1970. *Astrophys. J. Lett., 161*, L81.
CERN, HBC, and IEP groups. 1961. *Int. Conf. Elementary Particles*, Aix-en-Provence. *1*, 93.
Chapman, W. S. See Blair et al., 1966.
Cheng, C. C. 1967. *Nature, 215*, 1035.
Cheshire, I. M. 1964. *Proc. Phys. Soc., 83*, 227.
Cheung, A. C. See Evans et al., 1970.
Chinowsky, W. 1966. Private communication.
Clark, G. W. See Bradt et al., 1965.
Clark, G. W., Garmire, G. P., and Kraushaar, W. L. 1968. *Astrophys. J. Lett., 153*, L203.
Clark, G. W., Garmire, G. P., and Kraushaar, W. L. 1969. Proc. I.A.U. Symp. No. 37, Rome (L. Gratton, ed.), 269, Reidel Pub. Co., Dordrecht, Holland.
Clark, G. W., Garmire, G. P., and Kraushaar, W. L. 1970. Private communication.
Clauser, S. F. See Bartolot et al., 1969.
——— See Thaddeus and Glauser, 1966.
Cline, T. L., and Hones, E. W. 1968. *Can. J. Phys., 46*, S527.
Collins, G. B. See Anderson et al., 1966.
Connolley, P. L., Ellis, W. E., Hongh, P. V. C., Miller, D. J., Morris, T. W., Onannes, C., Panvini, R. S., and Thorndike, A. M. 1967. BNL internal report 11980.
Cooper, W. A. See Bartke et al., 1963.
Cork, B., Dahl, O. I., Miller, D. H., Tenner, A. G., and Wang, C. L. 1962. *Nuovo Cimento, 25*, 497.
Cowsik, R., and Pal, Y. 1969. *Phys. Rev. Lett., 22*, 550.
Culwick, B. B. See Baltay et al., 1964.
——— See Batson et al., 1959.
Czapp, B. See Bartke et al., 1963.
Dahl, O. I. See Cork et al., 1962.
Dalitz, R. H. 1953. *Phil. Mag., 44*, 1068.
Daniel, R. R. See Anand et al., 1968, 1969.
Daniel, R. R., Durgaprasad, N., Malhotra, P. K., and Vijayalakshmi, B. 1963a. *Nuovo Cimento*, Suppl. 1, 1169.

Daniel, R. R., Lavakare, P. J., Menon, M. G. K., Naranan, S., Nerurkar, N. W., Pal, Y., and Sreekantan, B. V. 1963b. *Proc. Int. Conf. Cosmic Rays*, Jaipur, *5*, 595.
Dekkers, D., Geibel, J. A., Mermod, R., Weber, G., Willitts, T. R., Winter, K., Jordan, B., Vivargent, M., King, N. M., and Wilson, E. J. N. 1965. *Phys. Rev.*, *137B*, 962.
Derrick, M. See Loken and Derrick, 1963.
Deutsch, M., 1953. *Prog. in Nuc. Phys.*, *3*, 131.
Diaz, J. See Böckmann et al., 1966.
Dicke, R. H., Peebles, P. J. E., Roll, P. G., and Wilkinson, D. T. 1965. *Astrophys. J.*, *142*, 414.
Dilworth, C., Maraschi, L., and Perola, G. C. 1968. *Nuovo Cimento*, *56B*, 334.
Dirac, P. A. M. 1930. *Proc. Cambridge Phil. Soc.*, *26*, 361.
Dobrotin, N. See Guseva et al., 1962.
Domingo, V. See Bradt et al., 1965.
Donahue, T. M. 1951. *Phys. Rev.*, *84*, 972.
Donn, B., Wickramasinghe, N. C., Hudson, J. P., and Stecher, T. P. 1968. *Astrophys. J.*, *153*, 451.
Doroshkevich, A. G., Zeldovich, Y. B., and Novikov, I. D. 1967. *Sov. Astr. AJ.*, *11*, 233.
Dorschner, J. von, Gürtler, J., and Schmidt, K. H. 1965. *Astronomische Nachrichten*, *288*, 149.
Dovzhenko, O. I., and Pomanskii, A. A. 1964. *Sov. Phys. JETP*, *18*, 187.
Durgaprasad, N. See Daniel et al., 1963a.
Durgaprasad, N., Fichtel, C. E., Guss, D. E., and Reames, D. V. 1968. *Astrophys. J.*, *154*, 307.
Eberhard, P. See Button et al., 1961.
Edelstein, R. M. See Anderson et al., 1966.
Ellis, W. E. See Connolley et al., 1967.
Ellis, W. E., Miller, D. J., Morris, T. W., Panvini, R. S., and Thorndike, A. M. 1968. *Phys. Rev. Lett.*, *21*, 697.
Encrenaz, P., and Partridge, R. S. 1969. *Astrophys. Lett.*, *3*, 161.
Epherre, M. See Audonze et al., 1967.
Escobar, I. See Bradt et al., 1965.
Evans, N. J., Cheung, A. C., and Sloanaker, R. M. 1970. *Astrophys. J. Lett.*, *159*, L9.
Fabri, E. 1954. *Nuovo Cimento*, *11*, 479.
Fan, C. Y., Gloeckler, G., McKibben, B., Pyle, K. R., and Simpson, J. A. 1968. *Can. J. Phys.*, *46*, S498.
Fazio, G. G. See Stecker et al., 1968.
——— See Pollack and Fazio, 1963, 1965.
Fazio, G. G., Stecker, F. W., and Wright, J. P. 1966. *Astrophys. J.*, *144*, 611.
Fazio, G. G., and Stecker, F. W. 1970. *Nature*, *226*, 135.
Feenberg, E., and Primikoff, H. 1948. *Phys. Rev.*, *73*, 449.
Feldman, P. D. See McNutt and Feldman, 1970.
Felten, J. E. 1965. *Phys. Rev. Lett.*, *15*, 1003.
Felten, J. E. 1966. *Astrophys. J.*, *144*, 241.
Felten, J. E., and Morrison, P. 1963. *Phys. Rev. Lett.*, *10*, 453.
Felten, J. E., and Morrison, P. 1966. *Astrophys. J.*, *146*, 686.
Ferbel, T. See Baltay et al., 1964.
Ferbel, T., Firestone, A., Johnson, J., Sandweiss, J., and Taft, H. D. 1965. *Nuovo Cimento*, *38*, 12.
Ferbel, T., Sandweiss, J., Taft, H. D., Gailloud, M., Kalogeropoulos, T. E., Morris, T. W., and Lea, R. M. 1962. *Phys. Rev. Lett.*, *9*, 351.
Fermi, E. 1934. *Z. Phys.*, *88*, 161.
Fermi, E. 1951. *Phys. Rev.*, *81*, 683.

Fichtel, C. E. See Durgaprasad et al., 1968.
Fichtel, C. E., Kniffen, D. A., and Ögelman, H. B. 1969. *Astrophys. J., 158*, 193.
Fichtel, C. E. See Kniffen and Fichtel, 1970.
Fidecaro, M., Finocchiaro, G., Gratti, G., Giacomelli, G., Middelkoop, W. C., and Yamagata, T. 1962. *Nuovo Cimento, 24*, 73.
Filippov, A. I. See Kozodaev et al., 1960.
Filthuth, H. See Bartke et al., 1963.
Finocchiaro, G. See Fidecaro et al., 1962.
Firestone, A. See Ferbel et al., 1965.
Focardi, S., Saporetti, F., Bertolini, E., Grigoletto, A., Peruzzo, L., Santangelo, R., and Gialanella, G. 1965. *Nuovo Cimento, 39*, 405.
Fowler, P. H., and Perkins, D. H. 1964. *Proc. Roy. Soc., 278A*, 401.
Fowler, W. B. See Baltay et al., 1964.
Frederick, C. L. See Hoffman and Frederick, 1969.
Friedman, H. See Henry et al., 1968.
Frier, P. S. See Valdez et al., 1969.
Fritz, G. See Henry et al., 1968.
Frye, G. M., and Smith, L. H. 1966. *Phys. Rev. Lett., 17*, 733.
Frye, G. M., Staib, J. A., Zych, A. D., Hopper, V. D., Rawlinson, W. R., and Thomas, J. A. 1969. *Nature, 223*, 1320.
Fujii, T. See Anderson et al., 1966.
Fujimoto, Y., and Hayakawa, S. 1967. *Handbuch der Physik, 46–2*, 115. Berlin: Springer-Verlag.
Gailloud, M. See Baltay et al., 1964.
——— See Ferbel et al., 1962.
Garmire, G. P. See Clark et al., 1968, 1969, 1970.
Garmire, G. P., and Kraushaar, W. L. 1965. *Space Sci. Rev., 4*, 123.
Garzoli, S. L., and Varsavsky, C. 1966. *Astrophys. J., 145*, 79.
Geibel, J. A. See Dekkers et al., 1965.
Giacomelli, G. See Fidecaro et al., 1962.
Gialanella, G. See Focardi et al., 1965.
Ginzburg, V. L., and Syrovatskii, S. I. 1964. *Origin of Cosmic Rays*. New York: Macmillan.
Ginzburg, V. L., and Syrovatskii, S. I. 1965. *Sov. Phys. Usp., 7*, 696.
Gloeckler, G. See Fan et al., 1968.
Gloeckler, G., and Jokipii, J. R. 1967. *Astrophys. J. Lett., 148*, L41.
Gold, T. See Gould et al., 1963.
Gold, T. 1969. *Nature, 221*, 25.
Goldschmidt-Clermont, Y. See Bartke et al., 1963.
Gould, R. J. 1965. *Phys. Rev. Lett., 12*, 511.
Gould, R. J., and Burbidge, G. R. 1965. *Ann. Astrophys., 28*, 171.
Gould, R. J., and Burbidge, G. R. 1967. *Handbuch der Physik, 46–2*, 265.
Gould, R. J., Gold, T., and Salpeter, E. E. 1963. *Astrophys. J., 138*, 408.
Gould, R. J., and Salpeter, E. E. 1963. *Astrophys. J., 138*, 393.
Gould, R. J., and Schréder. G. P. 1966. *Phys. Rev. Lett., 16*, 252.
Gould, R. J., and Schréder, G. P. 1967a. *Phys. Rev., 155*, 1404.
Gould, R. J., and Schréder, G. P. 1967b. *Phys. Rev., 155*, 1408.
Gratti, G. See Fidecaro et al., 1962.
Grigoletto, A. See Focardi et al., 1965.
Gruber, D. See Vette et al., 1969, 1970.
Gunn, J. E., and Peterson, B. A. 1965. *Astrophys. J., 142*, 1633.
Gürtler, J. See Dorschner et al., 1965.

Guseva, V. V., Dobrotin, N., Zelevinskaya, N., Kotchnikov, K., Lebedev, A., and Slavatinsky, S. 1962. *Proc. Int. Union Pure Appl. Phys. Conf.*, Kyoto, *3*, 375.
Guss, D. E. See Durgaprasad et al., 1968.
Harrison, E. R. 1967. *Phys. Rev. Lett.*, *18*, 1011.
Hartman, R. C. 1967. *Astrophys. J.*, *150*, 371.
Harwit, M. See Werner and Harwit, 1968.
——— See Shivanandau et al., 1969.
Hayakawa, S. See Fujimoto and Hayakawa, 1967.
Hayakawa, S. 1963. *Proc. Int. Conf. Cosmic Rays*, Jaipur, *3*, 125.
Hayakawa, S., and Okuda, H. 1962. *Prog. Theor. Phys. Japan*, *28*, 517.
Hayakawa, S., Okuda, H., Tanaka, Y., and Yamamoto, Y. 1964. *Prog. Theor. Phys. Japan*, Suppl. 30, 153.
Heeren, V. See Böckmann et al., 1966.
Heiles, C. E. 1968. *Astrophys. J.*, *151*, 919.
Heisenberg, W. 1952. *Z. Phys.*, *133*, 65.
Heitler, W. 1960. *The Quantum Theory of Radiation.* London: Oxford Press.
Henry, R. C., Fritz, G., Meekins, J. F., Friedman, H., and Bryam, E. T. 1968. *Astrophys. J. Lett.*, *153*, L11.
Hien, N. C. See Anderson et al., 1966.
Hoffman, W. F., and Frederick, C. L. 1969. *Astrophys. J. Lett.*, *155*, L12.
Hollenbach, D. J., and Salpeter, E. F. 1970. *J. Chem. Phys.*, *53*, 79.
Holmgren, S. O., Nilsson, S., Olhede, T., and Yamdagni, N. 1967. *Nuovo Cimento*, *51A*, 305.
Hones, E. W. See Cline and Hones, 1968.
Hongh, P. V. C. See Connolley et al., 1967.
Houck, J. R. See Shivanandan et al., 1969.
Hoyle, F. 1965. *Phys. Rev. Lett.*, *15*, 131.
Hudson, J. P. See Donn et al., 1968.
Hughes, V. See Morgan and Hughes, 1969.
Hutchinson, G. W., Pearce, A. J., Ramsden, D., and Wills, R. D. 1969. *Proc. XI Int. Conf. Cosmic Rays*, Budapest. *Acta Phys. 29*, Suppl. 1, 87 (1970).
Jauch, J. M., and Rohrlich, F. 1955. *The Theory of Photons and Electrons.* Cambridge, Mass.: Addison-Wesley.
Jelly, J. V. 1966. *Phys. Rev. Lett.*, *16*, 479.
Johnson, J. See Ferbel et al., 1965.
Jokipii, J. R. See Gloeckler and Jokipii. 1967.
Jones, F. C. 1963. *J. Geophys. Res.*, *68*, 4399.
Jones, F. C. 1965a. *Phys. Rev. Lett.*, *15*, 512.
Jones, F. C. 1965b. *Phys. Rev.*, *137*, B1306.
Jones, F. C. 1968. *Can. J. Phys.*, *46*, S1003.
Jordan, B. See Dekkers et al., 1965.
Kalbfleisch, G. R. See Button et al., 1961.
Källen, G. 1964. *Elementary Particle Physics.* Reading, Mass.: Addison-Wesley.
Kalmus, P. I. P. See Blair et al., 1966.
Kalogeropoulos, T. E. See Ferbel et al., 1962.
Kalyukin, M. M. See Kozodaev et al., 1960.
Kamata, K. See Bradt et al., 1965.
Kazuno, M. 1964. *Nuovo Cimento*, *34*, 303.
Kerr, F. J., and Westerhout, G. 1965. *Stars and Stellar Systems*, *5*, 167. [A. Blaauw and M. Schmidt, eds.]
Kidd, J. See Böckmann et al., 1966.

King, N. M. See Dekkers et al., 1965.
Kirz, J. See Rosenfeld et al., 1965.
Klepp, H. B. See Batson et al., 1959.
Koba, Z., and Takeda, G. 1958. *Prog. Theor. Phys. Japan, 19,* 269.
Kopp, J. K. See Baltay et al., 1964.
Kotchnikov, K. See Guseva et al., 1962.
Kozodaev, M. S., Kalyukin, M. M., Sulyaev, R. M., Filippov, A. I., and Shcherbakov, Yu. A. 1960. *Sov. Phys. JETP, 11,* 511.
Kniffen, D. A., and Fichtel, C. E. 1970. *Astrophys. J. Lett., 161,* L157.
Kniffen, D. A. See Fichtel et al., 1969.
Kraushaar, W. L. See Clark et al., 1968, 1969, 1970.
——— See Garmire and Kraushaar, 1965.
Kurt, V. G. See Zel'dovich et al., 1969.
Landau, L. D. 1953. *Izv. Akad. Nauk. SSSR Ser. Fiz., 17,* 51.
Lannutti, J. See Button et al., 1961.
LaPointe, M. See Bradt et al., 1965.
Lavakare, P. J. See Daniel et al., 1963.
Lea, R. M. See Baltay et al., 1964.
——— See Ferbel et al., 1962.
——— See Louttit et al., 1961.
Lebedev, A. See Guseva et al., 1962.
Lee, T. D., and Yang, C. N. 1956. *Nuovo Cimento, 3,* 749.
Lequeux, J. 1970. *Astrophys. J., 159,* 459.
Lieber, M., Milford, S. N., and Spergel, M. S. 1965. *Ann. Astrophys., 28,* 206.
Liebermeister, V. See Bockmann et al., 1966.
Lingenfelter, R. E. See Ramaty and Lingenfelter, 1966a, b, 1968, 1969.
Lingenfelter, R. E., and Ramaty, R. 1967. *High Energy Interactions in Astrophysics.* B. S. P. Shen, ed. New York: Benjamin.
Litt, J. See Blair et al., 1966.
Lohrmann, E. See Bockmann et al., 1966.
Loken, J. G., and Derrick, M. 1963. *Phys. Lett., 3,* 334.
Longair, M. S. 1966. *Mon. Not. Roy. Astron. Soc., 133,* 421.
Louttit, R. I. See Baltay et al., 1964.
Louttit, R. I., Morris, T. W., Rahm, D. C., Ran, R. R., Thorndike, A. M., Willis, W. J., and Lea, R. M. 1961. *Phys. Rev., 123,* 465.
Lynch, G. R. See Button et al., 1961.
Maglić, B. C. See Button et al., 1961.
Maksimenko, V. M. 1958. *Sov. Phys. JETP, 6,* 180.
Malhotra, P. K. See Daniel et al., 1963a.
Mandelli, L. See Böckmann et al., 1966.
Maraschi, L. See Dilworth et al., 1968.
Matsuda, S. 1966. *Phys. Rev., 150,* 1197.
Matteson, J. L. See Vette et al., 1969, 1970.
McCray, R. See Silk and McCray, 1969.
——— See Arons and McCray, 1969.
McKibben, B. See Fan et al., 1968.
McMahon, T. J. See Anderson et al., 1966.
McNutt, D. P., and Feldman, P. D. 1970. *Science, 167,* 1274.
Mebold, V. 1969. *Beitr. Radioastron., 1,* 97.
Meekins, J. F. See Henry et al., 1968.
Menes, J. See Anderson et al., 1966.

Menon, M. G. K. See Daniel et al., 1963.
Mermod, R. See Dekkers et al., 1965.
Metzger, A. E., Anderson, E. C., van Dilla, M. A., and Arnold, J. R. 1964. *Nature, 204,* 766.
Meyer, P. 1969. *Annu. Rev. Astron. Astrophys., 7,* 1.
Michel, L. 1949. *Nature, 163,* 959.
Middelkoop, W. C. See Fidecaro et al., 1962.
Milford, S. N. See Scanlon and Milford, 1965.
——— See Lieber et al., 1965.
Miller, D. H. See Cork et al., 1962.
Miller, D. J. See Connolley et al., 1967.
——— See Ellis et al., 1968.
Miller, M. C. See Blair et al., 1966.
Misra, D. See Ramaty et al., 1970.
Montanet, L. See Bartke et al., 1963.
Morgan, D., and Hughes, V. 1970. *Phys. Rev., D 2,* 1389.
Morris, T. W. See Baltay et al., 1964.
——— See Connolley et al., 1967.
——— See Ellis et al., 1968.
——— See Ferbel et al., 1962.
——— See Louttit et al., 1961.
Morrison, D. R. O. 1963. CERN Rpt. TC/Physics 63–1.
——— See Bartke et al., 1963.
Morrison, P. 1961. *Handbuch der Physik,* 46–1. Berlin: Springer.
——— See Brecher and Morrison, 1967.
——— See Felten and Morrison, 1963, 1966.
Mosca, L. See Böckmann et al., 1966.
Muirhead, H. 1965. *The Physics of Elementary Particles.* New York: Pergamon.
Murakumi, K. See Bradt et al., 1965.
Nadelhaft, I. See Anderson et al., 1966.
Naranan, S. See Daniel et al., 1963.
Nellen, B. See Böckmann et al., 1966.
Nelmes, A. T. 1953. National Bureau of Standards Circular 542 (Govt. Printing Office, Washington).
Nerurkar, N. W. See Daniel et al., 1963.
Neugebauer, G. See Becklin and Neugebauer, 1968.
Nikishov, A. I. 1961. *Sov. Phys. JETP, 14,* 393.
Nilsson, L. See Bartke et al., 1963.
Nilsson, S. See Holmgren et al., 1967.
Nishimura, J. 1967. *Handbuch der Physik,* 46–2. Berlin: Springer-Verlag. 1.
Novikov, I. D. See Doroshkevich et al., 1967.
Ögelman, H. B. 1969. *Nature, 221,* 753.
Ögelman, H. B. See Fichtel et al., 1969.
Okuda, H. See Hayakawa and Okuda, 1962.
——— See Hayakawa et al., 1964.
Olhede, T. See Holmgren et al., 1967.
Onannes, C. See Connolley et al., 1967.
Ore, A., and Powell, J. A. 1949. *Phys. Rev., 75,* 1696.
Osborne, J. L., and Wolfendale, A. W. 1963. *Proc. Int. Conf. Cosmic Rays,* Jaipur, *6,* 36.
Pal, Y. See Cowsik and Pal, 1969.
——— See Daniel et al., 1963.
Pal, Y., and Peters, B. 1964. *Danske Videnskab. Selskab, 33,* 1.

Palmiera, R. A. R. See Balasubrahmanyan et al., 1968.
Panvini, R. S. See Connolley et al., 1967.
——— See Ellis et al., 1968.
Parker, E. N. 1966. *Astrophys. J., 145*, 811.
Parker, E. N. 1968. *Stars and Stellar Systems*. B. M. Middlehurst and L. H. Aller, eds. 7, 707.
Partridge, R. B. See Stokes et al., 1967.
Partridge, R. S. See Encrenaz and Partridge, 1969.
Paul, E. See Böckmann et al., 1966.
Payne, A. D. 1969. *Aust. J. Phys., 22*, 59.
Peak, L. S., and Woolcott, R. L. S. 1965. *Proc. IX Int. Conf. Cosmic Rays*, London, *2*, 905.
Pearce, A. J. See Hutchinson et al., 1969.
Peebles, P. J. E. 1965. *Astrophys. J., 142*, 1317.
——— See Dicke et al., 1965.
Pelosi, V. See Böckmann et al., 1966.
Perkins, D. H. See Fowler and Perkins, 1964.
Perola, G. C. See Dilworth et al., 1968.
Perola, G. C., Scarsi, L., and Sironi, G. 1968. *Nuovo Cimento, 53B*, 459.
Peruzzo, L. See Focardi et al., 1965.
Peters, B. 1962. *J. Phys. Soc. Japan, 17*, Supp. A–III, 522.
——— See Pal and Peters, 1964.
Peterson, B. A. See Gunn and Peterson, 1965.
Peterson, L. E. See Vette et al., 1969, 1970.
Peyron, C. H. See Bartke et al., 1963.
Pollack, J. B., and Fazio, G. G. 1963. *Phys. Rev., 131*, 2684.
Pollack, J. B., and Fazio, G. G. 1965. *Astrophys. J., 141*, 730.
Pomanskii, A. A. See Dovzhenko and Pomanskii, 1964.
Powell, J. A. See Ore and Powell, 1949.
Primikoff, E. See Feenberg and Primikoff, 1948.
Prokoshkin, Yu. D., and Tiapkin, A. A. 1957a. *Sov. Phys. JETP, 5*, 618.
Prokoshkin, Yu. D., and Tiapkin, A. A. 1957b. *Sov. Phys. JETP, 6*, 245.
Pyle, K. R. See Fan et al., 1968.
Rahm, D. C. See Louttit et al., 1961.
Ramaty, R. See Lingenfelter and Ramaty, 1967.
Ramaty, R., and Lingenfelter, R. E. 1966a. *J. Geophys. Res., 71*, 3687.
Ramaty, R., and Lingenfelter, R. E. 1966b. *Phys. Rev. Lett., 17*, 1230.
Ramaty, R., and Lingengelter, R. E. 1968. *Phys. Rev. Lett., 20*, 120.
Ramaty, R., and Lingenfelter. 1969. *Astrophys. J., 155*, 587.
Ramaty, R., Stecker, F. W., and Misra, D. 1970. *J. Geophys. Res., 75*, 1141.
Ramsden, D. See Hutchinson et al., 1969.
Ratti, S. See Böckmann et al., 1966.
Rau, R. R. See Louttit et al., 1961.
Raubold, E. See Böckmann et al., 1966.
Reames, D. V. See Durgaprasad et al., 1968.
Rees, M. J. 1969a. *Astrophys. Lett., 4*, 61.
Rees, M. J. 1969b. *Astrophys. Lett., 4*, 113.
Reeves, H. See Audouze et al., 1967.
Riddiford, L. See Batson et al., 1959.
Rohrlich, F. See Jauch and Rohrlich, 1955.
Roll, P. G. See Dicke et al., 1965.
Roos, M. See Rosenfeld et al., 1965.

Rosenfeld, A. H., Barbaro-Galtieri, A., Barkas, W. H., Bastien, P. L., Kirz, J., and Roos, M. *Rev. Mod. Phys., 37*, 633.
Rowan-Robinson, M. 1968. *Mon. Not. Roy. Astron. Soc., 138*, 445.
Rubtzov, V. I. See Baradzei et al., 1962.
Sakurai, J. J. 1964. *Invariance Principles and Elementary Particles.* Princeton, N.J.: Princeton Univ. Press.
Salpeter, E. F. See Hollenbach and Salpeter, 1970.
——— See Gould and Salpeter, 1963.
——— See Gould et al., 1963.
——— See Caroll and Salpeter, 1966.
Saudri, G. See Balasubramanyan et al., 1968.
Sandweiss, J. See Baltay et al., 1964.
——— See Ferbel et al., 1962.
——— See Ferbel et al., 1965.
Sanford, J. R. See Baltay et al., 1964.
Santangelo, R. See Focardi et al., 1965.
Saporetti, F. See Focardi et al., 1965.
Scanlon, J. H., and Milford, S. N. 1965. *Astrophys. J., 141*, 718.
Scarsi, L. See Perola et al., 1968.
Schmidt, K. H. See Dorschner et al., 1965.
Schmidt, M. 1968. *Astrophys. J., 151*, 393.
Schréder, G. P. See Gould and Schréder, 1966, 1967a, b.
Schutt, R. See Baltay et al., 1964.
Schwinger, J. 1949. *Phys. Rev., 75*, 1912.
Scott, D. B. See Blair et al., 1966.
Serlemitsos, P. See Boldt and Serlemitsos, 1969.
Share, G. 1970. Private communication.
Shcherbakov, Yu. A. See Kozodaev et al., 1960.
Sherman, H. J. See Blair et al., 1966.
Shen, C. S. 1969. *Phys. Rev. Lett., 22*, 568.
Shivanandan, K. 1970. Personal communication.
Shivanandan, K., Houck, J. R., and Harwit, M. O. 1968. *Phys. Rev. Lett., 21*, 1460.
Shklovskii, I. 1960. *Cosmic Radio Waves.* Cambridge, Mass.: Harvard Univ. Press.
Silk, J. See Stecker and Silk, 1969.
Silk, J., and McCray, R. 1969. *Astrophys. Lett., 3*, 59.
Simpson, J. A. See Fan et al., 1968.
Sironi, G. See Perola et al., 1968.
Slavatinsky, S. See Guseva et al., 1962.
Sloanaker, R. M. See Evans et al., 1970.
Smith, A. M. 1969. *Astrophys. J., 156*, 93.
Smith, L. H. See Frye and Smith, 1966.
Smorodin, Y. A. See Baradzei et al., 1962.
Söding, P. See Böckmann et al., 1966.
Solovyev, M. V. See Baradzei et al., 1962.
Sood, R. K. 1969. *Nature, 222*, 650.
Sosnowski, R. 1963. See Bartke et al., 1963.
Spergel, M. S. See Lieber et al., 1965.
Sreekantan, B. V. See Daniel et al., 1963.
Stecher, T. P. See Donn et al., 1968.
Stecher, T. P., and Stecker, F. W. 1970. *Nature, 226*, 1234.
Stecher, T. P., and Williams, D. A. 1967. *Astrophys. J. Lett., 149*, L29.

Stecker, F. W. 1968. *Phys. Rev. Lett., 21*, 1016. See also Stecker, F. W. 1969. *Phys. Rev. 180*, 1264.
Stecker, F. W. 1969a. *Astrophys. and Space Sci., 3*, 579.
Stecker, F. W. 1969b. *Nature, 222*, 865.
Stecker, F. W. 1969c. *Astrophys. J., 157*, 507.
Stecker, F. W. 1970. *Astrophys. and Space Sci., 6*, 377.
Stecker, F. W. 1971. *Nature, 229*, 105.
——— See Fazio et al., 1966.
——— See Fazio and Stecker, 1970.
——— See Ramaty et al., 1970.
——— See Stecher and Stecker, 1970.
Stecker, F. W., and Silk, J. 1969. *Nature, 221*, 1229.
Stecker, F. W., Tsuruta, S., and Fazio, G. G. 1968. *Astrophys. J., 151*, 881.
Stephens, S. A. See Anand et al., 1968, 1969.
Stevenson, M. L. See Button et al., 1961.
Stokes, G. A., Partridge, R. B., and Wilkinson, D. T. 1967. *Phys. Rev. Lett., 19*, 1199.
Stonehill, D. L. See Baltay et al., 1964.
Stump, R. See Baltay et al., 1964.
Suess, H. E., and Urey, H. C. 1956. *Rev. Mod. Phys., 28*, 53.
Suga, K. See Bradt et al., 1965.
Sulyaev, R. M. See Kozodaev et al., 1960.
Syrovatskii, S. I. See Ginzburg and Syrovatskii, 1964, 1965.
Syunyaev, R. A. See Zel'dovich et al., 1969.
Taft, H. D. See Baltay et al., 1964.
——— See Ferbel et al., 1962.
——— See Ferbel et al., 1965.
Takeda, G. See Koba and Takeda, 1958.
Tallone, L. See Böckmann et al., 1966.
Tanaka, Y. 1968. *Can. J. Phys., 46*, S536.
——— See Hayakawa et al., 1964.
Taylor, A. E. See Blair et al., 1966.
Tenner, A. G. See Cork et al., 1962.
Thaddeus, P. See Bartolot et al., 1969.
Thaddeus, P., and Clauser, S. F. 1966. *Phys. Rev. Lett., 16*, 819.
Thorndike, A. M. See Baltay et al., 1964.
——— See Connolley et al., 1967.
——— See Ellis et al., 1968.
——— See Louttit et al., 1961.
Tiapkin. See Prokoshkin and Tiapkin, 1957a, b.
Tolkachev, B. V. See Baradzei et al., 1962.
Toyoda, Y. See Bradt et al., 1965.
Trower, W. P. 1966. Univ. of Cal., Lawrence Rad. Lab. Rpt. UCRL–2426, vol. 2.
Tsuruta, S. See Stecker et al., 1968.
Turkot, F. See Anderson et al., 1966.
Urey, H. C. See Suess and Urey, 1956.
Valdez, J. V., Frier, P. S., and Waddington, C. J. 1969. *Proc. XI Int. Conf. Cosmic Rays*, Budapest. *Acta. Phys. 29*, Suppl. 1, 79 (1970).
Van Dilla, M. A. See Metzger et al., 1964.
Varsavsky, C. See Garzoli and Varsavsky, 1966.
Vette, J. I., Gruber, D., Matteson, J. L., and Peterson, L. E. 1969. *Proc. I.A.U. Symp. No. 37*, Rome (L. Gratton, ed.), 335, Reidel Pub. Co., Dordrecht, Holland. *1970 Astrophys. J. Lett., 160*, L161.

Vijayalakshmi, B. See Daniel et al., 1963a.
Vivargent, M. See Dekkers et al., 1965.
Weddington, C. J. See Valdez et al., 1969.
Walker, T. G. See Blair et al., 1966.
Wang, C. L. See Cork et al., 1962.
Weber, G. See Dekkers et al., 1965.
Webster, M. S. See Baltay et al., 1964.
Werner, M. W., and Harwit, M. 1968. *Astrophys. J., 154*, 881.
Westerhout, G. See Kerr and Westerhout, 1965.
Weymann, R. 1967. *Astrophys. J., 147*, 887.
Wickramasinghe, N. C. See Donn et al., 1968.
Wigini, B. See Böckmann et al., 1966.
Wilkinson, D. T. See Dicke et al., 1965.
——— See Stokes et al., 1967.
Williams, D. A. See Stecher and Williams, 1967.
Williams, W. S. C. 1961. *An Introduction to Elementary Particle Physics.* New York: Academic Press.
Willis, W. J. See Baltay et al., 1964.
——— See Louttit et al., 1961.
Willitts, T. R. See Dekkers et al., 1965.
Wills, R. D. See Hutchinson et al., 1969.
Wilson, E. J. N. See Dekkers et al., 1965.
Winter, K. See Dekkers et al., 1965.
Wolfendale, A. W. 1963. *Cosmic Rays.* New York: Philosophical Library.
Wolfendale, A. W. See Osborne and Wolfendale, 1963.
Wolff, S. See Böckmann et al., 1966.
Woolcott, R. L. S. See Peak and Woolcott, 1965.
Wright, J. P. See Fazio et al., 1966.
Xuong, N. H. See Button et al., 1961.
Yamagata, T. See Fidecaro et al., 1962.
Yamamoto, Y. See Hayakawa et al., 1964.
Yamdagni, N. See Holmgren et al., 1967.
Yang, C. N. See Lee and Yang, 1956.
Yekutieli, G. 1961. Air Force Cambridge Research Laboratory Rept. No. 1089.
Zeldovich, Y. B. See Doroshkevich et al., 1967.
Zeldovich, Y. B., Kurt, V. G., and Syunyaev, R. A. 1969. *Sov. Phys. JETP, 28*, 146.
Zelevinskaya, N. See Guseva et al., 1962.

GAMMA-RAY TELESCOPES

DONALD KNIFFEN

A–1 INTRODUCTION

Even though astronomy is one of the oldest of the experimental sciences, dating back over 5000 years, investigations in the highest frequency portions of the electromagnetic spectrum have developed only within the last two decades. Atmospheric absorption of X-rays and γ-rays prevents their direct detection and study from ground-level observatories, hence data on these energetic photons were not available until high-altitude balloons, sounding rockets, and satellites became available to place instruments above the atmosphere. In this appendix we describe the telescopes which have been developed for such observations and outline the direction of future experimentation in γ-ray astronomy.

A–2 TECHNIQUES

There is no property of the γ-ray which allows it to be detected directly. It is thus necessary to use secondaries produced by the interaction of γ-rays with some suitable target material. Heavy-metal targets because of their large atomic number Z provide large interaction cross sections. (See ch. 4.) Figure A–1 shows that for energies above 1 MeV the most important interactions of photons in heavy-metal targets are the Compton scattering process up to a crossover energy of about 10 MeV and the electron-positron pair-production above 10 MeV.[1]

The reliability with which γ-rays may be detected by these interactions depends upon the discrimination between these events and those caused by interactions of unwanted particles in the cosmic-ray environment. In fact, this consideration plays a dominant role in the design of γ-ray telescopes, since the photons must be observed above a background of 10^4 times as many charged particles. Since the consequences of the de-

[1] The crossover energy increases with decreasing atomic number becoming about 55 MeV for hydrogen (fig. 4–2).

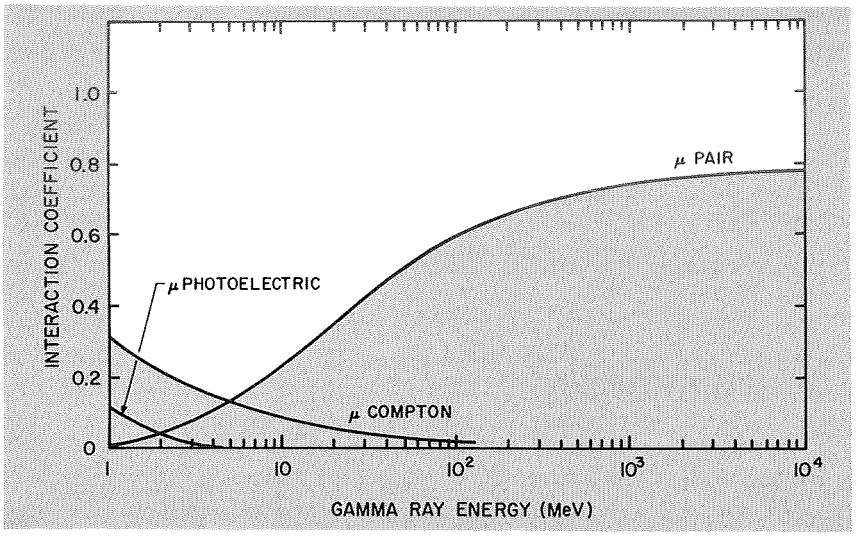

FIGURE A–1.—The interaction coefficients (proportional to cross sections) for interactions of energetic photons traversing a large atomic number ($Z=79$) medium, plotted as a function of photon energy. (For N_0 photons incident upon the material, $N=N_0e^{-\mu t}$ remain after passing through t radiation lengths of the material, where μ is the interaction coefficient; Kniffen, 1969.)

sign depend strongly on the particular objectives of the experiment, a variety of different types of detectors have been developed to search for extraterrestrial γ-rays with energies above 1 MeV. However, in each case the instrument must be able to have a reasonable detection efficiency for γ-rays with a high rejection efficiency for other types of events. In addition, it must have some degree of energy resolution and the ability to measure the arrival directions of the γ-rays in order to identify the source regions and to compare their γ-ray energy spectra with theoretical predictions, such as those presented in this monograph. The slowly varying nature of the expected continuum spectra for cosmic γ-rays above 1 MeV does not necessitate a particularly high energy-resolution for the detectors.

The telescopes currently being used in γ-ray investigations or planned for use in the near future consist of four basic types: The scintillator-Cerenkov detector telescope, pictorial-type detectors, gas Cerenkov telescopes, and ground-based night-sky Cerenkov detectors. Each of these types has its unique characteristics and advantages.

A–3 SCINTILLATOR-CERENKOV DETECTOR TELESCOPES

As the name implies, the basic element of this type of detector, as depicted in figure A–2, is a two-element telescope consisting of a scin-

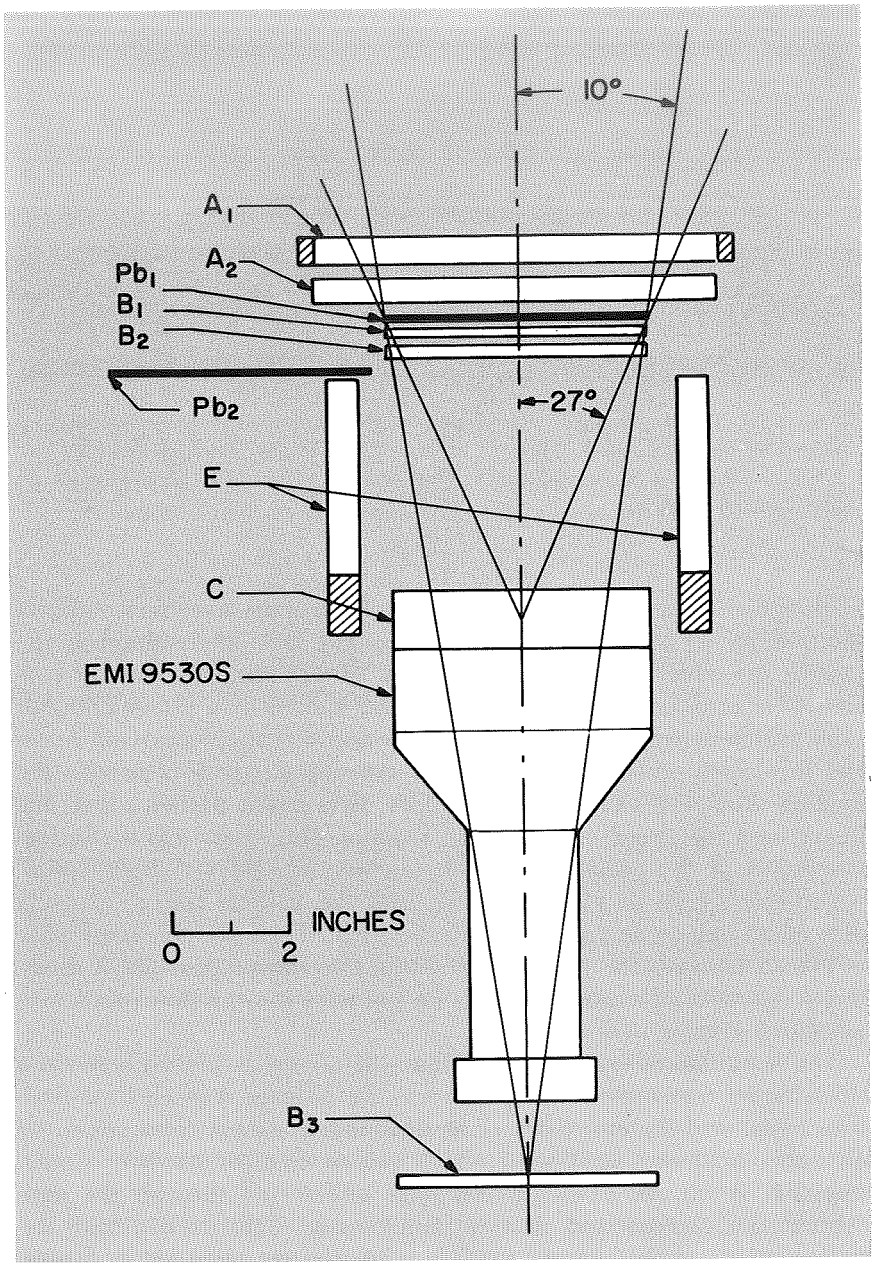

FIGURE A–2.—A schematic representation of the scintillator-Cerenkov counter of Duthie et al. (1963) with plastic scintillator anticoincidence counters, A_1, A_2, and E; a lead converter, Pb_1; scintillation counters, B_1 and B_2; and Cerenkov detector, C. The counter pairs are used for redundancy.

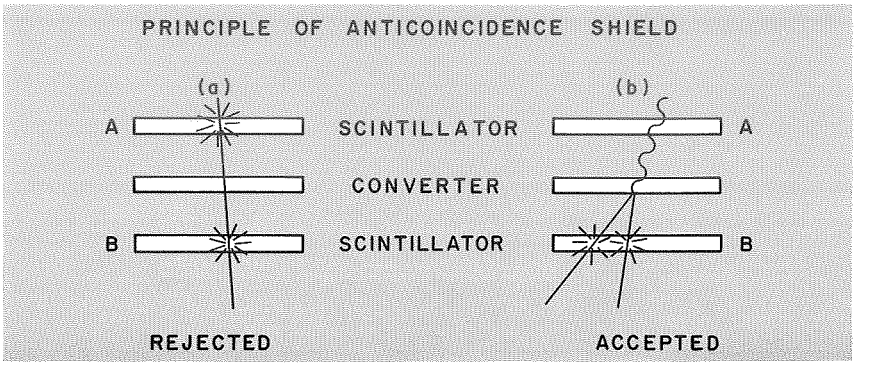

FIGURE A–3.—This figure depicts the principle of the anticoincidence shield. A charged particle (*a*) produces a flash in both scintillators A and B. The γ-ray conversion (*b*) produces two flashes in B, but none in A. Thus charged particle background events are discriminated against.

tillation counter and a Cerenkov detector. Each of these devices registers the passage of a charged particle by sensing the light emitted as the particle traverses the detecting medium. The scintillation counter consists of a translucent fluorescent material viewed by a photomultiplier tube, which converts the light flashes produced in the fluorescent material to electric pulses. The Cerenkov detector consists of a radiating medium (radiator) and a photomultiplier. Relativistic particles traveling faster than the speed of light in the radiator, c/n, where n is the refractive index of the radiator material, produce an optical "shock wave" which emits light in a forward cone with the particle trajectory as its axis and a half angle θ given by $\cos \theta = 1/\beta n$. When the photomultiplier is placed beneath the radiating medium, this device provides a directional detector which triggers only on particles moving downward with velocities greater than c/n.

The scintillator-Cerenkov coincidence telescope is placed beneath a thick target (converter) which converts the photons into electron-positron pairs; and the entire device is surrounded, except from below, by an anticoincidence scintillator which vetoes charged particle events. (See fig. A–3.) All events which pass undetected through the anticoincidence counter and provide simultaneous light flashes from the two elements of the charged particle telescope are recorded as γ-rays.

This instrument has the advantage of being relatively small, light, and simple, which makes it very useful as a space research detector. However, it has poor angular resolution and, most importantly, an inherent ambiguity in uniquely identifying weak γ-ray intensities, because of its lack of pictorial capabilities. Scintillator-Cerenkov telescopes

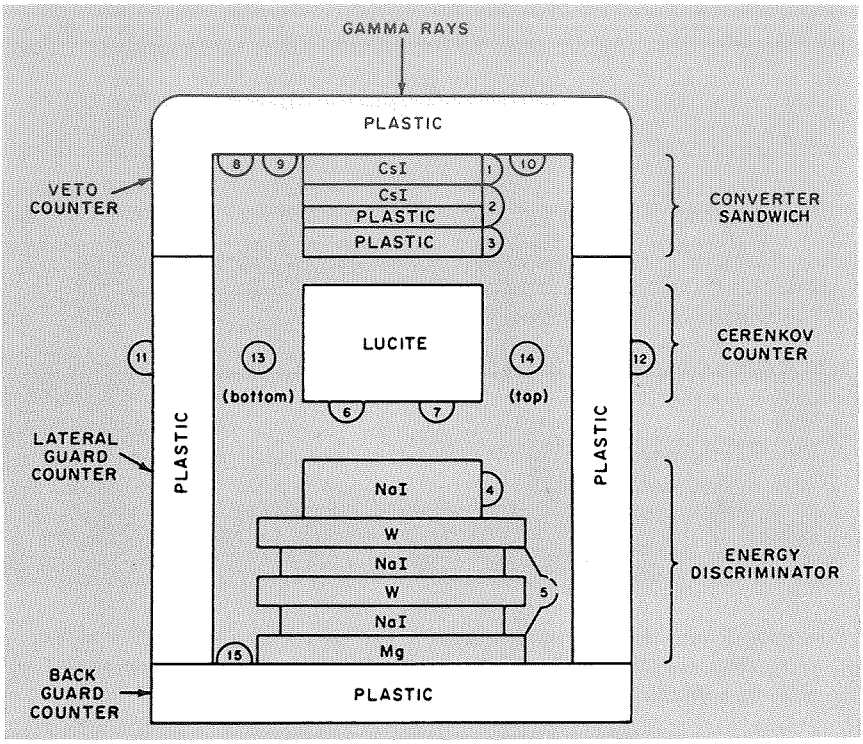

FIGURE A–4. — The OSO–3 γ-ray detector of Kraushaar et al. (1968). The principle of operation of this advanced scintillator-Cerenkov detector is discussed in the text.

have obtained very valuable data on γ-rays with energies above 50 MeV as "first-generation" γ-ray telescopes.

The counter-type detector has been used in balloon-borne experiments by Cline (1961) and Duthie et al. (1963) in search of a diffuse background intensity of cosmic γ-rays and in the satellite experiments of Kraushaar and Clark (1962) on Explorer 11; Fazio and Hafner on OSO–1 (1967); and Kraushaar, Clark, and Garmire (1968) and Valentine et al. (1970) on OSO–3. Figure A–4 is a schematic representation of the most advanced of this detector type, the OSO–3 instrument of Kraushaar et al. (1968), with a converter sandwich[2] designed to verify the electro-

[2] The converter sandwich consists of two different types of scintillators, each examined by separate photomultiplier tubes. Because cross sections for electromagnetic interactions have a different dependence on the atomic number Z than do those for nuclear interactions, the ratio of γ-ray conversions between the CsI and the plastic scintillation counters is 13:1. The expected ratio for neutrons converting to protons is 4:1.

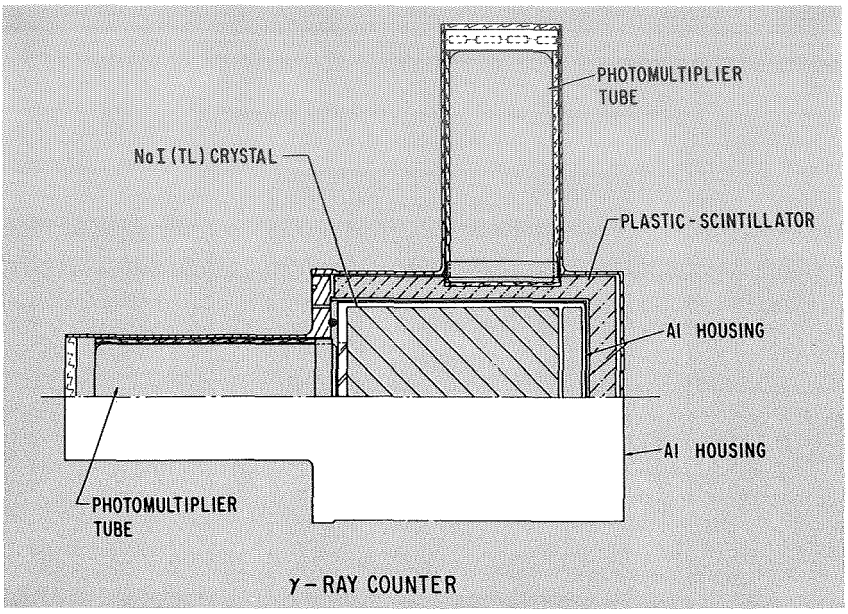

FIGURE A–5. — A schematic representation of the low-energy γ-ray counter of Peterson et al. (1968), consisting of a central totally absorbing crystal scintillator surrounded on all sides by a plastic scintillator anticoincidence counter.

magnetic nature of the suspected γ-ray events and an energy discriminator[3] to provide a crude energy measurement.

Modifications of this general type of telescope have been used in recent balloon studies of atmospheric γ-rays (Paolo, Paolo, and Constantinos, 1970) and the galactic line intensity (Sood, 1969).

The electrons and positrons produced by γ-rays below ~ 5 MeV in the converter do not have sufficient energy to penetrate both elements of the telescope; hence a different configuration is required. To detect these low-energy γ-rays, the Cerenkov element is removed and the scintillation detector is made sufficiently thick to absorb the converted electrons as their kinetic energy is lost in the scintillation material. Peterson et al. (1968) have developed such an instrument to measure the isotropic diffuse intensity of 0.25- to 6-MeV γ-rays. This detector, shown schematically in figure A–5, consists basically of a large thallium-doped sodium iodide

[3] The energy discriminator consists of alternating layers of tungsten targets, in which the incoming electron initiates an electromagnetic cascade, and scintillation counters, which measure the number of electrons existing at sample levels in the cascade. Comparison with shower theory allows a crude measurement of the energy of the incoming particles and also allows an additional discrimination against nuclear particles because of the different nature of the nuclear cascade.

crystal, surrounded on all sides by a plastic scintillator anticoincidence shield which rejects penetrating charged particles. Those γ-rays are recorded which produce high-energy electrons that are detected and totally absorbed by the crystal while no signal is recorded in the anticoincidence counter. Gamma rays in this energy range produce high-energy electrons predominately by Compton scattering rather than by pair-production. Since this scattering process destroys potential information on the direction of the incoming γ-ray, this type of detector is limited to studies of diffuse γ-ray distributions.

A-4 PICTORIAL-TYPE DETECTORS

By the early 1960's it had become clear from the results of experiments by Perlow and Kissinger (1951) and Critchfield and Ney (1952) that the primary γ-ray intensity at cosmic-ray energies is several orders of magnitude lower than the intensity of energetic charged nuclei. The many problems of identifying such a rare component in a high background led several groups to develop a variety of pictorial-type detectors in which the pair-production event could be uniquely identified and its properties studied to obtain detailed data on each of the detected γ-rays.

A-4a Nuclear Emulsions

The first pictorial detector to be used was the nuclear emulsion (Bracessi, Ceccarelli, and Salandin, 1960; Klarmann, 1962; Fichtel and Kniffen, 1965; and Frye, Reines, and Armstrong, 1965). The emulsion provides an excellent medium for the identification of the pair-production interaction, since the emulsion material serves as the conversion target as well as the detecting medium. This allows the electron pair to be observed at the point of formation, since rows of developed grains remain along the residual ion paths of the charged particles. This allows the properties of the electrons to be studied before they are modified by subsequent passage through the remainder of the converter. As a result, this medium provides a maximum of information on each detected γ-ray, with excellent determination of the energy and arrival direction of the incident photon down to a few megaelectron volts. Unfortunately, there are some very serious undesirable features of this technique which seriously limit its usefulness in γ-ray astronomy. First, it lacks time discrimination, since any γ-ray passing through the emulsion, from the time of its manufacture to the time of its development following exposure, is recorded. The resulting high background γ-ray intensity in the emulsion detector restricts its use to searches for discrete sources where its high angular resolution can be used to minimize the effect of the background. The

equation for the sensitivity of a detector for discrete source observations is given by

$$S = \frac{F_\gamma A \epsilon t}{(I_B A \epsilon t \pi \theta^2)^{1/2}} = \frac{F_\gamma}{\theta} \left(\frac{A \epsilon t}{I_B \pi} \right)^{1/2} \qquad \text{(A-1)}$$

where F_γ is the discrete γ-ray source flux, I_B the background γ-ray intensity, A the detector exposure area, ϵ the detection efficiency, t the time of exposure, and θ the angular resolution of the detector. It follows from equation (A–1) that for maximum detector sensitivity, good angular resolution is desirable, but not at the cost of a large sacrifice in background intensity. At low energies, ϵ is also a very critical parameter for emulsion detectors, since it is most tedious and time consuming to search for the low-energy electron pairs under a high-power microscope, with the resultant deterioration in accuracy and consistency. Finally, the necessity for recovery essentially limits the use of emulsions to balloon-borne experiments.

A-4b Spark Chambers

The advantages of the emulsion detector have led many experimenters to develop other types of pictorial detectors which incorporate, to as great an extent as possible, the advantages of that technique without its disadvantages. Of the other imaging detectors which might be considered for γ-ray telescopes, the spark chamber is the most advantageous for space research. A number of different approaches have been taken by experimenters in adapting this device to γ-ray observations.

Historically, the first spark chambers used in γ-ray astronomy (Cobb, Duthie, and Stewart, 1965; Frye and Smith, 1966; and Ögelman et al., 1966) incorporated the photographic readout system. In this type of device, the spark-chamber modular unit consists very simply of two parallel metal plates with a gap containing the spark gas. The gap is sufficiently large that the sparks formed in the gas between the plates can be viewed optically and recorded on film.

The first such instrument to be used in studies of extraterrestrial γ-rays with energies > 100 MeV was developed by the group under Duthie at the University of Rochester (Cobb et al., 1965). Ögelman et al. (1966) used a similar detector for studies of γ-rays above 1 GeV. In principle, this detector is similar to the counter-type detector shown in figure A–2, with sets of spark-chamber modules placed above the converter and between the scintillation and Cerenkov counters. Incoming γ-rays are converted into electron-positron pairs in the converter. As the pair electrons pass through the spark chambers the spark gas is ionized along the particle paths. When the scintillator-Cerenkov

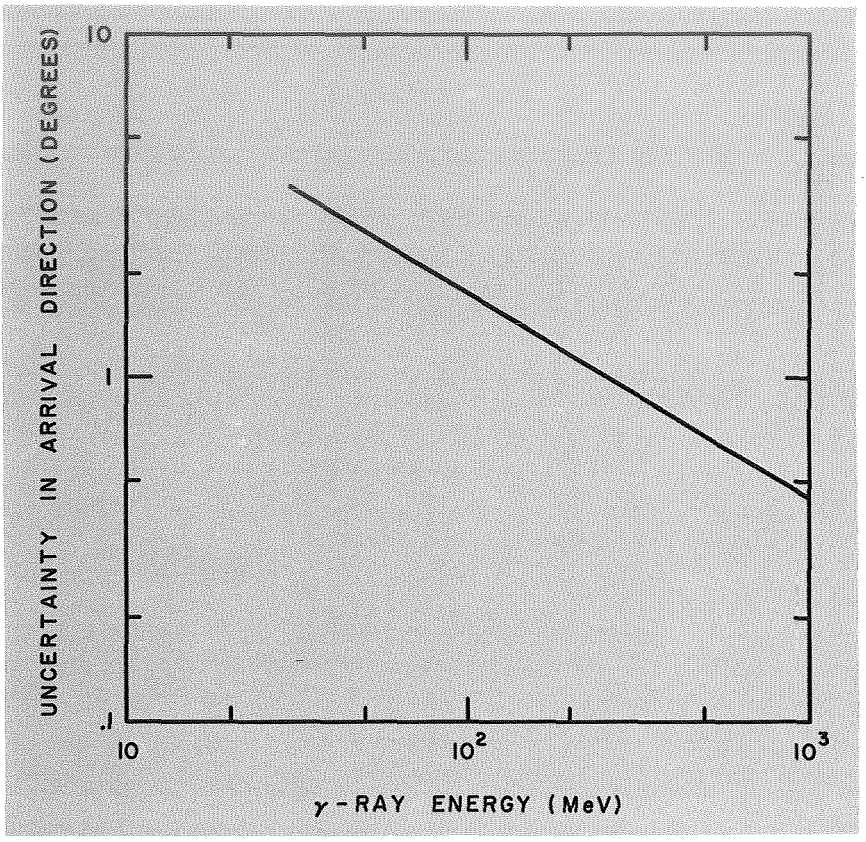

FIGURE A–6.—The one standard deviation error in determining the arrival direction of γ-rays in a typical spark chamber telescope as a function of γ-ray energy (Fichtel et al., unpublished).

telescope detects a γ-ray event, high voltage is applied across the plates, and the sparks which occur along the ion paths are recorded on photographic film. This determination of the trajectory results in a much-improved γ-ray event identification and an accurate determination of its arrival direction and maintains a wide acceptance angle. The spark chamber above the converter serves as a redundant anticoincidence indicator to prevent acceptance of charged particle events.

Frye and Smith (1966) and the group under Fichtel at Goddard Space Flight Center (Ehrmann et al., 1967) improved upon the spark chamber by distributing the converter as thin plates placed between the modules of the spark chamber. This feature provides more detail in the "picture" of the event, approaching more closely the advantages of the emulsion detector. The result is a still more reliable event identification and a more accurate determination of the γ-ray arrival direction. Figure A–6

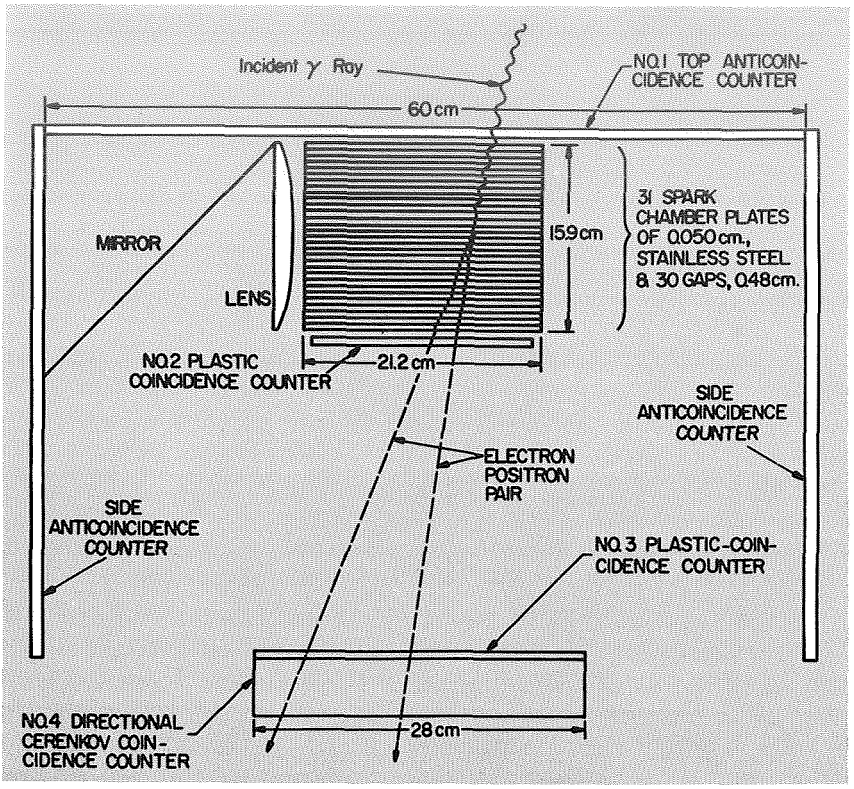

FIGURE A–7. – A recent version of the balloon-borne spark chamber γ-ray telescope of Frye et al. (1969).

shows the accuracy with which the γ-ray arrival direction can be obtained with such a configuration.

A recent version of the Case Western Reserve photographic chamber (Frye et al., 1969) is shown in figure A–7.

The balloon-borne detector of the GSFC group contains target plates between the modules beneath the scintillation counter, as shown in figure A–8. Such a configuration provides a better identification of the event, and a study of the coulomb deflections of the electrons in the plates allows a determination of the energy of each electron and hence the energy of the γ-ray (Pinkau, 1966; Kniffen, 1969). This energy information also improves the knowledge of the γ-ray arrival direction (Fichtel et al., 1969). The GSFC group (Ehrmann et al., 1967; and Ross et al., 1969) employs a ferrite core readout system consisting of a stack of spark modules. Each wire is threaded through a ferrite core and attached to a bus common to all wires of the same plane. As an event is detected and high voltage is applied across the grid, a spark breakdown

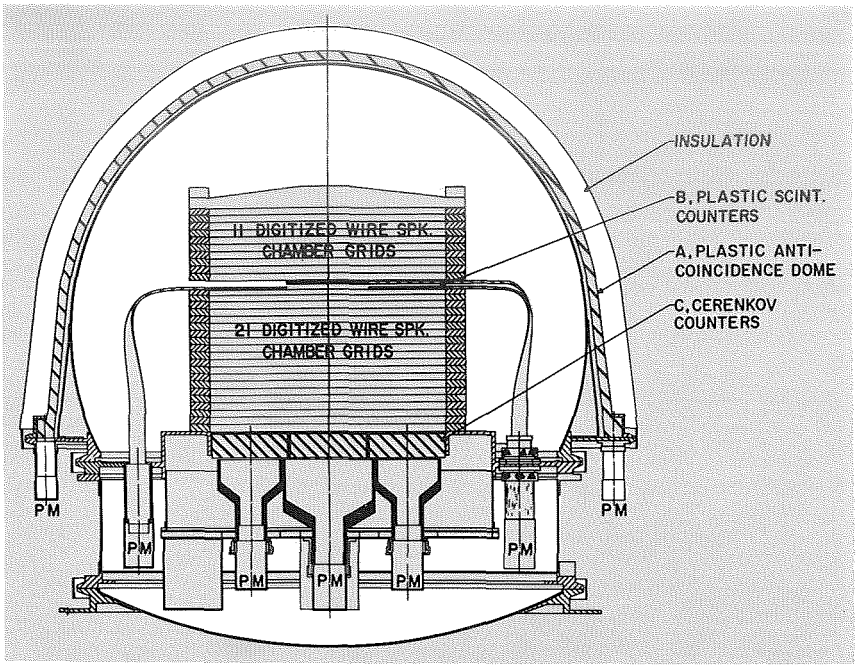

FIGURE A–8.—The ½- by ½-m digitized wire-grid spark chamber γ-ray telescope of the Goddard Space Flight Center group (Ross et al., 1969). [PM = photomultiplier tube.]

causes current to flow along the affected wires, "setting" the respective cores. Reading out the cores identifies an x and y spark location at each modular level, hence a stack of modules provides a three-dimensional "picture" of the charged particle trajectories. Figure A–9 presents a microfilm printout of such an event obtained in a balloon flight experiment. This type of readout system has the advantage that it does not require that large amounts of film be carried with the experiment, and the data can readily be transmitted to a ground-based receiving and recording station. This feature makes this system readily adaptable to a satellite configuration. Figure A–10 shows a satellite version of the telescope developed at Goddard Space Flight Center (Cline, Fichtel, and Kniffen, 1967).

Other remote readout systems have been devised for γ-ray telescopes, such as the video scanning technique developed by Fazio and Helmken (1968) for a balloon-borne detector and by a European collaboration (University of Milan; Centre d'Etudes Nucléaires de Saclay, France; Max Planck Institut für Extraterrestrische Physik, Munich) for a satellite γ-ray experiment. An acoustic readout chamber was flown by Hutchinson et al. (1970) on OGO–5.

In an attempt to improve the sensitivity of balloon-borne spark-

411-892 O - 71 - 16

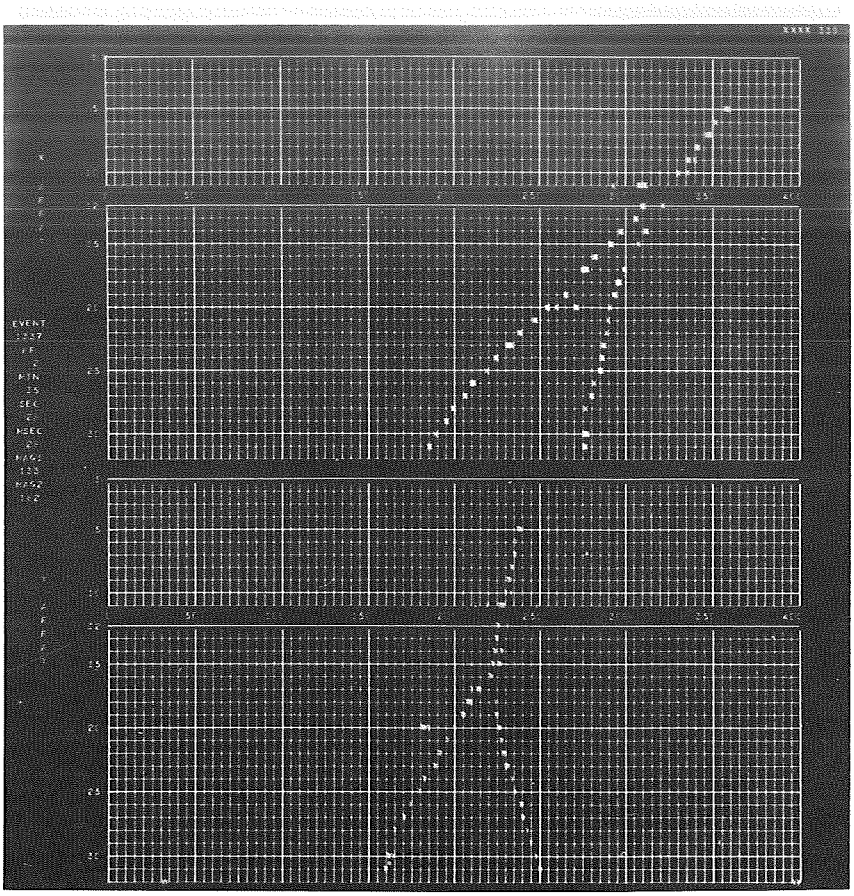

FIGURE A–9.—A computer microfilm printout of a γ-ray event observed in the spark chamber shown schematically in figure A–8. The x (top) and y (bottom) arrays represent two orthogonal views of the same pair-production event by sampling the charged particle trajectories at 32 modular or z-axis levels.

chamber telescopes for discrete source studies, May and Waddington (1969) and Share et al. (1968) have combined the excellent directional properties of nuclear emulsions with the time discrimination of spark chambers. Ross et al. (1969), Frye et al. (1969), and Board, Dean, and Ramsden (1968) have improved sensitivity by developing larger area detectors for balloon flight observations of γ-rays with energies above 30 MeV.

A xenon wide-gap spark chamber for directional studies of 1- to 100-MeV γ-rays is currently being developed by the NRL group (Kinzer et al., 1970). This device, shown in figure A–11, is a pictorial detector

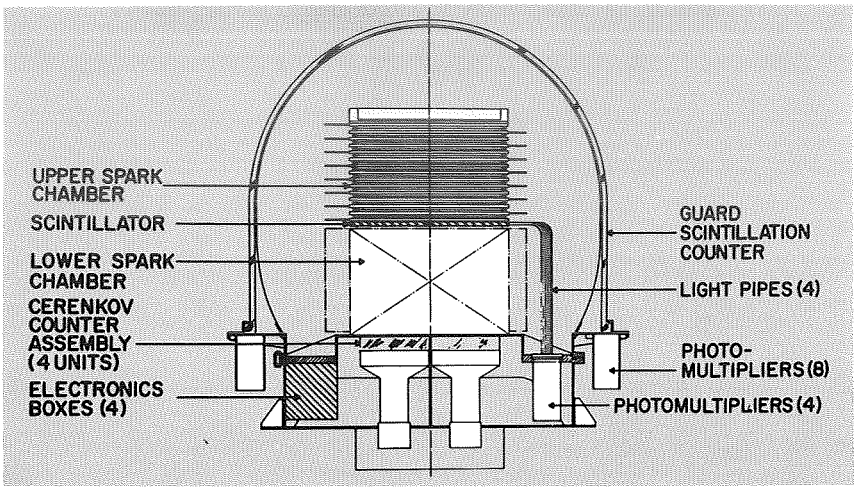

FIGURE A–10. – A schematic representation of the Goddard Space Flight Center SAS–B spark chamber γ-ray telescope (Cline, Fichtel, and Kniffen, 1967).

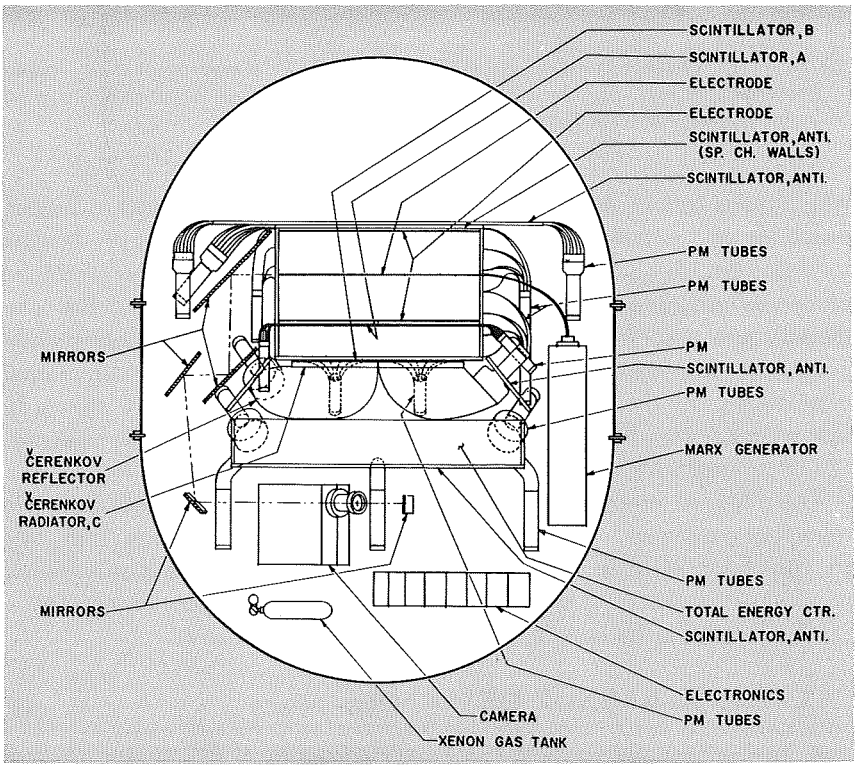

FIGURE A–11. – A schematic diagram of the NRL xenon spark chamber for 1- to 100-MeV γ-ray studies (Kinzer et al., 1970).

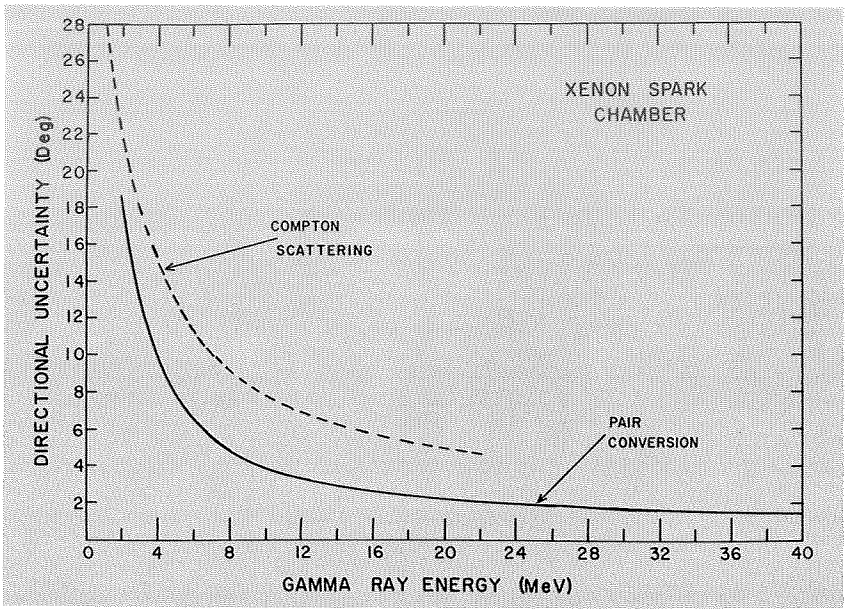

FIGURE A–12. – Root-mean-square directional uncertainty for γ-rays detected by Compton scattering and pair conversion interactions given as a function of γ-ray energy for the xenon chamber shown in figure A–11.

which uses xenon as the spark-chamber gas. Xenon, being a high-Z (large atomic number) material, acts as an effective pair-production material (ch. 4) as well as a detecting medium in which the produced electrons are photographed close to their origins. By use of the low-density gas, a sacrifice is made in conversion efficiency to obtain high-accuracy directional information. The root-mean-square directional uncertainty for the Compton scatter and pair conversion are shown in figure A–12. The detector has the additional advantage of event interpretation allowed with a "picture"-type detector.

The lack of unambiguous positive observations with balloon-borne telescopes, even with the increased accuracies and sensitivities, indicates the need for satellite detectors with sufficient energy and directional resolution to obtain a detailed map of both galactic and extragalactic γ-ray intensities as well as to observe discrete sources.

A–5 GAS CERENKOV DETECTORS

A new instrument concept has been devised by K. Greisen of Cornell University and G. Fazio of the Smithsonian Astrophysical Observatory and their collaborators for the examination of possible discrete source

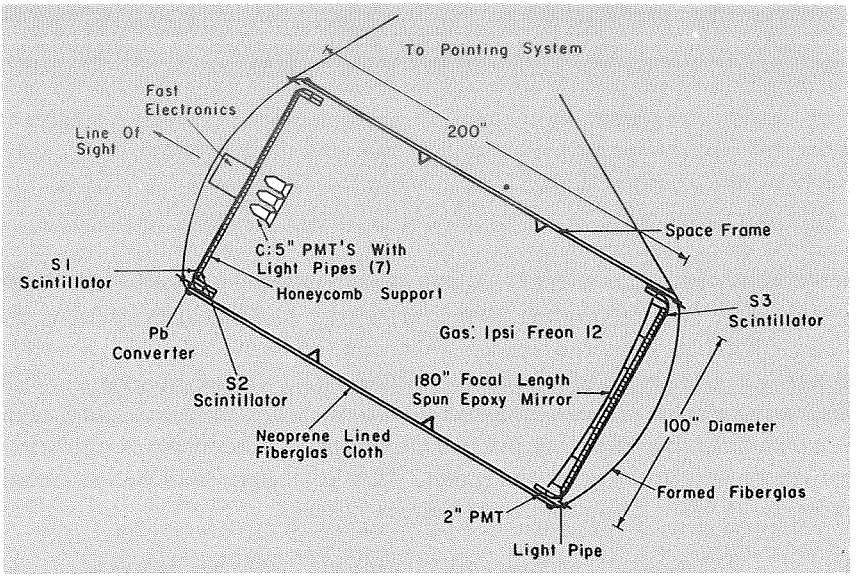

FIGURE A–13.—A schematic representation of the 100-in. telescope gas Cerenkov γ-ray detector of the Cornell and Smithsonian Astrophysical Observatory groups.

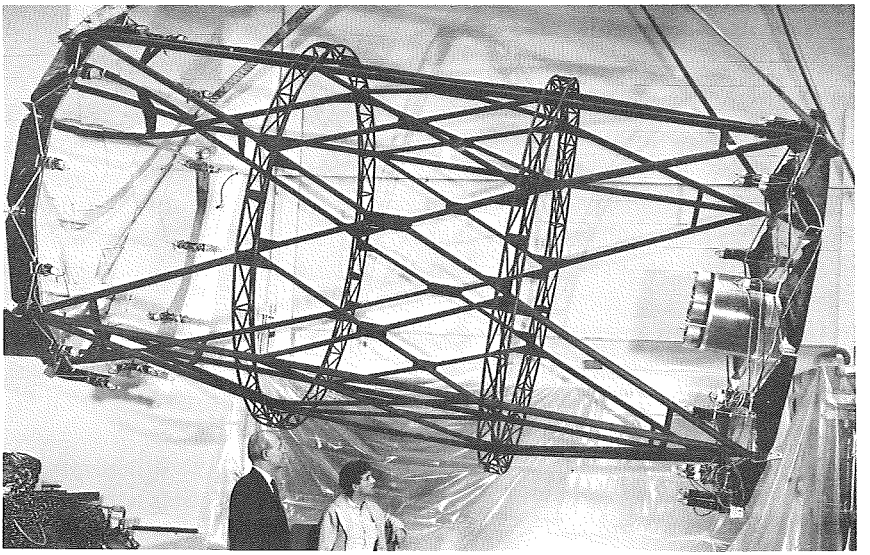

FIGURE A–14.—The 100-in.-diameter Cornell-SAO gas Cerenkov telescope. The telescope is shown pointing to the right with the mirror at the left of the picture. On the right end are the Cerenkov tubes, scintillators, and lead converter. (See fig. A–13.) The 20-ft-long instrument was designed and built at Cornell under the direction of Prof. Kenneth Greisen (shown at the bottom left with coworker Dr. Brian McBreen). (Courtesy K. Greisen.)

emitters. This instrument, depicted schematically in figure A–13 and shown in figure A–14, can be compared in principle to the scintillation-Cerenkov detector presented in figure A–2, with the solid radiator Cerenkov detector replaced by a gas Cerenkov detector. An event which is accepted passes undetected through the scintillation counter, S_1, converts to one or more charged particles in the lead converter, and is subsequently detected by a coincidence between the thin scintillator S_2 and the gas Cerenkov detector. The index of refraction of the gas is very near unity, giving it a high-velocity threshold and a small-angle light cone. Thus this detector is characterized by its simplicity, potentially large collecting area, low background, and moderate angular accuracy. A small acceptance angle limits its use to studies of discrete sources. The technique should provide excellent sensitivity for point sources, although it has the disadvantage that it lacks the unambiguous event identification provided by the imaging detectors. This technique can be extended down to 15 MeV (Helmken and Hoffman, 1970).

A–6 GROUND-BASED TELESCOPES FOR OBSERVATIONS OF 10^{11} TO 10^{12} eV γ-RAYS

Recent observations (Fazio et al., 1970a, b; Charman et al., 1970; Chatterjee et al., 1970; and Charman and Jelly, 1970) of 10^{11} to 10^{12} eV γ-rays have been made utilizing the Earth's atmosphere both as a converter and as a gas Cerenkov detector for the electrons produced by γ-rays. The background I_B in this case is the Cerenkov light produced by the isotropic background of charged particle cosmic rays, as well as starlight and other light which might appear in the night sky. This background is severe, but the small angle θ subtended by the source and the large collecting areas allow excellent sensitivities to be obtained with this type of detector.

The basic instrument is simply a large optical reflector which focuses the light onto a photoelectric device, where the detected light pulses are recorded for later analysis. Data are collected as the Earth's rotation causes the source to pass across the detector aperture, with background samples taken before and after each observation. In this observing mode, care is taken to keep the instrument stationary in order to minimize the variables encountered during the data-collection period. The high background involved makes it essential that the system be extremely stable. Observations in which the telescope is pointed at the source as it moves across the sky have also been made to increase sensitivity by increasing the observing time; but the background fluctuations involved in moving the system due to varying atmospheric depths, changing magnetic field configurations, etc., make this a most difficult mode.

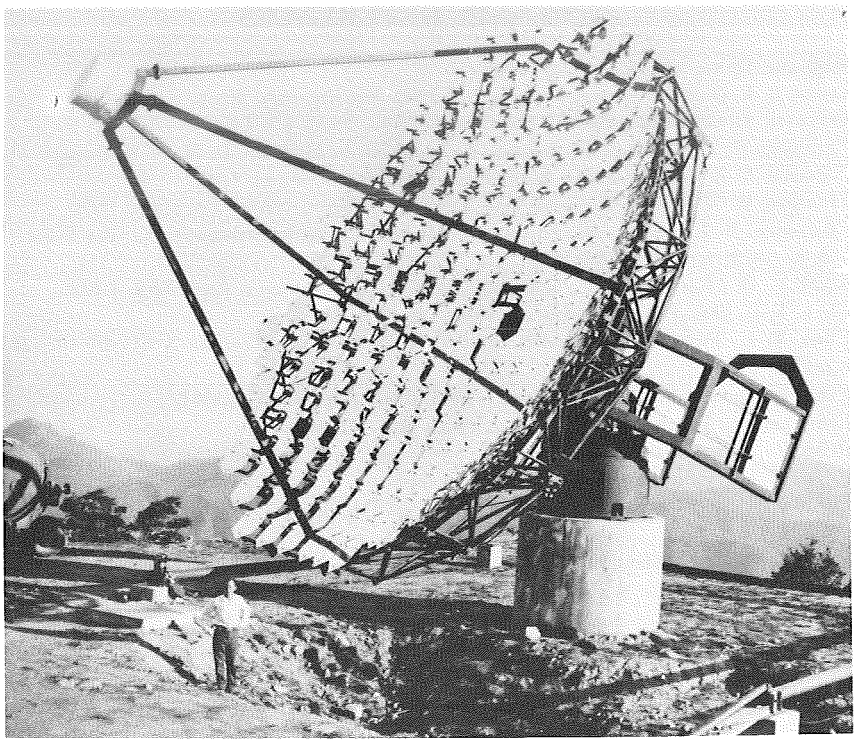

FIGURE A–15. – A picture of the 10-m reflecting night-sky Cerenkov telescope of the Smithsonian Astrophysical Observatory Mount Hopkins facility. (Courtesy G. G. Fazio.)

The 10-m telescope of the Smithsonian Astrophysical Observatory is shown in figure A–15.

A–7 SUMMARY

The detectors described in this brief survey represent the current instrumentation being used or planned for the near future in experimental γ-ray astronomy programs. Though intense effort has been put into this potentially fruitful observational field, the only unambiguous positive results obtained at this writing are the very significant results of the OSO–3 experiment of Clark, Garmire, and Kraushaar (1968) and Garmire (1970), and the ERS–18 results of Vette et al. (1970). There is a clear need for continued observations in all energy ranges with more sensitive detectors and improved techniques to map the detailed spectral and spatial structure of the celestial γ-ray distribution and to detect discrete sources and measure the characteristics of their emitted γ-radiation.

APPENDIX REFERENCES

Badhwar, G. See Valentine et al., 1970.

Board, S. J., Dean, A. J., and Ramsden, D. 1968. *Nuc. Instrum. Methods*, **65**, 141.

Bracessi, A., Ceccarelli, M., and Salandin, G. 1960. *Nuovo Cimento*, **17**, 691.

Charman, W. N., Fruin, J. H., Jelly, J. V., Fegan, D. J., Jennings, D. M., O'Mongain, E. P., Porter, N. A., and White, G. M. 1970. *Acta Phys.*, **29**, Suppl. 1, 59.

Charman, W. N., Jelly, J. V., and Drever, R. W. P. 1970. *Acta Phys.*, **29**, Suppl. 1, 63.

Chatterjee, B. K., Murthy, G. T., Ramana Murthy, P. V., Sreekantan, B. V., and Tonwar, S. C. 1970. *Acta Phys.*, **29**, Suppl. 1.

Clark, G. W., Garmire, G. P., and Kraushaar, W. L. 1968. *Ap. J. Lett.*, **153**, L203.

Cline, T. L. 1961. *Phys. Rev. Lett.*, **7**, 109.

Cline, T. L., Fichtel, C. E., and Kniffen, D. A. 1967. NASA Preprint X-611-67-135 (unpublished).

Cobb, R., Duthie, J. G., and Stewart, J. 1965. *Phys. Rev. Lett.*, **15**, 507.

Critchfield, C. L., and Ney, E. P. 1952. *Phys. Rev.*, **81**, 552.

Delvaille, J. P., Albats, P., Greisen, K. I., and Ogelman, H. B. 1968. *Can. J. Phys.*, **46**, 425.

Duthie, J. G., Hafner, E. M., Kaplon, M. F., and Fazio, G. G. 1963. *Phys. Rev. Lett.*, **10**, 364.

Ehrmann, C. H., Fichtel, C. E., Kniffen, D. A., and Ross, R. W. 1967. *Nuc. Instrum. Methods*, **56**, 109.

Fazio, G. G., and Hafner, E. M. 1967. *J. Geophys. Res.*, **72**, 2452.

Fazio, G. G., Hearn, D. R., Helmken, H. F., Rieke, G. H., Weekes, T. C. 1970a. *Acta Phys.*, **29**, Suppl. 1, 111.

Fazio, G. G., and Helmken, H. F. 1968. *Can. J. Phys.*, **46**, 5427.

Fazio, G. G., Helmken, H. F., Rieke, G. H., and Weekes, T. C. 1970b. *Acta Phys.*, **29**, Suppl. 1, 115.

Fichtel, C. E., and Kniffen, D. A. 1965. *J. Geophys. Res.*, **70**, 4227.

Fichtel, C. E., Kniffen, D. A., and Ögelman, H. B. 1969. *Ap. J.*, **158**, 193.

Frye, G. M., Reines, F., and Armstrong, A. H. 1966. *J. Geophys. Res.*, **71**, 3119.

Frye, G. M., and Smith, L. H. 1966. *Phys. Rev. Lett.*, **17**, 733.

Frye, G. M., Staib, J. A., Zych, A. D., Hopper, V. D., Rawlinson, W. R., and Thomas, J. A. 1969. *Nature*, **223**, 1320.

Garmire, G. 1970. *Bull. Am. Phys. Soc.*, **15**, 564.

Helmken, H., and Hoffman, J. 1970. *Nuc. Instrum. Methods*, **30**, 125.

Hutchinson, G. W., Pearce, A. J., Ramsen, D., and Wills, R. D. 1970. *Acta Phys.*, **79**, Suppl. 1, 89.

Kaplon, M. F. See Valentine et al., 1970.

Kinzer, R. L., Noggle, R. C., Seeman, N., and Share, G. H. 1970. *Bull. Am. Phys. Soc.*, **15**, 613.

Klarmann, J. 1962. *Nuovo Cimento*, **24**, 540.

Kniffen, D. A. 1969. NASA TR R-308, pp. 38-43.

Kraushaar, W. L., and Clark, G. W. 1962. *Phys. Rev. Lett.*, **8**, 106.

Kraushaar, W. L., Clark, G. W., and Garmire, G. 1968. *Can. J. Phys.*, **46**, 414.

May, T., and Waddington, C. J. 1969. *Ap. J.*, **156**, 437.

Ögelman, H. B., Delvaille, J. P., and Greisen, K. I. 1966. *Phys. Rev. Lett.*, **16**, 491.

Paolo, C., Paolo, D., Constantinos, P. 1970. Instituto di Fisica Preprint, Milan.

Perlow, G. J., and Kissinger, C. W. 1951. *Phys. Rev.*, **81**, 552.

Peterson, L. E., Gruber, D., Lewis, S. J., Stone, M. R., and Vette, J. I. 1968. University of California (San Diego) Preprint, UCSD-SP-68-5.

Pinkau, K. 1966. *Z. Phys.*, **96**, 163.

Ross, R. W., Ehrmann, C. H., Fichtel, C. E., Kniffen, D. A., and Ögelman, H. B. 1969. *IEEE Trans. Nucl. Sci.*, NS–16, 304.

Share, G., Kinzer, R. L., Noggle, R. Carl, and Seeman, N. 1968. *Bull. Am. Phys. Soc.*, **13**, 1459.

Sood, R. K. 1969. *Nature*, **222**, 650.

Valentine, D., Kaplon, M. F., and Badhwar, G. 1970. *Acta Phys.*, **29**, Suppl. I, 101.

Vette, J. I., Gruber, D., Matteson, J. L., and Peterson, L. E. 1970. *Ap. J. Lett.*, **160**, L161.

Additional Reading References

Fazio, G. G. 1970. *Nature*, **225**, 905.

Greisen, K. 1966. *Perspectives in Modern Physics* (R. E. Marshak, ed.) 355 (Interscience Publ. Co., New York).

Kraushaar, W. L. 1969. *Astronautics and Aeronautics*, **7**, 28.

U.S. GOVERNMENT PRINTING OFFICE : 1971 OL - 411-892

NATIONAL AERONAUTICS AND SPACE ADMINISTRATION
WASHINGTON, D. C. 20546

OFFICIAL BUSINESS

POSTAGE AND FEES PAID
NATIONAL AERONAUTICS AND
SPACE ADMINISTRATION
FIRST CLASS MAIL

POSTMASTER: If Undeliverable (Section 158 Postal Manual) Do Not Return

"The aeronautical and space activities of the United States shall be conducted so as to contribute . . . to the expansion of human knowledge of phenomena in the atmosphere and space. The Administration shall provide for the widest practicable and appropriate dissemination of information concerning its activities and the results thereof."

— NATIONAL AERONAUTICS AND SPACE ACT OF 1958

NASA SCIENTIFIC AND TECHNICAL PUBLICATIONS

TECHNICAL REPORTS: Scientific and technical information considered important, complete, and a lasting contribution to existing knowledge.

TECHNICAL NOTES: Information less broad in scope but nevertheless of importance as a contribution to existing knowledge.

TECHNICAL MEMORANDUMS: Information receiving limited distribution because of preliminary data, security classification, or other reasons.

CONTRACTOR REPORTS: Scientific and technical information generated under a NASA contract or grant and considered an important contribution to existing knowledge.

TECHNICAL TRANSLATIONS: Information published in a foreign language considered to merit NASA distribution in English.

SPECIAL PUBLICATIONS: Information derived from or of value to NASA activities. Publications include conference proceedings, monographs, data compilations, handbooks, sourcebooks, and special bibliographies.

TECHNOLOGY UTILIZATION PUBLICATIONS: Information on technology used by NASA that may be of particular interest in commercial and other non-aerospace applications. Publications include Tech Briefs, Technology Utilization Reports and Notes, and Technology Surveys.

Details on the availability of these publications may be obtained from:

SCIENTIFIC AND TECHNICAL INFORMATION OFFICE

NATIONAL AERONAUTICS AND SPACE ADMINISTRATION

Washington, D.C. 20546